Study of the muscle stem cell microenvironment in cancer cachexia and the benefits of a neuromuscular electrical stimulation therapy

Aliki Zavoriti

THESE de DOCTORAT DE L'UNIVERSITE CLAUDE BERNARD LYON 1

Ecole Doctorale N°205
ECOLE DOCTORALE INTERDISCIPLINAIRE SCIENCES-SANTE (EDISS)

Discipline : Biologie Cellulaire et Physiologie

Soutenue publiquement le 16/12/2022, par :
Aliki Zavoriti

Study of the muscle stem cell microenvironment in cancer cachexia and the benefits of a neuromuscular electrical stimulation therapy

Devant le jury composé de :

Pr Paloa Costelli	PR Université d'études à Turin	Rapporteure
Pr Vincent Martin	PR Université Clermont Auvergne	Rapporteur
Dr Athanassia Sotiropoulos	DR INSERM Université Paris Cité	Rapporteure
Pr Bruno Allard	PR UCBL1	Président
Dr Julien Gondin	CR CNRS UCBL1	Directeur de thèse

''Sans la curiosité de l'esprit, que serions-nous ? Telle est la beauté et la noblesse de la science : un désir sans fin de repousser les frontières du savoir, de traquer les secrets de la matière et de la vie sans idée préconçue des conséquences éventuelles''. Marie Curie

''Without the curiosity of the mind, what would we be? Such is the beauty and nobleness of science: a never-ending desire to expand the frontiers of knowledge, to track down the secrets of matter and life without any prejudice to the possible consequences''. Marie Curie

''Χωρίς την περιέργεια του νου, τι θα ήμασταν; Αυτή είναι η ομορφιά και η αρχοντιά της επιστήμης: μια ατελείωτη επιθυμία να διευρύνει τα σύνορα της γνώσης, να κυνηγήσει τα μυστικά της ύλης και της ζωής χωρίς προκατάληψη για τις πιθανές συνέπειες''. Μαρία Κιουρί

REMERCIEMENTS / ACKNOWLEDGMENTS

Tout d'abord, je voudrais remercier Julien Gondin, Bénédicte Chazaud et Rémi Mounier pour m'avoir fait confiance et m'avoir accordé l'opportunité d'effectuer une thèse dans leur équipe. Cette période de thèse fut une période enrichissante et riche d'émotions. Parfois difficile mais toujours intéressante.
Dans un deuxième temps je voudrais remercier spécialement mon directeur de thèse, Julien Gondin pour m'avoir accompagné durant ces trois ans de thèse. Grâce à lui, j'ai pu développer un regard critique sur des sujets divers et une démarche scientifique rigoureuse, tout en lui fournissant de beaux résultats, parfois dans de délais restreints (il adore la ponctualité !). Ensuite, je voudrais le remercier car il a toujours été disponible pour m'aider au moindre souci ou pour la moindre question, il a su très bien me guider à travers les différents travaux et me redonner confiance dans des moments critiques. Je reste cependant un peu sceptique par rapport à ses gouts de vin.

First of all, I would like to thank Julien Gondin, Bénédicte Chazaud and Rémi Mounier for having trusted me and having given me the opportunity to do a thesis in their team. This thesis period was an enriching and emotional period. Sometimes difficult but always interesting.
Secondly, I would like to thank especially my thesis director, Julien Gondin for having accompanied me during these three years of PhD. Thanks to him, I was able to develop a critical look on various subjects and a rigorous scientific approach, while providing him with beautiful results, sometimes within short deadlines (he loves punctuality!). Then, I want to thank him because he was always available to help me at the slightest concern or question, he knew very well to guide me through the various works and to give me confidence in critical moments. However, I am little skeptical about his taste in wine.

Je voudrais ensuite remercier mes collègues de labo avec lesquels j'étais le plus proche durant ma thèse, Clara et Charline. Nos rigolades et les moments passés ensemble vont me manquer, je suis triste d'être la première à partir et ainsi ne pas pouvoir assister aux derniers instants de votre thèse.

Peu importe le contexte, vous aviez toujours su être là quand j'avais besoin de votre aide et m'épauler. Malheureusement Clara, il faudra trouver une nouvelle personne pour remplacer la Queen du montage de muscles :-p
Je vous souhaite en tous cas, beaucoup de réussites dans l'aboutissement de vos projets et dans votre future vie postdoctorale.

I would like to thank my lab mates with whom I was the closest during my thesis, Clara and Charline. I will miss our laughs and the moments spent together, I am sad to be the first to leave and not be able to attend the last moments of your thesis. No matter the context, you were always there when I need your help and support. Unfortunately, Clara, we will have to find a new person to replace the Queen of muscle mounting. :-p
I wish you all the best for your projects and your future postdoctoral life.

Je tiens également à remercier Aurélie qui a été d'un grand soutien à la réalisation de mon projet de thèse. Grâce à son aide remarquable qu'elle a fourni lors des expériences, nous avons pu faire avancer le projet de manière optimale.

I would also like to thank Aurélie who has been a great support to the achievement of my thesis project. Thanks to the remarkable help she provided during the experiments, we were able to make the project progress in an optimal way.

Par la suite je voudrais également remercier Anita et Georgia. Anita, avec sa bonne humeur, a toujours apporté un grand intérêt pour mon projet de thèse. Les échanges que nous avons eu ensemble au fil et à mesure de mon doctorat, étaient toujours intéressants et certaines fois ont contribué à me donner des idées pour mon projet. Grâce à Georgia, ma compatriote, j'ai pu pratiquer ma langue maternelle tout au long de la thèse et ne pas l'oublier. Je la remercie également pour son soutient durant la rédaction de mon manuscrit et son aide pour utiliser le logiciel Word :-p

Afterwards, I would also like to thank Anita and Georgia. Anita, with her pleasant mood, has always brought great interest in my thesis project. Our discussions which we had together throughout my whole PhD, were always interesting and sometimes helped to give me ideas

for my project. Thanks to Georgia, my compatriot, I was able to practice my native language throughout the thesis and not forget it. I also thank her for her support during the writing of my manuscript and her help in using Word software :-p

Pour la fin, je voudrais également remercier les membres restants de l'équipe Chazaud et Mounier ; Gaëtan, Huong, Hamy, Sabrina, Michèle… Grâce à vos différentes expertises, chacune dans un domaine différent, nos échanges ont été très instructifs. Je vous souhaite que de belles surprises dans l'avenir!

For the end, I would also like to thank the remaining members of the Chazaud and Mounier team; Gaetan, Huong, Hamy, Sabrina, Michèle… Thanks to your different expertise, each in a different field, our exchanges were very instructive. I wish you many nice surprises in the future!

Et, et… En tout dernier sans les oublier, je voudrais remercier Carole et Audrey (les deux nouveaux bébés doctorantes) pour leur bienveillance et bonne humeur, apportant de la légèreté au quotidien. Je vous souhaite une belle aventure au sein de l'institut avec plein de beaux résultats !

And, and… as a last but not least, I would like to thank Carole and Audrey, the two new doctoral babies, for their warmth and good mood, bringing cheerfulness to the daily life. I wish you a happy adventure within the institute with many exciting results!

SCIENTIFIC PUBLICATIONS AND SUBMISSIONS

Bernard C*, Zavoriti A*, Pucelle Q, Chazaud B, Gondin J. Role of macrophages during skeletal muscle regeneration and hypertrophy-Implications for immunomodulatory strategies. **Published in** Physiol Rep. 2022 Oct;10(19): e15480. doi: 10.14814/phy2.15480
*Equally contributed

Zavoriti A, Fessard A, Rahmati M, Boyer N, Del Carmine P, Chazaud B, Gondin J. Neurommuscular electrical stimulation training induces myonuclear accretion and hypertrophy in mice without overt signs of muscle damage. **Submitted to** the Journal of physiology. JP-RP-2022-283984, http:/jp.msubmit.net
(Accessible : bioRxiv 2021.12.14.472254; doi: https://doi.org/10.1101/2021.12.14.472254)

Communications

Oral communications

Days of the French Society of Myology (18èmes Journées de la société Française de Myologie, Saint-Etienne, France – November 2021) '' Stem cell microenvironement and skeletal muscle function analysis during the progression of cancer cachexia in *Apc*$^{Min/+}$ mice''.

Internal seminar of the institute NeuroMyogène (Lyon, France – March 2022) '' Stem cell microenvironement and skeletal muscle function analysis during the progression of cancer cachexia in *Apc*$^{Min/+}$ mice.

Posters

PhD school day (26ème Journée de l'EDISS, Lyon, France – October 2021) '' Stem cell microenvironement and skeletal muscle function analysis during the progression of cancer cachexia in *Apc*$^{Min/+}$ mice'' - Best poster award!

4th International conference of Stem cells, Development and Cancer (Lyon, France – May 2022) ''Increased myofiber contractile activity promotes muscle stem cell fusion, reduces inflammation and improves muscle function in a mouse model of cancer cachexia''

ABREVIATIONS

BIA: Bioelectrical impedance analysis

BMI: Body Mass index

CC: Cancer-cachexia

COPD: Chronic obstructive pulmonary disease

CSA: Cross-sectional area

CT: computed tomography

DEXA: Dual-energy X-ray absorptiometry

ECM: Extracellular-matrix

EC: Endothelial cell

FAP: Fibro-adipogenic progenitor

FFM: Fat-free mass

MyHC: Myosin heavy chain

eMyHC: embryonic myosin heavy chain

NMES: Neuromuscular electrical stimulation

NMJ: neuromuscular junction

PDAC: Pancreatic ductal adenocarcinoma

SC: Satellite cell

SMI: Skeletal muscle index

SUMMARY

GENERAL INTRODUCTION

I. Preview: Cancer

Cancer arises when body's own cells become damaged and stop working normally as a result of mutations in genetic information. Cells can suddenly start to divide out of control, invade nearby tissues and travel to distant places in the body to form new tumors (*i.e.,* metastasis). Cancer is the second leading cause of death in the world, after cardiovascular disease[1] accounting for nearly 10 millions of deaths *per* year worldwide or nearly one in six deaths[2]. In 2020, breast and lung cancers were the most diagnosed cancers worldwide, contributing respectively to 12,5% and 12,2% of the global cancer incidence. Colorectal cancer was the third most common diagnosed cancer with 1.9 million new cases in 2020, contributing to 10,7% of global cancer incidence. In 2020, lung cancer comprised 18% of total cancer caused deaths while colorectal cancer was responsible for 9.4% of all cancer related deaths[3]. More than two thirds of cancer-related mortality occur in low- and middle-income countries[4,5] due to weak health care and economic infrastructure, these countries are least prepared to manage cancer burden[6,7]. Thus, large numbers of cancer patients globally do not have access to timely quality diagnosis and treatment[8]. Age is the biggest risk factor for the disease, for instance only 1.7% of all cancer-related deaths in both sexes occur before the age of 40 years in the United States of America (USA), and 90% of cancers are diagnosed in those aged up to 50 years[9]. As the world population is growing and aging the global number of cancer deaths is increasing[10,11].

Other risks related to greater cancer incidence are smoking, excess body weight, physical inactivity, poor diet and alcohol intake. It is estimated that at least 40 percent of cancer deaths in the USA may be prevented if people paid attention to these risk factors[12]. Thus, cancer is one of the world's most pressing problems to make progress against this disease.

II. Cancer cachexia: Definitions, prevalence, diagnostic tools and consequences

A. Definition of cancer cachexia

In the olden days, cachexia was described as a syndrome of irreversible muscle wasting in the terminally ill patients. The term ''cachexia'' comes from the Greek words ''*kakos*" and "*hexis*" which translate to "bad physical state".

The definition of cachexia has constantly evolved over the years. Historically, involuntary weight loss of >10% has been used to define cancer cachexia (CC)[13]. However, research shows that the underlying progressive muscle loss is the crucial factor, that is responsible for the most of the adverse effects of CC[14]. Therefore, the weight loss in cachexia differs from the weight loss in malnutrition or starvation, the loss of lean tissues compared to fat mass is accelerated in cachexia[15]. Furthermore, cachexia can occur with or without anorexia in mice and humans, and frequently it appears prior to decreases in food intake[16,17]. In 2007, an expert panel[18] from the Cachexia Consensus Conference proposed the following: « *Cachexia is a complex metabolic syndrome associated with underlying illness and characterized by loss of muscle with or without loss of fat mass*. *The prominent clinical feature of cachexia is weight loss in adults (corrected for fluid retention) or growth failure in children (excluding endocrine disorders)*. *Anorexia*, *inflammation*, *insulin resistance and increased muscle protein breakdown are frequently associated with cachexia*. *Cachexia is distinct from starvation*, *age-related loss of muscle mass (i.e., sarcopenia)*, *primary depression*, *malabsorption*, *and hyperthyroidism*, *and is associated with increased morbidity* ». In 2008, another definition was suggested by Evans et al.[19] including, weight loss with or without the loss of fat, in addition with three of the 5 following criteria such as decreased muscle strength, reduced muscle mass, fatigue, anorexia, or abnormal biochemistry including anemia, evidence of inflammation, or low albumin. These diagnostic criteria are applicable to all types of chronic disease-related cachexia when taking metabolism and nutrition into account.

In 2011, an agreement was made among an international group of experts[20], that provided the following definition specifically targeting CC, that emphasized weight loss factors and muscle loss: « *A multifactorial syndrome defined by ongoing loss of skeletal muscle with or without accompanying loss of fat that can be partially but not entirely reversed by conventional nutritional support and can lead to progressive functional impairment*». The same group of experts proposed three consecutive stages of clinical relevance to characterize CC comprising the pre-cachexia stage, the cachexia stage and the refractory cachexia stage. The latter also proposed five domains to assess CC including food intake, metabolic alterations, functional and psychosocial impact, and assessments of body composition including stores of adipose tissue and muscle mass. Additionally, it was advised for grading the severity of weight loss, to use the body mass index (BMI) and degree of weight loss (Figure 1). The early pre-cachexia stage features early clinical and metabolic signs such as impaired

glucose tolerance, anemia and general inflammation that can be present before significant uncontrolled body weight loss (*i.e,* ≤5%). The agreed diagnostic criterion for patients in cachexia stage was weight loss greater than 5% over six months prior to diagnosis, or a BMI <20 kg/m^2 combined to ongoing weight loss >2% or muscle mass loss (sarcopenia) combined to ongoing weight loss >2%. In refractory cachexia stage, due to higher level of active weight loss, management is no longer possible and patients are unlikely to benefit from any treatment. At this stage, patients usually have less than 3 months of survival and show low performance scores. The performance score in oncology is an attempt to quantify cancer patient's functional status and general well-being, the score ranges from 0 (Fully active) to 4 (complete disability) and grades how well the patient takes care for himself, performs daily tasks and activities[21].

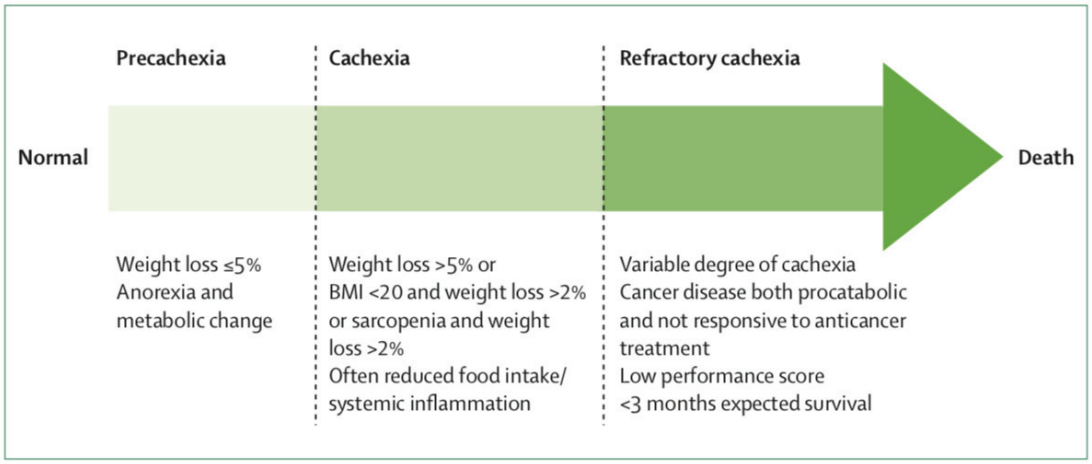

***Figure 1**: Progression of CC in clinical setting defined by 3 stages: pre-cachexia, cachexia, and refractory cachexia. Severity is classified according to degree of depletion of energy stores and body protein (reflected by BMI) in combination with degree of ongoing weight loss. An increase in anorexia, inflammation, metabolic dysregulation and a decrease in muscle strength, mobility and quality of life are additional clinical symptoms related to cachexia stage. (Adapted from Fearon et al.[20].*

This definition is currently considered by many as the gold standard of CC and has been validated in a follow-up study of 861 subjects with and without cachexia[22]. Further, this classification of CC progression emphasizes the relevant physiological changes that may be present long before the cutoff point of weight loss >5% is reached and that can be taken into account in CC prevention.

This type of grading allows also for patients to obtain more suitable treatment options at all stages of disease development. Yet cancer patients may not experience all three stages, the

severity of cachexia and incidence are quite heterogeneous and depend on the type, location and stage of the tumor.

B. Prevalence of CC

The overall prevalence of cachexia, among all diseases that cause cachexia (chronic kidney disease, chronic obstructive pulmonary disease, neurological disease, rheumatoid arthritis and cancer) currently affect around 0.5-1.0% of the population, (*i.e,* around 6-12 million people). It is estimated that 1.5-2 million people die annually worldwide due to the consequences of cachexia[23].

Half of all cancer deaths worldwide are attributed to the cancers most frequently associated with cachexia, mainly pancreatic, esophageal, gastric, lung, hepatic, and colorectal cancers[24,25,26,27,28]. Cachexia occurs in more than 50% of cancer patients and is depending on the type, site and stage of tumor[28,29,30,31]. All cancers can present with cachexia, but prevalence of CC is higher in some cancer types. Almost 80% of patients with pancreatic and upper gastrointestinal cancers suffer from cachexia[24,32,26,27] and those cancers are often diagnosed at an advanced stage[33] (Figure 2). In fact, the anatomical location of the tumor near structures that are directly related to nutrient intake such as the pancreas or the intestines can increase the risk of development and severity of CC[34,35,36,37,38,39]. On the other hand, patients with sarcomas, breast cancer and hematological malignancies display the lowest frequency of weight loss combined with cachexia[29,40]. Globally, over the course of their disease progression, 45% of patients lose more than 10% of their initial body weight[41]. Approximately 30% of all cancer-related deaths are thought to derive from CC rather than from tumor burden or metastasis spreading[42], with incidence predicted to grow in the future[43]. In accordance with a direct cause of death, cachexia can produce loss of respiratory muscle function conducting to death from hypostatic pneumonia[44] or might cause myocardium atrophy leading to heart failure[45].

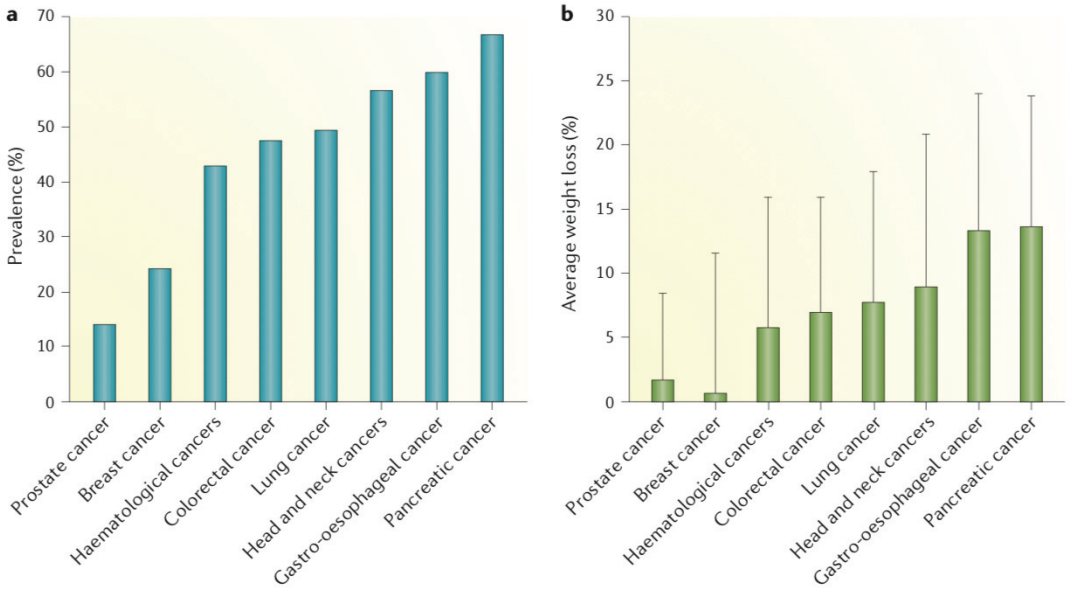

Figure 2: *a) The prevalence of cachexia and b) average body weight loss (in %) in cancer patients according to tumor location. Cachexia is most common in pancreatic, esophageal, stomach, lung, and colorectal cancers (Adapted from Baracos et al.*[32]*).*

Additional factors besides tumor type or stage, may contribute to variable prevalence of cachexia such as genetic factors, age, biological sex, chemotherapy administration or body composition.

Despite having the same tumor type and burden, one person may develop cachexia while another does not, such variation can be due to the interaction of cancer patient's genotype[46,47] regulating immunity and associated signaling pathways. The most common type of genetic variation among people are single nucleotide polymorphisms (SNPs). Even while the vast majority of SNPs have no functional impact, some of them can affect a gene's function by occurring within or close to it in a regulatory region. Numerous candidates of gene SNPs have been found to have functional association with CC prevalence, especially genes involved in inflammation[46,47]. Increase in levels of proinflammatory cytokines produced by the tumor or the host is likely the most frequent correlation between cancer and the occurrence of cachexia. SNPs in the IL-6, IL-10 and IL-1 genes linked to production rates of these cytokines have been associated with the prevalence of cachexia in pancreatic and gastric cancers[48]. Cachexia in pancreatic cancer has been associated with elevated tumor IL-6 production[49]. Moreover, two independent cohorts have confirmed that the 1082G allele in IL-10 promoter is a genetic polymorphism increasing the risk of cachexia in gastroesophageal cancers[50,51]. IL-10 has been shown to be elevated in a Myc/mTOR-driven murin model of CC[52], as well as in cachectic patients with colorectal cancer[53]. Moreover, separate studies conducted in a large

and diverse populations of cancer patients and animal models, showed that individuals carrying the C allele of the rs6136 polymorphism in the P-selectin gene are at reduced risk of developing cachexia[54,55]. These findings have been confirmed in chemo-naïve patients with locally advanced or metastatic pancreatic cancer[56]. Finally, pancreatic and non-small cell lung cancer patients which carry the mutant TNF-α variant of 308 *G/A* within the gene coding this pro-inflammatory cytokine together with high non-coding microRNA miR-155 are at greater risk of cachexia[57]. Collectively, these studies support genetic predisposition to CC.

Regarding age as a factor that might contribute to cachexia, a recent study showed that aging affects cachexia development and progression in tumor bearing mice in a strain-dependent manner[58]. In this study, aging aggravated weight loss onset and progression in tumor-bearing C57BL/6 mouse strain, while no impact of aging was observed in the tumor-bearing mice with BALB/c genetic background.

Regarding human cancer patients, a retrospective study reported that elderly patients ($\geq$ 70 years old) presented more frequently weight loss and malnutrition than younger patients (< 70 years) with 73,6 % and 67,6% weight loss respectively, since the diagnosis of the cancer disease[59]. Another study conducted in a specialized geriatric oncology clinic, reported that more than half of patients (65%) with a mean age of 80 years (range: 66-95 years) presented with cachexia[60]. However, at the moment no study has shown a direct association between the prevalence of cachexia and age in cancer patients, due to the fact CC is very poorly described in older adults with cancer. Sarcopenia, a common syndrome related to aging that contribute to muscle functional and mass decline, might amplify CC[61,62].

Biological sex has been recently reported as an important factor for CC. While both males and females exhibit CC, the development of CC is probably different between sexes[63]. Women generally appear to be less prone to muscle wasting caused by cancer in comparison to men[63]. Among 124 patients on first-line treatment for metastatic pancreatic cancer, only men displayed muscle loss with average muscle wasting being greater and more rapid than in women[64]. Yet, Baracos et al.[65] evaluated body composition in non-small lung cancer by analyzing diagnostic computed tomography images of 441 patients (229 men and 212 women). In this study, men (61%) presented with muscle wasting at a substantially higher rate than women (31%). Similar results were derived from a study comprising 471 patients (259 men and 212 women) where the prevalence of muscle depletion in the last 2 years of life was higher in male cancer patients (59%) than female patients (28%)[66]. These data show that male

cancer patients present generally greater loss of body weight and muscle mass and worse outcomes than female cancer patients. This fact may further relate to a higher prevalence of hypogonadism in males than females[67]. In experimental studies as well, male mice also show earlier and more severe body weight loss than female mice caused by accelerated loss of muscle mass[68,64].

Cachexia prevalence may also be affected by chemotherapy use. Pre-clinical models and clinical studies reveal that chemotherapies such as taxanes or vinka alkaloids can induce severe muscle weakness and wasting[69,70,71,72,73,74,75]. Thus, chemotherapy and radiotherapy could exacerbate CC[76,77,78,79,80] and reduce the physical fitness of cancer patients[81].

In a cohort of 150 patients[82] with advanced pancreatic ductal adenocarcinoma (PDAC), the incidence of post-chemotherapy cachexia was highest within 12 weeks from starting first-line chemotherapy (FLC). Chemotherapy-induced cachexia occurred in 64% of patients within 48 weeks of FLC. Among patients with basal cachexia, 51% experienced chemotherapy-induced cachexia following FLC while only 36% of patients without basal cachexia experienced cachexia following chemotherapy.

Interestingly, two studies[83,84] found that the prevalence of muscle mass loss was increased for post-chemotherapy patients as compared to pre-chemotherapy patients. Muscle mass loss occurred in the absence of any clinically significant reduction in body weight, suggesting that the prevalence of muscle wasting tends to be higher in patients that have received chemotherapy than patients with untreated cancers.

Medical oncologists at present are facing a new issue as 40-60% of their patients present with excess body weight (overweight and obese) at the time of cancer diagnosis[85]. Patients with both low skeletal muscle mass and excess fat mass (*i.e.,* sarcopenic obese) have a greater risk of negative outcomes. Obesity and CC, besides their dichotomy, these diseases share some common underlying mechanisms mediating profound metabolic alterations[86,87,88]. It was proposed that chronic inflammation and insulin resistance deriving from obesity could promote a suitable environment for cancer growth and the development of cachexia[89]. Hendifar et al.[90] reported an association between obesity and cachexia in their PDAC patient cohort. BMI higher than 30 was associated with considerably higher prevalence of cachexia (68% *vs* 32%). In another study[91], more than half of patients (52%) displaying variable levels of body weight loss, were presented as overweighted or obese. Overall, the findings imply that when cancer patients have obesity, it may promote CC development.

C. Diagnostic tools of CC

At present, there is no universal agreement on the criteria that should be applied to diagnose CC in clinical trials and healthcare decision making. Diagnosis for cachexia in cancer patients used routinely, is mainly based on parameters such as weight loss or BMI[20]. However, these parameters do not provide any information about body composition and particularly muscle mass[92]. Indeed, weight loss or BMI alone are not suitable methods to assess CC in sarcopenic obese patients (sarcopenic patients with high BMI) and patients with severe edema, because weight is rather increased due to increased fat mass and/or body water while skeletal muscle is decreased[91,93]. Body composition analysis as a complementary approach, can be used to overcome these limitations and to determine muscle wasting, the major feature of CC. The most commonly used tools to screen for muscle wasting in cancer patients include dual-energy X-ray absorptiometry (DEXA), computed tomography (CT) and bioelectrical impedance analysis (BIA).

DEXA evaluates human body composition using a three-compartment model including fat mass (FM), fat-free mass (FFM), and bone mineral content (Figure 3).

Figure 3: *DEXA provides precise measurements of total body composition such as fat and lean distribution in segmental regions like in arms and legs over time and is widely used to assess skeletal muscle based on analysis of the limbs[94,95] (Picture from Internal medicine of Arizona's website, topdocsaz.com).*

DEXA can identify early lean mass variations[96,97]. However, this approach does not differentiate between the different subsets of adipose tissue into intramuscular, visceral and subcutaneous or lean body mass into muscle, organ tissue, and tumor tissue[98,99]. Fat-free mass represents skeletal muscle in DEXA analysis. Thus, this technique can induce lack of accuracy in estimating muscle mass[94,95]. The latter consists of predominantly scanning appendicular

muscles using radiation[100,101,102,103]. The appendicular muscle (sum of muscle mass from arms and legs) evaluated with DEXA is expressed in kilograms and is used as a basic index. Due to the strong correlation between the body height and size with muscle mass, the skeletal muscle index (SMI) can be employed instead of using directly the appendicular skeletal muscle mass. SMI is defined as appendicular skeletal muscle mass (kg) normalized to each patient height^2 (kg/m^2)[104]. Baumgartner et al.[94] were the first to propose the following sex-specific cut-off values that define low appendicular muscle mass: 7.26 kg/m^2 in men and 5.45 kg/m^2 in women. Since then, several groups use these cut-off values as reference to evaluate muscle wasting[105,106].

CT scanning is the most commonly tool used in research and cancer care to assess muscle mass in patients[65,107]. CT scanning estimates axial skeletal muscle mass and quality by cross-sectional imaging [108]; Thus, CT data are presented in the units of the primary measure, cross-sectional areas (CSA) in cm^2. CSA of skeletal muscles at distinct anatomical landmarks were shown to give a good estimate of the whole skeletal muscle compartment and therefore may be used to identify patients with low muscle mass[103,109,110]. Therefore, in the last years, skeletal muscle wasting is most often determined from CT scan analysis of the area of either intra-abdominal musculature or psoas muscle, both located at the third-lumbar vertebra (L3) level[111,112,113] (Figure 4).

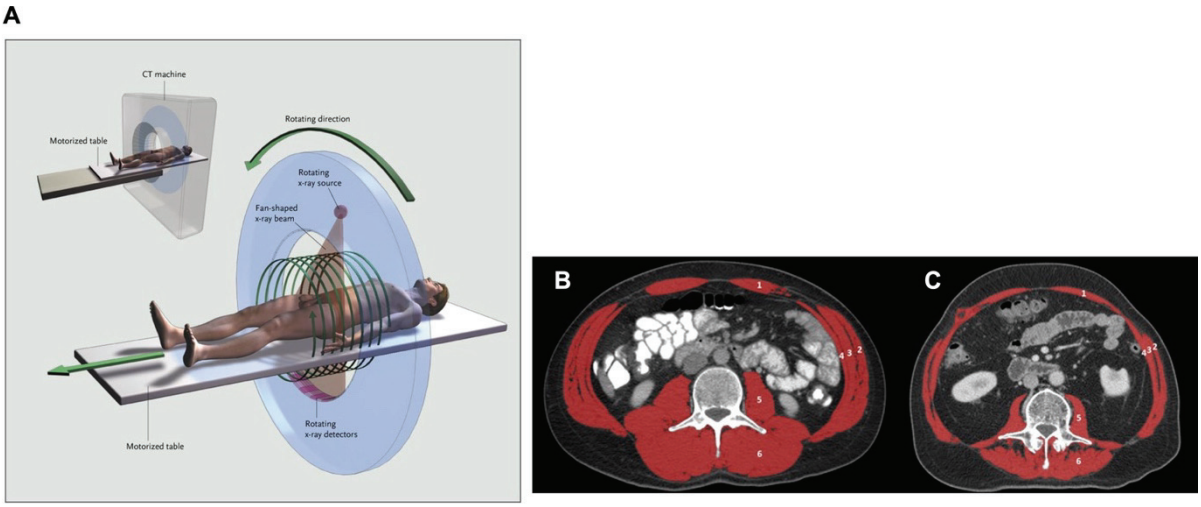

Figure 4: *A) A motorized table moves the patient through the CT imaging system. In parallel, a source of x-rays rotates within the circular opening, and a set of x-ray detectors in turn rotates synchronously on the far side of the patient. The x-ray source produces a narrow, fan-shaped beam. The table moves continuously as the x-ray source and detectors rotate, producing a spiral scan (Figure taken from Brenner et al.*[114]*,) Right panel: CT scans at the 3rd lumbar vertebra level in patient with B) normal (L3 SMI 60,04 cm²/ m²) and C) low (L3 SMI 39.19 cm²/ m²) skeletal muscle mass submitted to resection of perihilar cholangiocarcinoma. Skeletal muscle is colored in red (1: rectus abdominis, 2: external oblique, 3: internal oblique, 4: transverse abdominal, 5: psoas, 6: paraspinal). (Figure taken from Coelen et al.*[115]*).*

Lumbar SMI is defined by the ratio of skeletal muscle area (cm^2) normalized to each patient's height^2 (cm^2/ m^2). Studies have proposed different cut-off values specific to patients with CC. Prado et al.[14] defined cut-off values of 52.4 cm^2/ m^2 in men and 38.5 cm^2/ m^2 in women among a population of obese patients with respiratory or gastrointestinal tract cancers. Mourtzakis et al.[116] demonstrated strong correlation between CT analysis of skeletal muscle at L3 and appendicular skeletal muscle measured by DEXA. Thus, CT cut-off values were obtained by matching them to those of DEXA, corresponding to 55.4 cm^2/m^2 in men and 38.9 cm^2/m^2 in women. Finally, Fearon et al.[20] agreed on a new diagnostic criterion for cachexia to be based both on anthropometric measures and SMI cut-off values of 55 cm^2/m^2 in men and 39 cm^2/m^2 in women using CT scan analysis. As such, CT scanning is thought to be the most trustworthy and accurate procedure to evaluate muscle wasting.

BIA is an easy, affordable, rapid and non-invasive method to assess body composition. BIA can determine fat mass, fat-free mass or water composition, from whole body or from a specific region, based on the conduction of electrical current through the body[117] (Figure 5). A small electrical current is used to measure the resistance at different frequencies against various tissues in the body. Fat tissue has high resistance to the flow current, therefore shows a high impedance reading while lean muscle and water are good conductors of current, therefore

will show low resistance or impedance readings. The impedance readings are after translated using validated equations into estimations of body composition components. Appendicular skeletal muscle mass can be determined when the conversion equation is calibrated with a reference of DEXA-measured lean mass[118] in a specific population[119,120]. Similarly, to DEXA, appendicular SMI estimated with BIA is defined by the weight of fat-free compartment normalized to patient's height^2 (kg/m^2). The majority of studies are using the cut-off values from either the European[103] or Asian[121,122,123] consensus. The Asian consensus suggests cut-off values of appendicular SMI corresponding to 7.0 kg/m^2 in men and 5.7 kg/m^2 in women with BIA analysis.

The assessment of muscle mass by BIA has to be interpreted carefully. Body composition estimates rely on the brand of BIA device and equation used[124], therefore estimates of muscle mass might differ. In addition, BIA is highly dependent on patient hydratation state and muscle mass loss is biased[116] when patients exhibit pathological increase in water content like massive ascites or marked edema[125] .

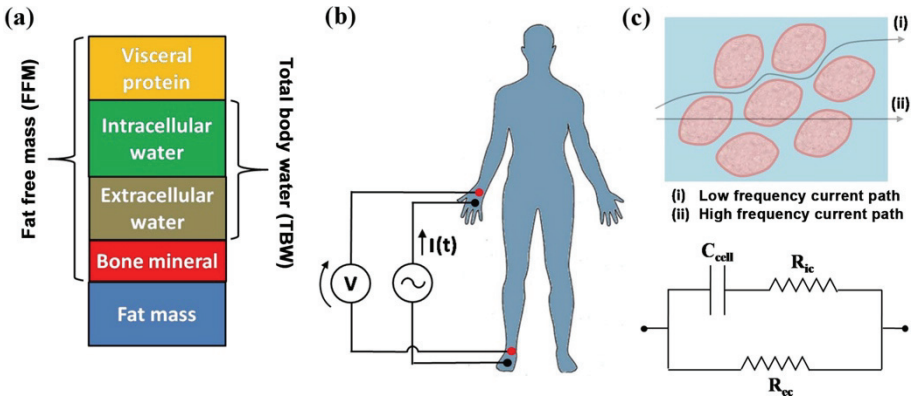

Figure 5: *a) Total body weight or fat-free mass are estimated based on conductivity by using empirical linear equations that take into account the height, the weight, and other parameters of the patient b) BIA technology uses electrodes (driving and sensing electrodes) applied to the skin of the patient to deliver a mild electrical voltage and assess tissue electrical conductivity. c) Electric current flows at different rates through the body depending upon its composition. (Picture taken from Grossi and Ricco[126]).*

DEXA and CT methods are preferentially used in the research field while BIA is frequently used in clinical practice. Unfortunately, the costs and availability of these methods, mainly offered only by large health care institutions yet limit their use[127]. To date, there is no consensus on how to choose the optimal modality to assess muscle mass in CC patients. SMI and muscle

mass distribution varies according the method and device used[128,129] and also to ethnicity and gender[130,131] therefore indicating that different standards for skeletal muscle should be applicable according to these elements.

The cachectic patient can be also assessed and characterized by anorexia or reduced food intake[20,132,133]. An additional key diagnostic factor for CC could be skeletal muscle force. Decrements in muscle function have been indirectly assessed and validated in research and preliminary studies on cancer patients with cachexia (defined by body weight loss) using physical performance tests such as the 6 min walk test or by directly *via* dynamometry to assess hand grip or leg muscle force[134,135,136]. However, still muscle force measurement is not a common tool used in clinics to stratify cancer patients with cachexia. Finally, a uniform methodology including consistent evaluation of muscle strength together with muscle mass to determine CC in cancer patients might be helpful for decision making on supportive treatment in patient care and especially for research to be able to compare clinical trials.

D. Consequences of CC

During CC, muscle strength and endurance are severely reduced[137,138,136,139,140] . Moreover, cachectic cancer patients experience decreased physical function[141] and have a higher chance of disabilities[142,143], extended hospital stays and of dying in hospitals[144,143,145] . Patients with CC consequently are less likely to tolerate anti-cancer therapies[146] and show worse quality of life and prognosis[147,148,149,150,151]. Therefore, because muscle depletion is associated with poorer survival[152] and decreased activity levels[153], it is used as a prognostic factor to predict survival in cancer patients[154,155,152].

A decrease in SMI or increase in muscle loss during chemotherapy or surgery is associated with poor survival in advanced-stage ovarian cancer[156]. Similarly, rapid depletion of skeletal muscle mass after treatment with chemotherapeutic drug sorafenib was linked with poor prognosis in hepatocellular carcinoma patients[77]. In fact, patients with depletion of skeletal muscle mass presented higher chemotherapy-induced toxicity compared with patients with larger amounts of lean body mass[157,112,158,159,160,161,36,162]. Wasting of skeletal muscle tissue, causes changes in body composition that alters the biotransformation and kinetics of chemotherapeutic substances in the body[163]. Thus, cancer patients are forced to reduce dosage or to delay the cycles of administration and ultimately have worsened outcomes[164].

Considered collectively, there is strong evidence that point out the skeletal muscle as the dominant target of CC.

III. Muscles: How CC impact skeletal muscle mass, fiber morphology and function

Skeletal muscles accounts for approximately 38% of total body weight for men and 30% for women[165] and are made up with 50 to 75% of total body proteins[166]. Skeletal muscle is one of the most dynamic and plastic tissues of the human body, it mainly contains water and proteins and to a lesser extent minerals, fat and carbohydrates. Muscle mass primarily relies on the balance between muscle protein synthesis and breakdown and both processes can be influenced by elements such as diet, hormonal balance, exercise, along with injury or disease. Fundamentally, the main function of skeletal muscle is to produce contractile force by transforming chemical energy into mechanical energy. The electrical activity of motor neurons is transmitted across the neuromuscular junctions (NMJ), by depolarizing the muscle membrane and produces muscle action potentials. Therefore, through this mechanism, muscles are essential to maintain posture and produce movement that makes possible to practice social activities and sports. In other words, skeletal muscle is essential for functional independence. Skeletal muscle also plays a role in the basal energy metabolism, by operating as storage for essential substrates such as amino acids and carbohydrates, producing heat to sustain core body temperature and maintaining the balance of oxygen consumption during exercise or physical activity.

A. Anatomical organization of skeletal muscle

An adult muscle is covered with an outermost layer of connective tissue known as the *epimysium*. Fibers inside that single muscle are organized into bundles and covered by another layer of connective tissue known as the *perimysium*. Individual muscle fibers are surrounded by a layer called the *endomysium*.

Single muscle fibers are for the most part made of proteins that have unique functions. Each muscle fiber contains many chains of myofibrils which are made up by filaments referred to as myofilaments that meet together in a well-organized and specific pattern. The two most

abundant myofilaments are actin and myosin, which compose the thin and thick myofilaments respectively and which are responsible for muscle contraction. The myofilaments are arranged into repeated subunits, called sarcomeres (smallest unit of the muscle fiber), along the length of the myofibril. The alignment between the sarcomeres of one myofibril with those of the myofibrils next to it, is responsible for the striated appearance of skeletal muscle (Figure 6).

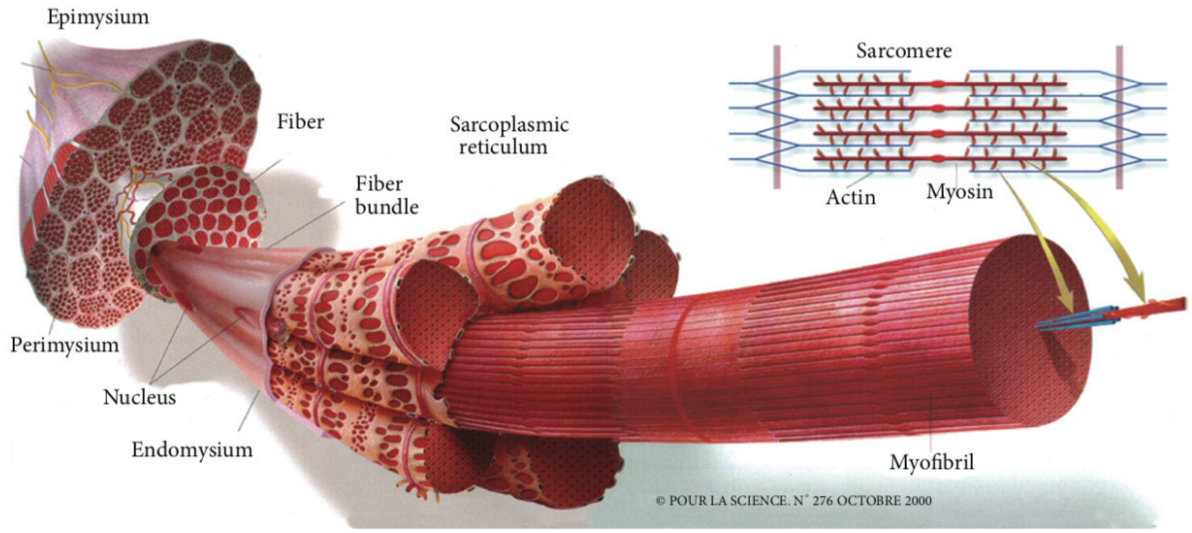

Figure 6: *Structural organization of the skeletal muscle (Picture taken from Listrat et al.[167]).*

The process by which a muscular action potential in the muscle fiber induces muscle contraction is known as excitation-contraction coupling[168].

Excitation-contraction coupling occurs when muscle fibers depolarize in response to nerve impulse allowing a muscle action potential to propagate along the NMJ. Acetylcholine is released, binds to receptors, and opens sodium ion channels allowing the action potential to travel along the muscle fiber membrane, called the sarcolemma. The muscle action potential then goes down the network of T-tubules (invaginations of the sarcolemma) depolarizing the inner part of muscle fiber. This leads to activation of the dihydropyridine (DHP) receptors which interact mechanically with the calcium-conducting ryanodine receptors (RyRs) on the adjacent sarcoplasmic reticulum membrane. As the RyRs open, calcium is released from the sarcoplasmic reticulum into the sarcoplasm (muscle cytosol), which subsequently initiates a cascade of events leading to muscle contraction. Calcium released in the cytosol binds to Troponin C and transmits information via structural changes throughout the actin-

tropomyosin filaments, activating myosin ATPase activity. Myosin converts chemical energy released from ATP into mechanical energy. This mechanical energy is then used to pull the actin filaments along, causing muscle fibers to contract and, thus, generating movement. The sarco-endoplasmic reticulum calcium-ATPase (SERCA) actively pumps calcium towards the sarcoplasmic reticulum. When the calcium returns to basal levels, the force decreases and relaxation occurs.

Muscle is a heterogeneous tissue composed of muscle fibers that differ with respect to their expression of the motor proteins myosin heavy chain (MyHC) isoforms conferring them distinct contractile and metabolic functions[169]. Based on MyHC gene isoform expression, it is possible to distinguish within a single mammalian muscle, type 1, 2A and 2X fibers, in mouse additional fiber type 2B is present. Fibers occur in varying proportions inside a single muscle, it can differ according to species, muscle function, and innervation but also it can reflect dynamic adaptations in response to metabolic demands, to neuromuscular activities or muscle injuries[169]. In addition, each muscle fiber type own different capacities to produce force, different fatigue rates and count on different energy systems in order to function. Type I (slow twitch fiber) and 2A fibers use commonly oxidative metabolism, conversely type 2X and 2B fibers (faster twitch fibers) rely on glycolytic metabolism (Table 1). Some muscles can be enriched with one specific type of muscle fibers, for instance the *soleus* muscle is predominantly composed of slow type I fibers while the *extensor digitorum longus* muscle is mainly composed of fast type IIB fibers[170].

Type of muscle fiber:	Type I	Type IIA	Type IIX	Type IIB
size	small	Large	Intermediate	Intermediate
Coding gene	*Myh7*	*Myh2*	*Myh1*	*Myh4*
Contraction duration	Slow	Moderately fast	Very fast	Very fast (Faster than IIX)
Power produced	Low	Medium	Very high	Very high
Endurance	Fatigue resistant	-/+ Fatigue resistant	Easily fatigued	Easily fatigued
Activity used for	Aerobic (Running a marathon, posture)	Long-term anaerobic (Sprinting, walking)	Short-term anaerobic (Identical to type IIB)	Short-term anaerobic (Short duration high-intensity or powerful movements, *e.g.,* hitting a baseball)
Capillary density	High	Intermediate	Low	Low
Oxidative capacity	High	High	Low	Low
Glycolytic capacity	Low	High	High	High
Mitochondria	Numerous	Moderate	Few	Few

Table 1: *Distinct skeletal muscle fibers compose a mammalian skeletal muscle. This table shows their structural and functional characteristics. (Table adapted from Talbot et al.*[171]*)*

Finally, several components of the skeletal muscle mentioned above can be affected during CC making the skeletal the main target of this syndrome.

B. Impact of CC on skeletal muscle mass

A systematic loss of the skeletal muscle mass displaying distinct metabolic and contractile properties has been reported in various animal models of CC such as in the colon-26 (C26) adenocarcinoma-bearing mice[172,173,174,175,176,177,178] in the *Apc*$^{Min/+}$ mouse model of colorectal cancer[179,180,181,182,183,184] in the Lewis Lung Carcinoma (LLC)-inoculated mouse model[185,186,187] ,

in rats bearing AH-130 hepatocellular carcinoma[178,188,189,190], and finally in the KPC genetically engineered mouse model of pancreatic cancer[191,64] (Figure 7).

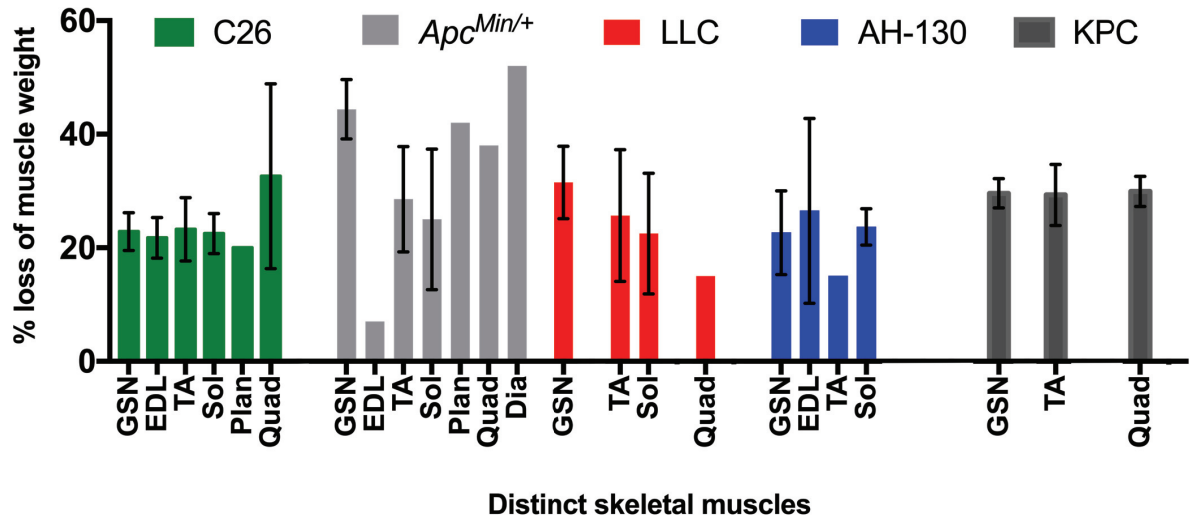

Figure 7: *Skeletal muscle loss proportion in rodent models of CC in comparison to either control or to weight stable tumor-bearing animals. Differences within an animal model of CC can be due to sex specificities (male vs female), age, tumor type or number of cells (cells or solid fragment), tumor growth kinetics, severity of cachexia (mild vs drastic).* ***GSN****: Gastrocnemius,* ***EDL****: Extensor digitorum longus,* ***TA****: Tibialis anterior,* ***Sol****: Soleus,* ***Plant****: Plantaris,* ***Quad****: Quadriceps,* ***Dia****: Diaphragm,* ***C26****: Colon-26 carcinoma tumor-bearing mouse model.* ***Apc$^{Min/+}$*** *mouse model bearing multiple intestinal neoplasia,* ***LLC****: Lewis lung carcinoma-bearing mouse model,* ***AH-130****: Yoshida AH-130 ascites hepatoma-bearing rats,* ***KPC****: PDAC-bearing mouse model.*

Interestingly, the extent of body weight loss, especially evident in the *Apc*$^{Min/+}$ mice, worsens the degree of muscle mass loss[192,193,194,195].

Lean body mass is found lower in cachectic cancer patients compared to non-cachectic cancer patients or healthy individuals according to evaluation of the whole-body composition using either BIA[196,197,134,123,136] or DEXA[198,199,200,201], indicating lower skeletal muscle mass. CT scans have revealed that skeletal muscle atrophy is proportional to the increase of body mass loss[92]. In fact, metastatic colorectal cancer patients experienced a 9% muscle loss when weight loss was between 5-20% and a 25% muscle loss when weight loss was above 20%.

Studies using magnetic resonance imaging to measure the lower limb CSA, found that cachectic cancer patients displayed a reduction in the *quadriceps* muscle area by up to 33% compared to healthy control subjects[136,202,203]. Interestingly there appear to be sex differences[202]. *Quadriceps* muscle CSA was similar in female cachectic patients and weight-stable cancer patients, while *quadriceps* CSA in male cachectic patients was 15% lower compared to the one of male non-cachectic patients. Thus, suggesting that body weight is not the best criterion of CC, at least for women, since skeletal muscle wasting appears to occur

earlier than body weight loss. Similarly, another study using CT-L3 scan reported lower loss of muscle area in females cachectic cancer patients than their counterparts males, with 8% and 13% loss respectively when compared to non-cachectic cancer patients[204] (Figure 8). Further, the mean percentage loss of skeletal muscle area (at the level of the first lumbar vertebra) was the highest (~17%) during the last 3 months of survival in squamous cell lung cancer patients when compared to baseline[205].

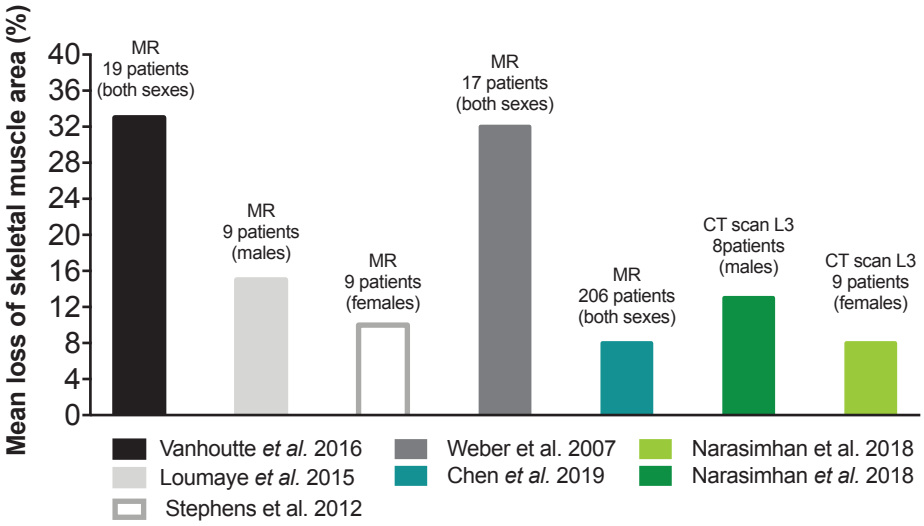

Figure 8: *Proportion of skeletal muscle area loss in cachectic cancer patients relative to either weight stable cancer or healthy individuals across different human studies. Fluctuations among studies are attributable to factors such as age, location and stage of tumor, severity of cachexia, the criterion used to define cachexia, anti-cancer treatment and the method of assessment.**MR**: Magnetic resonance, **CT scan**: Computed tomography.*

Finally, SMI of cachectic cancer patients was also consistently decreased relatively to non-cachectic cancer patients[134,206,196,204,207] (Figure 9).

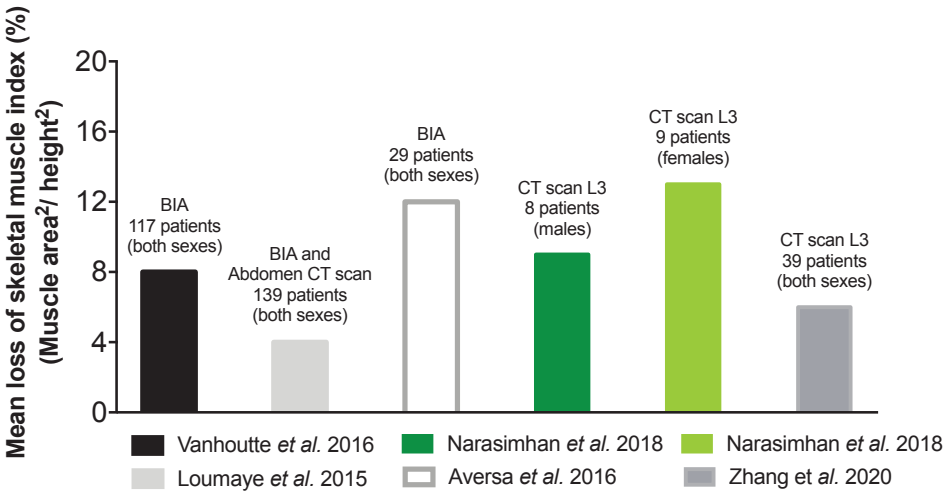

Figure 9: *Proportion of SMI loss in cachectic cancer patients relative to weight stable cancer patients, across different human studies. Fluctuations among studies are attributable to factors such as age, location and stage of tumor, severity of cachexia, the criterion used to define cachexia, anti-cancer treatment and the method of assessment.* ***BIA:*** *Bioelectrical impedance,* ***CT scan:*** *Computed tomography.*

Overall, these findings revealing declines in muscle area and SMI suggest muscle mass loss in cancer cachectic patients.

C. Impact of CC on skeletal muscle fiber size

Experimental models of CC show consistent decrease in muscle fiber CSA[208,209,210,211,178,175,212,213,214,186,180,215,216,217,218,219,220,221,193,222,191,138,223,224,] when compared to their non-cachectic cancer or healthy counterparts. Decreases in the size of muscle fibers expressing type 1, 2A or 2X/B MyHC isoforms occur at similar levels in the *tibialis anterior* and the *diaphragm* muscles. Yet, in the *gastrocnemius* muscle, fibers expressing type 2 MyHC isoform seem to be more prone to atrophy than type I muscle fibers from cancer cachectic animals, suggesting a preferential atrophy of type 2 muscle fibers in the *gastrocnemius* muscle Figure 10).

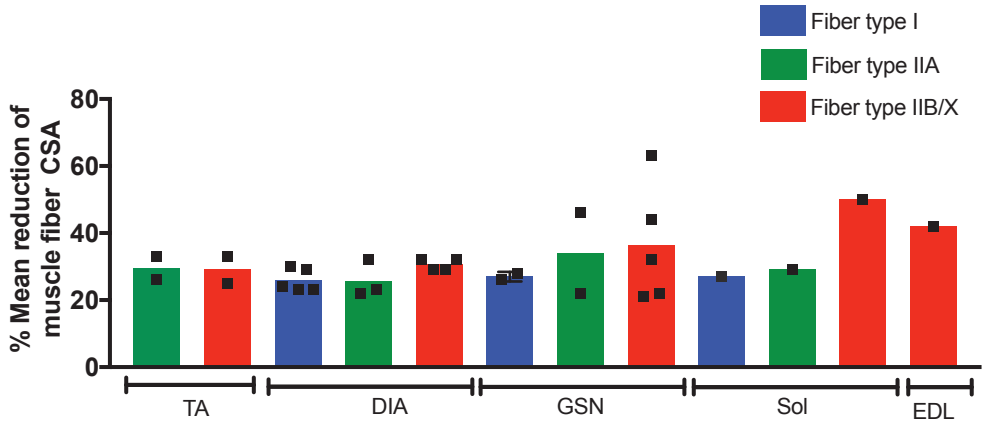

Figure 10: *Percentage of CSA reduction of the different types of muscle fiber for each muscle coming from rodent models of CC in comparison to either control or to weight stable tumor-bearing animals. Differences in the CSA of the different types of muscle fibers within a muscle could be explained by the animal model of CC that was used in the study. Each square represents the result from one study* ***GSN****: Gastrocnemius,* ***EDL****: Extensor digitorum longus,* ***TA****: Tibialis anterior,* ***Sol****: Soleus,* ***DIA****: Diaphragm. Each black square represents one study.*

Cancer patients suffering from cachexia also exhibit muscle atrophy indicated by a decrement in muscle fiber CSA by 25-70% when compared to healthy or non-cachectic cancer subjects[201,136,200,46,207,225].

D. Impact of CC on skeletal muscle typology

In experimental models of CC, data regarding the distribution of muscle fiber types is conflicting. Some studies demonstrated an increase in the percentage of 2A and 2B type fibers and a decline in the proportion of type 1 fibers in the *soleus* muscle of cachectic cancer mice compared with control mice[226,227,180]. These data suggested muscle transitioning toward a faster and higher force production phenotype that might serve as a compensatory mechanism to overcome muscle wasting. On the contrary, other studies did not observe changes in the muscle fiber distribution throughout distinct muscles such as in the *gastrocnemius*[228,184,227,223,224,229,230] *the tibialis anterior*[228,220,231,232] or even the *soleus*[228]. Differences among those studies could be explained by the experimental model of CC that was used and the severity of cachexia.

In general, distribution of type I and II skeletal muscle fibers seems to be constant between patients with CC and healthy subjects[233,203] or weight stable cancer patients[234,46,200]. One study has suggested a shift from slow towards faster contracting muscle fibers, but this was not yet significant[235].

E. Impact of CC on skeletal muscle function

1. Force

Decline in tetanic muscle force of distinct skeletal muscles was observed among several experimental models of CC[236,177,191,139,226,231,176,221,237] (Figure 11) as well as in grip strength[172,174,238,176,220,210,175,239,212,187,232,214,240,241,242,243,215,244,245,246,247,248,249,250,251,252,137,253] when cachectic animals were compared to their control counterparts or to weight stable animals[183]. Even after adjusting muscle tetanic force to body weight[176], muscle fiber CSA[236,183,226,221] or muscle mass[177,236], maximal muscle strength loss still occurs in the cachectic cancer mice, suggesting that decline in muscle force is not completely dependent on muscle mass but can also be due to intrinsic contractile alterations.

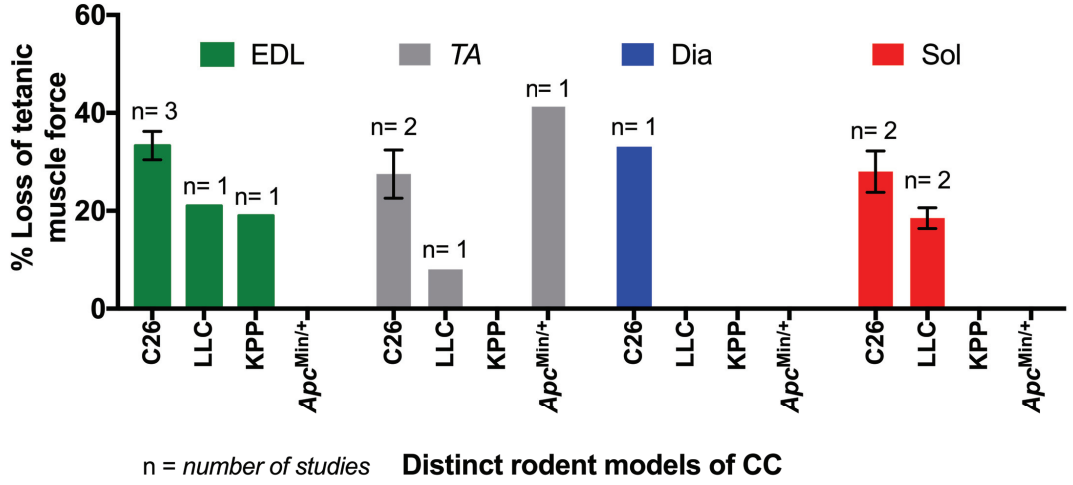

Figure 11: *Loss of tetanic skeletal muscle force in rodent models of CC. The loss of muscle strength is expressed as a percentage loss normalized to the muscle strength of control animals from each study. Differences can be due to age, experimental model, to tumor growth and cachexia severity (mild vs drastic), the distribution of fiber type composition and to experimental conditions. Muscle strength was assessed ex vivo.* ***EDL****: Extensor digitorum longus,* ***TA****: Tibialis anterior,* ***Sol****: Soleus,* ***Dia****: Diaphragm,* ***C26****: Colon-26 carcinoma tumor-bearing mouse model,* ***Apc$^{Min/+}$****: Mouse model bearing multiple intestinal neoplasia,* ***LLC****: Lewis lung carcinoma-bearing mouse model,* ***AH-130****: Yoshida AH-130 ascites hepatoma-bearing rats,* ***KPC****: PDAC-bearing mouse model.*

Patients with CC also showed a reduction in their handgrip strength[134,133,206,123,135,199] (Figure 12) as well as reduction in the absolute isometric strength of the *quadriceps* muscle[201,136,202,200] when compared to healthy volunteers (Figure 13). When normalized to body mass or cross-sectional area (specific force), *quadriceps* muscle strength still remains lower in the cachectic cancer patients[202].

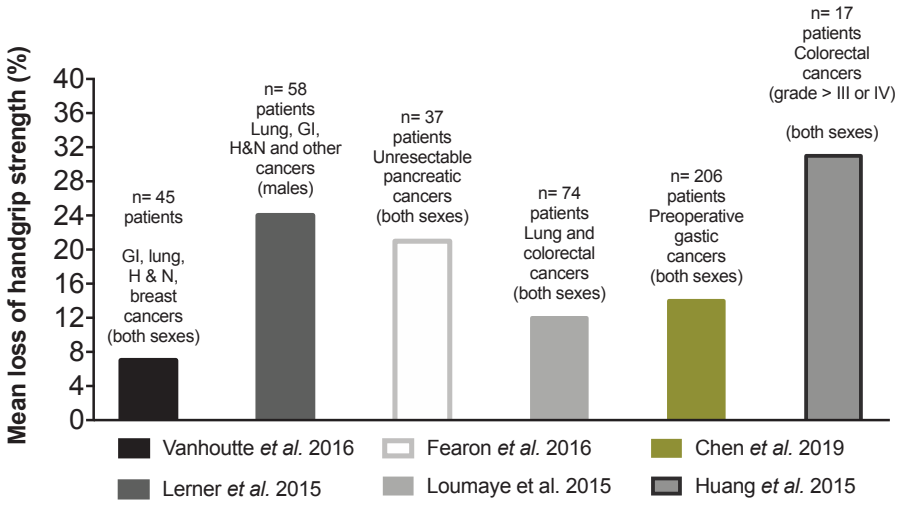

Figure 12: *Proportion of handgrip strength loss in cachectic cancer patients relative to healthy individuals across different human studies. Fluctuations among studies can be explained by factors such as age, gender, primary tumor location and stage, severity of cachexia, metastatic status, anti-cancer treatment modality or strength method. For all studies, grip strength (expressed in kg) was assessed with a hand-held dynamometer several times either from the dominant or non-dominant hand. Muscle strength was defined as the mean of repetitions or as the highest strength measure.* ***GI****: Gastrointestinal,* ***H & N****: head and neck.*

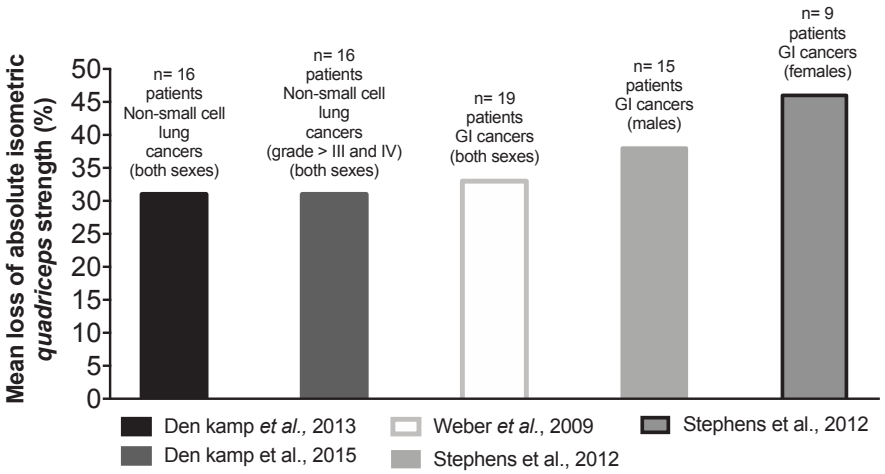

Figure 13: *Proportion of absolute isometric (static) quadriceps strength loss in cachectic cancer patients relative to either weight stable cancer or healthy individuals across different human studies. Values are quite consistent between studies, the small fluctuations can be due to age, gender, primary tumor location and stage, severity of cachexia, metastatic status, and anti-cancer treatment modality. For all studies, the maximum voluntary quadriceps force output (expressed in newtons or in newton meters) was recorded using a dynamometer.****GI****: Gastrointestinal.*

2. Physical activity

Rotarod movement and locomotor activity were reduced in preclinical models of CC[238,193,176,220]. Interestingly some pre-clinical models displayed low volitional physical activity even before body mass loss[193,137,254], reinforcing the notion that skeletal muscle force could be an important parameter to take into consideration for cachexia diagnosis. Moreover, decreased physical activity also occurs in cancer patients[255,200].

Together, these studies demonstrate muscle wasting and weakness as important mediators of CC, however to what extent these two events coordinate with each other to drive CC is still unclear. The aforementioned findings show that loss of muscle mass does not fully account for the decrease in force, and thus CC is probably linked with alterations of muscle intrinsic contractility. Factors needed for coordinated muscle contractile function include neuro-muscular junction integrity, excitation-contraction coupling and calcium handling, sarcomere structure, and energetic metabolism[169].

F. Impact of CC on skeletal muscle NMJ

One study suggested that CC does not affect NMJ integrity in cancer patients showing muscle weakness[256]. Indeed, NMJ morphology and structure were entirely conserved in the *rectus abdominis* muscles of patients with gastrointestinal CC when compared to control subjects or weight-stable cancer patients. Although this study did not rule out the possibility of a possible dysfunction of NMJ even if NMJ structure remains intact. In contrast, another study[257] reported upregulation of denervation markers in cachectic skeletal muscles from both gastrointestinal cancer patients and tumor-bearing mice, suggesting neurological perturbations of the muscle fibers that could contribute to muscle wasting. In this line, it has been recently demonstrated that disruption of NMJ and its subsequent dysfunction promotes muscle wasting in the C26 mouse model, through a mechanism dependent on noggin, a bone morphogenic protein (BMP) inhibitor[258]. In this study, excessive noggin and signs of denervation were also reported in patients suffering from CC. Restoration of BMP signaling in the muscles of tumor-bearing mice prevented muscle wasting and preserved the function of NMJ. Remarkably, type II muscle fibers also showed higher accumulation of denervation

markers suggesting that they might be more prone to wasting related with NMJ degeneration. Therefore, alteration of the crosstalk between muscle fibers and their innervating motor neurons could result in muscle deficiency to generate force.

G. Impact of CC on muscle fiber membrane and intracellular organelles

1. Sarcolemma and sarcomere structure alterations

Mouse models of CC[233,259,207,260,139] and cancer patients with cachexia[259,260] display either muscle membrane or basal lamina abnormalities (Figure 14). In patients with pancreatic cancer, the extent of skeletal muscle membrane disruptions correlated positively with cachexia severity[259]. An increase in the number of damaged[261] and shrunken fibers[225] also occurred in CC patients. Membrane damage could arise from tumor-induced dysregulation of muscular dystrophin glycoprotein complex in both cachectic cancer mice and patients[260].

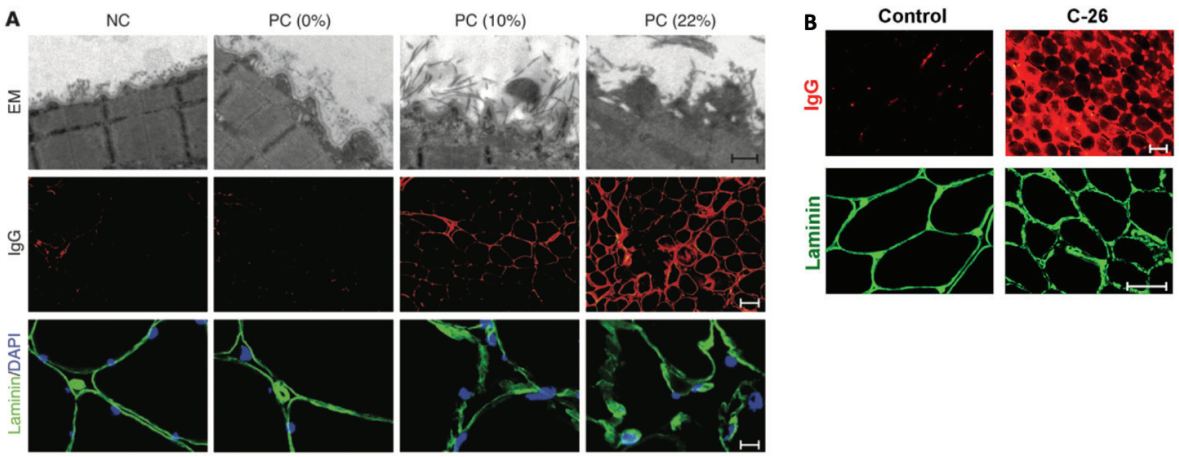

Figure 14: *Alterations of skeletal muscle fiber membrane in muscles from non-cancer individuals (NC) and from pancreatic cancer patients that exhibit varying degrees of body weight loss (A) and from control and C26-tumor bearing mice (B). Electron microscopy photos showing muscle fiber sarcolemma perturbations (A), pronounced accumulation of IgG (A, B), used as a marker of membrane damage and diffuse laminin staining (A, B) are shown (He et al.[259]).*

Disordered structure of the sarcomere was suggested to be a common feature in CC-associated muscle wasting[225,262]. Disruptions of sarcomere structure[139,263,264,265] have been observed in the skeletal muscles from animal models of CC indicated by disorganized myofibrils with increased interstitial spaces between them and comprising less well-defined myofilament proteins. Similarly, cancer patients with cachexia presented randomly oriented myofilaments with sarcomere disruptions in limb muscles[207,233]. Regarding myofilament

content, a case study showed loss of myosin in a patient with small-cell lung cancer cachexia while another study showed no difference in myosin content among a larger diversity of cancers in patients[266]. The latter study although showed reduced myosin-actin cross-bridge formation and kinetics. Further, in some studies, loss of cross-striation pattern was observed in skeletal muscles from cancer patients with cachexia[267,225,268,261].

These structural impairments could impact myofiber contractile performance and therefore attenuate muscle capacity to generate force.

2. Calcium mishandling

The maximal calcium activated force of muscle fibers from C26 mice was reduced[221] suggesting alteration of calcium handling. Vanderveen et al.[183] analyzed the calcium handling gene expression in cachectic cancer *Apc*$^{Min/+}$ mice. Notably, key calcium handling proteins, SERCA1 and RyR1 were found upregulated and the rate of relaxation following tetanic stimulation was reduced suggesting inadequate release and reuptake from the sarcoplasmic reticulum that can lead to calcium leak inside the muscle fiber and alter muscle function. Increased expression of SERCA1 and RyR1 in the *extensor digitorum longus* muscle was also reported in tumor-bearing rats[219]. Lastly, microarray analyses of gene expression performed in muscles of tumor-bearing rats showed downregulation of genes related to intracellular calcium homeostasis and to the excitation-contraction coupling[269]. Most importantly, the authors[269] identified genes that encode for proteins of calcium channels and calcium binding that could lead to excessive calcium amounts in the sarcoplasm.

Calcium deposition was found in skeletal muscles of cachectic pancreatic cancer patients[261]. Calcium overload within myofibers can induce cellular damage and death through activation of calcium-activated proteases[270]. Force response to increasing calcium concentrations of the contractile apparatus was surprisingly increased in skeletal muscle from cachectic cancer patients, which was associated with a transition from slow towards fast MyHC isoform expression[235]. All these findings, both in human and animal studies, suggests calcium disequilibrium that can contribute to uncoupling of muscle fiber excitation-contraction leading to loss of muscle function and mass.

3. Sarcoplasmic reticulum and mitochondrial structural alterations during CC

Sarcoplasmic reticulum and mitochondria relationship has crucial role in the regulation of calcium signaling during excitation-contraction coupling. Calcium in sarcoplasmic reticulum stimulates the generation of mitochondrial ATP to support the increased energy demand during muscle contractions[271]. Few studies performed in cancer patients[268,272] and in tumor-bearing animals[219] with cachexia have reported profound alterations of the sarcoplasmic reticulum in their skeletal muscles.

Research on exploring mitochondrial structural alterations in CC patients are scarce. Two studies[272,207] showed alterations in mitochondria structure in gastrointestinal cancer patients with cachexia compared to weight-stable patients while another one[233] noted no changes in mitochondrial size and shape in cachectic lung cancer patients compared with healthy controls. Therefore, it is still unclear whether human CC presents altered mitochondrial morphology that could lead to mitochondrial network or function deficiency in the skeletal muscle. On the other hand, electron microscopy analysis demonstrated distorted mitochondrial morphology[263,219,243,273,264,265] in experimental models of CC. Furthermore, studies also demonstrated mitochondrial dysfunction in tumor-bearing rodents during CC[264,274,275,276] and even prior to the development of muscle atrophy[277], suggesting that mitochondrial dysfunction could trigger muscle loss of muscle activity as well as exercise intolerance in CC.

IV. Intracellular molecular mechanisms of CC involved in skeletal muscle wasting

The most important component of muscle mass is its protein content. The majority of skeletal muscle is made up of myofibrillar proteins (contractile proteins: myosin, actin and regulatory proteins: tropomyosin, troponins), which account for 65-75% of all muscle proteins[278]. The other 20-30% of all proteins are sarcoplasmic proteins, and mostly consisting of enzymes that are involved in the biochemical reactions occurring in muscle tissue, as for stromal proteins (collagen and elastin), these are present in low content. The balance between the rates of synthesis and degradation of muscle protein pools controls the number of proteins in muscle.

Thus, muscle protein synthesis and degradation mechanisms dynamically work together to determine muscle size. Under basal condition, adult muscle mass stays relatively constant, ensuring that protein synthesis and degradation are kept in balance. Exercise or anabolic hormonal stimulation can promote muscle gains (*i.e.,* hypertrophy) by increasing the rates of protein synthesis and organelles in the cytosol to increase muscle fiber volume. During this process, the levels of muscle contractile protein synthesis is greater than protein degradation, resulting in greater amounts of actin and myosin filaments composing the myofibrils. In contrast muscle atrophy, occurring from a decrease in protein synthesis, an increase in protein degradation, or a combination of both[20], is characterized by loss of proteins and organelles inside the cytoplasm leading to shrinkage of the muscle fiber volume. In CC, skeletal muscle wasting occurs through an imbalance in the rate of protein synthesis and degradation[29,279,280,281,282] leading to the selective destruction of myofibrillar proteins[281,283,234] that form the sarcomeres that provide contractile functions to muscle. Therefore, loss of contractile proteins inevitably impacts muscle strength production[284].

A. Skeletal muscle protein degradation during CC

The most well-known cellular protein degradation system is the Ubiquitin-Proteasome System (UPS)[285], which is in charge of destroying the majority of the misfolded or otherwise dysfunctional cellular proteins[286]. The UPS is composed of ubiquitin and a series of related enzymes, including E1 ubiquitin-activating enzymes, E2 ubiquitin-conjugating enzymes, E3 ubiquitin-protein ligases and proteasomes[287]. In this system, proteins are targeted for degradation by covalent ligation to ubiquitin, a 76 amino acid residue protein[288]. Ubiquitin must first be activated by E1[289] and then transferred to E2[290]. E2 recognizes E3, which then specifically recognizes and binds to specific proteins to form a ubiquitin-protein chain[291]. A proteasome is a large, 26S, multi-catalytic protease that degrades polyubiquitinated proteins to small peptides[292] (Figure 15). Currently, two E3 protein ligases have been proven to be very active in the proteolysis of muscle wasting, namely, MAFbx/atrogin-1 and MuRF1/TRIM63[293]. These muscle-specific ubiquitin ligases (Ub-ligases) have been regarded as molecular markers of proteasome-dependent proteolysis.

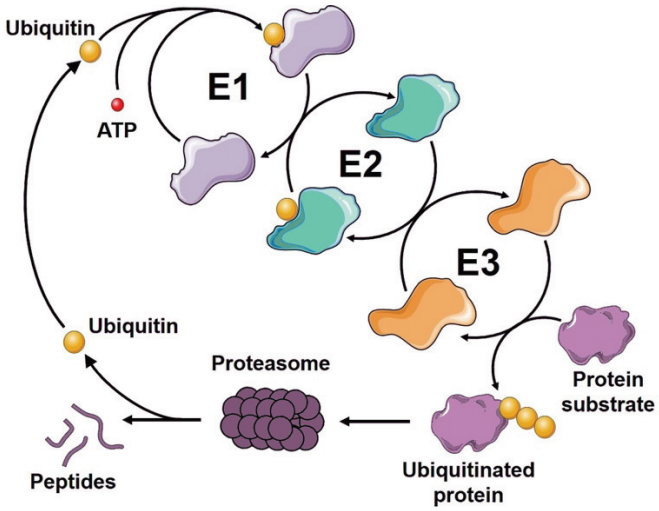

Figure 15: *Overview of the Ubiquitin-Proteasome system (UPS). Ubiquitin activating enzyme E1 signals the UPS for protein degradation through activation of ubiquitin, this leads to a cascade of enzymatic/substrate activity. E2 conjugating enzyme binds to the ubiquitin to form an E2-Ubiquitin conjugate intermediate. E3 such as MuRF1 or Atrogin takes the ubiquitin molecule from the Ubiquitin-E2 intermediate and conjugates the ubiquitin to the target substrate to complete the process. Ubiquitin is removed and the protein is linearized and delivered into the central core of the proteasome, where it is broken down into peptides (Picture taken from lifesensors.com).*

Increase in the mRNA levels of E3 Ub-ligases[294,40,295,296,242,251,192,297,298,299], ubiquitin and proteasome subunits, as well as in the proteasome activity have been reported in animal models of CC[300,301,192,302,303].

Some studies reported no changes in UPS activation or E3 Ub-ligases expression in cachectic cancer patients[304,305,198] while some other studies demonstrated UPS activation above physiological levels in cancer patients prior to[306,307] and during body weight loss[308,306,307]. The extent of UPS activation was suggested to be correlated with tumor stage.

Another way to degrade muscle proteins is autophagy. Autophagy is a physiological process in skeletal muscle that aims at removing misfolded proteins and clearing damaged organelles or at providing substrates under conditions of starvation allowing cells to reutilize their own constituents for energy[309,310]. Autophagy primarily relies on the sequestration of organelles and cytoplasmic fragments into double-membrane vesicles called autophagosomes, which then fuse with lysosomes for destruction. The material is degraded and the degradation products that result are made available for recycling[311]. Only in recent years[312], autophagy has been recognized to be essential for the degradation of damaged or misfolded proteins as well as the selective removal of damaged organelles like peroxisomes or mitochondria (Figure 16). Proteins such as beclin-1, a main upstream regulator of autophagic sequestration[313] and LC3-II[314], an autophagosome formation marker, are established markers of autophagy.

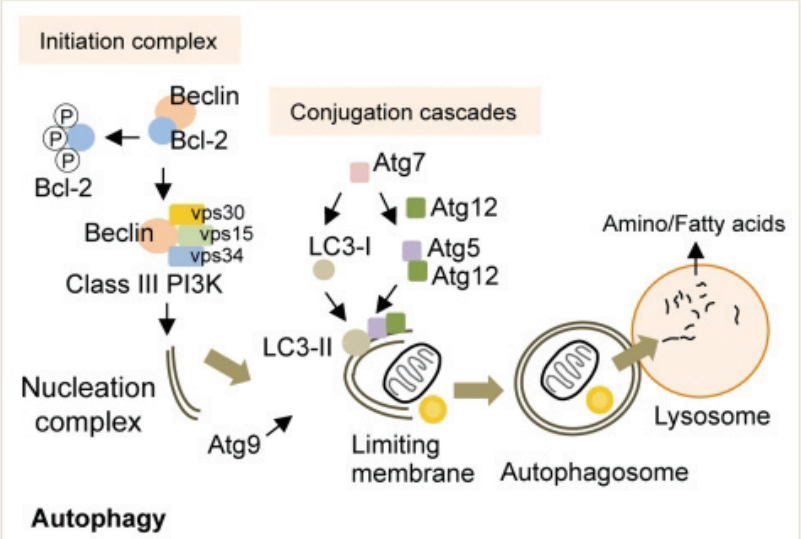

Figure 16: *Induction of autophagy relies on the release of Beclin from Bcl-2, which is then free to generate the Class III PI3K that contributes to the formation of the nucleation complex. The LC3-II and the Atg5-12 conjugation cascades elongate the nucleation complex to generate the limiting membrane. Transmembrane Atg9, delivers additional membranes for limiting membrane formation. As the limiting membrane elongates, it surrounds the cytoplasmic components, including organelle and long-lived proteins, to form the autophagosome. The latter fuses with lysosome, and consequently the trapped elements are degraded by lysosomal hydrolases.* ***Atg:*** *autophagy gene,* ***LC3:*** *light chain-3,* ***PI3K:*** *phosphoinoside 3-kinase,* ***vps:*** *vacuolar protein sorting (Picture taken from Singh et al.*[315]*).*

Results emerging from both experimental models and clinical research in the last years have clearly shown that the autophagic/lysosomal pathway also contributes to generate muscle wasting during CC. Increased mRNA and protein levels of Beclin-1 and LC3-II in the skeletal muscle of tumor-bearing animals indicate induction of autophagy[186,316,317,318,319]. Additionally, it has been observed that autophagy is increased during the later stages of cachexia in *Apc*$^{Min/+}$ mice[192]. In this model, it appears that increased UPS activation is the first cause of protein breakdown during the early stages of cachexia irrespective of autophagy/lysosomal activation. On the contrary, data regarding human studies are conflicting. One study revealed unchanged levels of autophagy markers in the skeletal muscles from CC patients[320], while two studies demonstrated increase activity levels of cathepsin B and L (two lysosomal proteases) as well as increased LC3B-II protein levels[198,196] suggesting induction of autophagy. In contrast to animal models of CC, autophagy induction was suggested to occur in the skeletal muscles from CC patients likely in the absence of UPS activation[201,198]. The considerable UPS activation in experimental models of CC could possibly be due to the rapid development of massive tumor burden that does not resemble human experience[321].

Taking together these data indicates that the proteolytic systems are redirected from their primary function which is to regulate muscle protein balance to instead accelerate degradation of functional proteins and contribute to muscle wasting and weakness.

B. Impact of CC on Skeletal muscle protein synthesis

The most significant role of insulin-like growth factor 1 (IGF-1) signaling is to regulate protein synthesis in skeletal muscle. A range of growth-related stimuli (insulin, amino acids) can be integrated into the IGF-1 signaling via the PI3K/Akt/mTOR pathway to control myofiber size and muscle mass[322] (Figure 17). Under physiological conditions, IGF-1 activates AKT through a PI3K-dependant process, leading to the activation of mTOR and thus resulting in the increased protein synthesis in muscle fibers. IGF-1/PI3K/Akt signaling can also suppress protein degradation. Akt can phosphorylate and inactivate forkhead box O (FoxO) proteins (FoxOs: FoxO1, FoxO3 and FoxO4) by promoting their export from the nucleus to the cytoplasm[323]. FoxO are transcriptional regulators of genes involved in autophagy and UPS-mediated protein turnover[324,325,326], their inhibition prevents the transcription of E3 ubiquitin ligases to process into protein degradation. It is likely that IGF-1 inhibits autophagy via mTOR and FoxO signaling[327,326,328] , but it is yet unknown what role autophagy regulation plays in IGF-1 mediated inhibition of skeletal muscle atrophy.

Several studies have demonstrated suppressed muscle protein synthesis and dysregulation of muscle protein synthesis signaling in animal models of CC[329,330,40,331,273,238,194] and humans[280,332,333] during CC. However, opposing evidence exists showing that muscle protein synthesis is not affected by cancer in patients[334]. The link between the dysregulation of muscle protein synthesis with that of protein degradation during CC is remaining questionable[335,300,]. The literature generally suggests that protein synthesis is decreased in the later stages of cachexia in both animals[194,336] and humans[280,332,337] while a large number of studies showed that protein degradation is predominantly occurring early in muscle depletion with one exception in *Apc*$^{Min/+}$ mice[192]. Cachexia in *Apc*$^{Min/+}$ mice develops over a much longer time of period. Thus, use of different experimental models of CC could be the cause of the inconsistent findings regarding protein synthesis rates during muscle atrophy.

C. Humoral factors as mediators of muscle wasting and weakness

Humoral factors arising from the tumor as well as by the crosstalk between the tumor and the immune system of the host, play a pivotal role in the pathogenesis of CC. Among humoral factors, several pro-inflammatory cytokines and growth factors are potential cachexia mediators. The latter have been shown to impact host physiology by inducing metabolic reprogramming of target tissues and create a chronic negative energy state[29,32]. Pro-inflammatory cytokines and growth factors can signal through their respective cell surface receptors in the muscle fiber and can activate transcription factors which in turn dysregulate muscle protein synthesis and degradation rates, leading to persistent muscle wasting[338,29,339,340,341].

Pro-inflammatory TNF-α cytokine has been reported to have direct catabolic effect on muscle through activation of the nuclear factor-κB (NF-κB) pathway[342]. Activation of NF-κB leads to its translocation to the nucleus where it induces expression of E3 ligases of the UPS[343,344,345]. TNF-α also downregulates the signaling pathways dependent on the IGF-1, reducing muscle anabolic capacity and enhancing the pro-catabolic stimuli[346,347]. Inhibition of NF-κB results in a significant decrease in tumor-induced muscle loss[348]. TWEAK (TNF-related weak inducer of apoptosis), is another potential procachectic cytokine that binds to TNF receptor superfamily member 12A: TNFRSF12A[349,350] and is involved in experimental CC[351].

IL-6 cytokine is secreted by several cell types located within the tumor microenvironment such as stromal cells, tumor-infiltrating immune cells and the tumor cells themselves[352,353,354,355]. The *Apc*$^{Min/+}$ mouse model, the C26-bearing mouse model as well as mice bearing the uterine cancer line, Yomoto, all experience IL-6-dependent loss of skeletal muscle mass[356,357,358,359,360]. Administration of an anti-IL-6 receptor antibody reverses cachexia in cancer patients[361,] and animal models with cachexia[362,363]. Pro-inflammatory cytokine IL-6 binding to its receptor (IL-6R) results in the activation of two main signaling pathways, JAK/STAT3 signaling and the mitogen-activated protein kinase (MAPK/ERK) cascade. STAT3 activates the transcription factor C/EBPδ (CCAAT-enhancer-binding protein d) causing an increased expression of myostatin, which consequently, upregulates E3 ligases of the UPS and increases protein degradation[364,365]. STAT3 activation and expression levels were found increased both in cachectic cancer patients[366] and tumor-bearing animals[367] suggesting activation of IL-6/JAK pathway to be determinant in inducing muscle wasting. Moreover, LIF (leukemia inhibitor

factor), a member of IL-6 cytokine family, has been shown to stimulate the JAK2/STAT3 signaling pathway and to participate in the initiation and progression of skeletal muscle atrophy in the C26 tumor-bearing mice[368,369,370].

IL-1 cytokine can be produced by the tumor cells or by immune cells infiltrating the tumor environment[371]. IL-1 exists in two forms: IL-1α and IL-1β . IL-1β signaling occurs *via* binding with the IL-1 receptor, which associated with IL-1 receptor-associated kinase that activates NF-κB[372,373] which enhances muscle protein degradation. Systemic IL-1β increased levels are often associated with upregulation of muscle catabolism components[374,375,376]. Interestingly, studies have suggested that inflammation in the central nervous system can trigger breakdown of proteins in the skeletal muscle[377,378]. It was suggested that high levels of IL-1β cytokine in the central nervous system of LLC tumor bearing mice can evoke a catabolic program in skeletal muscle resulting in atrophy[374].

The transforming growth factor β (TGF-β) pathways plays an important role in cell differentiation and inflammation[379]. TGF-β has been shown to mediate cachexia in cancer patients and tumor-bearing models[298,380] and is a blood biomarker of cachexia in cancer patients[381]. Several members of the TGF-β superfamily of growth factors have also been described as negative regulators of muscle mass, including myostatin[382] and Activin A[383] cytokines. Binding of myostatin and Activin A ligands to the Activin receptor type-2B (ActRIIB), a high affinity receptor[384,385,386] on the muscle cell membrane results in the activation of type-1 activin receptor serine kinases which then phosphorylate SMAD2/3[387,388] , which together with the common mediator, SMAD4, translocate to the nucleus. Activation of SMAD signaling, after binding of Activin A or myostatin regulates transcriptional responses leading to reduction in Akt/mTORC1 pathway[389,390,391] and activation of specific E3 Ub-ligases that facilitate the degradation of myofibrillar proteins[392,172,393]. Activin A is involved in many physiologic functions, including embryogenesis, cell growth, differentiation and the immune response[394]. Cachexia in tumor-bearing mice, is potentially triggered by Activin A *via* IL-6 signaling enhancement[395]. Increased Activin A circulating amounts are observed in CC patients which might participate in the development of CC[396,397,206]. In addition, skeletal muscle strength loss was positively correlated with Activin A concentrations, suggesting a role of Activin A in the decreased muscle function of CC patients[206]. Myostatin is predominantly secreted from skeletal muscle cells[398] and has a key role in limiting skeletal muscle growth. The loss of myostatin function in animals and humans which carry null mutations in myostatin gene, leads

to dramatic increase in muscle mass and size[399,400,]. In contrast, myostatin overexpression has been shown to contribute to muscle atrophy during a variety of illnesses, including chronic obstructive pulmonary disease (COPD) and chronic heart failure[401]. Myostatin expression is found to be upregulated in the muscle of animals with tumor-induced cachexia[172,402]. Importantly inhibition of myostatin expression or activity using either genetic[403] or pharmacological approaches[404,209,405,231,172] respectively, prevents or reverse muscle wasting in preclinical models of CC, indicating that myostatin is a potent factor in the wasting process during CC. As regards cancer patients with cachexia, a study reported paradoxically a decrease in myostatin plasma concentrations[206]. However, the authors measured total myostatin concentrations and not myostatin expression specifically in the muscles of these cancer patients, as it was done with the different animal models of CC described above. The authors support that myostatin might not have an endocrine activity but might act locally in the muscle level. Further, Activin A and myostatin are secreted *in vitro* by a large number of human tumor cell lines[172,318]. Finally, Waning et al.[406] showed that release of TGF-β from the bones, as consequence of metastasis-induced bone destruction, up-regulates NADPH oxidase 4 leading to oxidation of skeletal muscle proteins involved in muscle contraction such as RyR1. Hence, ligands of TGF-β family could signal to alter calcium homeostasis, leading to dysfunction of the sarcomeres and to muscle weakness.

D. Oxidative stress as mediator of muscle wasting and weakness

Oxidative stress arises from an imbalance in the increased production of reactive oxygen species (ROS) and nitrogen species (RNS) and those normally neutralized by the activity of the intracellular antioxidant systems[407,408,409]. ROS produce modifications to proteins which frequently results in protein loss of function or enhanced degradation of the oxidized proteins[410]. High levels of ROS and greater oxidative protein and lipid damage[411,223,412] in association with high rates of protein turnover[411,413,233] have all been linked to muscle wasting in cancer patients. Mouse models of CC also exhibit oxidative stress in conjunction with increased activity of muscle catabolic pathways[232,414,415,416]. Further, association between an increase in ROS and loss of muscle mass has been established in cancer cachectic animals[412,414]. Antioxidant treatment was demonstrated to attenuate muscle atrophy in CC by suppression ROS generation[417]. Increase in the amounts of IL-1, IL-6 and TNF-α or TGF-β can

also contribute to increase oxidative damage[357,418,419,420,421,422,406,373] likely *via* activation of NAD(P)H oxidases[422,406]. It was suggested that pathways involved in skeletal muscle proteolysis could accelerate muscle atrophy under oxidative stress. Oxidative stress could promote calcium overload and stimulate calcium-activated proteases such as calpains[423,424,425]. Further oxidative stress could activate the autophagy-lysosomal pathway[426] or overexpress muscle specific E3 Ub-ligases in muscle which subsequently stimulate the proteasome system[427,422]. Increase of ROS levels in the skeletal muscle from CC subjects can also rely in antineoplastic treatments[428,429,430] or can be generated as by-products of mitochondrial altered oxidative phosphorylation[431,421]. Mitochondria plays a major role in redox homeostasis of skeletal muscle[432]. In addition to impinge on muscle energy production, altered or damaged mitochondria can also favor the onset of oxidative stress, since they may be both act as a source of ROS and be a target of the latter[433,434,435,436]. In tumor-bearing mice with cachexia, muscle mitochondria exhibit reduced oxidative capacities that could trigger oxidative stress[437,264].

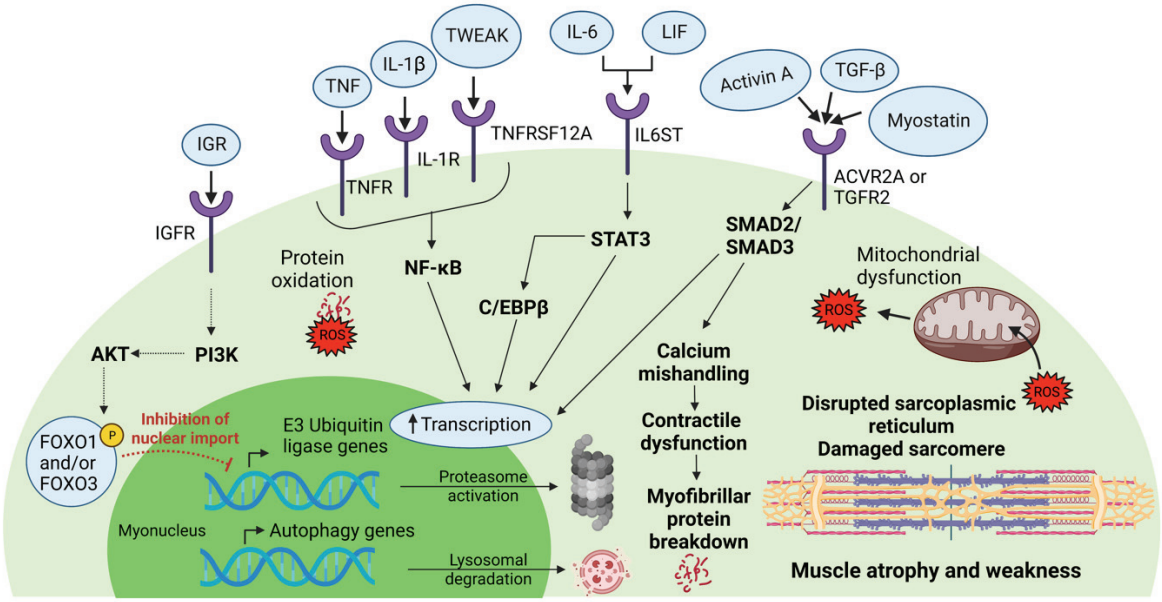

Figure 17: *Muscle fiber intracellular mechanisms resulting in muscle wasting and weakness. Immune and tumor cells produce and secrete multiple proinflammatory cytokines and growth factors. The humoral factors signal through their respective cell surface receptors at the muscle fiber to dysregulate signaling pathways that maintain the protein synthesis and degradation balance. Consequently, altered signaling pathway leads to increased transcriptional levels of genes involved in the proteolytic systems or to generation of reactive oxygen species (ROS) that damage proteins. Muscle weakness can also be mediated through dysfunction of intracellular components of the muscle fiber such as mitochondria or the sarcoplasmic reticulum. (Figure adapted from Baracos et al.[32]).*

So far regulation of multifactorial mechanisms that drive muscle wasting and weakness are considered to reside within the muscle fiber. Nevertheless, over recent years emerging literature suggests that muscle stem cells and their microenvironment, surrounding the muscle fibers, could also play an important role in CC.

V. Impact of CC on the extracellular environment of skeletal muscle

A. Satellite cells (SCs), the stem cells of skeletal muscle

Muscle fibers are surrounded by a population of committed myogenic stem cells, referred to as satellite cells (SCs). Based on electron microscopic analysis, SCs are located between the myofiber sarcolemma and basal lamina and are not easily distinguished from myonuclei[438] (Figure 18). In skeletal muscles from young perinatal mice which undergo muscle growth rapidly, SC nuclei represents approximately one-third of total muscle nuclei, but their proportion is reduced to below 10% in healthy adults[439,440]. SCs are required for muscle homeostasis, postnatal growth, regeneration[441,442,443] and to adaptation to overload or exercise[444,445]. Deregulation of SC function or number leads to a failure in muscle postnatal growth and muscle atrophy[446,447,448].

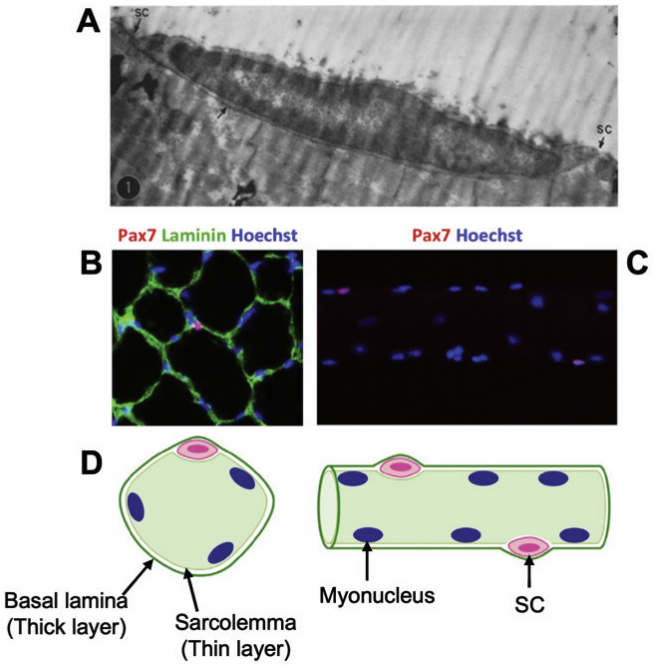

Figure 18: *A) Longitudinal view of SC close to a muscle fiber taken by electron microscopy. B) Muscle cross-sectional photo showing SC in red (stained for Pax7 marker) and the basal lamina in green (stained for laminin marker). C) Single muscle fiber showing SC in red. Nuclei or myonuclei are in blue (Hoechst marker). D) Schematic representations of cross-sectional and a longitudinal view of muscle fiber. (Adapted from Le Grand et al.[449]).*

1. Role of SCs in muscle homeostasis/regeneration

In uninjured muscle under physiological conditions, SCs are maintained in a cell-cycle-arrested state, called quiescence and therefore are transcriptionally inactive[450]. However, when muscle fibers become damaged following injury, the muscle fibers require the skills of SCs to be fixed or replaced by new muscle fibers[442]. In response to injury, SC exit dormancy, become activated and proliferate to produce muscle precursor cells which are called myoblasts[441]. These myoblasts commit to the myogenic lineage and differentiate by a variety of growth factors and mitogenic stimuli such as IGF-1, TGF-β and fibroblast growth factor[451,452]. SC differentiation can involve either fusion with each other to form *de novo* skeletal muscle fibers or fuse to an existing muscle fiber donating their nucleus to the fiber (*i.e.,* myonuclear accretion) to allow muscle fiber regeneration[453,454,455]. The peak of proliferating myoblasts tends to occur 3 days after cardiotoxin-induced muscle injury in healthy mice[456]. Nascent muscle fibers, called myotubes resulting from myoblast fusion take place 4 days after injury while growth of these myotubes can last until 10 days following injury[456]. The progression of the SC across the myogenic program is controlled by particular gene expression of paired box transcription factor 7 (Pax7) and of the myogenic regulatory factors (MRFs) in a time-ordered

fashion[447,457,458] (Figure 19). SCs express nuclear transcription factor Pax7, a well-established and exclusive marker of SCs, which is associated with SC quiescence[459] and required for SC specification and maintenance[447]. Further, Pax7 plays a crucial role in maintaining and regulating the expansion and differentiation of SCs during both neonatal and adult myogenesis[460,447,461,462,463]. Ablation of $Pax7^{+}$ SCs in the muscle leads to failure of muscle regenerative myogenesis[464,465,442] confirming that SCs are indispensable in muscle regeneration.

MRFs are important group of muscle-specific proteins which are only expressed in myogenic lineage-committed cells and comprise myogenic factor 5 (Myf5), myogenic differentiation (MyoD), myogenic regulatory factor 4 (MRF4) and myogenin. During the early phase of myogenic commitment, SC activation occurs by increased expression of My5f followed by the concomitant expression of MyoD[466,455,467,468,469]. After proliferation, differentiation of myoblasts, referred to as myocytes, involves down-regulation of Pax7[470,461] and induction of MRF4, myogenin and embryonic myosin heavy chain (eMyHC) expression, the latter occurring at late differentiation[471,472,473,474]. By contrast, some myoblasts retain Pax7 expression following proliferation and exit terminal differentiation to return back in quiescence to replenish the SC pool[475,463,476]. This process allows to maintain homeostatic numbers of SCs over several rounds of injury and regeneration. Both the regulation and disruption of SCs number, activation, proliferation and differentiation potentials have been widely examined for many years using numerous *in vivo* and *in vitro* animal models. Analyses have shown that Pax7 and myogenin expressions are mutually exclusive during differentiation[461]. Pax7 overexpression prevents myogenin induction, downregulates MyoD and results in inhibition of myogenesis in healthy conditions. On the other hand, muscles depleted for myogenin (*myog*$^{-/-}$) from adult zebrafish show reduced muscle fiber growth and nuclear accretion together with increased number of SCs[477].

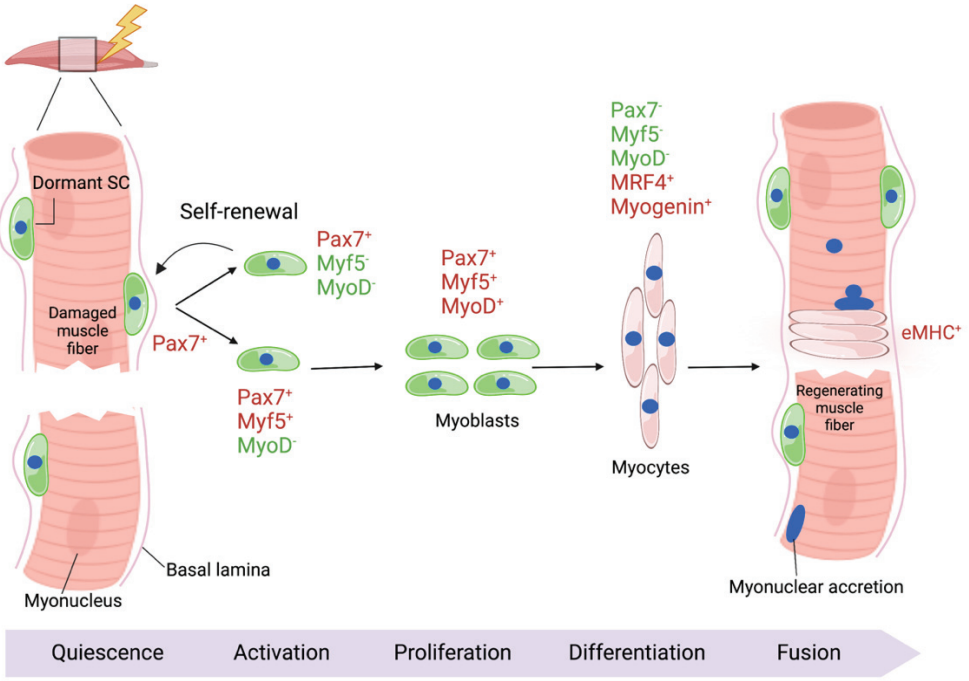

***Figure 19**: Scheme illustrating myogenesis: In healthy adult muscle, SCs remain in a quiescent, non-proliferative state and are characterized by Pax7 expression. Following injury, while Pax7 expression is reduced progressively, a genetic cascade including activation of the muscle-specific genes Myf5, MyoD, MRF4 and Myogenin tightly drive each step of SC proliferation, differentiation and fusion within the damaged muscle fiber to sustain muscle regeneration. Regenerating muscle fibers can be identified by eMyHC expression Activated SC can maintain Pax7 expression in order to return back to quiescence and supply the SC pool for future muscle regeneration.*

All together point out the crucial role of Pax7 and MRFs stepwise expression in regulating the expansion and differentiation of SC while acting as coordinators of muscle regeneration and homeostasis throughout life.

2. Role of SCs in exercise/overload-induced adaptations of skeletal muscle

The function of SCs in muscle regeneration has been relatively well investigated, yet SCs have been also suggested by several studies to support adult skeletal fiber plasticity in response to mechanical loading, such as during resistance training[478,479,480,481,482,483]; Depending on the stimulus[484] and on maturational age[481,485], muscle contractions during exercise could trigger SC proliferation, differentiation and fusion[486,487,488,489] with the pre-existing myofibers to provide them with new myonuclei (*i.*e., myonuclear accretion). Myonuclear accretion was demonstrated to depend entirely on SCs[490,491]. Fusion of SCs with the muscle fiber may provide new nuclei aiming to facilitate enhanced transcription of contractile proteins required for muscle growth[479], and maintenance of a consistent myonuclear domain may also be achieved by adding new nuclei to the myofiber[492]. It seems that myonuclear accretion occurs early

during training programs and precedes the increase in skeletal muscle size[492,478] suggesting early requirement of myonuclear accretion in hypertrophy. Upon increased load, blunting of SC fusion results in exercise intolerance and fibrosis[478,479] and to compromised muscle hypertrophy[478,479,493,480], indicating that myonuclei increase by SC is required for efficient muscle hypertrophy. Serum response transcription factor (Srf), a master regulator of F-actin scaffold, was identified as a master regulator of SC fusion during overload-induced hypertrophy[480]. Srf functions to convert the contractile forces delivered within myofibers into paracrine signals such as IL-6, cyclooxygenase-2 and IL-4, which in turn modulate SC fusion to promote muscle growth[493]. Noviello et al.[494] have recently unveiled RhoA GTPase protein, a regulator of Sfr and produced by overloaded myofibers, to be required for hypertrophy by regulating SC recruitment and fusion to the growing myofibers. In response to increased contractile activity, Rhoa is required to build a permissive SC microenvironment for muscle growth and for SC fusion through ECM remodeling and macrophage recruitment, by controlling the expression of ECM regulators *Mmp9/Mmp13/Adam8* and of macrophage chemo-attractants *Ccl3/Cx3c11.* Collectively these results suggest that increased contractile activity can improve SC fate to promote hypertrophy.

So far, the role that SCs play in muscle overload hypertrophy has been demonstrated using non-physiological models of hypertrophy such as synergist ablation- or tenotomy-induced muscle overload models[495,496,478]. The extent of muscle injury generated by these invasive models would trigger muscle regeneration. Thus, it is still unclear to what extent overload alone regulates SC activation/proliferation/fusion, independently of the added effects of an ongoing muscle regeneration. In addition, models of muscle hypertrophy are not always appropriate to study SC-mediated myonuclear accretion due to excessive and rapid increase in muscle mass for some models, far exceeding that accomplished by humans in resistance training[495,497,484] . Overall, the use of non-damaging models of muscle hypertrophy would allow to improve our understanding of the role of SCs in the regulation of muscle mass.

3. Role of SCs during CC

In the last decade, there is a growing interest from researchers in trying to understand the effect of CC on SC function, which may have a direct impact on the reduced skeletal muscle function and mass[498,174,259,499]. Deficits in the capacity for myogenesis, required for a

successful muscle regeneration, have been reported in skeletal muscle from preclinical models of cachexia and cancer patients, and implicate impairment of SCs fate[174,259,173].

Skeletal muscles from distinct mouse models of CC[173,174,259,187,500,208] as well as from cancer cachectic patients[259,501] display increased $Pax7^+$ cells, Pax7 protein or Pax7 mRNA levels. In the C26 tumor-bearing mouse model, Pax7 protein expression was induced prior to muscle atrophy and steadily increased during CC[259]. Upregulation of Pax7 protein was associated with increased numbers of proliferating SC ($Pax7^+BrdU^+$) that were tightly associated with cachectic muscle fibers of both tumor bearing animals at an early stage of cachexia development and in CC patients[259]. These findings raise the possibility that activated myoblasts may accumulate during CC due to either enhanced proliferation or impaired differentiation or both. Indeed, reduced myogenin mRNA and protein expressions were observed in both animal models of CC[174,259] and CC patients[501] suggesting impairment of myogenic differentiation. Oppositely, one study[500] found increased myogenin protein levels in tumor-bearing animals, such increase could rather indicate ongoing muscle regeneration under cachectic conditions. The difference between studies could be explained by the severity of CC in the experimental model, as well as by the genetic background and the age at which mice were scarified. He et al.[259] was the first to demonstrate that muscle wasting in CC was mediated by deregulation of Pax7 expression. The team showed that overexpression of Pax7 results in inhibition of myogenesis by negatively acting on MyoD and myogenin that in turn restricts myoblast fusion to tumor-induced damaged myofibers.

Further several studies have reported muscle membrane alterations in both tumor-bearing animals and CC patients[233,207,261,259,208,260,139,502,503,316]. He et al.[259] suggested that tumor circulating factors could trigger muscle damage and in turn activation of SCs. Indeed, cachexia severity positively correlated with the extent of muscle membrane damage and Pax7 protein expression in patients and mice with CC suggesting that the extent of tumor-induced muscle damage correlates with SC expansion. On this point Inaba et al.[504] failed to show a significant increase in SC numbers from muscles of C26 mice and did not report ongoing muscle membrane damage, further strengthening the notion that muscle damage could be related to SC activation. The absence of significance of an increase in SC number could also be due to the fact that *Inaba et al.* used a different marker, here M-cadherin, that is maybe not as specific as Pax7 to properly stain SCs. A greater fragility of the skeletal muscle to micro-lesions and injuries in the cachectic muscle, that could derive from circulating tumor factors under

physiological state is plausible and could lead to events of continuous degeneration/regeneration, thus triggering repeatedly activation of SCs. Occurrence of continuous episodes of regeneration in cachectic skeletal muscles is supported by the observation that skeletal muscle of cachectic cancer patients[261,505,316,506] and of CC murine models[180,223,224,229,230] displays a higher number of muscle fibers with centralized nuclei, indicating the presence of regenerating muscle fibers under physiological conditions.

Some studies went further and examine the ability for muscle regeneration of cachectic tumor-bearing mice in response to injury. Muscle damage was induced by either exposing cachectic mice to cardiotoxin[504] or freeze-injury[173] or using tumor-bearing *mdx* mouse model of Duchenne muscular dystrophy[259], whose muscles undergo repeated cycles of acute degeneration and regeneration, after tumor implantation. Regeneration was assessed at similar time-points in the following studies. Post-injured muscles from the distinct tumor-bearing cachectic animals exhibited severe deficit in regeneration, as indicated by a profound reduction in newly generated muscle fibers marked by the presence of centrally located nuclei[259,173] and eMyHC[259,504] and by persistence of damaged/necrotic muscle fibers associated with inflammation[259,504,173] when compared to healthy controls or to tumor-bearing mice without cachexia. CC muscles displayed lower number of regenerating muscle fibers post-injury over time[173] further suggesting progressive blockade in muscle regeneration during CC. Transplantation with Tomato$^+$ SC into freeze-injured muscles from tumor-bearing mice was performed to assess SC fusion within the damaged muscle fibers following injury[259]. One week after, fewer Tomato$^+$ muscle fibers were observed in the tumor-bearing mice compared to controls suggesting that muscle regeneration delay is due to SC fusion defect in CC following acute injury. Moreover, Costamagna et al.[500] showed persistent expression of eMyHC protein expression in muscles of tumor-bearing cachectic mice after 10 days from cardiotoxin-induced muscle injury compared to control mice, indicating additionally a delay in muscle regeneration. A possible explanation regarding the differences between the latter and the previous studies could be the time point of muscle regeneration assessment. Yet, considering muscle regeneration in a unphysiological context by inducing damage with myonecrotic agents is not representative of what happens in muscles during CC.

Nevertheless, all together suggest that an accumulation of unresolved or delayed episodes of muscle repair in the presence of tumor could enhance the loss of skeletal muscle mass and function during CC. Different studies wanted to assess the intrinsic regenerative ability of SC

from cachectic muscles of tumor-bearing mice in the absence of tumor. Isolated SC from muscles of cachectic C26 tumor-bearing mice exhibit normal[504] or even higher[500] proliferation rates compared to their control counterparts *in vitro*. Likewise, SC extracted from muscles of cachectic C26 tumor-bearing mice were able to differentiate and fuse equally[500,504] or even more[259] than their control counterparts, suggesting that SC retain their myogenic capacities when they are no longer under the influence of the cachectic SC microenvironment. However, these studies assessed SC myogenic potential in relatively distinct culturing conditions, the purity of myoblasts culture following isolation and the initial density in which myoblasts were seeded for each experiment were not specified among experimental conditions. Thus, lack of technical accuracy between these studies makes the results questionable.

Studies have gone further and investigated potential signaling pathways that might drive SC defect in myogenesis during CC[259,507,500,508]. Importantly, NF-κB aberrant activation within SC during CC was shown to lead directly to sustained Pax7 protein expression[259]. Further, Pax7 protein accumulation in SCs from cachectic tumor-bearing mice was prevented by systemic administration of a MEK-dependent signaling inhibitor[174] or by IL4 cytokine[500], suggesting that both IL-4 and ERK/MAPK signaling pathways within the muscle microenvironment indirectly regulate Pax7 expression in SC during CC. Addition of Wnt7a protein, *in vitro,* reversed the impairment of SCs differentiation caused by cancer-induced factors, suggesting also an involvement of Wnt7a-mediated AKT/mTOR anabolic pathway in SC regulation during CC[508]. A mathematical modeling performed in C26 tumor-bearing mice has recently predicted that blocking the myostatin/activin A pathway could alleviate cancer-induced muscle loss by restoring the activation and proliferation of the SC with a functional differentiation program[509,510] , although this was not experimentally demonstrated. Finally preclinical studies have demonstrated that ZIP14[242], a metal-ion transporter involved in zinc homeostasis, and twist1[251], a transcription factor which regulates activin/myostatin signaling, are overexpressed in SCs of tumor-bearing animals and lead to muscle wasting. Consistently, overexpression of ZIP14 in C2C12 myoblasts blocks differentiation in the presence of zinc, suggesting a role of cellular zinc homeostasis in SC fate during CC. Taken together these data suggests multiple extracellular and intracellular pathways that can interfere with SC function in CC. Hence reinforcing the notion that SC defect might not simply be a consequence, but a contributing factor for the wasting process.

In the interstitial space between the muscle fibers, SCs are surrounded by an environment that defines the ''niche'' of these resident stem cells and which is a complex network of structural proteins, blood arteries, and nerves that support the muscle's main function of producing force for movement. In addition to these components, the SC niche houses a variety of mononuclear cell types such as endothelial cells (ECs), fibro/adipogenic progenitors (FAPs), and foremost, immune cells such as macrophages and neutrophils. The composition of the SC niche plays a crucial role in ensuring the maintenance, activation and functions of SC[511,512,513,514,515]. Under homeostatic conditions, the SC is relatively static; but after injury, the niche undergoes dynamic remodeling. Activity of immune cells, FAPs and ECs that is tightly coordinated regulates SC proliferation, differentiation and fusion during the regenerative response by interacting directly together through cell-to-cell interactions, by releasing growth factors into the milieu, or by remodeling the extracellular matrix (ECM)[515,516,514]. Evidence from mouse models of CC and cancer patients reveal alterations in the SC niche composition that could affect SC fate through impairment of interactions between the SC and the other cell types and therefore perturbing muscle homeostasis during CC (Figure 20).

B. Immune cells in the SC niche

1. Role of immune cells in muscle homeostasis/regeneration

In healthy condition, very few immune cells reside inside the SC niche. On the other hand, upon acute muscle injury multiple immune cells such as neutrophils, monocytes, eosinophils and lymphocytes are recruited and engaged to effectively regenerate muscle tissue. Muscle injury causes release of molecules containing damage-associated molecular patterns (DAMPs) that recruit immune cells to the site of injury[517] .Within the first two hours, the first to invade the damaged muscle are neutrophils, expressing Ly6G and high levels of CD11b, their numbers are peaking approximately 24h following injury and rapidly decline afterwards[518,519]. Neutrophils prepare the proinflammatory response together with resident macrophages and $CD8^{+}$T cells by releasing cytokines and chemokines, especially CCL2 (CC-chemokine ligand 2) and CXCL1 (CXC-chemokine ligand 1) to promote recruitment of blood monocytes through the CCL2-CCR2 axis[520,521,522]. Infiltrated monocytes secrete specialized pro-resolving mediators such as annexins in order to induce neutrophil apoptosis and activate monocyte phagocytosis[523]. This consists to monocyte transformation into inflammatory macrophages

expressing high levels of Ly6C. Proinflammatory macrophages promote the expansion of SCs by stimulating their proliferation through the delivery of soluble factors and metabolites, among which IL-6, TNF-α, VEGF, IGF1, IL1β, IL13, NAMPT and glutamine[524,525,526,527,528,529]. Proinflammatory macrophages also control the number of FAPs by triggering their apoptosis through TNFα production[530]. The proinflammatory phase is usually short (2-3 days) and ends with the shift towards the acquisition of anti-inflammatory phenotype by macrophages, characterized by low expression of Ly6C[531,532,533]. A major role of macrophage is efferocytosis, which consists in the phagocytosis of dead cells and muscle fiber debris. This process resolves inflammation by the modification of the macrophage inflammatory status. Engulfment of dead myoblasts inhibits TNFα secretion and induces that of anti-inflammatory effectors such as TGF-β and IL-10[534,535,536,537,538,539]. The macrophage shift is characterized by metabolic changes, notably from a glycolytic to oxidative and glutamine metabolism[540,523]. Perturbation in the switch of macrophage/monocytes hampers skeletal muscle regeneration[541]. Anti-inflammatory macrophages exert a series of functions while dampening the inflammatory response. They stimulate terminal myogenic differentiation and fusion of SC via the secretion of factors (IGF-1, TGF-β, GDF3…)[536,537,525,539]. Moreover, anti-inflammatory macrophages also promote angiogenesis[542] and regulate FAPs functions[530,543]. Further, they were shown to stimulate fibroblastic cells for ECM remodeling and secrete themselves ECM components (*e.g.,* proteoglycans, matricellular proteins and assembly proteins)[531,544,545]. Depletion of macrophages is associated with the development of severe fibrosis[546,547]. The early phase of muscle regeneration is also associated with rapid accumulation of eosinophils[548]. Eosinophils secrete IL-4 to enhance the regenerative ability of FAPs[549]. Activation of IL-4/IL-13 signaling within FAPs control their functions and fate by promoting their proliferation while blocking them from differentiating into adipocytes and simultaneously helps them support SC proliferation[549].

2. Role of immune cells during CC

Few studies exist and have provided conflicting results when assessing the content of immune cells inside the skeletal muscles during CC.

Regarding experimental model of CC, one study[260] reported no statistically significant differences in the number of lymphocytes and macrophages between control and C26 tumor-

bearing, although quantified data are not shown in the paper. Similarly, Costamagna et al.[500] detected no differences of F4/80 protein expression in the muscles of C26 mice suggesting no changes in the whole macrophage content while they report a tendency of decreased CD206 protein expression, which could depict smaller proportion of anti-inflammatory macrophages. In the latter study, administration of IL-4 cytokine, a potent stimulator of anti-inflammatory macrophage[550,551], in C26-bearing cachectic mice increased muscle CD206 expression which was associated with increased muscle mass, suggesting that immunosuppression of the muscular cachectic micro-environment could limit muscle wasting. However, IL-4 treatment in the C26 mice also resulted in increased tumor mass due to greater accumulation of inflammatory cells surrounding the tumor necrotic areas, indicating a change in tumor inflammatory status that could in turn affect inflammation of skeletal muscles. In contrast to these studies that have not find statistical differences in total amount of muscle macrophages during CC, one study[552] reported a decline in macrophages at late-stage cachexia close to survival limit in C26-bearing animals as well as a tendency of decrease in $CD8^+$ and $CD3^+$ lymphocytes analyzed by flow cytometry. However, here the authors used esterase histochemistry for macrophage detection which is not a specific method to identify macrophages[553,554].

Two studies have assessed the recruitment of immune cells in the cachectic skeletal muscles of tumor bearing animals in response to muscle injury. Using histological and FACS quantitative analysis, Inaba et al.[504] have demonstrated reduced numbers of infiltrating neutrophils and $F4/80^+$ macrophages in the *tibialis anterior* muscle from C26 mice compared to weight-stable cancer mice, 4 days following cardiotoxin-induced injury. In this study, the exceptional drop in SCs numbers that was observed following injury could be explained by the reduction in neutrophil infiltration to activate the regeneration process. On the other hand, Colleti et al.[173] suggested higher burden of recruited macrophages from histological sections within regenerative areas in the *tibialis anterior* muscle from C26 mice, peaking at 8 days following freeze-injury, when compared to control mice. Although, here again the authors used esterase staining to highlight the presence of macrophages in the damaged muscles and that without showing any quantification. These two studies suggest a defect in macrophage recruitment and a delay to progress through muscle regeneration in CC muscles following injury. Beside the difference regarding the time point of macrophage assessment and the method used in these two studies, the conflicting results could also be explained by the type

of muscle-injury induced, the stage of cachexia, the sex and the genetic background of mice, which were different between studies.

In human cancer patients, findings are more consistent. Judge et al.[261] detected significant infiltration of $CD68^+$ macrophages in the *rectus abdominis* muscles of cachectic PDAC patients with cachexia relative to healthy individuals. Further transcriptional profiling performed in PDAC cachectic patients identified upregulation of gene clusters related to inflammation notably enrichment of genes involved in leukocyte activation and migration[261]. Moreover, recruitment of $CD163^+$ macrophages in the skeletal muscles were also found increased from PDAC patients compared to non-cachectic PDAC patients[555]. In the latter study, macrophage infiltration was negatively correlated with muscle fiber CSA, strongly suggesting a potential role of macrophages in muscle wasting and muscle repair alterations in PDAC patients. Furthermore, macrophage depletion, irrespective of macrophage subtype, restored total protein content and muscle strength in tumor-bearing mice, suggesting critical role of macrophages in altering muscle strength[555]. Although it is not clear whether this was caused by the absence of macrophage infiltrating the muscle tissue or the macrophages associated with the tumor. With regard to the results derived from PDAC patients, recently transcriptomic analysis revealed increased expression of genes related with macrophage activation in the *diaphragm* muscle from cachectic PDAC-xenograft mice compared to controls[503].

Taking together, these results suggest a prominent role for immune cell modulation in the skeletal muscle microenvironment during CC that might contribute to muscle wasting.

C. Fibroadipogenic-progenitors (FAPs) in the SC niche

1. Role of FAPs in muscle homeostasis/regeneration

FAP cells are muscle resident multipotent mesenchymal stem cells that can be identified by the cell surface markers stem cell antigen-1 (Sca1) and platelet-derived growth factor receptor-α (PDGFRα)[556]. They also express CD34, like SCs and ECs[557]. FAPs exhibit bipotential properties, capable of facilitating skeletal muscle regeneration as fibroblasts or to contribute to its fatty degeneration as adipocytes under specific conditions[558,559]. In healthy muscles, FAPs are one of the most common mononuclear cell population and likewise SC and muscle-resident macrophages, FAPs are found in a quiescent state[560]. Several studies have highlighted

the importance of FAP cells on maintaining skeletal muscle homeostasis in steady state conditions[561,559]. Depletion of FAP^{+} stromal cells from skeletal muscles induced by diphtheria toxin treatment results in loss of skeletal muscle mass and myofiber size[562]. Moreover, depletion of FAPs in PDGFRα^{CreER} mice leads to SC number decrease under homeostatic conditions, suggesting that FAPs are required for maintenance of the SC pool[561]. Upon acute muscle injury, FAPs expand rapidly[563,558], and become highly abundant around 3 to 4 days post-injury in accordance to the type and severity of injury, which coincides with the peak of SC proliferation[516,465]. After that, FAPs gradually decrease to baseline through apoptosis likely induced by macrophage release of TNFα[530]. During chronic injury, like in muscular dystrophies, it was suggested that disruption of the precisely synchronized progression from TNFα-rich to a TGF-β1-rich muscle environment prevents apoptosis of FAPs and favors FAPs differentiation into matrix-producing cells[530]. Therefore, the tightly regulated phenotypic switch of macrophages is crucial to preserve FAP number and function and prevent fibrotic degeneration in skeletal muscle. On the other hand, FAPs express high levels of immunomodulatory cytokines that regulate the accumulation and function of monocytes and neutrophils[564,565]. In addition, activated FAPs upregulate the expression of IL-10 upon muscle damage[566], this cytokine is a major effector triggering the switch of macrophages into anti-inflammatory phenotype[534]. During the skeletal muscle injury, the structural composition of the niche is strongly remodeled by *de novo* deposition of several ECM components produced by FAPs such as collagen, fibronectin and basement constituents[567,568,569] that sustain the SC niche. Lack of collagen and fibronectin secreted by fibroblasts contributes to reduced SC self-renewal and proliferation capabilities as well as to muscle regeneration impairment[570,571,572,573,574]. On the other hand, ablation of SCs leads to dysregulation of fibroblasts and to strong increase of connective tissue suggesting that SCs and FAPs mutually interact to promote myogenesis and muscle regeneration[465]. Thus, sustained poor interactions between the various cell types in the SC niche during muscle regeneration, can result in the replacement of injured muscle fibers by stromal components that do not assist muscle contraction leading consequently to muscle motor function and mass loss.

2. Role of FAPs during CC

To date, few articles have directly examined the alterations of skeletal muscle FAPs in CC. Using flow cytometry and immunofluorescence analysis, results from two separate studies

revealed greater expression of Sca1[500,552] and PDGFRα[500] markers in the skeletal muscles from C26-bearing mice compared to control mice suggesting expansion of FAPs with CC. Interestingly, when removed from the muscles of the C26-bearing mice and cultured, FAPs degenerated into adipocyte-like cells, revealing an adipogenic shift that is maintained *in vitro*[500]. Hence, FAPs could be responsible for muscle fat infiltration (*i.e,* myosteatosis) which commonly occurs in cancer patients affected by cachexia[575,576,261]. Moreover IL-4/IL-13 signaling is possibly altered in the C26-bearing mice, reinforcing the idea of FAPs degeneration in CC[500]. Histological analysis using Masson's trichrome staining on limb and respiratory muscles from PDAC-patient derived xenograft (PDX) cachectic mice showed significant increase in collagen content compared to controls[503]. Further, genome-wide microarray analysis of the *diaphragm* muscle revealed up-regulation of genes encoding for ECM structural proteins such as *Collagens I*, *III* and *VI* and for ECM-degrading proteases that function in ECM turnover and fibrosis such as *Mmp3, Hpse* and *Lox*. These findings by Nosacka et al.[503] suggest expansion of FAPs, which are the predominant source of ECM-protein expression following injury[577,578]. In addition, the authors detected greater expression of IL-33 cytokine in the *diaphragm* from PDAC-PDX mice. IL-33 is a cytokine mostly released by FAPs following injury and inflammation in skeletal muscle[577,578] which stimulates proliferation of regulatory T cells[579] suggesting that FAPs could stimulate accumulation of immune cells in the skeletal muscle during CC.

As to human cancer patients, Judge et al.[261] demonstrated increased number of FAPs and greater areas with collagen and fat deposition in the damaged skeletal muscles of cachectic PDAC patients compared with non-cancer-control patients. Occurrence of fat infiltration in human cachectic muscles is in line with the findings of Costamagna et al.[500] which observed a transition of FAPs towards an adipocyte-like phenotype from muscles of tumor-bearing mice, although data was not quantified. Further increased collagen content is positively associated with body weight loss, lymph node metastasis and survival in PDAC patients[261], demonstrating a link between the extent of muscle fibrosis and oncologic outcomes in pancreatic cancer. Genome wide microarray analysis and qRT-PCR of skeletal muscles from PDAC cachectic patients identified elevated transcripts involved in TGF-β activation and its target genes known to be involved in tissue fibrosis[580,581] suggesting TGF-β-dependent mechanism of FAPs to stimulate muscle fibrosis in CC. To conclude, explicit evidence from both mouse models of

CC and human cancer patients is strongly suggesting alterations of FAPs function in skeletal muscles that could impinge on SC regulation and thus impair muscle regeneration during CC.

D. Endothelial cells (ECs) in the SC niche

1. Role of ECs in muscle homeostasis/regeneration

ECs are the major cell type that compose the inner layer of capillary blood vessels. They penetrate the interstitial space of muscle fibers to provide oxygen and nutrient supply and control immune cell invasion[582]. In healthy individuals, the vasculature is stable and ECs are constantly maintained through life. Autocrine vascular endothelial growth factor (VEGF) pathway is required for EC survival under non pathological conditions[583]. Strikingly, histological analyses have revealed that SC are located in close proximity to capillary ECs[584,585]. Christov et al.[584] notably found that in resting conditions, the number of SC attached to a muscle fiber is significantly correlated with the number of ECs of the same myofiber. Verma et al.[586] showed that SCs recruits ECs to establish a juxavascular niche for SCs, through production of VEGF4. Blockage of VEGF4 using either VEGF inhibitor or SC-specific VEGF4 gene deletion, decrease the proximity of SCs to capillaries. Interestingly this proximity to the blood vessels was associated with SC renewal, in which notch signaling pathway mediated by EC induced quiescence in SC. These results suggest that the cross talk between EC and SC is crucial for replenishment and maintenance of SC quiescence. During particular physiological response like in muscle growth, injury or exercise there is a need for formation of capillaries from existing blood vessels, a mechanism called angiogenesis[587,588]. During muscle regeneration, number of capillaries increases[589] which is expectedly associated with the activation of ECs[590]. EC and SC proliferation occur concomitantly after an injury[591]. *In vitro* and *in vivo* studies have revealed that ECs promote myoblast proliferation[584,592], while SC exhibit angiogenic-like properties[584,593,594], through combined delivery of soluble factors like IGF-1, basic fibroblast growth factor (bFGF), hepatocyte growth factor (HGF) and vascular endothelial growth factor (VEGF)[595,596,592]. These findings highlight the interplay between SCs and ECs to stimulate each other in order to sustain both angiogenesis and myogenesis. Macrophages were also shown to stimulate angiogenesis during muscle regeneration[597,598,542] highlighting the complexity of the interactions between the different type of cells in the SC niche during muscle regeneration.

2. Role of ECs during CC

According to studies performed in animal models of CC, the role that ECs could play in muscle wasting is yet unclear due to contradictory results.

Wang et al.[242] reported no variation in the ratio of EC numbers *per* muscle fiber between muscles on a small cohort of control and tumor-bearing cachectic mice (n=3), as determined by histological staining with the endothelial marker CD31, indicating preserved vascularization. In contrast, two studies[260,599] have reported significantly increased number of blood vessels in *gastrocnemius* and *quadriceps* muscles from C26 mice compared to control mice. The difference in ECs number among these studies could be due to the difference in the stage and metabolism of cancer inoculated in the mice to investigate on CC. The first study by Wang et al.[242] used metastatic cancer mouse model while the other two studies[260,599] used mice bearing primary cancers. Moreover, another explanation could be the method of counting the number of ECs within the cachectic muscle, indeed the last study[599] determined capillary density by counting the number of capillaries per unit of muscle surface area (reported by mm^2). Therefore, the increase in capillary numbers could be due to smaller muscle fiber width in the absence of *de novo* angiogenesis. Although the reduced muscle fiber diameters could lead to reduced diffusion distance that may result in greater exposure of muscle tissue to pro-inflammatory factors secreted by the tumor[260]. Moreover, *He et al.*[259] showed increased expression levels of endothelial markers CD31, VWF (von Willebrand factor) and CD133 in $Sca1^+$ $CD34^+$ flow cytometry-sorted cells characterizing mesoangioblasts/pericytes from muscles of C26-tumor mice compared to control.

Conversely, where ECs are increased in the muscles of C26-bearing mice, two studies[600,601] performed in muscles from rats bearing the AH-130 Yoshida ascites hepatoma, reported decline in capillary-to-fiber ratio associated with increase expression levels of HIF-1α, suggesting decreased vascularization and hypoxia. According to these observations, FSTL-1 (follistatin-like protein1), a myokine required to increase capillary density and improve EC function in the skeletal muscle[602], was found downregulated in the skeletal muscles from rats bearing the AH-130 Yoshida hepatoma[269].

PGC1α (peroxisome proliferation activator receptor-γ coactivator1-α) is a transcriptional factor important in maintaining the integrity of skeletal muscle vascular barrier[603]. Recently it was demonstrated that PGC1α expression was significantly decreased in ECs from skeletal

muscles of melanoma bearing mice compared with control mice[604]. Further, tumor bearing mice lacking PGC1α gene in ECs, showed decreases in muscle mass and weight, as well as in grip strength and greater vascular leak than control tumor bearing mice. Thus, endothelial dysfunction in the skeletal muscle could result in the development of cachexia in cancer through suppression of PGC1α in the skeletal muscle endothelium. Vascular leak could result from excess vascular permeability to allow extravasation of inflammatory cells penetrating the muscle during CC[605,606].

In respect to human cancer patients, very little is known about the role of ECs during CC. To date, one study reported that CC does not seem to impact capillary density and microcirculation in cancer patients[136]. Taken all together, these results suggest that EC numbers and function are probably altered, at least in experimental CC.

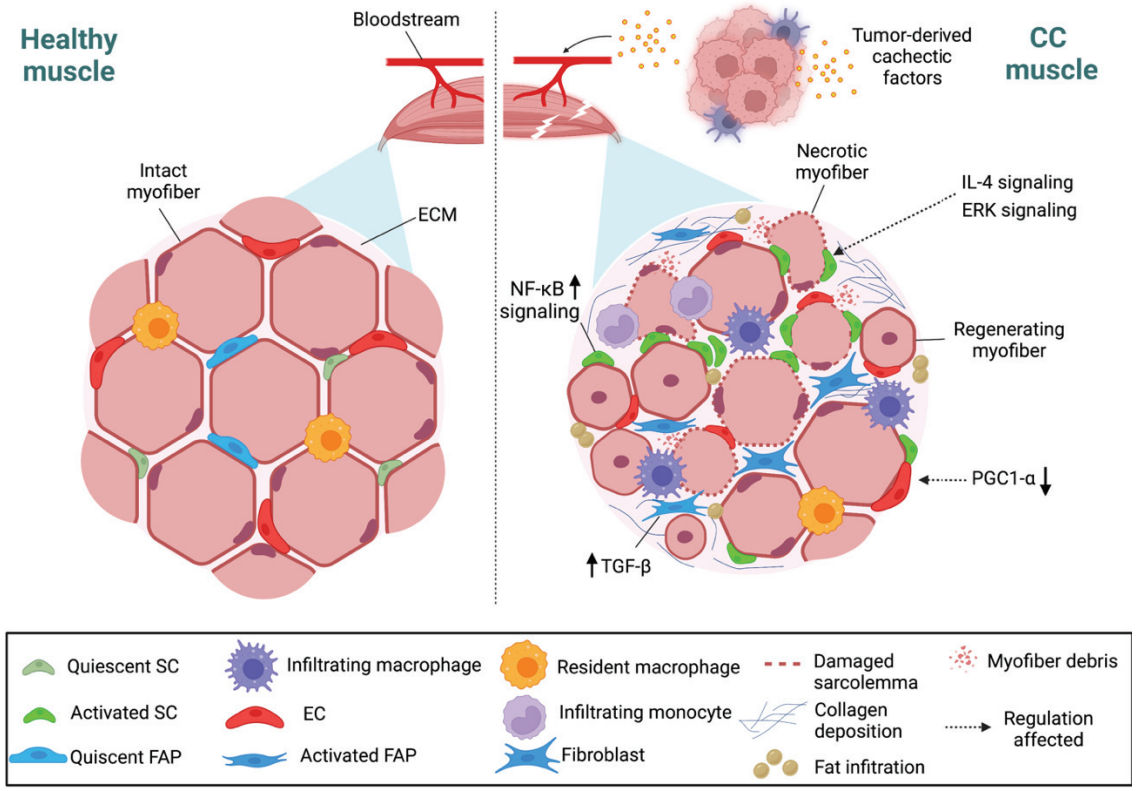

Figure 20: *Summary of the alterations occurring in the SC niche during CC. Image on left represents the muscle fibers and the SC niche under healthy homeostatic state. Image on right represents the possible alterations occurring in the SC niche and muscle fibers during CC under steady state in animal models of CC and cancer cachectic patients. Tumor circulating factors damage the membrane of muscle fibers, as a result SCs become aberrantly activated through upregulation of Pax7 mediated by NF-kB signaling. SC commit into myogenesis but are unable to complete proper differentiation and fusion to regenerate the damaged myofibers. Potent mechanisms that contribute to the altered SC fate during muscle regeneration could be a continuous muscle inflammation caused by immune cells accretion and dysfunction of FAPs and ECs to support SC myogenesis. Lack of replacement of the damaged myofibers leads to tissue fibrosis and fat infiltration by FAPs.*

Beyond the multifactorial causes that affect the internal mechanisms of the muscle fiber in CC, a growing body of evidence from experimental models of CC and human cancer patients shows disruption of the microenvironment surrounding the muscle fibers. Imbalance of the content of macrophages, FAPs and ECs and the ECM that compose the SC niche during CC might deregulate the interactions between those cells and with SCs. As a consequence, SC myogenic capacities might be altered prompting SC to be unable to support the muscle fiber homeostasis and to regenerate the muscle in response to damage induced by the tumor. Finally, because of the multitude of mechanisms that affect the muscles fibers from the inside and the outside, it is currently challenging to establish treatments that target muscle wasting during CC.

VI. Therapeutic approaches of CC

A. Pharmacological treatments

Considering the importance of skeletal muscle mass in oncological outcomes, pharmacological strategies to optimize body composition are a crucial component of effective cancer treatment. Various drugs have been proposed to counteract CC and have been conducted to clinical trials of phase I, II or III. Mechanisms of action of these drugs rely on increasing food intake and improving muscle protein metabolism. Such drugs consist of anti-inflammatory molecules or molecules that enhance muscle growth such as androgens or anabolic steroids. Appetite stimulants, such megestrol acetate, improve appetite and body weight in patients with cancer cachexia[607,608] but in most cases these drugs did not show efficacy in improving muscle mass[609,610,611,612,613]. Anabolic androgens have been shown to improve lean body mass[614,615] but they may be inappropriate for use due to their negative androgenic effects such as increased risk of hepatic toxicity, virilization and issues related to prostate cancer in men[616,617,618]. In clinical phase I and II trials, ALD518 targeting IL-6 ameliorated loss of lean mass in lung cancer patients[619] however its effect on muscle mass still remains unknown. TNF-α inhibitors such as Infliximab[620,621] or Etanercept[620] have failed to prevent CC and were associated with increased fatigue and neuromotor adverse events.

Finally, in light of the fact thar myostatin inhibition was able to rescue muscle mass and function in preclinical studies[249,231], some myostatin inhibitors have proceeded to clinical

development but a link between improvements in muscle mass and clinically significant functional outcomes has still not been validated[622].

Despite the several agents being in clinical development to overcome CC, in the present most of them have little or no effect on muscle wasting as the mechanisms involved in the development and progression of CC are multifactorial. Finally, these studies point out the fact that CC cannot be fully treated by targeting a single component but rather requires a multidimensional therapy in order to target multiple pathways underlying the pathogenicity of CC to achieve maximum benefit[140,623]. Thus, nowadays CC remains incurable.

B. Non-pharmacological treatments

1. Effects of exercise training in CC

To limit the alterations related to CC, physical activity has been recently introduced, alone it can target multiple pathways responsible for the pathogenesis of CC. Exercise is known to have positive effects on health of various organ systems. In response to muscle contraction, skeletal muscle was established to be a secretory immunogenic organ, producing and releasing cytokines[624], called myokines, that exert local and distant effects. Locally, myokines support muscle growth[625], for instance by enhancing muscle capillarization[626,627] and muscle metabolic homeostasis[628]. At distance, they mediate muscle-organ crosstalk to several organs such as the immune system[629,630], the adipose tissue[631] and the cardiovascular system[625]. One of the key roles of myokines is their capacity to reduce systemic inflammation[632,633,634,635]. Exercise also improves muscle protein metabolism[636,637]. Production of anti-inflammatory IL-6 myokine by muscle fibers during physical activity is widely recognized[638,639] and has been proposed to limit the activity the inflammatory activity of other cytokines such as TNFα[640] involved in muscle protein degradation. Moreover, exercise is able to increase both endurance and muscle strength in healthy and diseased conditions[641,642], improve insulin resistance[643] as well as to modulate the SC function[644,445] and niche[645,646,647]. Therefore, exercise represents a promising non-pharmacological intervention to attenuate or prevent muscle wasting in CC[648,649,650].

Robust body of research suggests that physical activity may have an impact on cancer features related to its emergence[651,652], progression[652,653] and outcome[654,655]. For instance, numerous

researches have looked at how aerobic exercise training affects the onset and progression of cancer[656,657], but only few studies conducted in both clinical and experimental contexts directly evaluate the usefulness of exercise on progression of cachexia and prevention of muscle loss and strength.

Physical activity can be classified as endurance (aerobic) or resistance (anaerobic) exercise/training. Endurance training often includes repetitive, low-resistance activities like running, cycling and swimming for periods of time ranging from a few minutes to several hours. On the other hand, resistance training comprises short-duration activities at high or maximal exercise intensities, and increases the capacity to perform high intensity, high-resistance exercise of a single or few repetitions such as bodybuilding or weightlifting. Endurance training favors the conversion of fibers toward oxidative type I fibers *via* a mechanism involving AMP kinase mediated-activation of PGC1α[658,659], promoting mitochondrial biogenesis[660], and thus stimulating oxidative metabolic adaptions with little changes in muscle mass[661]. In contrast, resistance training exhibit anabolic functions by enhancing synthesis of contractile proteins through stimulation of Akt/mTOR signaling[662], stimulates mitochondrial biogenesis, and ultimately triggers hypertrophy, preferentially of glycolytic fibers, thus increasing muscle strength[663,664].

Endurance or resistance training in the majority of preclinical studies that aim to overcome CC, has been performed as a preventive approach, started prior to tumor inoculation[601,665,666] and sometimes even maintained during CC progression[667,668,669,670,217]. In tumor-bearing animals, treadmill training[667,668] or wheel running[671] started prior to tumor growth and carried out during CC progression could retard tumor growth[667,668], increase muscle mass[667,668], function[671] and protein synthesis[667]. Increase in muscle mass in response to treadmill training improved insulin sensitivity as well as muscle oxidative metabolic capacity, despite persistence in muscle inflammatory signaling[668]. Treadmill running[672] or voluntary wheel running[316,173] started from the day after tumor implantation rescued muscle atrophy[672,316,173] and function[316] in C26-bearing mice. Further, voluntary wheel running downregulated Pax7 protein expression and activated NF-κB from muscles of C26 bearing-mice closely to the control levels, suggesting improvement of myogenesis regulation[173]. Morinaga et al.[672] went further on the molecular mechanisms by which endurance exercise could improve muscle wasting, by showing activation of adiponectin signaling in the C26-tumor bearing mice submitted to treadmill running protocol. Adiponectin has been reported to enhance insulin

signaling[673,674]. Addition of adiponectin prevented the atrophy of myotubes exposed to C26-conditioned medium *in vitro* through increased production of phosphorylated-mTOR and suppression of LC3-II.

Resistance exercise has long been advocated as a treatment for cachexia and other types of muscle atrophy[675] due to its powerful anabolic stimulus that promotes muscle hypertrophy, enhance contractile function and signaling responses favoring muscle growth and preservation[676,677]. Increased resistance load is a successful way to stimulate IGF-1 pathway activation and block myostatin signaling to preserve muscle mass in other disorders of cachexia[678]. Therefore, resistance training may hold promise for stimulating IGF-1 activity as well as diminishing myostatin activation, observed in CC models. In pre-clinical models of CC, resistance training is often modeled using electrical stimulation protocols combined with lengthening contractions or the surgical ablation of the synergistic muscles or tenotomy[665,679,680]. Functional overload surgeries or eccentric contractions performed in experimental models of CC, to mimic the effect of resistance exercise training, limited muscle wasting whether it was carried at tumor inoculation[679] or after[216,680]. The above studies did not evaluate muscle functional decline after resistance exercise. In one study, resistance exercise consisted of a set ladder-climbing, as previously described[681] and started two days after tumor cell inoculation in animals, counteracted the loss of muscle mass and strength and prevented muscle STAT3 excessive activation[682].

Finally, C26-bearing mice trained with a mixed endurance-resistance exercise starting the day after tumor implantation[414] were partially protected from the loss of muscle mass and strength without further impact on tumor mass. Such beneficial effects on muscle mass and function were accompanied by reduced levels of ROS, carbonylated proteins and markers of autophagy indicating decreased muscle protein catabolism and oxidative stress.

Taking together, the majority of the above-described studies showing improvement on muscle mass and function during CC did not employed exercise at the onset of CC but rather at the initiation of tumor growth. Thus, making difficult at present, to judge the rationale for the use of exercise as a treatment for CC which often develops in the late stages of the disease in humans.

In the clinical field, few data exist. Preliminary findings from trials with advanced cancer patients demonstrated that multimodal interventions, including notably resistance exercise, might contribute to body weight and muscle mass stabilization in cancer patients susceptible

for cachexia[683,684,685]. Progressive resistance exercise alone for 20 weeks increased significantly muscle strength and endurance of prostate cancer patients from baseline, receiving androgen deprivation for prostate cancer[686]. Although comparison to a control group was lacking from the study and patients were not screened for ongoing cachexia. In pancreatic cancer patients, 6 months of progressive resistance exercise led to significant increases in muscle mass and improved muscle strength, while body weight remained unchanged compared to control group[687]. However, in this study, only about half of the patients were cachectic before the beginning of resistance training. Similarly, progressive resistance exercise during radiotherapy of advanced lung cancer patients with cachexia who participated in exercise program consisting of aerobic and weight training over an 8-week period maintained or even improved their muscle strength over the course of the study[688]. Despite these promising results for the use of exercise in therapeutic practice, there is clearly a lack of cancer patients for adhesion in exercise trials that are specifically screened for cachexia and a lack of criteria to stratify those who used or not to exercise before cancer diagnosis.

2. Limitations of exercise training in cancer patients

Despite these optimistic results emerging in the preclinical and clinical fields, cancer patients are frequently too weak to complete physical activity interventions, especially if they are in advanced state of their disease, leading to a substantial proportion of patients (30-85%) who remain sedentary in the long term[689,690,691]. Factors such as increased treatment complications, heart dysfunction, anemia, tiredness and functional limitations restrict cancer patient's capacity to exercise[692,693]. Bowel symptoms, mainly related to radiotherapy or surgery, decrease the ability of cancer patients to exercise[694,695,696]. Chemotherapy can also impair peak oxygen capacity (VO_{2peak}), resulting in poorer exercise tolerance[697]. In addition, heart function is compromised as a result of CC, patients as well as animals bearing cancer cells exhibit cardiac shrinkage at the advanced stages of the illness[698]. Cachectic cancer patients often suffer from anemia, which can also exacerbate weight loss and tolerance to physical exercise[699]. Correspondingly mild endurance training worsened the condition of tumor-bearing mice suffering from a significant decrease in hematocrit[243]. Cancer complications can also lead to changes in eating habits which might affect how the muscle adapt to exercise and lose exercise benefits if the body lacks adequate food availability. In

addition, weakened patients with advanced cancer that are not able to attempt hospital-based exercise, rather prefer to undertake exercise at home[700,701] in the absence of medical supervision. Thus, it is necessary to propose alternative exercise regimens in severely cancer cachectic patients, which would consist to stimulate muscle activity artificially. Neuromuscular electrical stimulation (NMES) might represent a good alternative to voluntary exercise training. NMES is able to elicit muscle contractions, imitating those generated during exercise, and this without any physical effort, making it a promising therapy to overcome muscle wasting and weakness.

VII. Neuromuscular electrical stimulation (NMES)

A. Principle, current use in the clinical field and possible molecular and cellular mechanisms of NMES

NMES consists of repeated application of electrical current over muscles that depolarizes local intramuscular nerve branches[702,703] to generate muscle contractions without voluntary effort[704,705]. The electrical impulses are delivered to the muscles through electrodes connected to a portable device with a stimulator unit, and which are placed on the skin near the muscles (Figure 21), or directly over a motor nerve[706]. NMES training has been applied in various muscles such as *quadriceps*[707], which is the most often stimulated muscle, the *abdominals*[708] or the *triceps surae*[709]. NMES, which involves cycles of stimulation and rest, can be also delivered at a variety of frequencies in accordance with the objectives of the intervention[710]. At very low frequencies (2-10 Hz), NMES can be delivered at intensity below the motor threshold to overcome pain impulses by targeting specifically sensory nerve fibers[711]. When delivered at high frequencies (>50 Hz) and at intensity higher than the motor threshold, NMES produces muscle tetany and contraction aiming to improve muscle strength[712].

Figure 21: *Application of NMES in patient after anterior cruciate ligament reconstruction. Patient is seated and the knee is placed at 60° of flexion (different angles can be used according on pain or comorbidities). Electrical stimulation is used to contract the patient's muscles to 50% of its maximum voluntary isometric contraction against a fixed resistance (Picture taken from Adams et al.[713]).*

NMES produces muscle contractions in a different pattern from that of voluntary motor contractions[714,715] (Figure 22). During voluntary contractions, the recruitment order of muscle fibers follows an orderly fashion[716]. The muscle fibers activated are distributed over the entire muscle. First small fibers consisting generally of type I muscle (slow twitch, fatigue resistant) are selectively recruited, then progressively larger ones are recruited consisting of type II muscle fibers (fast twitch, fast fatiguing)[717] according to the intensity of the voluntary contraction. In turn, during NMES, muscle fibers are activated by an electrical current that is applied externally to the intramuscular nerve axons, thus the order of recruitment depends on spatial distance from the stimulating electrodes. Muscle fibers located directly beneath the stimulation electrodes, at the surface of the muscle are recruited preferentially, involving random recruitment of both slow and fast fibers that are activated simultaneously[714]. As NMES intensity rises the recruitment of fibers lying deeper in the muscle increases[718].

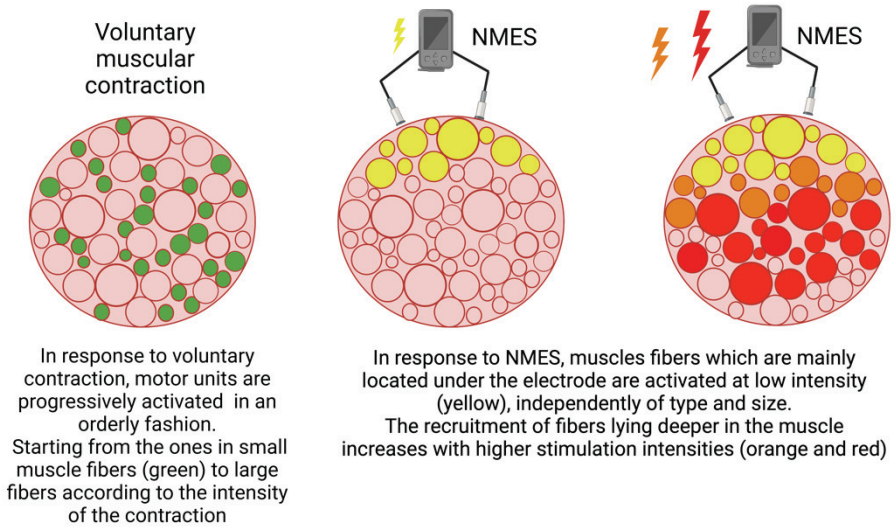

***Figure 22**: Comparison of muscle fiber recruitment in voluntary contraction vs in NMES.*

Like voluntary exercise, repeated muscle contractions, generated by NMES over time, can promote muscle hypertrophy, neural adaptations, improve muscle force and well-being[719,720]. In healthy individuals, NMES seems to be less[721] or equally[722,723] effective than identical voluntary training programs. Additionally, it has been shown that the improvements observed at the end of the training session is dependent on the intensity of the electrically elicited contractions[724]. Further, NMES is largely adopted to increase muscle strength in athletes that require high levels of muscle strength[725,726,727]. Therefore, NMES can be promising for muscle weakness and wasting in patients with advanced disease that show impaired voluntary contraction capacity. Strong evidence for improving altered muscle function and mass by NMES was observed in patient groups that are usually not allowed to exercise due to progression of their underlying disease, such as patients with COPD[728,729,730,731], chronic heart failure[730,732] or other critical illnesses[733,734]. In chronic heart failure and COPD patients, long term NMES caused the same positive muscle adaptations, such as increased oxidative capacity carried on by changes in oxidative enzyme levels and changes in type of muscle fiber[735,736,737]. Increasing body of research also has shown the benefits of NMES to improve muscle strength, muscle mass and cardiorespiratory performance in sedentary elderly subjects[738,739,740]. NMES has also the potential to prevent muscle wasting and loss of function during prolonged periods of disuse or immobilization[741,742].

Brief periods of NMES were shown to maintain muscle protein synthesis in men with fractured tibia[741] while in elderly type 2 diabetic patients, NMES was shown to exhibit large increase in skeletal muscle protein synthesis rates[743].

Increase in muscle CSA was observed in healthy young[719] and older adults[744,745,746] following NMES training. In healthy subjects, 8 weeks of NMES training induced muscle hypertrophy and increase in muscle force which were accompanied by a conversion of MyHC type IIX muscle fibers (fast twitch fibers, glycolytic) to MyHC type IIA and I muscle fibers (slower twitch, oxidative) and by an upregulation of oxidative enzymes[719]. Moreover, proteomic analysis in healthy individuals, allowed to identify upregulation of desmin, cofinilin-2, tubulin-β2 and actin induced following NMES training[719]. Thereby, these results suggest that NMES remodel the cytoskeleton and modulate the metabolic characteristics of muscle fibers that might support the increases in muscle fiber CSA and force. NMES in healthy elderly subjects was shown to lead to muscle hypertrophy in conjunction with increase in SC cell proliferation and in myonuclear density indicating that NMES could enhance the SC fusion and fate to sustain muscle hypertrophy[746]. In point of fact, administration of an electrical current has been shown to promote myotube activity and proliferation of SC and rescue the loss of myonuclei in murine disuse muscle atrophy[747,748,749].

B. Use of NMES in CC

Despite the data supporting NMES efficacy in other patient populations, published data regarding the usefulness of NMES to improve cachexia in cancer patients are quite limited and conflicting. Use of NMES on *quadriceps* and *gluteus* during 4 weeks (60 min daily, 5 times a week) from a single patient with extensive metastatic lung cancer improved mobility, physical endurance and quality of life[750]. On the other hand, Windholz et al.[751] did not demonstrate improvement of physical functioning in cancer patients with poor performance status submitted to 6-week NMES on both *quadriceps* muscles. Direct measurement of muscle strength or CSA as outcome measures of muscle improvement by NMES were missing from both studies. Instead, these studies used tests that quantified functional mobility and exercise capacity such as timed up and go test or the 6-min walk test, which do not reflect absolute muscle strength. Further, in a pilot study[752], a group of advanced NSCLC patients were submitted to a 4-week NMES (50hz, 30-60min daily, minimum 3 times a week) of the

quadriceps. NMES improved leg muscle strength and physical activity by 22% and 11 % respectively compared to control group, although differences were not statistically significant. In a follow-up phase II study[753], the same authors applied NMES training protocol alongside to palliative chemotherapy in patients with NSCLC for a duration of 8 to 11 weeks. In this latter study, NMES had not significant improvements on *quadriceps* muscle strength, thigh and body lean mass or physical activity when compared to control group. Although only half of the lung cancer patients receiving palliative chemotherapy completed NMES training in this study. In the two last studies[752,753] patients were motivated to increase the stimulation amplitude as much as they could tolerated it, thus the amplitude of stimulation was often not controlled. Recently, meta-analyses, performed by O'Connor et al.[754] , and including nine studies for the use of NMES in adult cancer survivors highlighted methodological limitations (*e.g.,* small sample size, timing of intervention), uncontrolled application as well as lack of standardization among the different NMES protocols. Finally, the strong discomfort felt by the cancer patients due to the electric current remains the main limitation of NMES use[705]. In addition, the force produced by the muscle in response to stimulation which represents the only criterion to measure NMES efficacy, has never been controlled in CC patients[705]. To minimize these limitations, researchers in the cancer field should adapt the intensity of stimulation according to muscle force production so to minimize the discomfort felt while also achieving the greatest muscle force gains. For instance, NMES intensities adjusted to 15-25% of the maximum voluntary contraction are well tolerated and lead to functional improvements in COPD patients[728]. Collectively, these findings underly the lack of methodological consistency in NMES use. As a result, the effectiveness of NMES to prevent muscle wasting and weakness in CC is still not evident.

SPECIFIC AIMS

It is now well recognized that CC is driven by systemic inflammation which leads to muscle protein imbalance and subsequently to muscle wasting by taking over molecular pathways inside the muscle fiber. Yet, recent studies have revealed alterations on the outside of the muscle fibers, that affect the SCs and their myogenic program and prevent them from sustaining muscle homeostasis in the presence of the tumor. SC fate relies on the dynamic interactions between the SCs with the immune cells, FAPs and ECs composing the SC niche and these interactions may be compromised in CC leading to inefficient myogenesis. At present, the interactions of SC with their niche remain poorly characterized in the context of CC.

In light of the SC dysfunctions induced by CC, evidence is emerging illustrating that contractile activity *per se* can promote SC fusion with existing myofibers (myonuclear accretion). Although existing models of hypertrophy that have been used to demonstrate SC contribution to muscle growth lead also to muscle damage. SC fusion-induced muscle hypertrophy might not only be driven by increased mechanical loading in these models, but may occur, at least in part, in response to (overload) exercise-induced muscle injury. Therefore, the possibility of rigorously monitoring muscle activity by a standardized and controlled NMES protocol would allow a better understanding of the role of SC in a physiological context of muscle hypertrophy. This is particularly relevant, since NMES has recently been introduced in cancer patients approach of reconditioning. Although, the effectiveness of NMES to overcome muscle weakness and wasting in CC patients remains equivocal due to uncontrolled application that limits the scope and interpretation of these results. Pertinently, the muscle force produced in response to the stimulation, which is the main determinant of NMES effectiveness, has never been monitored in CC patients.

The first aim was to determine whether an increase in contractile activity carried out by a controlled and individualized NMES protocol could promote SC fusion (myonuclear accretion) and muscle growth without inducing muscle damage.

In our second study the objective was to determine alterations of SC and their cellular interactions within the SC niche in association to muscle weakness and wasting in experimental CC. Then our goal was to determine the beneficial effects of NMES on muscle weakness and wasting during CC and decipher the cellular mechanisms of NMES underlying the regulation of the SCs and their niche. Two complementary mouse models of CC were used to that aims. The colon-26 (C26) carcinoma tumor-bearing mouse model is a widely used

model of CC. Growth of C26 tumor causes drastic cachexia in a short and established time of period. Thus, it takes less time to evaluate our goals using the C26 mouse model. *Apc*$^{Min/+}$ mouse model is another mouse model commonly used to study CC. Similar to patients with colorectal cancer, *Apc*$^{Min/+}$ mice carry a mutation in the adenomatous polyposis coli (*Apc*) gene, which causes intestinal polyps to form spontaneously and progress into colon cancer over a longer period of time. Therefore, *Apc*$^{Min/+}$ mouse model better recapitulates the progressive nature of human CC and can allows to have more accurate results.

STUDY #1

(Submitted for publication to the Journal of physiology, JP-RP-2022-283984)

NEUROMUSCULAR ELECTRICAL STIMULATION TRAINING INDUCES MYONUCLEAR ACCRETION AND HYPERTROPHY IN MICE WITHOUT OVERT SIGNS OF MUSCLE DAMAGE

Running title: Skeletal muscle plasticity to NMES

Aliki Zavoriti[1], Aurélie Fessard[1], Masoud Rahmati[1,2], Natacha Boyer[1], Peggy Del Carmine[1], Bénédicte Chazaud[1], Julien Gondin[1]

[1] Institut NeuroMyoGène, Unité Physiopathologie et Génétique du Neurone et du Muscle, Université Claude Bernard Lyon 1, CNRS UMR 5261, Inserm U1315, Univ Lyon, Lyon, France.

[2] Department of Exercise Physiology, Faculty of Literature and Human Sciences, Lorestan University, Khoramabad, Iran.

Corresponding author:
Julien GONDIN
Institut NeuroMyoGène (INMG)
CNRS 5310 – INSERM U1217 – UCBL1
Faculté de Médecine et de Pharmacie
8 Avenue Rockefeller
69008 LYON, FRANCE
Julien.gondin@univ-lyon1.fr
ORCID : 0000-0002-3108-605X

This manuscript was first published as a preprint: Zavoriti *et al.* Individualized isometric neuromuscular electrical stimulation training promotes myonuclear accretion in mouse skeletal muscle. https://doi.org/10.1101/2021.12.14.472254

Key points

It is still unclear whether muscle overload-induced myonuclear accretion is driven by increased mechanical loading *per se*, or occurs, at least in part, in response to exercise-induced muscle injury.

We assessed the impact of individualized and carefully monitored neuromuscular electrical stimulation (NMES) protocols performed at low force level under isometric conditions on skeletal mouse muscles.

NMES led to both a robust myonuclear accretion and higher muscle stem cell content in two mouse strains, without overt signs of muscle damage/regeneration.

NMES-induced myonuclear accretion was an early event preceding muscle hypertrophy.

NMES-induced myonuclear accretion and hypertrophy were driven by a mild increase in mechanical loading in the absence of muscle injury.

Abstract

Skeletal muscle is a plastic tissue that adapts to increased mechanical loading/contractile activity through fusion of muscle stem cells (MuSCs) with myofibers, a physiological process referred to as myonuclear accretion. However, it is still unclear whether myonuclear accretion is driven by increased mechanical loading *per se,* or occurs, at least in part, in response to muscle injury. Here, we developed a non-damaging protocol to evaluate contractile activity-induced myonuclear accretion in a physiological context. Contractile activity was generated by applying repeated electrical stimuli over the mouse plantar flexor muscles. This method is commonly referred to as NeuroMuscular Electrical Simulation (NMES) in Human. Each NMES training session consisted of 80 isometric contractions at ∼15% of maximal tetanic force to avoid muscle damage. C57BL/6J and BALB/c male mice were submitted to either a short (*i.e.*, 6 sessions) or long (*i.e.*, 12 sessions) individualized NMES training program while unstimulated mice were used as controls. The two NMES training programs led to both a robust myonuclear accretion and an increased MuSC content in the two mouse strains without overt signs of muscle damage/regeneration. We further demonstrated that NMES-induced myonuclear accretion was an early event preceding muscle hypertrophy inasmuch as an increased myofiber cross-sectional area was only observed in response to the long-term NMES training protocol. We conclude that NMES-induced myonuclear accretion and muscle hypertrophy are driven by a mild increase in mechanical loading in the absence of muscle injury.

Keywords: Muscle stem cells, skeletal muscle plasticity, force production, contractile activity, resistance training.

Table of contents category: Exercise

Introduction

Skeletal muscle is a remarkably plastic tissue that both regenerates *ad integrum* after an acute injury and adapts to changes in mechanical loading/contractile activity (*e.g.*, disuse, overloading). This plasticity widely relies on muscle stem cells (aka satellite cells, MuSCs) which are located beneath the basal laminal, *i.e.*, at the periphery of the myofibers. While MuSCs are indispensable for muscle regeneration (Lepper *et al.*, 2011; Murphy *et al.*, 2011; Sambasivan *et al.*, 2011), during which they exit quiescence, expand, differentiate and fuse to form new functional myofibers, emerging evidence illustrates their roles in skeletal muscle hypertrophy (Murach *et al.*, 2021).

Over the last few years, it was demonstrated that mechanical overload leads to MuSC fusion with existing myofibers, a physiological process referred to as myonuclear accretion. Thanks to the development of genetic mouse models either ablated for MuSCs (McCarthy *et al.*, 2011; Egner *et al.*, 2016) or deleted for transcription factors involved in MuSC myogenesis (Goh & Millay, 2017; Fukuda *et al.*, 2019) or in myofiber homeostasis (Noviello *et al.*, 2022), the requirement of MuSC-mediated myonuclear accretion for hypertrophy was demonstrated in young animals (McCarthy *et al.*, 2011; Egner *et al.*, 2016; Goh & Millay, 2017) and in protocols associated with long-term muscle overload (Fry *et al.*, 2014). However, the interpretation of these pioneer findings is limited by the use of non-physiological models of muscle overload consisting in either surgical ablation of synergist muscles or tenotomy (McCarthy *et al.*, 2011; Fukuda *et al.*, 2019). Indeed, the relevance of these models has been questioned regarding the magnitude of hypertrophy (*i.e.*, +30%-200% of muscle mass in 1-3 weeks post-surgery; (McCarthy *et al.*, 2011; Fukuda *et al.*, 2019)), that largely exceeds what can be achieved in humans after resistance training (*i.e.*, +5-10% of muscle mass after 20-24 weeks of training) (Reggiani & Schiaffino, 2020). Moreover, these models may also lead to muscle injury so that it is still unclear whether MuSC fusion is only driven by increased mechanical loading, or due, at least in part, to the confounding effects of overload-induced muscle regeneration (Egner *et al.*, 2016; Murach *et al.*, 2017; Fukuda *et al.*, 2019).

To overcome these limitations, weighted voluntary wheel running (Dungan *et al.*, 2019; Masschelein *et al.*, 2020) or high-intensity interval treadmill (Goh *et al.*, 2019) protocols were recently introduced to decipher the contribution of MuSCs to exercise-induced myonuclear accretion and/or hypertrophy. Myonuclear accretion occurs early during training

(Goh *et al.*, 2019; Englund *et al.*, 2021) while MuSC depletion blunts myofiber hypertrophy (Englund *et al.*, 2021). Although these physiological models of exercise greatly contributed to improve our understanding on the role of MuSCs in skeletal muscle hypertrophy, running activity relies on repeated eccentric muscle contractions where the muscle is stretched beyond its optimal length (Katz, 1939), potentially leading to muscle damage. In addition, exercise design usually involves the same absolute increment of wheel load (Dungan *et al.*, 2019) or running speed (Goh *et al.*, 2019) for all mice so that the training load is not adjusted according to the individual performance capacity. The lack of running exercise individualization might further aggravate the extent of muscle damage (Goh *et al.*, 2019; Murach *et al.*, 2020*a*). As a consequence, myonuclear accretion-induced muscle hypertrophy might not only be driven by increased mechanical loading, but may occur, at least in part, in response to running exercise-induced muscle injury in these models.

Here, we developed a non-damaging protocol to evaluate contractile activity-induced myonuclear accretion/hypertrophy in physiological conditions. In this context, contractile activity was generated by applying repeated electrical stimuli over the mouse plantar flexor muscles and was carefully monitored in response to each stimulation train and for each trained mouse. This method is commonly referred as to NeuroMuscular Electrical Simulation (NMES) in Human (Gondin *et al.*, 2005, 2006, 2011*b*) and was performed under isometric conditions to avoid muscle damage (Gondin *et al.*, 2011*a*). NMES led to a robust myonuclear accretion and higher MuSC content in two mouse strains, without overt signs of muscle damage/regeneration. We further demonstrated that NMES-induced myonuclear accretion is an early event preceding muscle hypertrophy.

Materials and Methods

Animals

Experiments were conducted on both C57BL/6J and BALB/c males (Janvier Labs, Le Genest-Saint-Isle, France) at 10-12 weeks of age. These two genetic backgrounds are commonly used to investigate the impact of cancer cachexia (Gallot *et al.*, 2014; Penna *et al.*, 2016) or sepsis (Morel *et al.*, 2017) on skeletal muscle homeostasis. Mice were housed in an environment-controlled facility (12-12-hour light-dark cycle, 25°C), received water and standard food *ad libitum*. All of the experiments and procedures were conducted in accordance with the guidelines of the local animal ethics committee of the University Claude Bernard Lyon 1 and in accordance with French and European legislation on animal experimentation and approved by the ethics committee CEEA-55 and the French ministry of research (APAFIS#12794-2017122107228405).

Experimental device

In order to propose individualized and carefully monitored NMES training protocols, we used a strictly non-invasive ergometer (NIMPHEA_Research, AII Biomedical SAS, Grenoble, France) offering the possibility to electrically stimulate the plantar flexor mouse muscles and to record the resulting force production (Fig. 1A). Mice were initially anesthetized in an induction chamber using 4% isoflurane. The right hindlimb was shaved before an electrode cream was applied over the plantar flexor muscles to optimize electrical stimulation. Each anesthetized mouse was placed supine in a cradle allowing for a strict standardization of the animal positioning in ~1 min (Supplemental Video 1). Throughout a typical experiment, anesthesia was maintained by air inhalation through a facemask continuously supplied with 1.5-2.5% isoflurane. The cradle also includes an electrical heating blanket in order to maintain the animal at a physiological temperature during anesthesia. Electrical stimuli were delivered through two electrodes located below the knee and the Achille's tendon. The right foot was positioned and firmly immobilized through a rigid slipper on a pedal of an ergometer allowing for the measurement of the force produced by the plantar flexor muscles (*i.e.*, mainly the *gastrocnemius* muscle). The right knee was also firmly maintained using a rigid fixation in order to optimize isometric force recordings (Fig. 1A).

***In vivo* maximal force measurements and NMES training**

Transcutaneous stimulation was first elicited on the plantar flexor muscles using a constant-current stimulator (Digitimer DS7AH, Hertfordshire, UK; maximal voltage: 400 V; 0.2 ms duration, monophasic rectangular pulses). The individual maximal current intensity was determined by progressively increasing the current intensity until there was no further peak twitch force increase. This intensity was then maintained to measure maximal isometric force production (F_{max}) in response to a 250-ms 100 Hz tetanic stimulation train (Fig. 1B).

NMES mice were then submitted to a NMES protocol performed under isometric conditions at a submaximal mechanical intensity corresponding to ~15% of F_{max} in order to i) avoid muscle damage (Gondin *et al.*, 2011*a*); ii) mimic the application of NMES in severely impaired patients (Maddocks *et al.*, 2016) for whom higher force levels are difficult to reach due to discomfort associated with electrical stimuli (Gondin *et al.*, 2011*c*). As a consequence, the current intensity was carefully adjusted at the beginning of each NMES training session in order to reach 15% of F_{max} (*i.e.*, initial intensity $I_{15\%}$; range: 12.5-17.5% of F_{max}) in response to a 250-ms 50 Hz stimulation train (Fig. 1C). Each NMES session consisted of 80 stimulation trains (2-s duration, 8-s recovery) delivered at a frequency of 50 Hz. Every 10 contractions, the current intensity was increased by 50% from $I_{15\%}$ in order to minimize muscle fatigue and maintain a force level of ~15% of F_{max} throughout the NMES protocol (Fig. 1D). Current intensity (in mA) was consistently recorded and averaged for all stimulation trains for each training session. For all NMES training sessions and for each mouse, the force produced in response to each stimulation train was quantified and normalized to F_{max} recorded at the beginning of the corresponding session. Control mice were not stimulated but were kept under anesthesia for the same duration as an NMES session. F_{max} was recorded in both NMES and control mice for each training and testing session (Fig. 1E-F). Force data was sampled at 1000 Hz with a PowerLab8/35 (ADinstruments, Sydney, Australia) and analyzed with LabChart software (v8.1.17 ADInstruments, Sydney, Australia).

Considering that myonuclear accretion is an early process preceding muscle hypertrophy (Bruusgaard *et al.*, 2010; Goh *et al.*, 2019), two NMES protocols were designed with different number of training sessions. For the short-term NMES training program (Fig. 1E), NMES mice were stimulated for 2 × 3 consecutive days separated by one day of rest, for a total of 6 sessions corresponding to a total muscle contractile activity of only 16 min (*i.e.*, 6 sessions x 80 trains x 2 sec). For the long-term NMES training program (Fig. 1F), 12 sessions were

performed over a 3 week-period corresponding to a total muscle contractile activity of 32 min (*i.e.*, 12 sessions x 80 trains x 2 sec). The two NMES training protocols and control interventions were performed in both C57BL/6J and BALB/c males.

Tissue preparation and immunofluorescence analyses

All animals were sacrificed by cervical dislocation after deep isoflurane anesthesia. The right *gastrocnemius* muscle was harvested, weighted and then frozen in isopentane placed in liquid-nitrogen, and kept at -80°C until use. Cryosections (10 µm) were prepared for immunohistochemical analyses.

Cryosections were permeabilized in Triton-X100 0.5% for 10 min at room temperature, washed 3 times in PBS and then blocked in BSA 4% for 1 hour at room temperature. Cryosections were then incubated with primary antibodies overnight at 4°C, washed 3 times with PBS and further incubated with secondary antibody for 1 hour at 37°C. The following primary antibodies were used: anti-MYH3 (1/200, mouse, sc-53091, Santa Cruz Biotech) and anti-PCM1 (1/1000, rabbit, HPA023370, Sigma) with anti-Laminin (1/200, rabbit, L9393, Merck) and anti-Laminin α2 (4H8-2) (1/1000, rat, sc-59854, Santa Cruz Biotech), respectively. Secondary antibodies were: Alexa Fluor 488 AffinePure Goat Anti-Mouse (1/200, ref: 115-545-205), Cy3 AffinePure Donkey Anti-Rabbit (1/200, ref: 711-165-152), Cy3 AffinePure Donkey Anti-Mouse (*i.e.*, for determining IgG^+ myofibers; 1/200, ref: 715-165-150), Fluorescein (FITC) AffinePure Donkey Anti-Rabbit (1/200, ref: 711-095-152), and Cy3 AffinePure Donkey Anti-Rat (1/200, ref: 712-165-153) supplied from Jackson ImmunoResearch. Slides were washed with PBS, counterstained with Hoechst and mounted in Fluoromount-G medium

For Pax7 immunostaining, cryosections were first fixed with PFA 4% for 10 min, washed 3 times in PBS, permeabilized in Triton-X100 0.1% + 0.1M Glycine for 10 min, washed 3 times in PBS, then immerged into citrate buffer 10mM in 90°C hot water bath twice, washed 3 times in PBS and blocked in donkey serum 5% BSA 2% and MOM 1/40 for 1 hour. Every step was performed at room temperature, unless indicated otherwise. Cryosections were then incubated with antibodies as described above except that primary (anti-Pax7; 1/50, mouse, DSHB) and secondary antibodies were diluted in blocking buffer containing donkey serum 5% and BSA 2%.

Image capture and analysis

Ten to fifteen images were recorded from each section with an Imager Z1 Zeiss microscope at 20x magnification connected to a CoolSNAP MYO camera for the quantification of the number of $PCM1^+$ nuclei *per* fiber and $Pax7^+$ cells using ImageJ software. The number of nuclei positive for PCM1 (*i.e.*, considered as myonuclei, (Winje *et al.*, 2018)) was divided by the number of fibers analyzed on the same picture. The number of $Pax7^+$ cells was also divided by the number of fibers analyzed on the same picture (Theret *et al.*, 2017). For whole cryosection analysis, slides were automatically scanned at × 10 of magnification using an Axio Observer.Z1 (Zeiss) connected to a CoolSNAP HQ2 CCD Camera (photometrics). The image of the whole cryosection was automatically reconstituted in MetaMorph Software (Desgeorges *et al.*, 2019).

The number of IgG positive fibers (*i.e.*, based on staining with cy3 anti-mouse), embryonic MyHC positive fibers and myofibers with central nuclei were quantified on the whole section and normalized to the total number of myofibers. Myofiber cross-sectional area (CSA) was determined on whole gastrocnemius muscle sections labeled by anti-laminin antibody using the Open-CSAM program, as previously described (Desgeorges *et al.*, 2019).

Statistical Analysis

Statistical analysis was performed using GraphPad Prism Software (version 9.0). Data distribution was initially investigated using Shapiro-Wilk test. Two-factor (group x time) analysis of variance (ANOVAs) with repeated measures on time was used to compare maximal tetanic force during the short-term NMES training protocol. Unpaired student t-test or Mann-Whitney was used to assess differences between control and NMES mice for other variables. Data are presented as mean ± SD with significance set at $p < 0.05$.

RESULTS

Individualization and monitoring of NMES training program

Thanks to our original device allowing for longitudinal force recordings in response to electrical stimulation applied on the surface of the plantar flexor muscles (Fig. 1A & Supplemental video 1), F_{max} was recorded at the beginning of each NMES training session for each NMES trained mouse (Fig. 1B). Then, the current intensity was carefully adjusted to reach 15% of F_{max} on the basis of a 250-ms testing train delivered at 50 Hz (Fig. 1C). The corresponding current intensity was applied for the first 10 stimulation trains and was increased every 10 stimulation trains by 50% of the initial current intensity. This strategy allowed to minimize the reduction of force production due to the repeated application of electrical pulses (Fig. 1D) and to maintain a mean force production (*i.e.*, training intensity) around 15% of F_{max} for each NMES session. The training intensity expressed in percentage of F_{max} slightly varied between mice and between sessions (Supplemental Fig. 1). For the short-NMES training program (Fig.1E), the mean training intensity was 12.6 ± 2.7% of F_{max} and 13.6 ± 2.6% of F_{max} in C57BL/6J and BALB/c mice, respectively. For the long-NMES training program (Fig.1F), the mean training intensity was 12.3 ± 2.4% of F_{max} and 12.6 ± 4.0% of F_{max} in C57BL/6J and BALB/c mice, respectively. For both NMES training programs and mouse strains, the mean current intensity ranged from 3.7 ± 1.3 mA to 5.5 ± 1.4 mA.

Short-term NMES training promotes myonuclear accretion and increases MuSC content

Gastrocnemius cryosections were immunostained for PCM1, laminin and Hoechst in both NMES and control mice in order to specifically label myonuclei (Fig. 2A-B) (Winje *et al.*, 2018) and to evaluate the effects of the above described individualized NMES training sessions on myonuclear accretion. The number of myonuclei *per* fiber was higher in C57BL/6J (+15%, $P<0.05$) and tended to increase in BALB/c (+15%, $P=0.10$) NMES trained mice as compared with controls, respectively (Fig. 2C-D). These results clearly demonstrate that a short-term NMES training protocol performed at a submaximal mean force level of ∼15% of F_{max} leads to myonuclear accretion.

Next, we investigated whether NMES-induced myonuclear accretion was also associated with an increased number of MuSCs. *Gastrocnemius* cryosections were immunostained for Pax7 to label MuSCs in both NMES and control mice (Fig. 3A-B; arrowheads). The number of $Pax7^+$

related to the number of myofibers was higher in C57BL/6J (+67%, P<0.001) and tended to increase (+48%, P=0.11) in BALB/c NMES trained mice as compared with controls, respectively (Fig. 3C-D). This indicates that NMES increases the MuSC content in the two different mouse strains.

Short-term NMES training does not induce overt signs of muscle damage

Considering that myonuclear accretion may be driven by muscle damage and/or regeneration (Murach *et al.*, 2020*a*), we immunostained IgG trapping on *gastrocnemius* cryosections of both NMES and control mice as an index of increased membrane permeability (Supplemental Fig. 2A-B). The proportion of myofibers positive for IgG was negligible in both NMES and control mice (*i.e.*, < 0.5%) (Fig. 4A-B; Supplemental Fig. 2A-B), showing that NMES did not induce membrane leakage. We also investigated whether signs of muscle regeneration can be observed in *gastrocnemius* muscles of both NMES and control mice. Cryosections were immunostained for embryonic MyHC (eMyHC) that labels newly formed myofibers. The proportion of myofibers positive for eMyHC was counted on the whole section. The percentage of myofibers positive for eMyHC was very low (*i.e.*, < 1%) in both control and NMES mice of the two different mouse strains (Fig. 4C-D; Supplemental Fig. 2C-D). Finally, we counted the number of myofibers with central nuclei, as central positioning of nuclei in myofibers is commonly used as a marker of regeneration (Matsuda *et al.*, 1983). In agreement with the eMyHC staining, the percentage of myofibers with central nuclei was very low (*i.e.*, < 1-2%) in all mice (Fig. 4E-F). Overall, on the basis of those three different markers of muscle damage/regeneration, our results illustrate the non-damaging effects of a short-term NMES protocol on *gastrocnemius* muscle.

Short-term NMES training does not induce muscle hypertrophy or force improvement

Considering that myonuclear accretion has been reported as an early event occurring before (or in absence of) muscle hypertrophy (Bruusgaard *et al.*, 2010; Goh *et al.*, 2019; Masschelein *et al.*, 2020), *gastrocnemius* muscle weight and myofiber CSA were quantified in both control and NMES mice as indices of muscle hypertrophy. These two parameters were not significantly different between control and NMES mice in the two mouse strains, indicating that short-term NMES-induced myonuclear accretion was not associated with an increase in muscle mass and myofiber size (Fig. 5A-D).

Finally, we investigated whether the changes in both myonuclear and MuSC content might have a functional effect in terms of muscle force production. Maximal tetanic force (*i.e.*, F_{max}) was recorded longitudinally in both control and NMES mice throughout the duration of the experiment (*i.e.*, Fig. 1E). Our functional analysis reveals that short-term NMES did not increase muscle force in either C57BL/6J and BALB/c mice (Fig. 5E-F).

Long-term NMES training promotes myonuclear accretion and muscle hypertrophy in the absence of overt signs of muscle damage/regeneration

On the basis of the robust myonuclear accretion induced by a short-term NMES training program, we next assessed whether a longer NMES training program could result in muscle hypertrophy in mice. Twelve NMES training sessions were delivered over a 3-week period (Fig. 1F) in the two mouse strains. In agreement with the results obtained after short-term NMES training, the number of myonuclei *per* fiber significantly increased by 16% ($P<0.01$) and by 27% ($P<0.001$) in C57BL/6J and BALB/c NMES trained mice as compared with controls, respectively (Fig. 6A-B). In the same way, the number of $Pax7^+$ cells *per* myofibers increased by 54% ($P<0.01$) and by 37% ($P<0.01$) in C57BL/6J and BALB/c NMES trained mice as compared with controls, respectively (Fig. 6C-D). Interestingly, the magnitude of changes for both the number of myonuclei and $Pax7^+$ cells was roughly similar than that observed after short-NMES training, indicating NMES-induced myonuclear accretion and increase in MuSC content were independent of the training duration.

Then, we investigated whether myonuclear accretion induced by the long-term NMES training protocol was associated with muscle hypertrophy. We found that NMES induced a significant shift towards a higher proportion of myofiber with large CSA in the two mouse strains (Fig. 6E-F), illustrating muscle hypertrophy. However, these changes in myofiber CSA were not associated with a significant variation in both *gastrocnemius* muscle mass and force production between controls and NMES mice (Fig. 6G-J).

In agreement with the results obtained in response to the short-term NMES training protocol, the proportion of myofibers positive for IgG or for eMyHC was negligible (*i.e.*, < 0.5%) in both control and NMES trained mice. Finally, the percentage of myofibers with central nuclei was very low (*i.e.*, ∼1-3%) and not significantly different between control and NMES mice, which further confirms the absence of overt signs of muscle injury/regeneration even after a longer NMES training program.

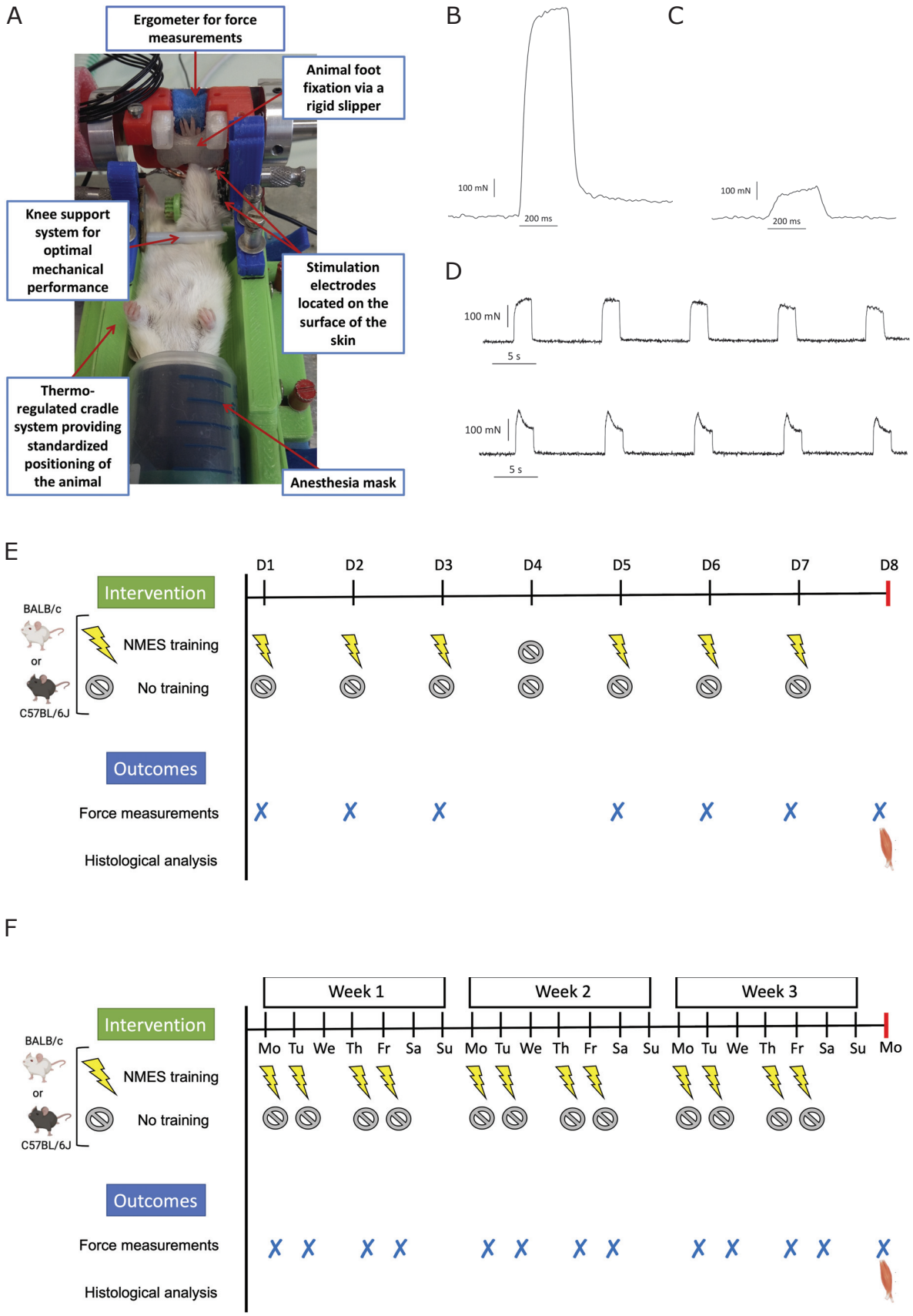
A
Ergometer for force measurements
Animal foot fixation via a rigid slipper
Knee support system for optimal mechanical performance
Stimulation electrodes located on the surface of the skin
Thermo-regulated cradle system providing standardized positioning of the animal
Anesthesia mask
B
100 mN
200 ms
C
100 mN
200 ms
D
100 mN
5 s
100 mN
5 s
E
D1
D2
D3
D4
D5
D6
D7
D8
Intervention
BALB/c
or
C57BL/6J
NMES training
No training
Outcomes
Force measurements
Histological analysis
F
Week 1
Week 2
Week 3
Mo Tu We Th Fr Sa Su Mo Tu We Th Fr Sa Su Mo Tu We Th Fr Sa Su Mo
Intervention
BALB/c
or
C57BL/6J
NMES training
No training
Outcomes
Force measurements
Histological analysis

FIGURE 1

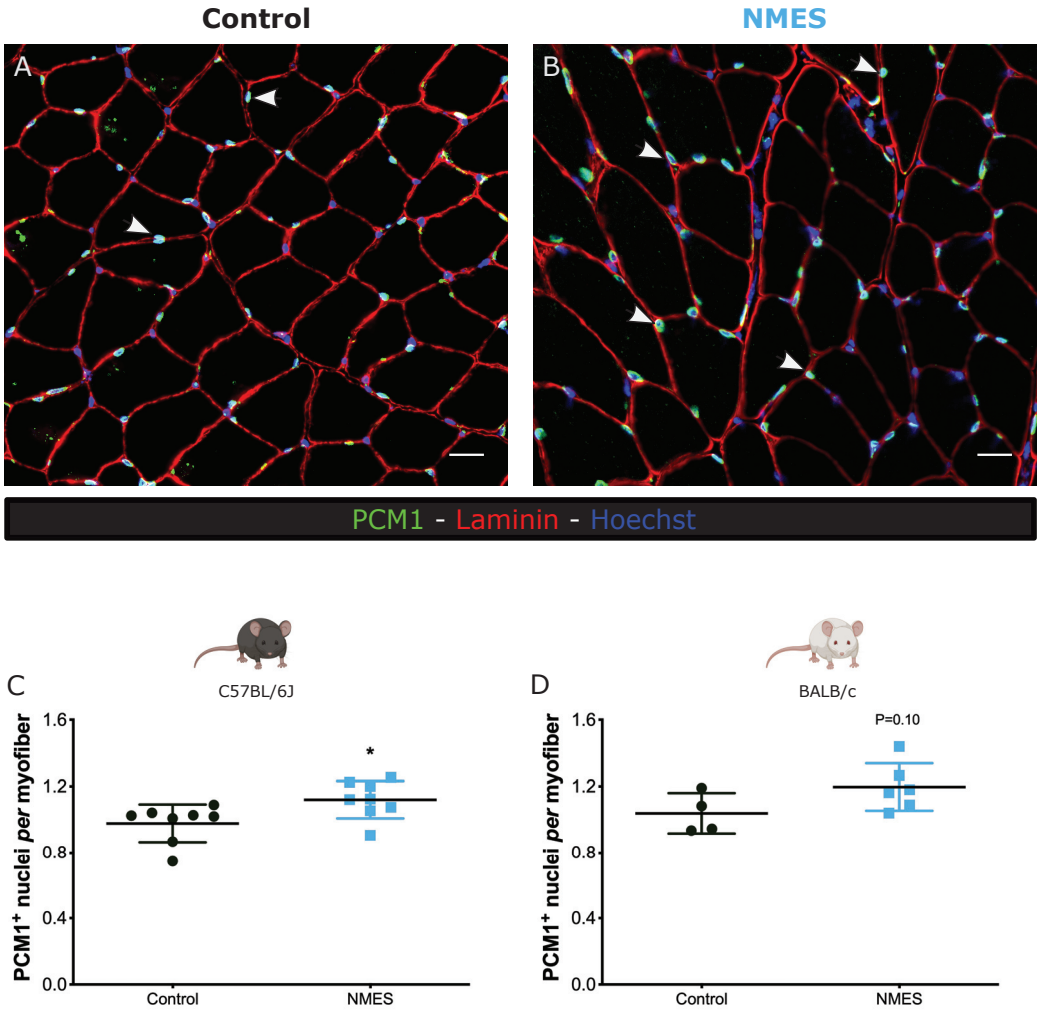
Control
NMES
A
B
PCM1 - Laminin - Hoechst
C
C57BL/6J
PCM1⁺ nuclei per myofiber
1.6
1.2
0.8
0.4
0.0
*
Control
NMES
D
BALB/c
P=0.10
PCM1⁺ nuclei per myofiber
1.6
1.2
0.8
0.4
0.0
Control
NMES

FIGURE 2

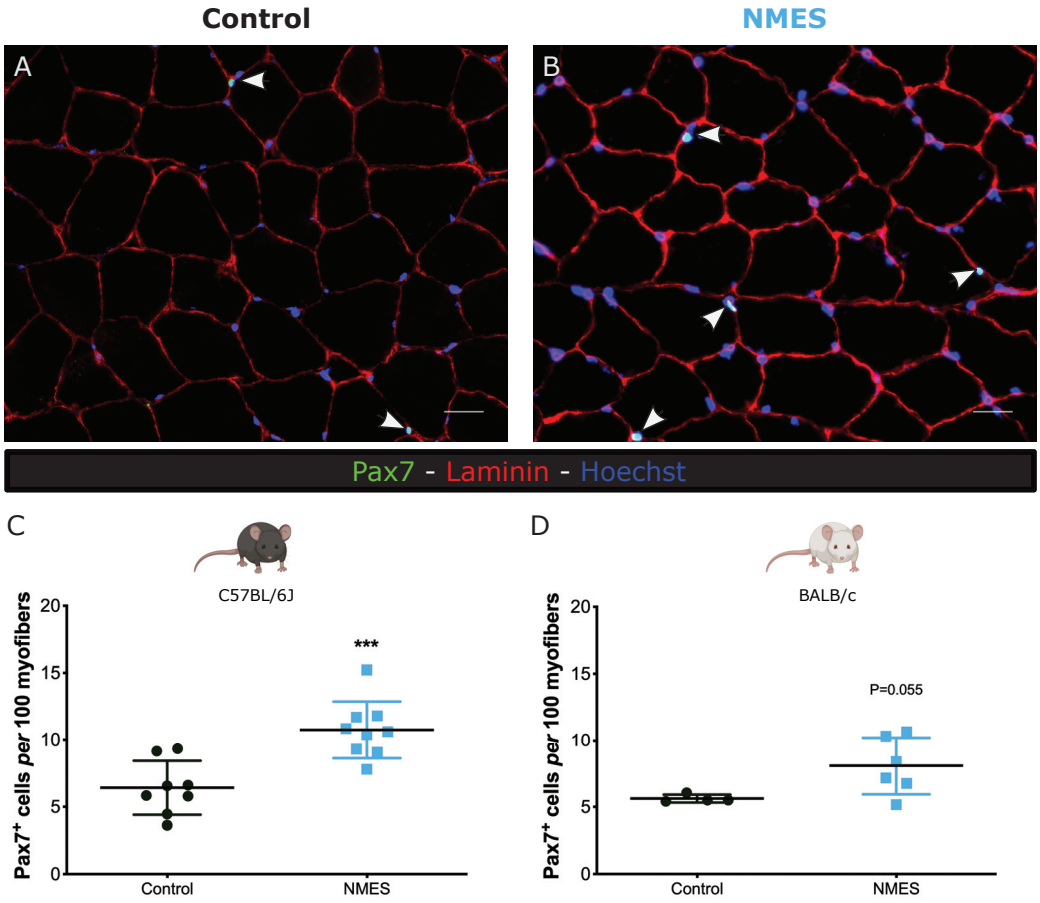
Control
NMES
A
B
Pax7 - Laminin - Hoechst
C
C57BL/6J
***
Pax7+ cells per 100 myofibers
20
15
10
5
0
Control
NMES
D
BALB/c
P=0.055
Pax7+ cells per 100 myofibers
20
15
10
5
0
Control
NMES

FIGURE 3

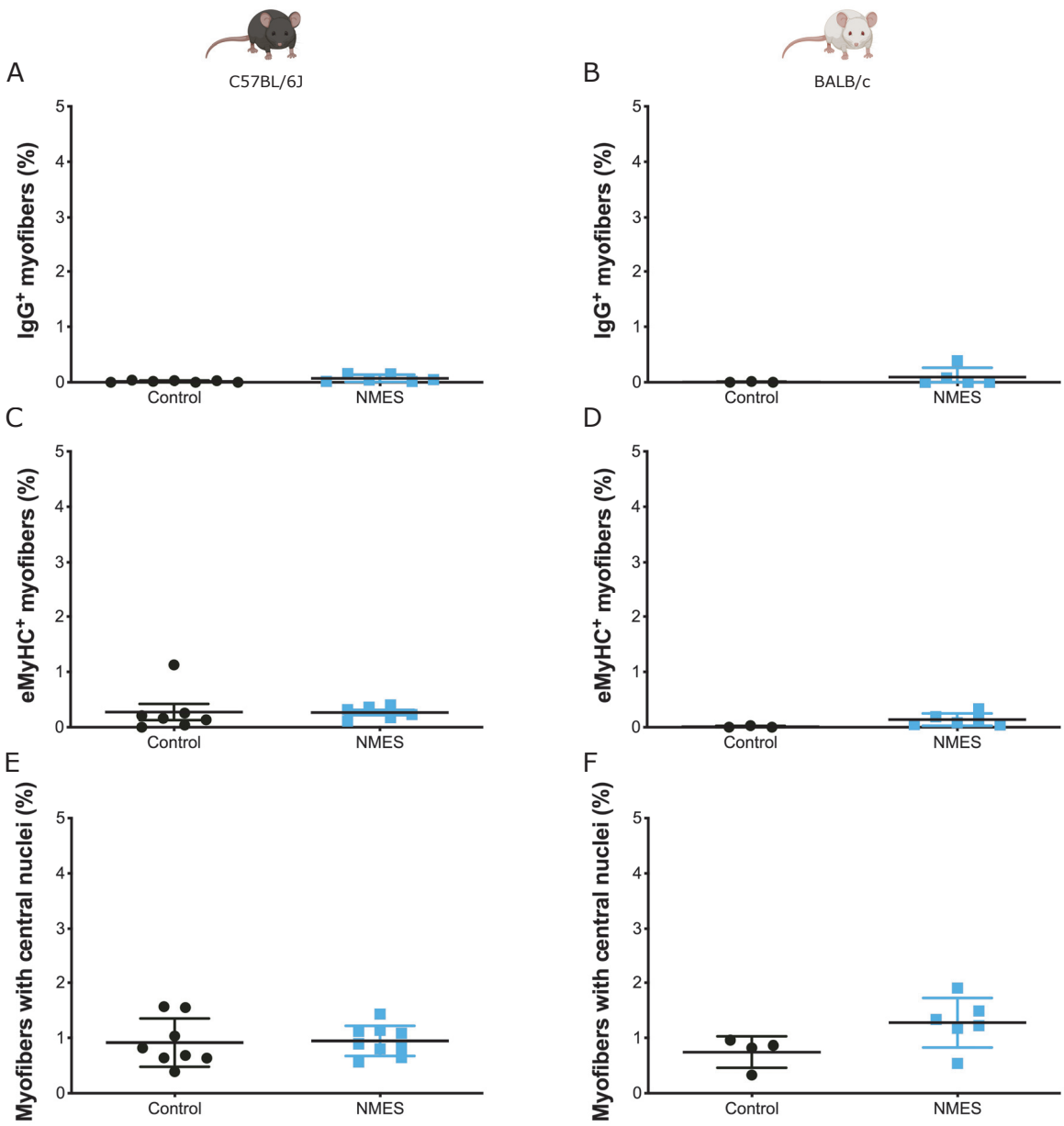
A
C57BL/6J
B
BALB/c
IgG+ myofibers (%)
C
eMyHC+ myofibers (%)
D
E
Myofibers with central nuclei (%)
F
Control
NMES
0
1
2
3
4
5

FIGURE 4

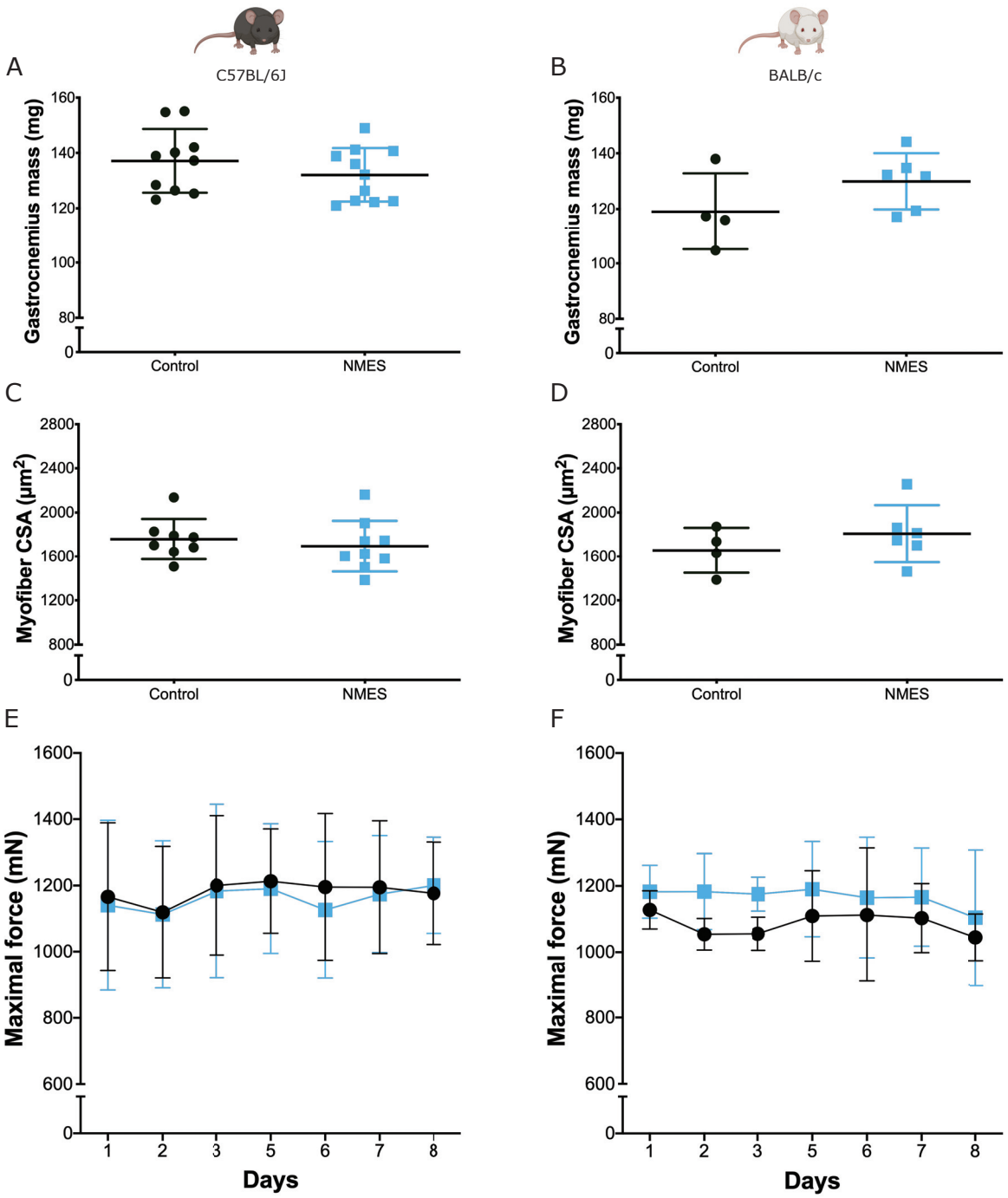
A
C57BL/6J
Gastrocnemius mass (mg)
160
140
120
100
80
0
Control
NMES
B
BALB/c
Gastrocnemius mass (mg)
160
140
120
100
80
0
Control
NMES
C
Myofiber CSA (µm²)
2800
2400
2000
1600
1200
800
0
Control
NMES
D
Myofiber CSA (µm²)
2800
2400
2000
1600
1200
800
0
Control
NMES
E
Maximal force (mN)
1600
1400
1200
1000
800
600
0
1
2
3
5
6
7
8
Days
F
Maximal force (mN)
1600
1400
1200
1000
800
600
0
1
2
3
5
6
7
8
Days

FIGURE 5

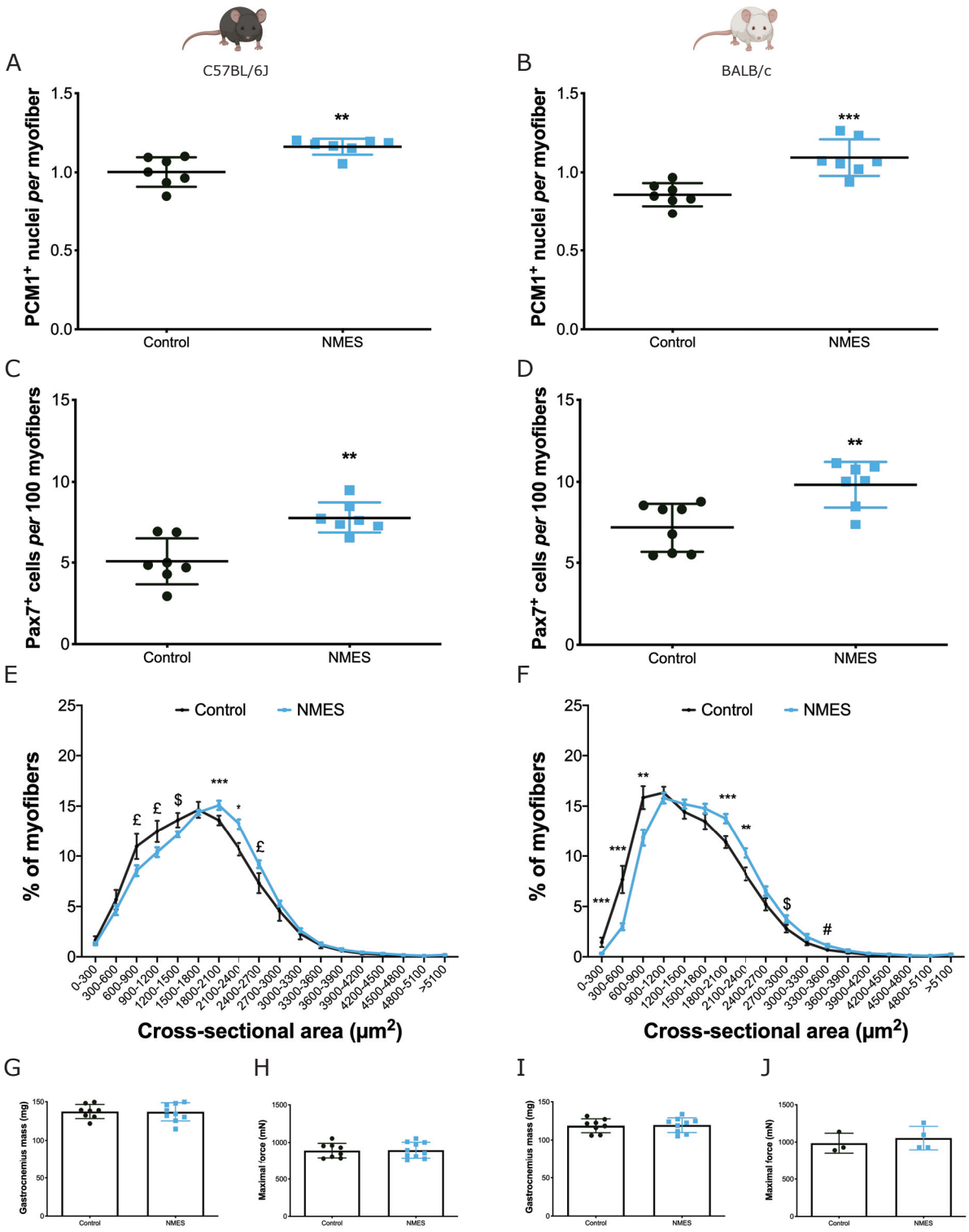
A
C57BL/6J
PCM1⁺ nuclei per myofiber
Control
NMES
B
BALB/c
C
Pax7⁺ cells per 100 myofibers
D
E
% of myofibers
Cross-sectional area (µm²)
F
G
Gastrocnemius mass (mg)
H
Maximal force (mN)
I
J

FIGURE 6

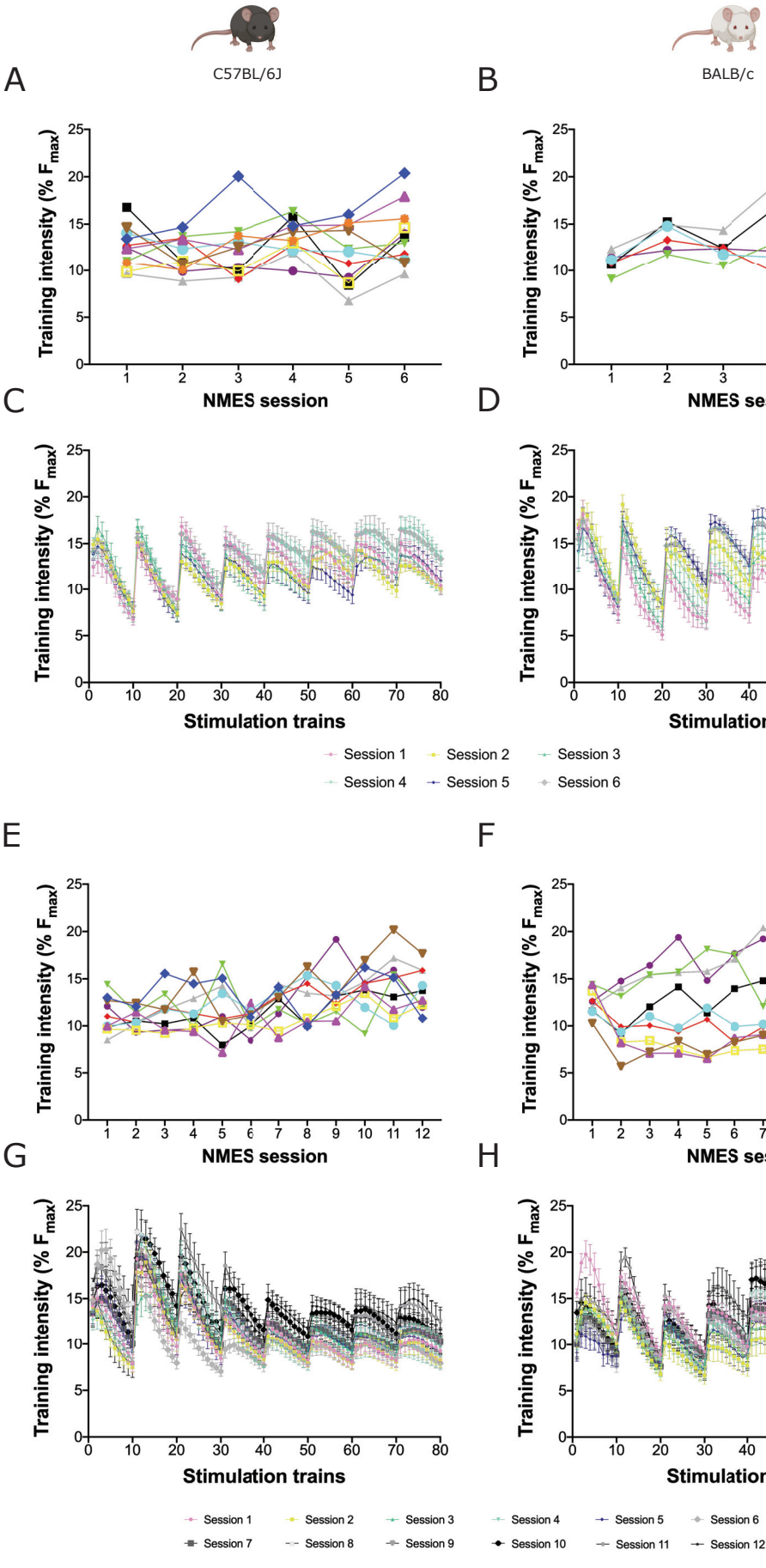

SUPPLEMENTAL FIGURE 1

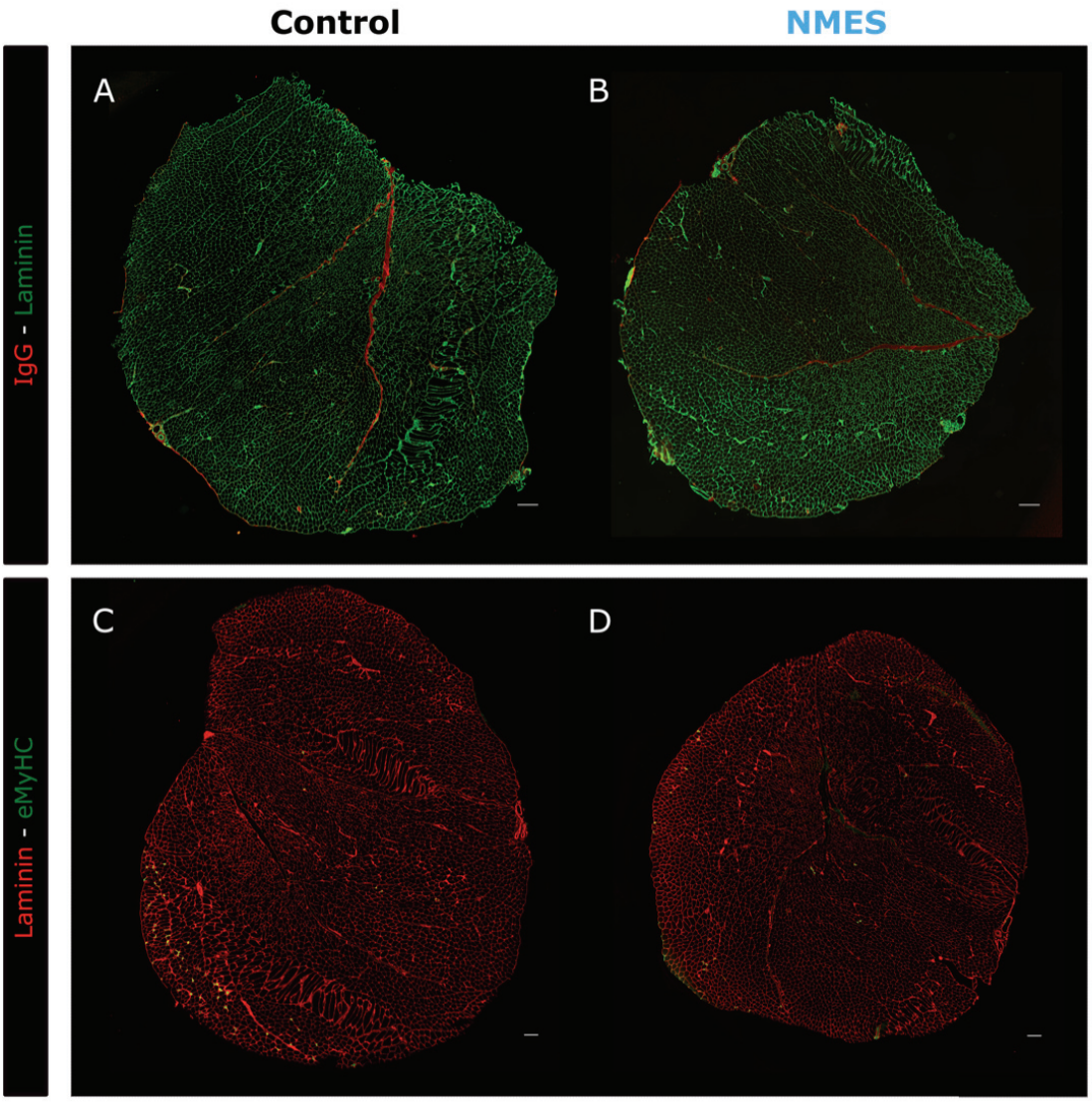

SUPPLEMENTAL FIGURE 2

Figure legends

Figure 1 – **A)** Experimental device allowing for non-invasive longitudinal force measurements and individualized neuromuscular electrical stimulation (NMES) training protocol in response to electrical stimuli applied over the plantar flexor muscle belly. **B)** Typical mechanical trace obtained in response to a 250-ms 100 Hz tetanic stimulation train allowing for maximal isometric force production measurement. **C)** Typical mechanical trace obtained in response to a 250-ms 50 Hz subtetanic stimulation train allowing for the determination of the training intensity corresponding to 15% of maximal isometric force. **D)** Typical mechanical traces obtained during the first five (top) and last five (bottom) stimulation trains during a typical NMES training session. **E)** Schematic representation of the short-term NMES training protocol. C57BL/6J or BALB/c were submitted to either 6 individualized NMES training sessions or a control intervention over a 8-day period. Maximal force production was recorded at the beginning of each NMES or control interventions as well as at day 8. Then, animals were sacrificed and *gastrocnemius* muscle was harvested. **F)** Schematic representation of the long-term NMES training protocol. C57BL/6J or BALB/c were submitted to either 12 individualized NMES training sessions or a control intervention over a 3-week period. Maximal force production was recorded at the beginning of each NMES or control interventions as well as at 3 days after the last training session. Then, animals were sacrificed and *gastrocnemius* muscle was harvested.

Figure 2 – **A-B)** Immunostaining for laminin (red), PCM1 (green) and Hoechst (blue) on *gastrocnemius* muscle section from mice submitted either to the control procedure or to the short-term NMES training program (*i.e.*, 6 sessions). Arrowheads show myonuclei, *i.e.*, nuclei positive for PCM1. Scale bar = 25 µm. **C)** Number of myonuclei (*i.e.*, $PCM1^+$ nuclei) *per* myofiber in C57BL/6J mice submitted either to the control procedure (n=8) or to the short-term NMES training program (n=8). **D)** Number of myonuclei (*i.e.*, $PCM1^+$ nuclei) *per* myofiber in BALB/c mice submitted either to the control procedure (n=4) or to the short-term NMES training program (n=6). Significantly different from control: $^*P< 0.05$. Data were obtained from two to three separate experiments Values are reported as mean ± SD.

Figure 3 – **A-B)** Immunostaining for laminin (red), Pax7 (green) and Hoechst (blue) on *gastrocnemius* muscle section from mice submitted either to the control procedure or to the short-term NMES training program (*i.e.*, 6 sessions). Arrowheads show $Pax7^+$ cells. Scale bar = 25 µm. **C)** Number of $Pax7^+$ cells *per* 100 myofibers in C57BL/6J mice submitted either to the control procedure (n=8) or to the short-term NMES training program (n=9). **D)** Number of $Pax7^+$ cells *per* 100 myofibers in BALB/c mice submitted either to the control procedure (n=4) or to the short-term NMES training program (n=6). Significantly different from control: $^{***}P<0.001$. Data were obtained from two to three separate experiments. Values are reported as mean ± SD.

Figure 4 – **A)** Proportion of myofibers positive for IgG in C57BL/6J mice submitted either to the control procedure (n=7) or to the short-term NMES training program (*i.e.*, 6 sessions, n=6). **B)** Proportion of myofibers positive for IgG in BALB/c mice submitted either to the control procedure (n=3) or to the short-term NMES training program (n=5). **C)** Proportion of myofibers positive for embryonic myosin heavy chain in C57BL/6J mice submitted either to the control procedure (n=7) or to the short-term NMES training program (n=6). **D)** Proportion of myofibers positive for embryonic myosin heavy chain in BALB/c mice submitted either to the control procedure (n=3) or to the short-term NMES training program (n=6). **E)** Proportion of myofibers with central nuclei in C57BL/6J mice submitted either to the control procedure (n=8) or to the short-term NMES training program (n=9). **F)** Proportion of myofibers with central nuclei in mice submitted either to the control procedure (n=4) or to the short-term NMES training program (n=6). Data were obtained from two to three separate experiments. Values are reported as mean ± SD.

Figure 5 – **A)** *Gastrocnemius* muscle weight of C57BL/6J mice submitted either to the control procedure (n=10) or to the short-term NMES training program (*i.e.*, 6 sessions, n=11). **B)** *Gastrocnemius* muscle weight of BALB/c mice submitted either to the control procedure (n=4) or to the short-term NMES training program (n=6). **C)** *Gastrocnemius* myofiber cross-sectional area of C57BL/6J mice submitted either to the control procedure (n=8) or to the short-term NMES training program (n=9). **D)** *Gastrocnemius* myofiber cross-sectional area of BALB/c mice submitted either to the control procedure (n=4) or to the short-term NMES training program

(n=6). **E)** Maximal isometric force production longitudinally recorded throughout the study design in C57BL/6J mice submitted either to the control procedure (n=10; black circles) or to the short-term NMES training program (n=11; blue squares). **F)** Maximal isometric force production longitudinally recorded throughout the study design in BALB/c mice submitted either to the control procedure (n=4; black circles) or to the short-term NMES training program (n=6; blue squares). Data were obtained from two to three separate experiments. Values are reported as mean ± SD.

Figure 6 – **A)** Number of myonuclei (*i.e.*, $PCM1^+$ nuclei) *per* myofiber in C57BL/6J mice submitted either to the control procedure (n=7) or to the long-term NMES training program (*i.e.*, 12 sessions, n=7). **B)** Number of myonuclei (*i.e.*, $PCM1^+$ nuclei) *per* myofiber in BALB/c mice submitted either to the control procedure (n=7) or to the long-term NMES training program (n=7). **C)** Number of $Pax7^+$ cells *per* 100 myofibers in C57BL/6J mice submitted either to the control procedure (n=7) or to the long-term NMES training program (n=7). **D)** Number of $Pax7^+$ cells *per* 100 myofibers in BALB/c mice submitted either to the control procedure (n=8) or to the long-term NMES training program (n=7). **E)** *Gastrocnemius* myofiber cross-sectional area distribution in C57BL/6J mice submitted either to the control procedure (n=8) or to the long-term NMES training program (n=8). **F)** *Gastrocnemius* myofiber cross-sectional area distribution in BALB/c mice submitted either to the control procedure (n=8) or to the long-term NMES training program (n=9). **G-H)** *Gastrocnemius* muscle mass and force production in C57BL/6J mice submitted either to the control procedure (n=8) or to the long-term NMES training program (n=10). **I-J)** *Gastrocnemius* muscle mass and force production in BALB/c mice submitted either to the control procedure (n=8 and n= 3, respectively) or to the long-term NMES training program (n=9 and n=4, respectively). Significantly different from control: $^{*}P< 0.05$, $^{**}P< 0.01$; $^{***}P<0.001$. $^{\#}P=0.06$; $^{\$}P=0.08$; $^{£}P=0.09$. Data were obtained from two to three separate experiments. Values are reported as mean ± SD expect for myofiber cross-sectional area distribution where values are reported as mean ± SEM for the sake of clarity.

Supplemental Materials

Supplemental video 1. A video clip illustrating the positioning of a BALC/c mouse in the ergometer. The application of electrode cream on the right plantar flexor muscles as well as the position of the foot on the pedal are also shown.

Supplemental Figure 1. A-B) Individual training intensity (expressed in percentage of maximal isometric force) obtained during each session of the short-term NMES training protocol in C57BL/6J (n=11) and BALB/c mice (n=6). Each symbol represents an individual mouse. **C-D)** Mean training intensity (expressed in percentage of maximal isometric force) obtained during each session of the short-term NMES training protocol throughout the 80 stimulation trains in C57BL/6J (n=11) and BALB/c mice (n=6). **E-F)** Individual training intensity (expressed in percentage of maximal isometric force) obtained during each session of the long-term NMES training protocol in C57BL/6J (n=10) and BALB/c mice (n=9). Note that session #8 of one C57BL/6J mouse was not recorded due to technical issue. Each symbol represents an individual mouse. **G-H)** Mean training intensity (expressed in percentage of maximal isometric force) obtained during each session of the long-term NMES training protocol in C57BL/6J (n=10) and BALB/c mice (n=9). Data were obtained from two to three separate experiments. Values are reported as mean ± SD.

Supplemental Figure 2. A-B) Immunostaining for IgG (red) and laminin (green) on *gastrocnemius* muscle section from C57BL/6J control and NMES trained mice. Scale bar = 250 µm. **C-D)** Immunostaining for laminin (red) and embryonic myosin heavy chain (green) on *gastrocnemius* muscle section from C57BL/6J control and NMES trained mice. Scale bar = 250 µm.

DISCUSSION

In the present study, we took advantage of our original device allowing for non-invasive force measurements in response to electrical stimuli applied over the plantar flexor muscle belly to design individualized and carefully monitored isometric NMES training sessions in two mouse strains. We observed a robust myonuclear accretion and higher MuSC content in two mouse strains, without overt signs of muscle damage/regeneration. We further demonstrated that NMES-induced myonuclear accretion is an early event preceding muscle hypertrophy.

The individualized isometric NMES training programs led to a robust myonuclear accretion as illustrated by the ∼15-27% increase in number of myonuclei *per* myofiber in C57BL/6J and BALB/c mice, respectively. These results are consistent with the ∼15-25% increase in myonuclei *per* fiber reported in various muscles (*e.g., soleus*, *gastrocnemius*, *plantaris*) after voluntary wheel running (Dungan *et al.*, 2019; Masschelein *et al.*, 2020) or high-intensity interval treadmill (Goh *et al.*, 2019). However, it is worth noting that the rate of myonuclear accretion is higher after NMES than after running exercise. Indeed, the duration of NMES-induced contractile activity was less than 3 min *per* session (*i.e.*, 80 stimulation trains lasting 2 s) for a total contractile activity of ∼16-32 min over a one-to three-week training period while treadmill or wheel running exercises usually involve 60-300 min session duration with 3-7 sessions *per* week for ∼8 weeks (Goh *et al.*, 2019; Masschelein *et al.*, 2020; Murach *et al.*, 2020*a*). One can therefore estimate that the increase of myonuclei *per* fiber *per* min of stimulation/exercise is ∼100-fold higher after NMES as compared with running exercise. Interestingly, NMES-induced myonuclear accretion was associated with a large increase in the number of MuSCs present in the trained muscle (*i.e.*, +∼40-70%). This is also consistent with the results obtained after voluntary wheel running (+44% (Dungan *et al.*, 2019)), even though the rate of changes in MuSC content is also more pronounced after NMES as compared with running protocols. Our innovative NMES training protocol appears therefore as a method of choice for investigating the contribution of MuSCs to myonuclear accretion. The use of genetically engineered mouse models ablated for MuSCs (McCarthy *et al.*, 2011; Egner *et al.*, 2016), deleted for transcription factors involved in MuSC myogenesis (Goh & Millay, 2017; Fukuda *et al.*, 2019) or in myofiber homeostasis (Noviello *et al.*, 2022) would allow to decipher MuSC communication with myofibers (Murach *et al.*, 2020*b*) in response to NMES .

The present study also demonstrates that NMES-induced myonuclear accretion occurs in the absence of overt signs of muscle damage/regeneration whatever the training duration. Indeed, the proportion of myofibers positive either for IgG labeling or embryonic MyHC (*i.e.*, < 0.5-1%) as well as the percentage of myofibers with central nuclei was very low (*i.e.*, ∼1-3%) after NMES and was never different between control and NMES mice, independent of their genetic background. On the contrary, around 30% of myofibers displayed centrally located nuclei in response to synergist ablation-induced muscle hypertrophy (McCarthy *et al.*, 2011). Furthermore, the proportion of myofibers with central nuclei was significantly higher in trained mice as compared with control animals in response to wheel running exercise (Masschelein *et al.*, 2020; Murach *et al.*, 2020*a*) and reached a mean value of ∼5-8% (range: ∼2-10% in the *soleus* muscle; (Murach *et al.*, 2020*a*)) with (Murach *et al.*, 2020*a*) or without (Masschelein *et al.*, 2020) the co-expression of embryonic MyHC. This indicates that the individualized isometric NMES training protocol performed at low force levels (*i.e.*, ∼15% of F_{max}) can be considered as a non-damaging modality of increased mechanical loading, whereas running exercise contains a component of damaging eccentric contractions. This is further supported by our functional analyses showing that NMES does not lead to acute force reduction (*i.e.*, after a single NMES training session, see Fig. 5E-F), this parameter being considered as the best indirect marker of muscle damage (Warren *et al.*, 1999). Our data therefore show for the first time that myonuclear accretion is primarily mediated by NMES-induced myofiber contractile activity rather than by muscle damage. The increase in MuSC content after NMES indicates that MuSC can sense changes in muscle activity and that necrosis/massive damage are not required for MuSC expansion (Darr & Schultz, 1987; Fukuda *et al.*, 2019). Our findings are in agreement with recent studies showing differences in MuSC dynamics during muscle regeneration and overload (Fukuda *et al.*, 2019; Fukada *et al.*, 2022). Indeed, and contrarily to what is usually observed during muscle regeneration, muscle overload led to MuSC proliferation in the absence of detectable MyoD protein expression (Fukada *et al.*, 2022). It is however noteworthy that these results were obtained in a mouse model of tenotomy which induces a strong mechanical stimulus as illustrated by the large increase in muscle mass (Fukuda *et al.*, 2019). In the present study, NMES training was performed at a mild mechanical intensity corresponding to a mean force level of ∼15% F_{max}, illustrating the sensitivity of MuSCs to detect subtle changes in myofiber contractile activity.

We further demonstrate that NMES-induced myonuclear accretion is an early event occurring before muscle hypertrophy. Indeed, while mice submitted to the short-term NMES training protocol showed an increase in the number of myonuclei without any changes in myofiber CSA, the longer NMES training protocol led to both myonuclear accretion and increased proportion of myofiber with large CSA in the two mouse strains. This is in agreement with previous studies showing that myonuclear accretion precedes muscle hypertrophy in response to mechanical overload (Bruusgaard *et al.*, 2010) or treadmill exercise (Goh & Millay, 2017). Overall, NMES-induced myonuclear accretion and muscle hypertrophy would be relevant to further identify the cellular and molecular mechanisms involved in MuSC regulation (*i.e.*, from activation to fusion) in overloaded muscle (Goh & Millay, 2017; Fukuda *et al.*, 2019). In addition, it would allow to decipher the role of cell-cell interactions (Peck *et al.*, 2022; Kaneshige *et al.*, 2022) and related secreted factors (Serrano *et al.*, 2008; Guerci *et al.*, 2012; Noviello *et al.*, 2022) in a physiological context of muscle hypertrophy. Finally, our NMES training protocol could be of interest to further improve our understanding on the role of muscle memory in the context of muscle adaptations, *i.e.*, to assess whether myonuclei gained during hypertrophy are lost during detraining (Venturelli *et al.*, 2019; Snijders *et al.*, 2020; Kirby & Dupont-Versteegden, 2022; Schwartz & Gundersen, 2022).

In the present study, experiments were performed in mice with two different genetic backgrounds (*i.e.*, C57BL/6J and BALB/c) that are commonly used to investigate the impact of cancer cachexia (thanks to the inoculation of LLC or C26 tumor cells; (Gallot *et al.*, 2014; Penna *et al.*, 2016)) or sepsis (*i.e.*, using cecal ligation and puncture (Morel *et al.*, 2017)) on skeletal muscle homeostasis. Indeed, recent evidence is emerging regarding the key role of defective regulation of MuSCs on cancer cachexia- (He *et al.*, 2013) or sepsis-induced (Rocheteau *et al.*, 2015) muscle atrophy. On that basis, NMES could be a relevant method to promote MuSC fusion in these two pathological contexts. However, additional investigations are warranted to determine whether and to what extent NMES is a relevant non-pharmacological approach to minimize the deleterious consequences of cancer cachexia or sepsis on the regulation of MuSCs. In addition, considering the widespread use of NMES in chronic diseases (Maddocks *et al.*, 2016; Jones *et al.*, 2016), our work paves the way of identifying the cellular and molecular adaptations to this artificial training method in severely deconditioned patients.

In conclusion, we demonstrate that an individualized and carefully-controlled isometric NMES training protocol promotes a robust myonuclear accretion, an increase in MuSC content and muscle hypertrophy without inducing muscle damage/regeneration. We show for the first time that myonuclear accretion is primarily driven by increased mechanical loading rather than muscle injury. NMES-induced myonuclear accretion will be of utmost interest to further understand the role of MuSCs in skeletal muscle plasticity.

REFERENCES

Bruusgaard JC, Johansen IB, Egner IM, Rana ZA & Gundersen K (2010). Myonuclei acquired by overload exercise precede hypertrophy and are not lost on detraining. *Proc Natl Acad Sci U S A* **107,** 15111–15116.

Darr KC & Schultz E (1987). Exercise-induced satellite cell activation in growing and mature skeletal muscle. *J Appl Physiol (1985)* **63,** 1816–1821.

Desgeorges T, Liot S, Lyon S, Bouvière J, Kemmel A, Trignol A, Rousseau D, Chapuis B, Gondin J, Mounier R, Chazaud B & Juban G (2019). Open-CSAM, a new tool for semi-automated analysis of myofiber cross-sectional area in regenerating adult skeletal muscle. *Skelet Muscle* **9,** 2.

Dungan CM, Murach KA, Frick KK, Jones SR, Crow SE, Englund DA, Vechetti IJ, Figueiredo VC, Levitan BM, Satin J, McCarthy JJ & Peterson CA (2019). Elevated myonuclear density during skeletal muscle hypertrophy in response to training is reversed during detraining. *Am J Physiol, Cell Physiol* **316,** C649–C654.

Egner IM, Bruusgaard JC & Gundersen K (2016). Satellite cell depletion prevents fiber hypertrophy in skeletal muscle. *Development* **143,** 2898–2906.

Englund DA, Figueiredo VC, Dungan CM, Murach KA, Peck BD, Petrosino JM, Brightwell CR, Dupont AM, Neal AC, Fry CS, Accornero F, McCarthy JJ & Peterson CA (2021). Satellite Cell Depletion Disrupts Transcriptional Coordination and Muscle Adaptation to Exercise. *Function (Oxf)* **2,** zqaa033.

Fry CS, Lee JD, Jackson JR, Kirby TJ, Stasko SA, Liu H, Dupont-Versteegden EE, McCarthy JJ & Peterson CA (2014). Regulation of the muscle fiber micro environment by activated satellite cells during hypertrophy. *FASEB j* **28,** 1654–1665.

Fukada S-I, Higashimoto T & Kaneshige A (2022). Differences in muscle satellite cell dynamics during muscle hypertrophy and regeneration. *Skelet Muscle* **12,** 17.

Fukuda S, Kaneshige A, Kaji T, Noguchi Y-T, Takemoto Y, Zhang L, Tsujikawa K, Kokubo H, Uezumi A, Maehara K, Harada A, Ohkawa Y & Fukada S-I (2019). Sustained expression of HeyL is critical for the proliferation of muscle stem cells in overloaded muscle. *Elife* **8,** e48284.

Gallot YS, Durieux A-C, Castells J, Desgeorges MM, Vernus B, Plantureux L, Rémond D, Jahnke VE, Lefai E, Dardevet D, Nemoz G, Schaeffer L, Bonnieu A & Freyssenet DG (2014). Myostatin gene inactivation prevents skeletal muscle wasting in cancer. *Cancer Res* **74,** 7344–7356.

Goh Q & Millay DP (2017). Requirement of myomaker-mediated stem cell fusion for skeletal muscle hypertrophy. *eLife* **6,** e20007.

Goh Q, Song T, Petrany MJ, Cramer AA, Sun C, Sadayappan S, Lee S-J & Millay DP (2019). Myonuclear accretion is a determinant of exercise-induced remodeling in skeletal muscle. *Elife* **8,** e44876.

Gondin, Giannesini B, Vilmen C, Le Fur Y, Cozzone PJ & Bendahan D (2011*a*). Effects of a single bout of isometric neuromuscular electrical stimulation on rat gastrocnemius muscle: a combined functional, biochemical and MRI investigation. *J Electromyogr Kinesiol* **21,** 525–532.

Gondin J, Brocca L, Bellinzona E, D'Antona G, Maffiuletti NA, Miotti D, Pellegrino MA & Bottinelli R (2011*b*). Neuromuscular electrical stimulation training induces atypical adaptations of the human skeletal muscle phenotype: a functional and proteomic analysis. *J Appl Physiol* **110,** 433–450.

Gondin J, Cozzone PJ & Bendahan D (2011*c*). Is high-frequency neuromuscular electrical stimulation a suitable tool for muscle performance improvement in both healthy humans and athletes? *Eur J Appl Physiol* **111,** 2473–2487.

Gondin J, Duclay J & Martin A (2006). Soleus- and gastrocnemii-evoked V-wave responses increase after neuromuscular electrical stimulation training. *J Neurophysiol* **95,** 3328–3335.

Gondin J, Guette M, Ballay Y & Martin A (2005). Electromyostimulation training effects on neural drive and muscle architecture. *Med Sci Sports Exerc* **37,** 1291–1299.

Guerci A, Lahoute C, Hébrard S, Collard L, Graindorge D, Favier M, Cagnard N, Batonnet-Pichon S, Précigout G, Garcia L, Tuil D, Daegelen D & Sotiropoulos A (2012). Srf-dependent paracrine signals produced by myofibers control satellite cell-mediated skeletal muscle hypertrophy. *Cell Metab* **15,** 25–37.

He WA, Berardi E, Cardillo VM, Acharyya S, Aulino P, Thomas-Ahner J, Wang J, Bloomston M, Muscarella P, Nau P, Shah N, Butchbach MER, Ladner K, Adamo S, Rudnicki MA, Keller C, Coletti D, Montanaro F & Guttridge DC (2013). NF-κB-mediated Pax7 dysregulation in the muscle microenvironment promotes cancer cachexia. *J Clin Invest* **123,** 4821–4835.

Jones S, Man WD-C, Gao W, Higginson IJ, Wilcock A & Maddocks M (2016). Neuromuscular electrical stimulation for muscle weakness in adults with advanced disease. *Cochrane Database Syst Rev* **10,** CD009419.

Kaneshige A, Kaji T, Zhang L, Saito H, Nakamura A, Kurosawa T, Ikemoto-Uezumi M, Tsujikawa K, Seno S, Hori M, Saito Y, Matozaki T, Maehara K, Ohkawa Y, Potente M, Watanabe S, Braun T, Uezumi A & Fukada S-I (2022). Relayed signaling between mesenchymal progenitors and muscle stem cells ensures adaptive stem cell response to increased mechanical load. *Cell Stem Cell* **29,** 265-280.e6.

Katz B (1939). The relation between force and speed in muscular contraction. *J Physiol* **96,** 45–64.

Kirby TJ & Dupont-Versteegden EE (2022). Cross Talk proposal: Myonuclei are lost with ageing and atrophy. *J Physiol* **600,** 2077–2080.

Lepper C, Partridge TA & Fan C-M (2011). An absolute requirement for Pax7-positive satellite cells in acute injury-induced skeletal muscle regeneration. *Development* **138,** 3639–3646.

Maddocks M, Nolan CM, Man WD-C, Polkey MI, Hart N, Gao W, Rafferty GF, Moxham J & Higginson IJ (2016). Neuromuscular electrical stimulation to improve exercise capacity in patients with severe COPD: a randomised double-blind, placebo-controlled trial. *Lancet Respir Med* **4,** 27–36.

Masschelein E, D'Hulst G, Zvick J, Hinte L, Soro-Arnaiz I, Gorski T, von Meyenn F, Bar-Nur O & De Bock K (2020). Exercise promotes satellite cell contribution to myofibers in a load-dependent manner. *Skelet Muscle* **10,** 21.

Matsuda R, Spector DH & Strohman RC (1983). Regenerating adult chicken skeletal muscle and satellite cell cultures express embryonic patterns of myosin and tropomyosin isoforms. *Dev Biol* **100,** 478–488.

McCarthy JJ, Mula J, Miyazaki M, Erfani R, Garrison K, Farooqui AB, Srikuea R, Lawson BA, Grimes B, Keller C, Van Zant G, Campbell KS, Esser KA, Dupont-Versteegden EE & Peterson CA (2011). Effective fiber hypertrophy in satellite cell-depleted skeletal muscle. *Development* **138,** 3657–3666.

Morel J, Palao J-C, Castells J, Desgeorges M, Busso T, Molliex S, Jahnke V, Del Carmine P, Gondin J, Arnould D, Cécile Durieux A & Freyssenet D (2017). Regulation of Akt-mTOR, ubiquitin-proteasome and autophagy-lysosome pathways in locomotor and respiratory muscles during experimental sepsis in mice. *Sci Rep* **7,** 10866.

Murach KA, Fry CS, Dupont-Versteegden EE, McCarthy JJ & Peterson CA (2021). Fusion and beyond: Satellite cell contributions to loading-induced skeletal muscle adaptation. *FASEB J* **35,** e21893.

Murach KA, Mobley CB, Zdunek CJ, Frick KK, Jones SR, McCarthy JJ, Peterson CA & Dungan CM (2020*a*). Muscle memory: myonuclear accretion, maintenance, morphology, and miRNA levels with training and detraining in adult mice. *J Cachexia Sarcopenia Muscle* **11,** 1705–1722.

Murach KA, Vechetti IJ, Van Pelt DW, Crow SE, Dungan CM, Figueiredo VC, Kosmac K, Fu X, Richards CI, Fry CS, McCarthy JJ & Peterson CA (2020*b*). Fusion-Independent Satellite Cell Communication to Muscle Fibers During Load-Induced Hypertrophy. *Function (Oxf)* **1,** zqaa009.

Murach KA, White SH, Wen Y, Ho A, Dupont-Versteegden EE, McCarthy JJ & Peterson CA (2017). Differential requirement for satellite cells during overload-induced muscle hypertrophy in growing versus mature mice. *Skelet Muscle* **7,** 14.

Murphy MM, Lawson JA, Mathew SJ, Hutcheson DA & Kardon G (2011). Satellite cells, connective tissue fibroblasts and their interactions are crucial for muscle regeneration. *Development* **138,** 3625–3637.

Noviello C, Kobon K, Delivry L, Guilbert T, Britto F, Julienne F, Maire P, Randrianarison-Huetz V & Sotiropoulos A (2022). RhoA within myofibers controls satellite cell microenvironment to allow hypertrophic growth. *iScience* **25,** 103616.

Peck BD, Murach KA, Walton RG, Simmons AJ, Long DE, Kosmac K, Dungan CM, Kern PA, Bamman MM & Peterson CA (2022). A muscle cell-macrophage axis involving matrix metalloproteinase 14 facilitates extracellular matrix remodeling with mechanical loading. *FASEB J* **36,** e22155.

Penna F, Bonetto A, Aversa Z, Minero VG, Rossi Fanelli F, Costelli P & Muscaritoli M (2016). Effect of the specific proteasome inhibitor bortezomib on cancer-related muscle wasting. *J Cachexia Sarcopenia Muscle* **7,** 345–354.

Reggiani C & Schiaffino S (2020). Muscle hypertrophy and muscle strength: dependent or independent variables? A provocative review. *Eur J Transl Myol* **30,** 9311.

Rocheteau P, Chatre L, Briand D, Mebarki M, Jouvion G, Bardon J, Crochemore C, Serrani P, Lecci PP, Latil M, Matot B, Carlier PG, Latronico N, Huchet C, Lafoux A, Sharshar T, Ricchetti M & Chrétien F (2015). Sepsis induces long-term metabolic and mitochondrial muscle stem cell dysfunction amenable by mesenchymal stem cell therapy. *Nat Commun* **6,** 10145.

Sambasivan R, Yao R, Kissenpfennig A, Van Wittenberghe L, Paldi A, Gayraud-Morel B, Guenou H, Malissen B, Tajbakhsh S & Galy A (2011). Pax7-expressing satellite cells are indispensable for adult skeletal muscle regeneration. *Development* **138,** 3647–3656.

Schwartz LM & Gundersen K (2022). Cross Talk opposing view: Myonuclei do not undergo apoptosis during skeletal muscle atrophy. *J Physiol* **600,** 2081–2084.

Serrano AL, Baeza-Raja B, Perdiguero E, Jardí M & Muñoz-Cánoves P (2008). Interleukin-6 is an essential regulator of satellite cell-mediated skeletal muscle hypertrophy. *Cell Metab* **7,** 33–44.

Snijders T, Aussieker T, Holwerda A, Parise G, van Loon LJC & Verdijk LB (2020). The concept of skeletal muscle memory: Evidence from animal and human studies. *Acta Physiol (Oxf)* **229,** e13465.

Theret M, Gsaier L, Schaffer B, Juban G, Ben Larbi S, Weiss-Gayet M, Bultot L, Collodet C, Foretz M, Desplanches D, Sanz P, Zang Z, Yang L, Vial G, Viollet B, Sakamoto K, Brunet A, Chazaud B & Mounier R (2017). AMPKα1-LDH pathway regulates muscle stem cell self-renewal by controlling metabolic homeostasis. *EMBO J* **36,** 1946–1962.

Venturelli M, Schena F, Naro F, Reggiani C, Pereira Guimarães M, de Almeida Costa Campos Y, Costa Moreira O, Fernandes da Silva S, Silva Marques de Azevedo PH, Dixit A, Srivastav S, Hinkley JM, Seaborne RA, Viggars M, Sharples AP, Mahmassani ZS, Drummond MJ &

Gondin J (2019). Commentaries on Viewpoint: “Muscle memory” not mediated by myonuclear number? Secondary analysis of human detraining data. *J Appl Physiol* **127,** 1817–1820.

Warren GL, Lowe DA & Armstrong RB (1999). Measurement tools used in the study of eccentric contraction-induced injury. *Sports Med* **27,** 43–59.

Winje IM, Bengtsen M, Eftestøl E, Juvkam I, Bruusgaard JC & Gundersen K (2018). Specific labelling of myonuclei by an antibody against pericentriolar material 1 on skeletal muscle tissue sections. *Acta Physiol (Oxf)* **223,** e13034.

Ethics approval and consent to participate

All of the experiments and procedures were conducted in accordance with French and European legislations on animal experimentation and approved by the local ethic committee CEEA-55 and the French ministry of research (APAFIS#12794-2017122107228405).

Consent for publication

Not applicable

Availability of data and materials

The datasets used and/or analyzed during the current study are available from the corresponding author on reasonable request.

Competing interests

The authors declare that they have no competing interests

Funding

This study was supported by Partenariats Hubert Curien (PHC) - Programme GUNDISHAPUR 2020 and Oncostarter – Cancéropôle CLARA.

Authors' contributions

Concept/idea/research design: J. Gondin. Writing: J. Gondin. Data collection: A. Zavoriti, A. Fessard, M. Rahmati, N. Boyer, P. Del Carmine, J. Gondin. Data analysis: A. Zavoriti, A. Fessard, N. Boyer, P. Del Carmine, J. Gondin. Project management: J. Gondin. Consultation (including review of manuscript before submitting): A. Zavoriti, A. Fessard, M. Rahmati, N. Boyer, P. Del Carmine, B. Chazaud, J. Gondin. All the authors read and approved the final version of manuscript. Masoud Rahmati acted as a visiting scientist at INMG (from September 2019 to July 2020) where he was trained to NMES training protocol and muscle analysis.

Acknowledgments

We thank Dr Rémi Mounier and Dr Anita Kneppers for their useful comments on a previous version of the manuscript.

STUDY #2

NEUROMUSCULAR ELECTRICAL STIMULATION LIMITS MUSCLE WEAKNESS AND WASTING AND MODULATES SATELLITE CELL FUNCTION AND NICHE DURING CANCER CACHEXIA

Aliki Zavoriti[1], Aurélie Fessard[1], Eugénie Moulin[1], Peggy Del Carmine[1], Bénédicte Chazaud[1], Julien Gondin[1]

[1] Institut NeuroMyoGène, Unité Physiopathologie et Génétique du Neurone et du Muscle, Université Claude Bernard Lyon 1, CNRS UMR 5261, Inserm U1315, Univ Lyon, Lyon, France.

Corresponding author :
Aliki Zavoriti
Institut Neuromyogène (INMG)
CNRS 5310 – INSERM U1217 – UCBL1
Faculté de Médecine et de Pharmacie
8 Avenue Rockefeller
69008 LYON, France
aliki.zavoriti@univ-lyon1.fr

Keywords: Cancer cachexia, contractile activity, training, satellite cells, myogenesis, microenvironment

Abstract

Cancer cachexia (CC) is characterized by systemic inflammation resulting in extensive body weight loss, skeletal muscle wasting (*i.e.*, reduced muscle mass) and weakness (*i.e.*, reduced force production). CC worsens patient survival and no curative therapies exist. Recent works reveal that CC may result from dysfunction of muscle stem cells, or satellite cells (SCs) as well as alterations in other cell types that harbor the SC niche. We recently demonstrated that increased muscle fiber contractile activity by neuromuscular electrical stimulation (NMES) promotes SC fusion in healthy muscles. We aimed to determine whether NMES reduces muscle weakness and wasting trough improvement of SC fate and niche alterations from two complementary mouse models of CC, the Colon-26 (C26)-tumor bearing and the *Apc*$^{Min/+}$ mouse models.

Our analyzes showed that muscle wasting and weakness occur in conjunction with alterations in SC content and function and accumulation of macrophages within the cachectic muscles. We showed that the NMES training improved muscle force, mass and SC fate in the C26 cachectic mice. These improvements were associated with reduction of inflammation, depicted by a transition toward an anti-inflammatory status of macrophages in muscle, validated by both *in vivo* and *in vitro* studies. Further NMES training in the *Apc*$^{Min/+}$ mice failed to prevent muscle weakness but increased muscle fiber size regardless of regulation in SC fate. These findings reveal a critical role of NMES-induced muscle contractions on SC fate and tissue inflammation to counteract the deleterious effects of CC.

Introduction

Cancer cachexia (CC) is a multi-organ syndrome, most prevalent in patients suffering from gastrointestinal and lung malignancies[1]. It is estimated that up to 30 % of cancer patients die directly of cachexia rather of the tumor burden[2]. CC is characterized by pronounced body weight loss (> 5% over the preceding 6 months of diagnosis) mainly due to loss of skeletal muscle mass (*i.e.,* muscle wasting), with or without loss of fat mass[3]. Muscle wasting, the major feature of CC, leads to progressive decline in muscle force (*i.e.,* muscle weakness), exercise capacity and endurance. Consequently, to these events, muscle wasting dramatically impact the quality of life, response in chemotherapy as well as the survival of cancer patients[4,5,6]. Cancer patients die faster[7] and currently no approved therapies exist to efficiently treat or prevent CC.

The causes underlying CC are multifactorial. Muscle wasting is considered to be mainly triggered by systemic inflammation resulting from host immune system in response to tumor presence[1]. Release of pro-inflammatory cytokines and growth factors leads to negative protein and energy balance driven by an association of anemia, anorexia and abnormal metabolism[1]. So far, the underlying mechanisms that drive muscle wasting and weakness have been predominantly considered to reside within the muscle fiber. Transiently, inflammation triggers muscle proteolysis, oxidative stress and mitochondrial dysfunctions[8,9] .

Emerging studies however reveal that muscle fibers become atrophic during CC due to alterations in the function of muscle stem cells, referred to as satellite cells (SCs). SCs are localized beneath the basal lamina of the muscle fiber, and exclusively express Pax7, a transcriptional factor important for their specification and maintenance[10]. SC myogenic function is crucial for muscle homeostasis and regeneration[11]. Upon muscle injury, SCs exit from quiescence, become activated, proliferate, differentiate into myocytes and eventually fuse with each other or with the existing muscle fibers to recover muscle damage and give rise to new functional muscle fibers[12]. Myogenesis was shown to be altered in the presence of tumor as illustrated by the increased number of SCs in both tumor-bearing animals[13,14,15] and cancer patients[13,16] and their inability to differentiate and fuse properly[13,14] during CC. SC fate across myogenesis also relies on the dynamic and tightly coordinated interactions between SCs with the other cell types composing its niche. Importantly, macrophages[17,18] removing the dead muscle fibers, fibro-adipogenic progenitors (FAPs)[19,20] secreting components of the

extracellular matrix and endothelial cells (ECs)[21,22] that make up the capillaries. Hence, a growing body of literature reveals changes in the number of macrophages[23,24,25,26,27], FAPs[15,23] and ECs[28,29,30,31] from skeletal muscles of tumor-bearing mouse models and human cancer patients. Altogether, defects in myogenesis due to altered cellular interactions within the SC niche likely play a key role in the development of cancer cachexia. However, characterization of these dysfunctions remains largely unknown in this context.

The SC fate and its niche are influenced by muscle contractile activity[32,33,34,35,36,37]. Outside of regeneration, SCs support skeletal muscle fiber adaptations to exercise/overload by fusing and providing new myonuclei (*i.e.,* myonuclear accretion) to muscle fibers[38,39]. Moreover, exercise could regulate macrophage inflammatory status to facilitate muscle adaptation to exercise[40,41]. In addition, macrophages have been proposed to be required for muscle growth by actively promoting SC fusion and extracellular matrix remodeling in overloaded muscles[32,35]. We recently showed that applying controlled and individualized electrical stimulations over the skeletal muscle, a technique known as neuromuscular electrical stimulation (NMES), positively regulates SC fate by inducing myonuclear accretion/SC fusion in healthy mice[42]. On that basis, the possibility of using a standardized NMES protocol to counteract the alterations of SC fate and its niche within the cachectic muscles, appears relevant, inasmuch as cachectic patients show difficulty to perform voluntary muscle contractions and the efficacy of NMES in CC patients remains unclear due to uncontrolled application[43,44,45]. The muscle force produced by the cachectic patients, in response to the stimulation, representing the main determinant of NMES efficacy[46], has never been monitored.

The present study aimed to investigate whether and to what extent an increased contractile activity induced by a carefully controlled NMES training protocol can improve SC fate and minimize the altered cellular interactions within the SC niche induced by CC. For this purpose, we used the allograft Colon-C26 (C26) carcinoma bearing mouse model, a classical model of CC which develops rapidly muscle wasting and the *Apc*$^{Min/+}$ mouse model, a mouse model that instead is predisposed to develop progressive colon cancer and cachexia such as in humans.

Materials and Methods:

Animals

Nine-week-old Balb/c male mice were purchased from Janvier-Labs (Le Genest-Saint-Isle, France) and were housed individually. Mice in animal facility stayed in incubation period at least for one week before inoculation of C26 tumor cells.

Heterozygous C57BL/6-*Apc*$^{Min/+}$ male mice, carrying a chemically induced mutation (*i.e.*, multiple intestinal neoplasia, Min) on the Adenomatous polyposis coli gene, were originally purchased from Jackson Laboratories (Bar Harbor, ME USA). Breeding was maintained by crossing heterozygous male *Apc*$^{Min/+}$ mice with female C57BL/6-WT mice. WT and *Apc*$^{Min/+}$ were genotyped for the WT (primer sequence F: -TAAAGACCAGGAAGCCTTGT- R: AATACCTCGCTCTCTCTCTCCA) and mutant *Apc* allele (primer sequence F: -TGAGAAAGACAGAAGTTA - R:TTCCACTTTGGCATAAGGC). Only male *Apc*$^{Min/+}$ and WT littermates were used for analysis.

Mice were housed in a humidity- and temperature-controlled animal facility (12:12-h light cycle, 25°C) with free access to water and food. All of the experiments and procedures were conducted in accordance with the guidelines of the local animal ethics committee CEEA-55 and the French ministry of research (APAFIS@12794-2017122107228405).

Experimental design

C26

Colon C26 cells were cultured in classic medium (Gibco's DMEM high glucose supplied with 10 % fetal bovine serum and 1 % penicillin/streptomycin (Thermo Fisher Scientific)) and maintained in a 5 % CO_2 37°C humidified incubator. Cells were passaged when sub-confluent and they were injected in the mice allocated to the tumor-bearing group at third passage. Five x 10^5 cells diluted in 100µL of PBS were injected subcutaneously in their right flank per mouse under general anesthesia. Control mice received an equivalent PBS vehicle injection. C26 mice displayed a tumor mass observable after 7 days following injection, and were either assigned to a NMES protocol (C26+NMES) or to a control procedure (C26). C26+NMES trained mice were submitted to 6 sessions of NMES protocol, with one session daily starting from 7 to 14 days after injection. Food intake, body weight and Fmax, were recorded two days before injection and daily from 7 to 14 days after injection for all groups. At 14 days following

injection, all mice were sacrificed by cervical dislocation under deep isoflurane anesthesia. Tumors were directly harvested and weighted.

***Apc*$^{Min/+}$**

Body weight and Fmax were weekly monitored in age-matched WT and *Apc*$^{Min/+}$ mice to assess loss of body weight and muscle force over time. Investigations were performed in 8-week-old mice and ended when *Apc*$^{Min/+}$ mice reached the ethical endpoint (*i.e., severe body weight loss and inability*). At this specific timepoint, age-matched *Apc*$^{Min/+}$ and WT mice were sacrificed by cervical dislocation under deep isoflurane anesthesia.

To analyze the effects of NMES, a cohort of *Apc*$^{Min/+}$ mice were trained 4 times *per* week for a total of 3 weeks, starting at 16 weeks of age. At the end of the protocol, mice were sacrificed as described above and intestines were harvested to count the number of polyps.

From both mouse models, the *gastrocnemius* muscles were harvested, weighted and used for histology or flow cytometry analysis. Muscles from the entire hindlimbs were also harvested to perform the *in vitro* experiments (see below)

Experimental device, force measurements and NMES protocol

Our individualized and carefully monitored NMES training protocol was performed in mice as previously described[42]. Briefly, a strictly non-invasive ergometer was used to electrically stimulate the right plantar flexor of mouse muscles and at the same time record the resulting force production. First maximal tetanic force (F_{max}) was recorded in response to 100 Hz tetanic stimulation. Stimulation intensity was carefully adjusted at the beginning of each NMES training session in order to reach 15% of Fmax. Each NMES session consisted of 80 stimulation trains delivered at a frequency of 50Hz. Every 10 contractions, the stimulation intensity was increased in order to minimize muscle fatigue and maintain a force level of 15% of Fmax throughout the NMES protocol

Tissue preparation and *in vivo* immunofluorescence analysis

Gastrocnemius muscles of the right limbs were dissected, frozen in liquid nitrogen-cooled isopentane and kept at -80°C until use. Cryosections (10µm) were prepared for immunohistochemical analysis with a NX 50 cryostat. Cryosections were permeabilized in 0.05% Triton-X100 in PBS for 10 min at room temperature, washed 3 times in PBS and then blocked in 4% BSA for 1 hour at room temperature. Cryosections were then incubated with

primary antibodies overnight 4°C, washed 3 times with PBS and further incubated with secondary antibodies for 1 hour at 37°C (See table 1 for the list with antibodies). Slides were washed with PBS, counterstained with Hoechst and mounted in fluoromount-G medium.

For Pax7/Laminin immunostaining and Pax7/Ki67/Myogenin immunostaining, cryosections were first fixed with PFA 4% for 10 min, washed 3 times in PBS, permeabilized in 0.1% triton-100X + 0.1M Glycine for 10 min, washed 3 times in PBS, then immerged into citrate buffer 10mM in 90° hot water bath twice, washed 3 times in PBS and blocked in 5% donkey serum 2% BSA and 1/40 M.O.M blocking reagent (MKB-2213, Vector Laboratories) in PBS for 1 hour. Every step was performed at room temperature, unless indicated otherwise. Cryosections were then incubated with antibodies as described below except that primary and the corresponding secondary antibodies were diluted in blocking buffer containing 5% donkey serum and 2% BSA in PBS.

For myosin heavy chain (MyHC) I/IIA/IIB/Laminin immunostaining, slides were neither fixed with PFA nor premetallized with triton. Slides were washed once with PBS, incubated with M.O.M blocking reagent (one drop in 1.25 ml) for 1 hour at room temperature and then washed again 3 times. Cryosections were incubated with antibodies as described above except that primary and the corresponding secondary antibodies were diluted in blocking buffer containing 0.5% BSA in PBS.

List of antibodies used for muscle tissue sections:

Primary Ab	**Reference of primary Ab and dilution**	**Secondary Ab: Reference* and dilution**
Anti- Laminin (rabbit)	L9393-2ml (Sigma); 1:200	• For F4/80, PDGFRα and CD31 stainings: Donkey Anti-Rabbit Fluorescein FITC 711-095-152; 1:200 • For Pax7 staining: Donkey Anti-Rabbit Cyanine Cy3 711-165-152; 1:200 • For MyHC I/IIA/IIB staining: Donkey Anti-Rabbit Cyanine Cy5 711-175-152; 1:200

Anti-F4/80 (rat)	Ab6640 (Abcam); 1:400	Donkey Anti-Rat Cyanine Cy3 712-165-153; 1:200
Anti-PDGFRα (goat)	AF1062 (R&D Systems); 1:200	Donkey Anti-Goat Cyanine Cy3 705-165-147; 1:200
Anti-CD31 (Rat)	Ab7388-50 (Abcam); 1:200	Donkey Anti-Rat Cyanine Cy3 712-165-153; 1:200
Anti-Pax7 (mouse)	DSHB; 1:30	• For Pax7/Ki67/Myogenin staining: Donkey Anti-Mouse Cyanine Cy3 715-165-150; 1:200. • For Pax7/Laminin staining: Donkey Anti-mouse Fluorescein (FITC) 715-095-150; 1:200
Anti-Ki67 (sheep)	AF7649 (R&D Systems); 1:200	Donkey Anti-Sheep Fluorescein (FITC) 713-095-003; 1:200
Anti-Myogenin (rabbit)	Ab124800 (Abcam); 1:500	Donkey Anti-Rabbit Cyanine Cy5 711-175-152; 1:200
Anti-PCM1 (rabbit)	HPA023370 (Sigma); 1:1000	Donkey Anti-Rabbit Fluorescein FITC 711-095-152; 1:200
Anti-Laminin α2 (4H8-2) (rat)	SC-59854 (Santa Cruz); 1:1000	Donkey Anti-Rat Cyanine Cy3 712-165-153; 1:200 (For PCM1/Laminin staining)
Anti-myosin I (mouse)	BA-D5 (DSHB); 1:100	Donkey Anti-Mouse BLUE-Alexa Fluor 405 IgG2b; 1:200
Anti-myosin IIA (mouse)	SC-71 (DSHB); 1:100	Anti-Mouse GREEN-Alexa Fluor 488 IgG1; 1:150
Anti-myosin IIB (mouse)	BF-F3 (DSHB); 1:100	Anti-Mouse RED-Alexa Fluor 546 IgM; 1:150
Anti-Immunoglobulin G (IgG)	none	Anti-Mouse Cyanine Cy3 715-165-150; 1:200
Anti-iNOS (rabbit)	Ab15323 (Abcam) 1:25	Donkey Anti-Rabbit Fluorescein FITC 711-095-152; 1:200
Anti-COX2 (goat)	Ab23672 (Abcam)1:50	Donkey Anti-Goat Fluorescein FITC 705-095-147; 1:200
Anti-CD206 (rabbit)	Ab64693 (Abcam) 1:200	Donkey Anti-Rabbit Fluorescein FITC 711-095-152; 1:200
Anti-IL-10 (rabbit)	Ab9969 (Abcam)1:50	Donkey Anti-Rabbit Fluorescein FITC 711-095-152; 1:200

*All secondary antibodies were supplied from Jackson ImmunoResearch

In vitro experiments

Murine Myoblasts isolation

Myoblasts were isolated from both C26 and *Apc*$^{Min/+}$ mice and their respective controls to assess the different steps of myogenesis. All steps were performed on ice unless indicated. The entire hindlimb muscles were dissected, minced and incubated with muscle dissociation buffer (Ham's F10 medium, 10% horse serum, 1 + penicillin-streptomycin, Collagenase II 800 U/ml, Gibco) during 1 hour at 37°C in a gently shaking hot-water bath. Muscle pieces were washed and digested further by incubating with additional 3000 U/ml of collagenase II and 33 U/ml of dispase, during 30 min at 37°C with agitation. After filtration to remove muscle bones, muscle chunks and tendons, red blood cells in the cell suspension were lysed by adding ACK buffer. Then cells were incubated with the satellite cell isolation kit mouse (Miltenyi biotec) in PBS, 0.5% BSA, 2mM EDTA during 30 min in the refrigerator. SCs were collected (unlabeled cells) using magnetic-activated cell sorting consisting of passing the cells through magnetic LC columns carried by a magnetic stand. After sorting, SC were cultured in growth medium (DMEM F-12, 20% fetal bovine serum, 2% ultroser G, 1% penicillin-streptomycin) within flasks coated with 0.02% of gelatin, during 3 to 4 days for myoblast expansion. Based on the *in vitro* experiments, myoblasts were passaged every two days until 2 passages.

Proliferation assay

After one passage, MACS-sorted myoblasts were plated in growth medium at 3 000 cells/cm^2 in a 48 Nunc™ well plate (Thermo Fisher Scientific, #150687) coated with 0.1% low growth factor matrigel (Corning #31550023). Twenty-four hours later, EdU (Click-iT EdU Alexa Fluor 488 Imaging kit, Thermofisher C10337) was added to each well to the growth medium at a final concentration of 1 µg/ml and cells were further incubated for 1 hour. Cells were then washed with PBS, fixed with 4% PFA for 15 min, washed again twice with PBS and permeabilized with 0.5% Triton-X100 during 15 min. Cells were washed again before coupling of EdU with Alexa fluor-488 substrate of the Click-iT kit reaction mixture during 30 min in dark, following the manufacturer's instructions. Cells then were then washed twice in PBS and blocked in 4% BSA for 1 hour. One hour later, myoblasts were incubated with primary antibody anti-desmin (1:200, Abcam #32362, Rabbit) overnight at 4°C. The day after, myoblasts were washed 3 times in PBS, incubated with secondary antibody Donkey Anti-Rabbit Cyanine

Cy3 (Jackson Immunoresearch #711-165-152; 1:200) for 1 hour at 37°C, washed 3 times in PBS and counterstained with Hoechst.

Myogenic differentiation and fusion assays

After two passages, MACS-sorted myoblasts were plated in growth medium at 1000 cells/cm^2 in a 24 Nunc™ well plate (Thermo Fisher Scientific, #142475) coated with 0.1% low-growth factor matrigel (Corning #31550023) to assess their intrinsic differentiation properties. Six hours later, growth medium was replaced by differentiation medium (DMEM F-12, 2% Horse serum, 1% penicillin-streptomycin) and cells were further incubated for 48 hours before the fixation. Fusion assay was performed at the same conditions but cells were seeded to a higher density of 30 000 cells/cm^2. For both assays, cells were washed once with PBS, fixed with 4 % PFA for 10 min, washed 3 times with PBS, permeabilized in 0.05% Triton-X100 for 10 min, washed 3 times with PBS, and then blocked in 4% BSA for 1 hour. Cells in differentiation assay were incubated with anti-myogenin primary antibody (1:50, Abcam #124800) and cells in the fusion assay were incubated with anti-desmin primary antibody (1:200, Abcam #32362, Rabbit) overnight at 4°C, respectively. The day after, myoblasts were further washed 3 times in PBS, incubated with secondary antibody Donkey Anti-Rabbit Cyanine Cy3 (Jackson Immunoresearch #711-165-152; 1:200) during 1 hour at 37°C and washed again 3 times with PBS. Then myoblasts were counterstained with Hoechst and were ready for microscope analysis. All steps were performed at room temperature, unless indicated.

Muscle protein extracts

Protein extracts were obtained from *gastrocnemius* muscles of the right limb. Briefly, 10-15 sections of 25µm were produced using the NX 50 cryostat, then sections were incubated with the Sigma's mammalian cell lysis kit (#087K4074) for 10 min at 4°C on a shaker plate. Further, tissue homogenate was centrifuged at 13 000 rpm for 10 min at 4°C and supernatant was collected and sonicated during 5 on-off cycles of 15-60 s. Protein extracts concentrations were determined using the Thermo Scientific Micro BCA™ Protein Assay kit. Samples were kept at -80°C until use.

Myogenesis assessment of SC exposed directly to muscle protein extracts

Myoblasts from WT Balb/c and C57bl/6j mice were isolated by MACS and frozen in 90% FBS – 10% DMSO. For proliferation assay, WT myoblasts were thawed, counted and seeded directly at 3000 cells/cm^2 in a matrigel-coated 48 well plate as described previously. Six hours later, growth medium was replaced by new growth medium containing 1 µg/ml of muscle protein extracts (from each mouse group). Proliferation assay was performed as described in the section dedicated.

For differentiation and fusion assays, WT myoblasts were thawed and recovered in growth medium during 2-3 days. Myoblasts were then counted and seeded at 1000 cells/cm^2 for differentiation and at 30 000 cells/cm^2 for fusion assay in a matrigel-coated 24 well plate as described previously. Six hours later, growth medium was replaced by differentiation medium containing 1 µg/ml of muscle protein extracts (from each mouse group). Differentiation and fusion assays were performed as described above (Myogenic differentiation and fusion assays sections).

Murine BMDMs isolation

Bone marrow-derived macrophages (BMDMs) were prepared from adult male WT Balb/c mice, same as the genetic background from the C26 mouse model. Mice were killed by cervical dislocation under isoflurane anesthesia, and marrow was flushed from tibiae and femurs. Cells were plated, washed and grown in 6-7 days in DMEM high Glucose High pyruvate, in 20% fetal bovine serum, 30% L929-derived supernatant, 1% amphotericin B (2.5 µg/ml; Thermo Fisher Scientific), and 100 µg/ml streptomycin. BMDMs were passaged once and frozen in 90% FBS – 10% DMSO.

Preparation of conditioned media from BMDMs exposed prior to *muscle protein extracts*

WT BMDMs were thawed and cultured in DMEM medium containing 20% of L929-derived supernatant to allow for BMDMs amplification during 3 days. BMDMs then were counted and cultured at 110 000 cells/cm^2 in 48 and 24 well plates with classic medium. Six hours later, the medium was replaced by classic medium supplied with 1µg/ml of muscle protein extracts. After 48 hours, cells were washed and serum-free DMEM was added for 24 hours more to obtain macrophage conditioned-medium. Myoblasts from WT Balb/c mice obtained by MACS, were thawed, counted, and cultured at 3 000 cells/cm^2 in BMDM conditioned-medium

containing 20% fetal bovine serum and 2% ultroser G to assess proliferation ability as described in the section dedicated.

Further thawed and counted myoblasts were cultured in BMDM conditioned-medium containing 2% horse serum at 1000 cells/cm^2 and at 30 000 cells/cm^2 densities to assess differentiation and fusion properties respectively.

Assessment of BMDM inflammatory status exposed to muscle protein extracts

In addition, ~200 000 BMDMs were seeded separately into cover-slips and were incubated similarly with protein extracts to assess BMDMs inflammatory status in response to the protein extracts. Two days after, cells were fixed and proceeded for immunostaining analysis using TNFα (Rabbit, Abcam #34839, 1:50) and CD206 (Rabbit, Abcam #64693) primary antibodies.

Flow cytometry analysis of macrophage phenotype from C26 muscles

Gastrocnemius muscles of the right limb from C26 and C26+NMES mice (n= 2-4) were dissected to characterize macrophage subtypes of the muscle trained with NMES using flow cytometry. Muscles were minced in very small pieces and digested with Collagenase B 0.2% (Roche #11088815001) during 1 hour at 37°C with agitation. Collagenase activity was blocked by the addition of 5 ml DMEM:FBS (1:1). The samples were filtered in cell strainer 100 and 30 µm. After several washing steps, cell suspension was incubated with magnetic beads conjugated to anti-CD45 antibody (Miltenyi Biotec) for 30 min at 4°C and CD45$^+$ cells (hematopoietic cells) were isolated by MACS. Then CD45$^+$ cells were incubated with Fc block (Miltenyi Biotec) for another 30 min at 4°C. Finally, CD45$^+$ cells were stained with antibodies against CD64 (BioLegend #139321), Ly-6C (BioLegend #128007), CD206 (Invitrogen #53-2061-82) and CCR2 (BioLegend #150605). Dead cells were excluded by fixable viability Ghost dye (eBioscience) by labeling during 15 min. In both conditions, 10 000 to 15 000 events were acquired using a FACSCanto II flow cytometer (BD Biosciences). Percentages of CD64$^+$, CD64$^+$Ly-6C$^+$ and CD64$^+$Ly-6C$^-$ were calculated among total CD45$^+$ cells after analysis by flow cytometry with BD FACSDiva™ Software.

Polyp count

The intestinal tract was harvested from *Apc*$^{Min/+}$ -control and -NMES mice, cut out in 4 pieces, washed with PBS and fixed in 10% PFA during 24 hours. The next day, intestines were washed with PBS overnight at 4°. The day after, intestines were washed twice with PBS, incubated in 70% alcohol during 3 hours and then in methylene blue solution (Sigma #03978) overnight. The total number of polyps was counted using a binocular microscope.

Image capture and analysis

In vivo

Ten to fifteen images were recorded from each section with an Imager Z1 Zeiss microscope at 20 x magnification connected to a CoolSNAP MYO camera. ImageJ software was used for the quantification of the number of myonuclei, PCM1$^+$ nuclei, Pax7$^+$, F4/80$^+$, PDGFRα^+ and CD31$^+$ cells. Myonuclei were first stained using Hoechst and laminin and were defined as the nuclei with their geometric center within the inner rim of the laminin ring[47,48]. Although, this technique is not sufficient to discriminate myonuclei, as it labels nuclei from other cell types that reside in the muscle and which are pressed tightly against the muscle fiber membrane. PCM1 (Pericentriolar material 1) antibody was then used to specifically label all myonuclei[49]. The number of cells stained for a given marker or the number of myonuclei and PCM1$^+$ nuclei were either divided by the number of fibers or by the area expressed in mm^2 from one picture. For quantification of type I collagen, twenty-five to thirty images were recorded similarly with the imager Z1 Zeiss microscope at 20 x magnification from each muscle section. Type I collagen - labeled areas for each image were quantified with ImageJ software. Briefly, images were converted into 8-bit binary image using an Otsu threshold filter, and white pixels were enumerated and expressed as a percentage of the total pixels in the muscle section. The mean intensity of type I collagen labelled-areas from one muscle section was reported for each mouse.

For whole cryosection analysis, slides were automatically scanned at 10 x magnification using the Axio Observer.Z1 (Zeiss) connected to CoolSNAP HQ2 CCD Camera (photometrics). The image of the whole cryosection was automatically reconstituted in MetaMorph Software[50]. The number of IgG positive fibers (*i.e.,* based on staining with Cy3 anti-mouse) and MyHC of type I, IIA, IIX and IIB positive muscle fibers were quantified on the whole section and normalized to the total number of myofibers. Muscle fiber CSA was determined on the whole

gastrocnemius muscle sections labeled by anti-laminin antibody using the Open-CSAM program, as previously described[50].

In vitro

For myoblasts assessment of myogenesis *in vitro*, 10 to 20 images were recorded from each well of the cell culture plate at 10 x magnification using the Axio Observer.Z1 (Zeiss) connected to CoolSNAP HQ2 CCD Camera. Quantification of EdU^+ nuclei, $Desmin^+$ cells and $Myogenin^+$ nuclei was performed with ImageJ software. The percentage of proliferative myoblasts was calculated using the number of $Desmin^+$ cells with EdU^+ nuclei over the total $Desmin^+$ cells. The percentage of differentiating cells was calculated using the number of cells containing $myogenin^+$ nuclei over the total cell number. The fusion index was calculated using the number of nuclei of myotubes presenting two or more nuclei over the total number of nuclei (in both myoblasts and myotubes). Purity was assessed by counting the number of $Desmin^+$ cells over the total number of cells (without desmin staining). Experiments were performed with purity higher than > 89%.

Statistical analysis

Statistical analysis was performed using GraphPad Prism Software (version 7.0a). Unpaired student t-test (nonparametric Mann-Whitney test) was used to test differences between WT and $Apc^{Min/+}$ mice or to compare C26 with PBS or C26 with C26+NMES. For flow cytometry analysis, paired t-test (parametric test) was used to determine differences between C26 and C26 NMES. One-way ANOVA test with repeated measures on session or week was used to compare body weight and force production between PBS, C26 and C26+NMES or between WT, $Apc^{Min/+}$, $Apc^{Min/+}$ + NMES and was also used for other variables among these groups. Data are presented as mean $\pm$ SD with significance set at $p < 0.05$.

RESULTS

NMES limits muscle weakness and wasting in C26 mice independently of tumor growth

C26 + NMES mice were stimulated for 2 x 3 consecutive days separated by one day of rest, for a total of 6 sessions starting at 7 days after injection, when tumor became visible, while PBS and C26 mice served as controls (Fig. 1). In order to avoid the bias of a possible contribution of anorexia to muscle force and mass, PBS mice were fed equally as C26 mice from 7 days following injection.

PBS and C26 mice lost around 15% of their initial body weight recorded at baseline (2 days prior to injection) while NMES did not prevent body weight loss in C26 mice (Fig. 2A). NMES did not impact the tumor mass of C26 mice (Fig. 2B). Our device that was used to perform NMES, served also for non-invasive daily maximal force (F_{max}) measurement in all mice groups throughout the experimental protocol. F_{max} started to decrease drastically from day 7 post-injection, prior to body weight loss, in the C26-bearing mice (Fig. 2C). After 14 days post-injection, loss of F_{max} was significantly greater in C26 mice (-36 $\pm$ 12%,) than C26 + NMES (-28 $\pm$ 12%) (Fig. 2C-D) indicating that NMES limited muscle weakness in the C26 mice. Further, when F_{max} was normalized to muscle mass (specific force) for each mouse, muscle force loss still occurred in the C26 mice, suggesting that decline in muscle force does not rely entirely on muscle mass but can also be triggered through intrinsic functional alterations (Fig. S1A). The muscle mass of C26 mice was significantly reduced by 12% compared to PBS mice whereas muscle mass was 6% higher in C26+NMES mice compared to C26 mice suggesting that NMES was able to partially revert the loss of *gastrocnemius* muscle mass (Fig. 2E). The mean CSA of muscle fibers was established by measuring the area of the whole muscle fibers on one muscle section and used as a parameter of muscle atrophy. After NMES training, the muscle fiber CSA in C26 mice remained 14% lower than in PBS mice, indicating that NMES did not prevent the reduction of CSA observed in C26 mice (Fig. 2F). Muscle mass increase with NMES could result from changes in the composition of muscle fibers with distinct phenotype. We next assessed whether NMES affected the distribution of the different MyHC isoforms by quantifying I, IIA, IIX and IIB muscle fibers in the PBS, C26 and C26 trained mice with NMES. Indeed, we find out increased proportion of muscle fibers expressing MyHC type IIB while muscle fibers expressing MyHC of type I and IIX were decreased in C26 +NMES mice compared to C26 untrained mice

(Fig. 2G), suggesting a shift from slow to faster contracting muscle fibers with NMES that could influence muscle mass and force.

NMES improves *in vivo* SC fusion in the C26 mice

We recently demonstrated that increased muscle fiber contractile activity by NMES promotes SC fusion in healthy mice[42]. We subsequently aim to determine whether NMES beneficial effects on muscle force and mass are associated with an improvement of SC fusion in the cachectic C26 mice. The number of SCs ($Pax7^+$ expressing cells) was significantly increased in the muscles of C26 mice compared with PBS mice. The increase of SC in our analysis is consistent with previous work that found a persistent increase in Pax7 protein expression from C26 muscles[13,14], suggesting aberrant proliferation of SC during CC. The abnormal increase in SC numbers from C26 mice was nearly reversed by NMES, bringing them close to those of PBS mice (Fig. 3A). In addition, the number of myonuclei *per* fiber significantly increased in C26 mice following NMES as compared with PBS and C26 controls (Fig. 3B). We further validated the increase in the number of myonuclei by labelling PCM1 protein which is specifically found on the nuclear envelope of adult skeletal muscle fibers[51,52]. A proportion of $PCM1^+$ nuclei greater than 30% was found in the C26+NMES mice in comparison to PBS and C26 control mice (Fig 3C). These findings suggest that NMES improves SC fusion in CC mice. We next used IgG labeling as a marker for membrane damage to assess whether NMES induces muscle damage in the C26 mice. The proportion of IgG^+ muscles fibers were negligible in both C26 and C26 + NMES mice (Fig.S1B), suggesting that NMES induces SC fusion in the absence of overt signs of muscle damage. Using Ki67 as a cell proliferation marker and myogenin as a marker of terminal differentiation to stain the SC, we attempted to determine if NMES influences SC proliferation and differentiation in the C26 mice. Levels of $Pax7^+Ki67^+$ cells tend to increase while $myogenin^+$ cells tend to decrease in the C26 mice relative to PBS mice suggesting alterations in SC proliferation and differentiation. NMES training in the C26 mice appeared to minimize the rise in $Pax7^+Ki67^+$ cells but seemed to have no effect on the amount of $myogenin^+$ cells. Due to high variability, additional replicates are required to refine our observations. To address whether the impairment in SC fate from C26 mice was triggered by the muscle cachectic microenvironment or by intrinsic alterations of SCs to commit into myogenesis, SCs from PBS and C26 muscles were isolated and cultured *in vitro* (Fig. S2A). Assays were performed with cell culture purity above 90% (Fig. S2B). The proportion of EdU^+

myoblasts derived from C26 mice was equivalent to that of myoblasts derived from PBS mice (Fig. 3F), demonstrating that C26-SC ability to proliferate was not impaired. When exposed to differentiation medium, isolated C26- and PBS-myoblasts were able to differentiate (Fig. 3G) and fuse (Fig. 3H) into multinucleated myotubes similarly. These results indicate that the myogenic properties of C26-SCs are retained when removed from the muscle cachectic environment.

NMES reduces neutrophil content and induces macrophage switching toward an anti-inflammatory state

The next step was to establish whether NMES may improve SC function by affecting the other cell types that are present in the SC niche and which are known to interact with SC and contribute to SC fate regulation. The numbers of FAPs (PDGFRα^+ cells) and ECs (CD31$^+$ cells) remained constant between the C26 and PBS mice from histological muscle sections (Fig. S3A and B), therefore we did not go further to examine if NMES affects the levels of these cells.

Muscles from C26 mice displayed intense accumulation of macrophages (F4/80$^+$ cells) compared to PBS mice (Fig. 4A), suggesting uncontrolled inflammation in the muscles of C26 mice. The total number of macrophages (F4/80$^+$ cells) was not impacted following NMES in the C26 mice (Fig. 4A). It is now well established that macrophages play crucial role in SC fate regulation after muscle injury[53]. Pro-inflammatory macrophages enhance SC proliferation while anti-inflammatory macrophage dampen inflammation and promote SC differentiation and fusion[53]. Therefore, we addressed whether NMES could differently impact macrophage inflammatory status in the C26 mice by quantifying the expression of different pro- (COX2 and iNOS) and anti- inflammatory (CD206 and IL-10) surface markers. NMES in the C26 mice did not change the proportion of macrophages expressing COX2 and iNOS (Fig. 4B and C). Likewise, NMES did not either alter the percentage of macrophages expressing the CD206 (Fig. 4D) but did increase the percentage of macrophages expressing IL-10 in the C26 mice compared to untrained C26 mice (Fig. 4E). IL-10 cytokine is released by anti-inflammatory macrophages and was shown to promote macrophage shift towards anti-inflammatory phenotype during muscle regeneration[54]. To validate a potential shift towards an anti-inflammatory status of macrophages within the C26 muscles induced by NMES, flow cytometry analysis was performed. Among CD45$^+$ sorted cells, macrophage population was defined by the expression of CD64 marker. Ly6C, CD206 and CCR2 markers were used to

characterize macrophage inflammatory phenotype (Fig. S4A). By using the expression of CD64 and Ly6C, we also succeeded in distinguishing neutrophils. NMES significantly decreased the proportion of neutrophils ($CD45^+CD64^-Ly6C^+$) (Fig. 4F) and tented to increase the overall proportion of macrophages ($CD45^+CD64^+$) (Fig. 4G) in the C26 muscles. The proportion of $Ly6C^+$ macrophages decreased (Fig. 4H) while that of $Ly6C^-$ macrophages increased (Fig. 4I) following NMES, suggesting a transition of macrophage from pro- into anti-inflammatory status. We further investigate whether NMES modifies the expression of additional pro- and anti-inflammatory markers among the different subtypes of $Ly6C^+$ and $Ly6C^-$ macrophages. Pro- CCR2 and anti-inflammatory CD206 expression did not vary in response to NMES training in the C26 mice (Fig. S4B, C, D and E). Overall, these findings suggest that NMES dampens muscle inflammation in the C26 mice by reducing neutrophil content and by switching macrophage status into anti-inflammatory.

NMES regulates macrophage function to guide SC differentiation and fusion *in vitro*

Thereafter, we wanted to go further in understanding how macrophages could regulate SC fate in response to NMES in the C26 muscles. Primary BMDMs taken from WT mice were cultured classically and exposed to muscle protein extracts derived either from PBS, C26 or C26+NMES muscles (Fig. 5A). First, the pro- and anti-inflammatory status of macrophages after exposure to extracts were assessed by quantifying the expression of pro-TNFα and anti-inflammatory CD206 markers. Macrophages exposed to extracts from C26 muscles appear to express greater TNFα and less CD206 levels compared to those exposed with extracts from PBS muscle (Fig. 5B and C). When exposed to extracts from C26+NMES muscles, macrophages conversely tend to express less TNFα and higher CD206 levels compared to C26 muscle, suggesting that factors released in the muscle microenvironment following NMES induce macrophages to acquire an anti-inflammatory phenotype. However, more replicates and additional markers (*e.g.,* IL-10) are needed to confirm our hypothesis. Next, the conditioned medium from BMDMs following their exposure to those extracts was used to assess SC myogenic properties *in vitro* (Fig. 5A). The proportion of proliferating myoblasts remained constant regardless of the BMDM-conditioned medium in which they were cultured (Fig. 5D), suggesting that factors released by macrophages in response to NMES do not impact SC proliferation in the C26 muscles. Treatment of myoblasts with conditioned medium from BMDMs exposed to C26 extracts trends to increase the levels of differentiation (Fig. 5E) and

to decrease the fusion index (Fig. 5F). Myoblasts cultured in conditioned medium from BMDMs exposed prior to C26+NMES muscle protein extracts tend to reverse the differentiation and fusion defects relative to C26 muscles (Fig. 5E and F). These results indicate that factors released in the cachectic muscle microenvironment in response to NMES may control macrophage function to improve SC differentiation and fusion.

Macrophage activity is required to improve SC function in the C26 mice in response to NMES

To rule out the possibility that SC function could be influenced by factors released in the muscle cachectic environment independently of macrophage activity, myoblasts were directly cultivated with the muscle protein extracts for the different *in vitro* assays (Fig. 6A). The percentage of proliferation, differentiation and fusion index of myoblasts treated either with extracts from C26 or C26 + NMES muscles did not vary (Fig. 6B, C and D) suggesting that macrophages are required for NMES to positively regulate SC function in the C26 mice.

Taken together, NMES training over 7 days for a total duration of only 16 minutes was able to improve SC fate, muscle inflammation and weakness in the C26-colon bearing mouse model of CC.

Longitudinal monitoring of body weight and muscle function decline in the *Apc*$^{Min/+}$

Growth of C26 tumor rapidly results in severe cachexia that might not reflect the progressive nature of cachexia often experienced by cancer patients. On the other hand, the *Apc*$^{Min/+}$ mouse model carries a mutation in the adenomatous polyposis coli (*Apc*) gene, which in humans is the genetic cause of the majority of sporadic colon cancers. Similarly, to humans, the *Apc*$^{Min/+}$mice are prone to develop intestinal adenomas (*i.e.,* polyps) resulting in progressive formation of colon cancer associated with cachexia.

Having the possibility to assess the effects of NMES in a much larger window with the *Apc*$^{Min/+}$ mouse model, we first aimed at determining the time-point of CC onset and further characterize skeletal muscle alterations. Body weight and muscle force of *Apc*$^{Min/+}$ mice were weekly monitored from 8 to 27 weeks of age. The median survival of *Apc*$^{Min/+}$ was 20 weeks (Fig. S5A). Body weight gain was progressively restricted in *Apc*$^{Min/+}$ from 12 weeks in comparison to WT mice (Fig. 7A). By 18 weeks of age, body weight began to decrease drastically in *Apc*$^{Min/+}$ mice resulting in 15% loss of their maximal body weight at ethical endpoint (Fig. 7A and C). At 16 weeks of age, the muscle force production was significantly

reduced by 26% in the *Apc*$^{Min/+}$ mice compared to WT mice (Fig. 7B). At the ethical endpoint, *Apc*$^{Min/+}$ lost 34% of their initial muscle force (Fig. 7D). Because *Apc*$^{Min/+}$ mice presented high variability in body weight and muscle force production, they were also stratified according to survival (Low survival $\leq$ 20 weeks *vs* High survival > 20 weeks) (Fig. S5B and C). *Apc*$^{Min/+}$ mice with high survival did not present body weight and muscle force loss before 18 weeks. At 16 weeks, low survival *Apc*$^{Min/+}$ mice display a F_{max} *of* 13 $\pm$ 3 mN.m while high survival *Apc*$^{Min/+}$ mice display a F_{max} *of* 16 $\pm$ 3 mN.m, therefore due to this overlap it was not possible to use the force production as a predicting factor for *Apc*$^{Min/+}$ mice survival. At the study's endpoint, muscle mass and muscle fiber CSA were both dramatically reduced in *Apc*$^{Min/+}$ compared to WT mice (Fig. 7E and G) by 26% and 23%, respectively. Furthermore, no overt signs of muscle membrane damage were detected in *Apc*$^{Min/+}$ (Fig. 7F). Specific muscle force was lower in *Apc*$^{Min/+}$ mice (Fig. S5D), indicating that the loss in skeletal muscle mass is not entirely responsible for the force loss. The number of myonuclei remained constant in both WT and *Apc*$^{Min/+}$ mice (Fig. 7H).

Increased macrophage and FAP accumulation in the skeletal muscles of *Apc*$^{Min/+}$ mice

Alterations in the SC niche have been mainly described in the C26 tumor-bearing mouse model of CC[13,15,24]. Here for the first time, we aimed at finding potential alterations in the different muscle cell populations from the SC niche of *Apc*$^{Min/+}$ mouse model which recapitulates more closely human CC. Immunofluorescence analysis from muscles of *Apc*$^{Min/+}$mice, performed at the ethical endpoint (~ mice 20 weeks old), revealed significantly decreased number of SCs (-35%) and increased number of total macrophages (+132%), while no differences were observed for ECs, as compared to WT mice (Fig. 8A, B and C). *Apc*$^{Min/+}$ mouse muscle also displayed higher number of FAPs (+ 67%) which was associated with significant increase in type I collagen content (Fig. 8D and E), suggesting that muscle fibrosis occurred in cachectic *Apc*$^{Min/+}$ mice at the advanced stage of CC.

The SC differentiation and fusion capacities are impaired in the cachectic *Apc*$^{Min/+}$ mice

We then investigated whether these alterations in the SCs number and in the different cell types composing the SC niche could be associated with defects in myogenesis. SCs were isolated from muscles of both WT mice and *Apc*$^{Min/+}$ mice with severe CC to evaluate their ability of proliferation, differentiation and fusion. The rates of EdU^+ myoblasts among WT and

cachectic *Apc*$^{Min/+}$ was equivalent (Fig. 9A), indicating that the intrinsic ability of SCs to proliferate is not impaired in *Apc*$^{Min/+}$ mice. In differentiation conditions, myoblasts from cachectic *Apc*$^{Min/+}$ muscles tend to differentiate less (-14%, *p=0,1*) relative to WT mice (Fig. 9B). Importantly, the fusion index of myoblasts derived from cachectic *Apc*$^{Min/+}$ mice was significantly (-15%) lower from the one of WT-myoblasts (Fig. 9C), indicating that SCs from *Apc*$^{Min/+}$ mice at the endpoint possess impaired fusion ability.

It was shown that expression of *Apc* by SCs is required for regenerative myogenesis and SC survival[55]. Disruption of *Apc* gene in SCs leads to loss of myogenic potential and SCs undergo apoptosis upon activation in healthy mice. In order to rule out the possibility that *Apc* gene mutation could be at the origin of SC myogenic defect in our cachectic animals, we assessed SC myogenesis from young *Apc*$^{Min/+}$ mice (8-9 weeks) that had not yet developed cachexia. The proliferation and differentiation rates as well as the fusion index of myoblasts isolated from young *Apc*$^{Min/+}$ mice were not impaired as compared to WT (Fig. 9D, E and F), suggesting that the differentiation and fusion intrinsic defects observed in the cachectic *Apc*$^{Min/+}$ mice are probably caused by the cachectic muscle environment.

NMES prevents muscle atrophy in the *Apc*$^{Min/+}$ mice

So far, we identified muscle weakness and atrophy occurring in *Apc*$^{Min/+}$ mice, both associated with impairment of the SCs and their niche. We then intended to determine whether our NMES protocol could be applied as therapeutic strategy to reverse these alterations, as in the C26 mouse model. We have previously shown that applying our individualized NMES protocol to healthy muscle for a longer period of time (4x *per* week, during 3 weeks), further induces myonuclear accretion and hypertrophy. Muscle force decline resulted from 16 weeks of age in our previous *Apc*$^{Min/+}$ mice cohort, therefore we employed our extended NMES protocol in the *Apc*$^{Min/+}$ mice, starting from 16 weeks of age and covering the time frame of the progressive muscle force decline (Fig. 10A). Three days after the last NMES session, the *gastrocnemius* muscles were harvested for histological analysis. NMES had no effect on variations of body weight (Fig. 10B) and muscle force production (Fig. 10C). However, the *Apc*$^{Min/+}$ mice assigned to the control group did not display decrease in muscle force from 16 weeks, indicating that severe cachexia might had not yet started. Perhaps, another possibility is that the repeated muscle force measurements performed on control *Apc*$^{Min/+}$ mice contributed to limit the functional alterations. The great variation regarding the onset and

progression of cachexia in these animals made it difficult for us to predict which animals would be susceptible to cachexia (Fig. S5A and B). The total number of polyps in the small intestine and colon was not different between *Apc*$^{Min/+}$ mice and *Apc*$^{Min/+}$+ NMES (Fig. 10F). On average less than 35 polyps in total were detected for each mouse group which does not correspond to the average number of polyps seen in *Apc*$^{Min/+}$ at an advanced stage of disease (> 70 polyps)[56], confirming that *Apc*$^{Min/+}$ mice had not yet developed severe cachexia. Moreover, NMES did not prevent the reduction of muscle mass by 11% in the *Apc*$^{Min/+}$ mice compared to PBS mice (Fig. 10D). Finally, *Apc*$^{Min/+}$ mice showed a 20% reduction in muscle fiber size compared to WT mice (Fig. 10E). Interestingly *Apc*$^{Min/+}$ +NMES mice showed a 16% higher muscle fiber CSA values compared to *Apc*$^{Min/+}$ mice and not different from WT mice. Thus, 3 weeks of NMES training preserved muscle fiber size in the *Apc*$^{Min/+}$ mice.

NMES does not improve SC alterations within the muscle of *Apc*$^{Min/+}$ mouse

Six sessions of NMES seemed to be effective at improving SC fate and muscle inflammation in the C26 tumor-bearing model, next we wanted to see if a prolonged NMES training protocol which increase muscle fiber size in the *Apc*$^{Min/+}$, contributes to minimize the SC dysfunction and SC niche alterations occurring in these mice. NMES training on *Apc*$^{Min/+}$ mice failed to restore SC numbers, proliferation and differentiation at physiological levels (Fig. 11A, B and C). In contrast to healthy and C26-cachectic muscles, where NMES increased the amount of myonuclei, NMES was unable to achieve this increase in the muscles of *Apc*$^{Min/+}$ mice (Fig. 11D). This result strongly suggests that NMES failed to overcome the SC fusion defect in the *Apc*$^{Min/+}$ mice. To determine whether NMES cannot exert its beneficial effect on SC fusion due to a deficient mechanism residing within the SCs in the *Apc*$^{Min/+}$, we assessed the fusion ability of control myoblasts cultured with protein extracts obtained from WT, *Apc*$^{Min/+}$ and *Apc*$^{Min/+}$+NMES muscles. When cultured with *Apc*$^{Min/+}$ muscle protein extracts, myoblasts fused less relative to WT (Fig. 11E) indicating that the cachectic muscle microenvironment further contributes to the defect of SC fusion in the *Apc*$^{Min/+}$ mice. On the other hand, the fusion of control myoblasts cultured with protein extracts obtained from *Apc*$^{Min/+}$+NMES muscles was restored compared to those cultured with *Apc*$^{Min/+}$ extracts (Fig. 11E). Even when the muscle microenvironment improves with NMES training, the SC fusion defect in the *Apc*$^{Min/+}$ mice still persists, indicating that SCs are intrinsically impaired.

NMES training on *Apc*$^{Min/+}$ mice did not show any effect on the number of total macrophages, FAPs or type I collagen composition (Fig. 11F, G and H). It is noteworthy to mention that macrophage and collagen accumulation were not observed in our cohort of control *Apc*$^{Min/+}$ mice, assuming again that they might had not yet developed severe cachexia. This could mean that macrophage and collagen alterations depend on cachexia severity. Overall, NMES appears to exert beneficial effect for treating muscle atrophy regardless of SC regulation and its cellular partners in the *Apc*$^{Min/+}$ mice.

Figure 1

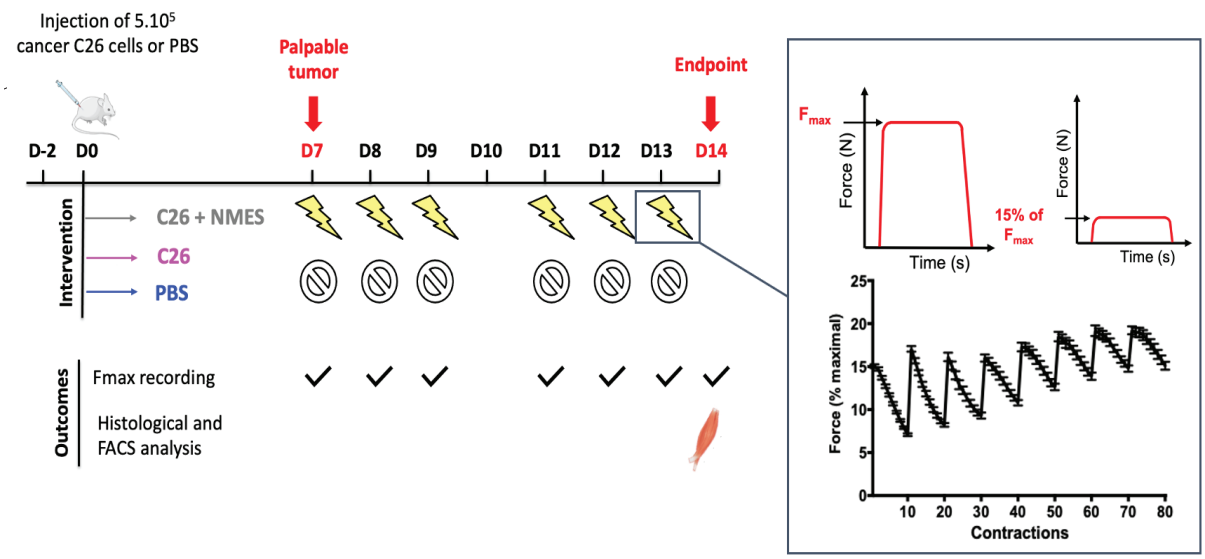
Injection of 5.10⁵
cancer C26 cells or PBS
Palpable
tumor
Endpoint
D-2
D0
D7
D8
D9
D10
D11
D12
D13
D14
Intervention
C26 + NMES
C26
PBS
Outcomes
Fmax recording
Histological and
FACS analysis
Fmax
Force (N)
Time (s)
15% of
Fmax
Force (N)
Time (s)
Force (% maximal)
25
20
15
10
5
0
10
20
30
40
50
60
70
80
Contractions

Figure 2

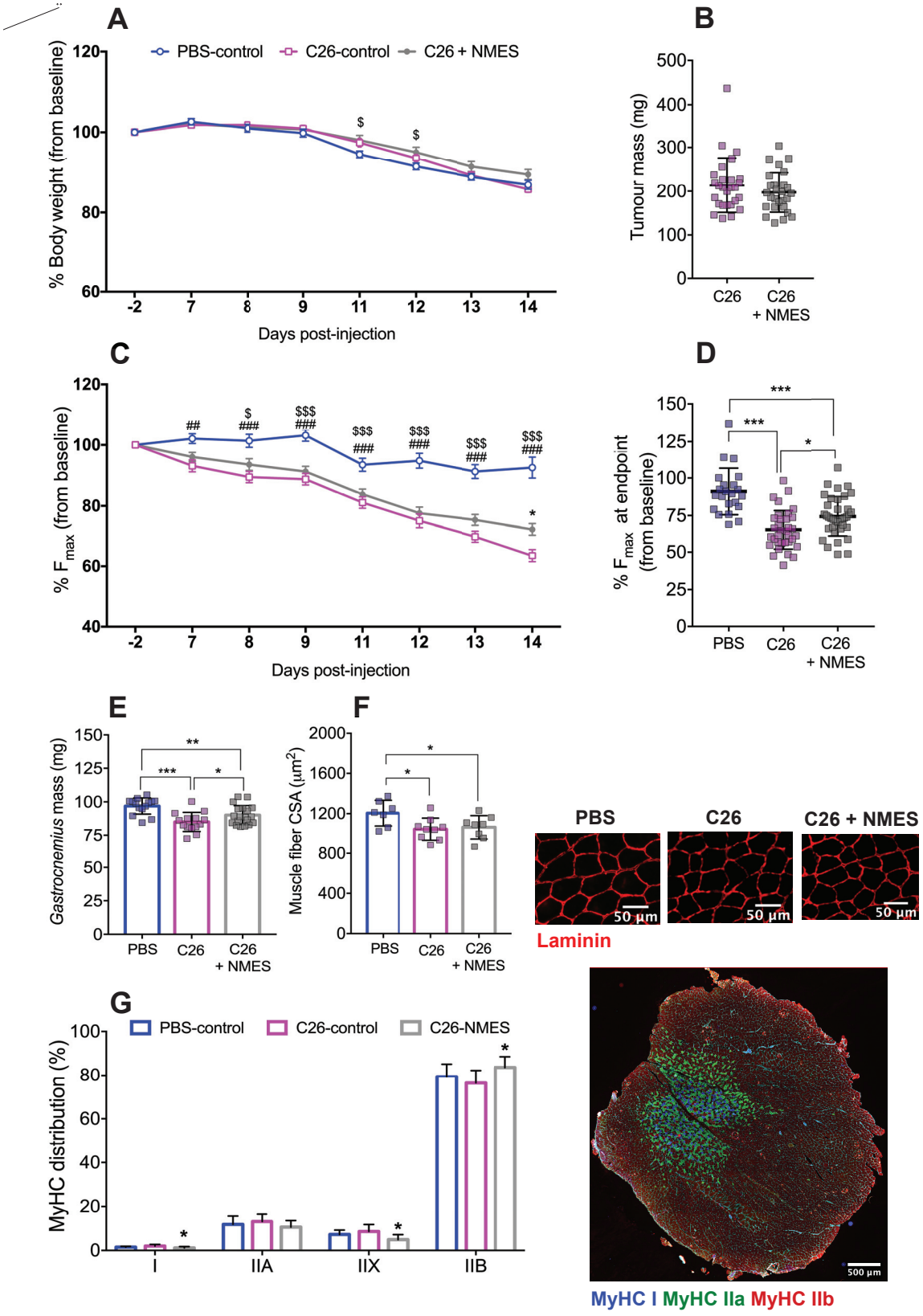
A
PBS-control
C26-control
C26 + NMES
% Body weight (from baseline)
Days post-injection
B
Tumour mass (mg)
C26
C26 + NMES
C
% F max (from baseline)
Days post-injection
D
% F max at endpoint (from baseline)
PBS
C26
C26 + NMES
E
Gastrocnemius mass (mg)
F
Muscle fiber CSA (µm²)
PBS
C26
C26 + NMES
PBS
C26
C26 + NMES
50 µm
Laminin
G
PBS-control
C26-control
C26-NMES
MyHC distribution (%)
I
IIA
IIX
IIB
500 µm
MyHC I MyHC IIa MyHC IIb

Figure 3

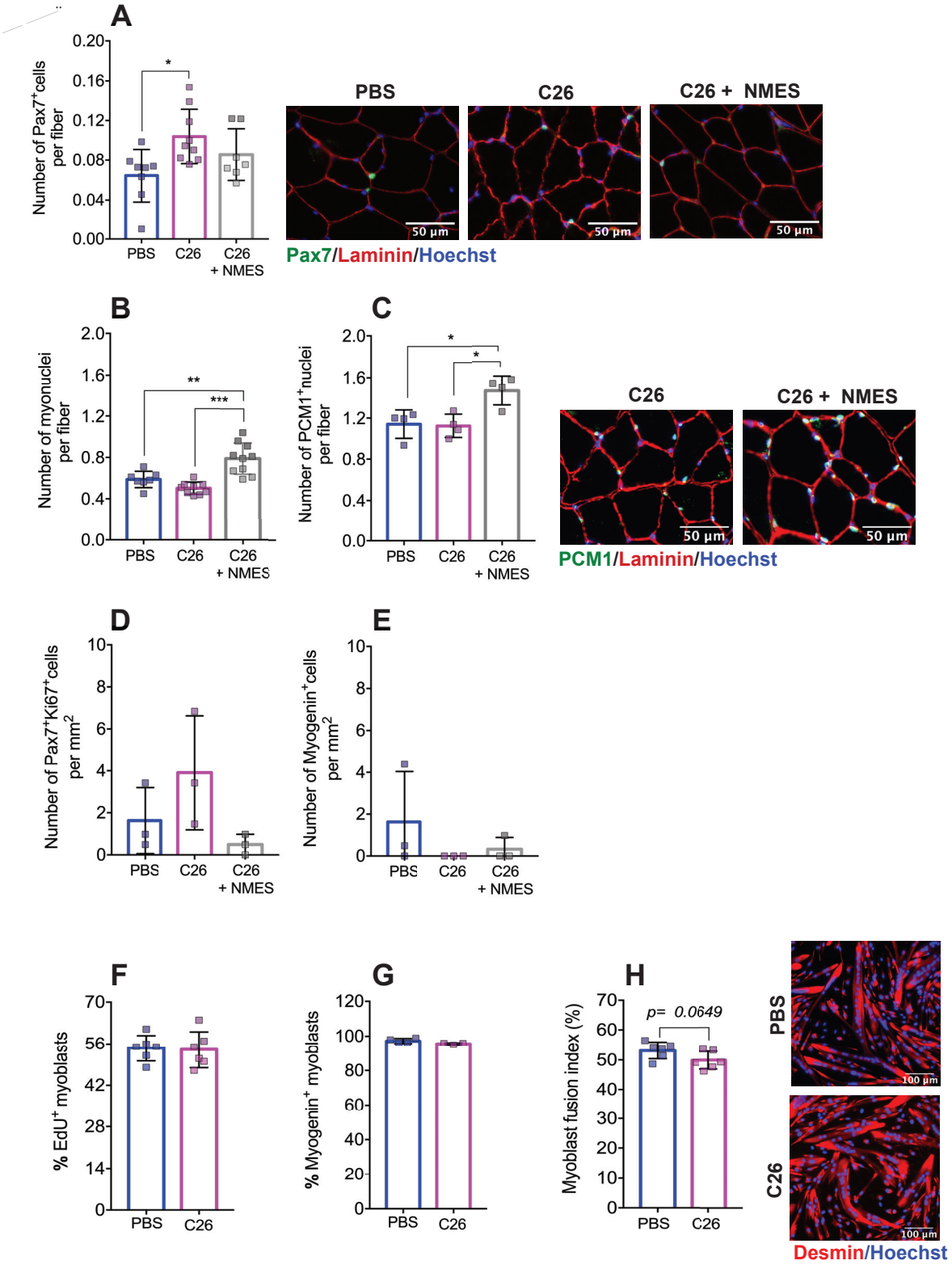
A
Number of Pax7+cells per fiber
0.20
0.16
0.12
0.08
0.04
0.00
*
PBS
C26
C26 + NMES
PBS
C26
C26 + NMES
50 µm
Pax7/Laminin/Hoechst
B
Number of myonuclei per fiber
2.0
1.6
1.2
0.8
0.4
0.0
**
***
PBS
C26
C26 + NMES
C
Number of PCM1+nuclei per fiber
2.0
1.6
1.2
0.8
0.4
0.0
*
*
PBS
C26
C26 + NMES
C26
C26 + NMES
50 µm
PCM1/Laminin/Hoechst
D
Number of Pax7+Ki67+cells per mm2
10
8
6
4
2
0
PBS
C26
C26 + NMES
E
Number of Myogenin+cells per mm2
10
8
6
4
2
0
PBS
C26
C26 + NMES
F
% EdU+ myoblasts
70
56
42
28
14
0
PBS
C26
G
% Myogenin+ myoblasts
120
100
80
60
40
20
0
PBS
C26
H
Myoblast fusion index (%)
70
60
50
40
30
20
10
0
p= 0.0649
PBS
C26
PBS
C26
100 µm
Desmin/Hoechst

Figure 4

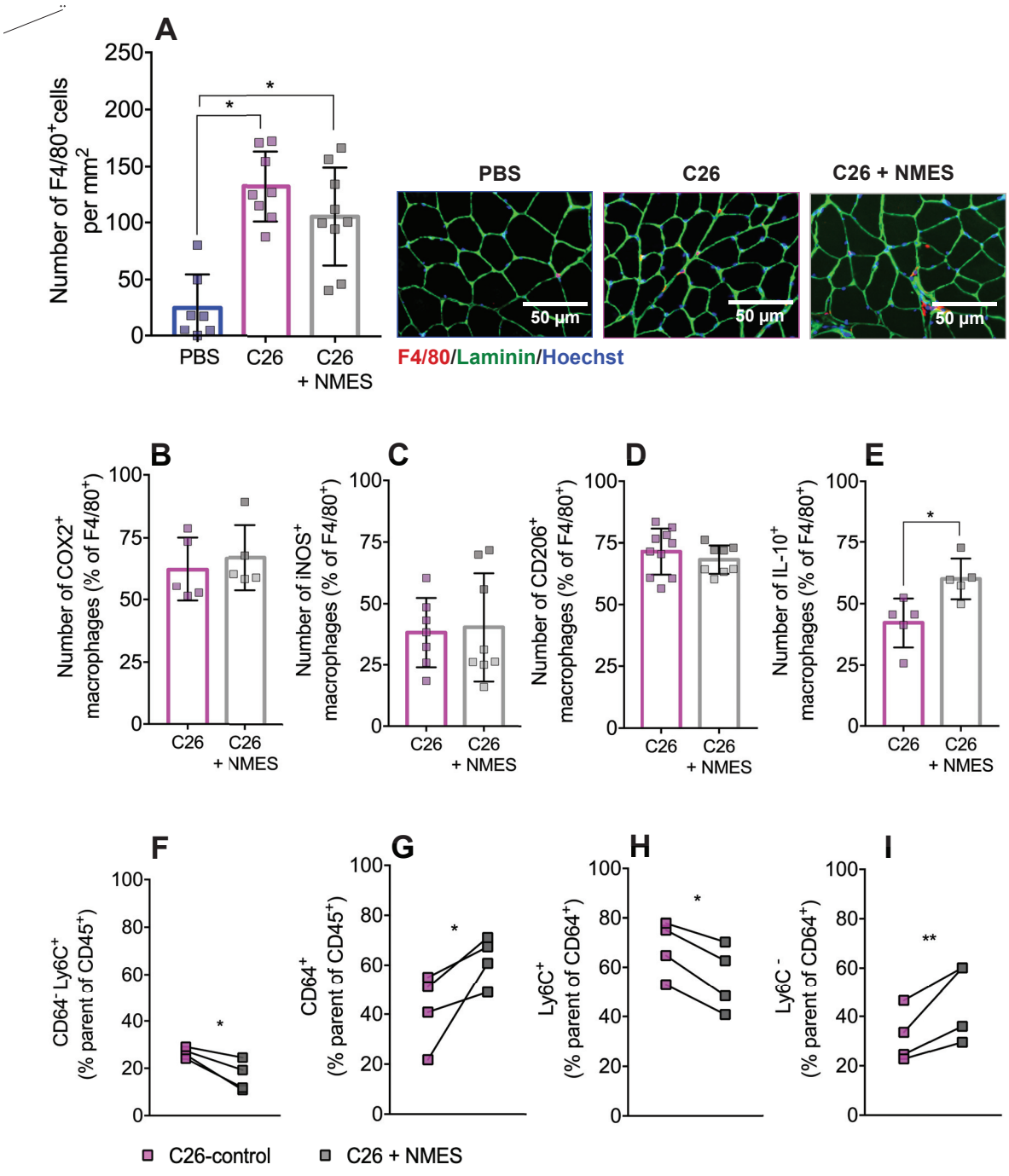
A
Number of F4/80+cells per mm2
PBS
C26
C26 + NMES
F4/80/Laminin/Hoechst
50 µm
B
Number of COX2+ macrophages (% of F4/80+)
C
Number of iNOS+ macrophages (% of F4/80+)
D
Number of CD206+ macrophages (% of F4/80+)
E
Number of IL-10+ macrophages (% of F4/80+)
F
CD64+Ly6C+ (% parent of CD45+)
G
CD64+ (% parent of CD45+)
H
Ly6C+ (% parent of CD64+)
I
Ly6C- (% parent of CD64+)
C26-control
C26 + NMES

Figure 5

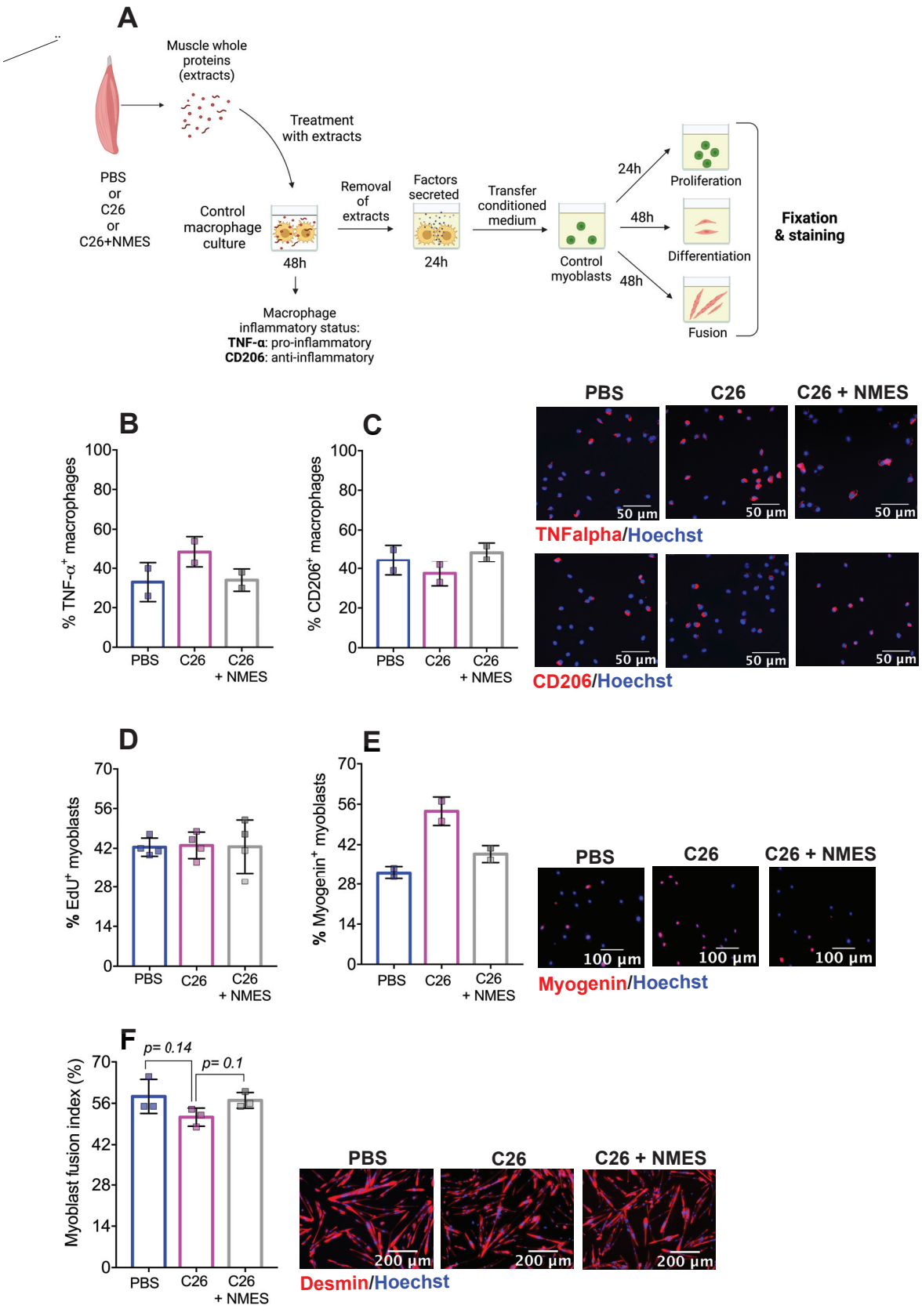
A
Muscle whole proteins (extracts)
Treatment with extracts
PBS or C26 or C26+NMES
Control macrophage culture
48h
Removal of extracts
Factors secreted
24h
Transfer conditioned medium
Control myoblasts
24h
48h
48h
Proliferation
Differentiation
Fusion
Fixation & staining
Macrophage inflammatory status:
TNF-α: pro-inflammatory
CD206: anti-inflammatory
B
% TNF-α+ macrophages
PBS
C26
C26 + NMES
C
% CD206+ macrophages
PBS
C26
C26 + NMES
PBS
C26
C26 + NMES
50 µm
TNFalpha/Hoechst
CD206/Hoechst
D
% EdU+ myoblasts
PBS
C26
C26 + NMES
E
% Myogenin+ myoblasts
PBS
C26
C26 + NMES
PBS
C26
C26 + NMES
100 µm
Myogenin/Hoechst
F
p= 0.14
p= 0.1
Myoblast fusion index (%)
PBS
C26
C26 + NMES
PBS
C26
C26 + NMES
200 µm
Desmin/Hoechst

Figure 6

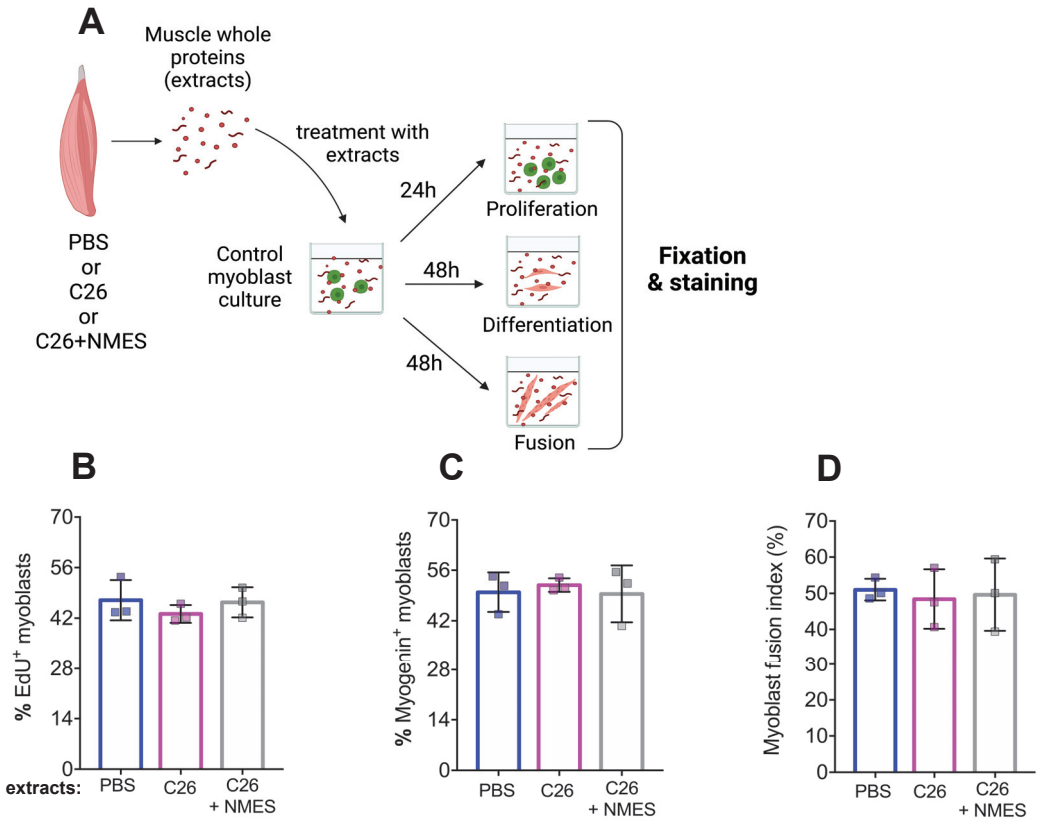
A
Muscle whole proteins (extracts)
treatment with extracts
PBS or C26 or C26+NMES
Control myoblast culture
24h
48h
48h
Proliferation
Differentiation
Fusion
Fixation & staining
B
% EdU+ myoblasts
70
56
42
28
14
0
extracts:
PBS
C26
C26 + NMES
C
% Myogenin+ myoblasts
70
56
42
28
14
0
PBS
C26
C26 + NMES
D
Myoblast fusion index (%)
70
60
50
40
30
20
10
0
PBS
C26
C26 + NMES

Figure 7

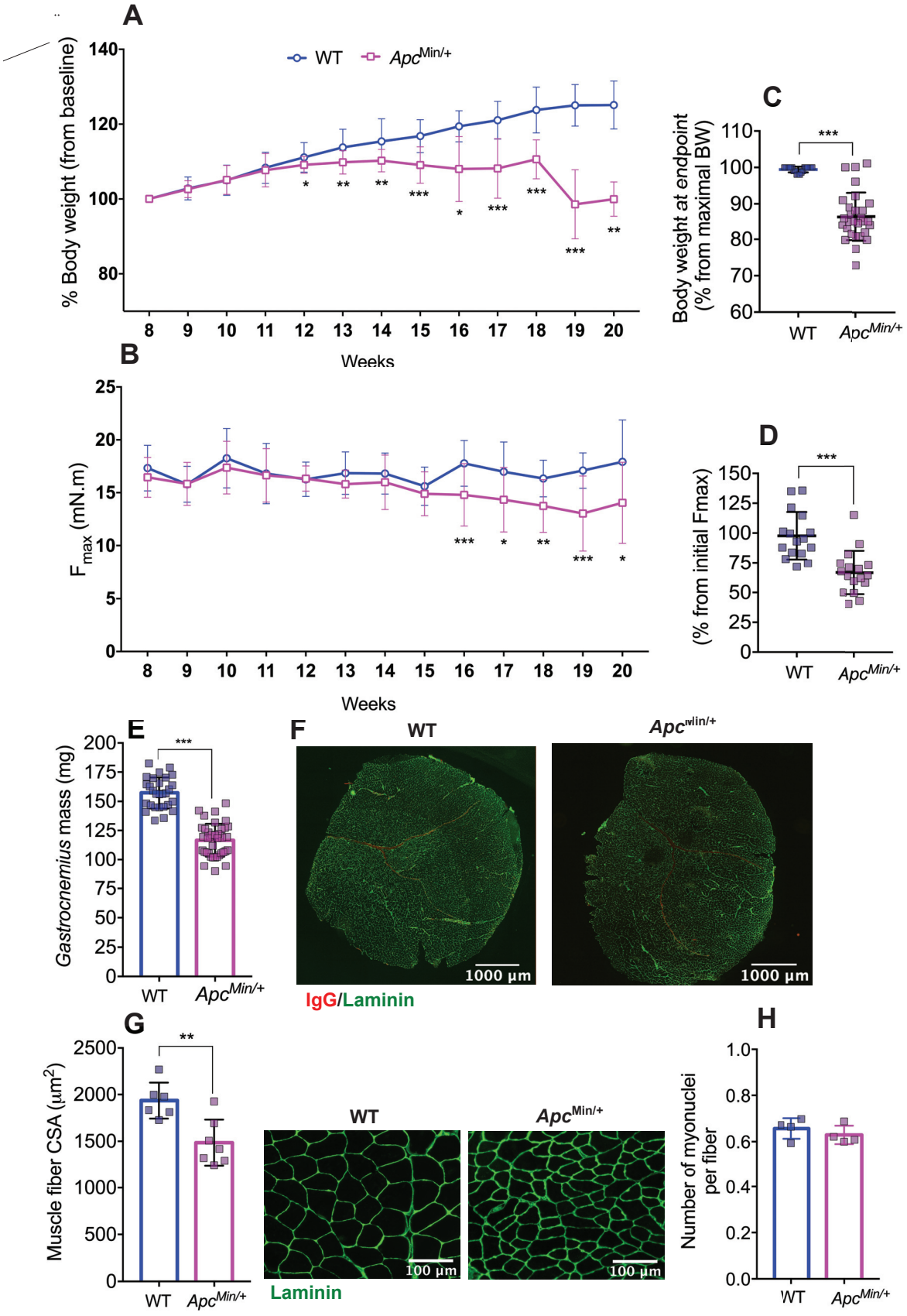
A
WT
ApcMin/+
% Body weight (from baseline)
Weeks
B
Fmax (mN.m)
Weeks
C
Body weight at endpoint (% from maximal BW)
WT
ApcMin/+
D
(% from initial Fmax)
WT
ApcMin/+
E
Gastrocnemius mass (mg)
WT
ApcMin/+
F
WT
ApcMin/+
1000 µm
1000 µm
IgG/Laminin
G
Muscle fiber CSA (µm2)
WT
ApcMin/+
WT
ApcMin/+
100 µm
100 µm
Laminin
H
Number of myonuclei per fiber
WT
ApcMin/+

Figure 8

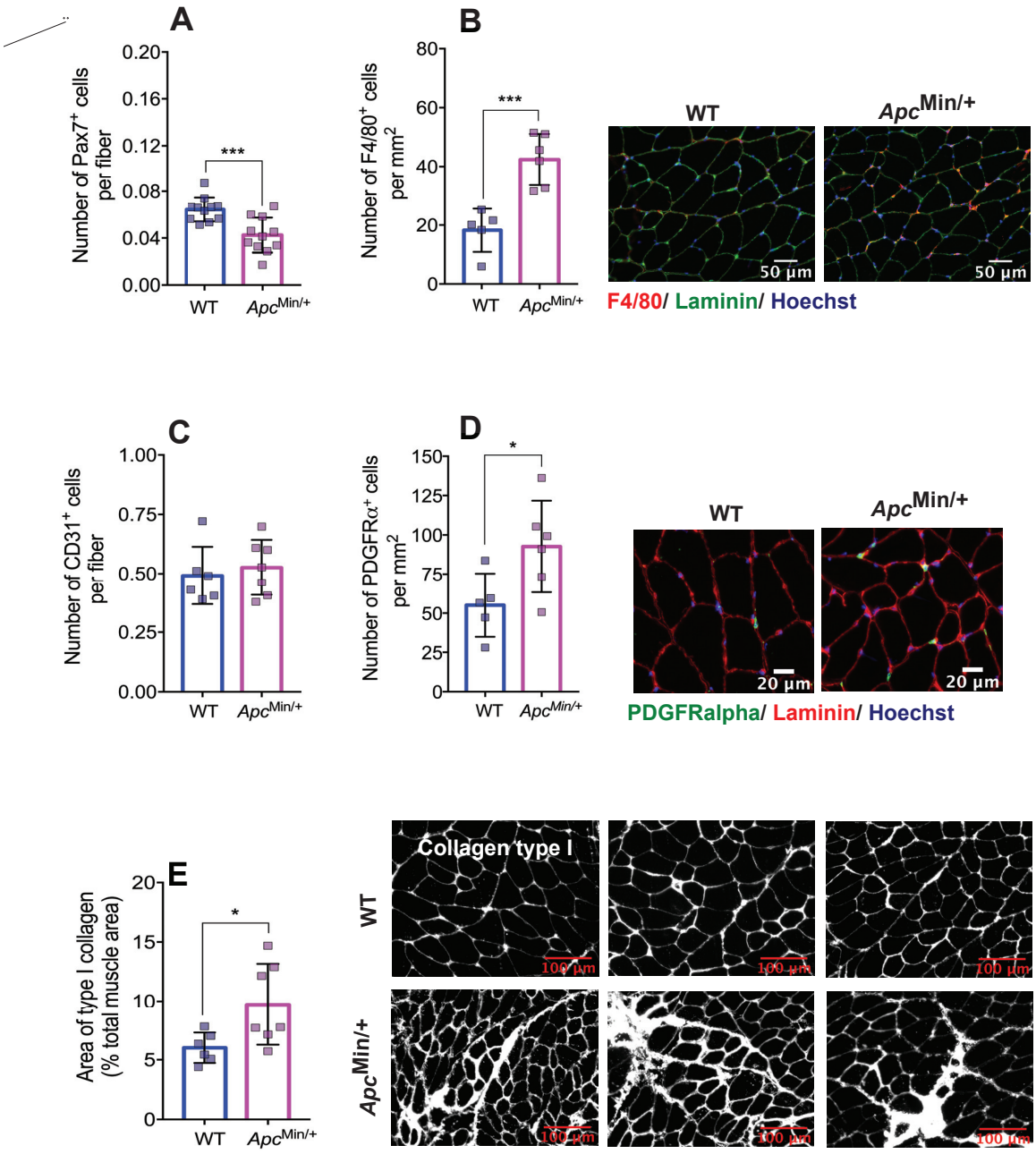
A
Number of Pax7+ cells per fiber
0.20
0.16
0.12
0.08
0.04
0.00
***
WT
ApcMin/+
B
Number of F4/80+ cells per mm2
80
60
40
20
0
***
WT
ApcMin/+
WT
ApcMin/+
50 µm
50 µm
F4/80/ Laminin/ Hoechst
C
Number of CD31+ cells per fiber
1.00
0.75
0.50
0.25
0.00
WT
ApcMin/+
D
Number of PDGFRα+ cells per mm2
150
125
100
75
50
25
0
*
WT
ApcMin/+
WT
ApcMin/+
20 µm
20 µm
PDGFRalpha/ Laminin/ Hoechst
E
Area of type I collagen (% total muscle area)
20
15
10
5
0
*
WT
ApcMin/+
Collagen type I
WT
ApcMin/+
100 µm
100 µm
100 µm
100 µm
100 µm
100 µm

Figure 9

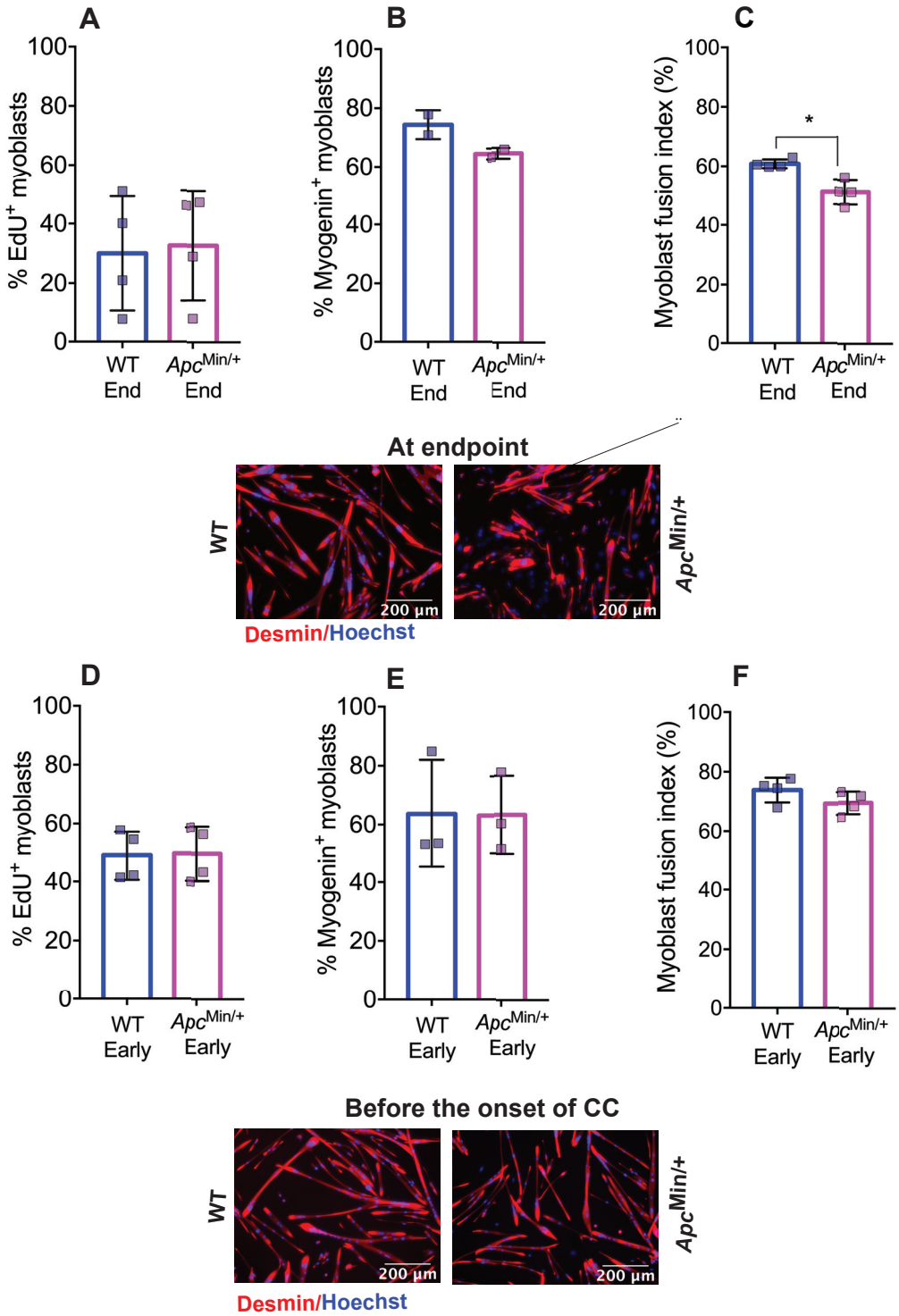
A
B
C
% EdU+ myoblasts
% Myogenin+ myoblasts
Myoblast fusion index (%)
100
80
60
40
20
0
WT End
ApcMin/+ End
*
At endpoint
WT
ApcMin/+
200 µm
Desmin/Hoechst
D
E
F
WT Early
ApcMin/+ Early
Before the onset of CC

Figure 10

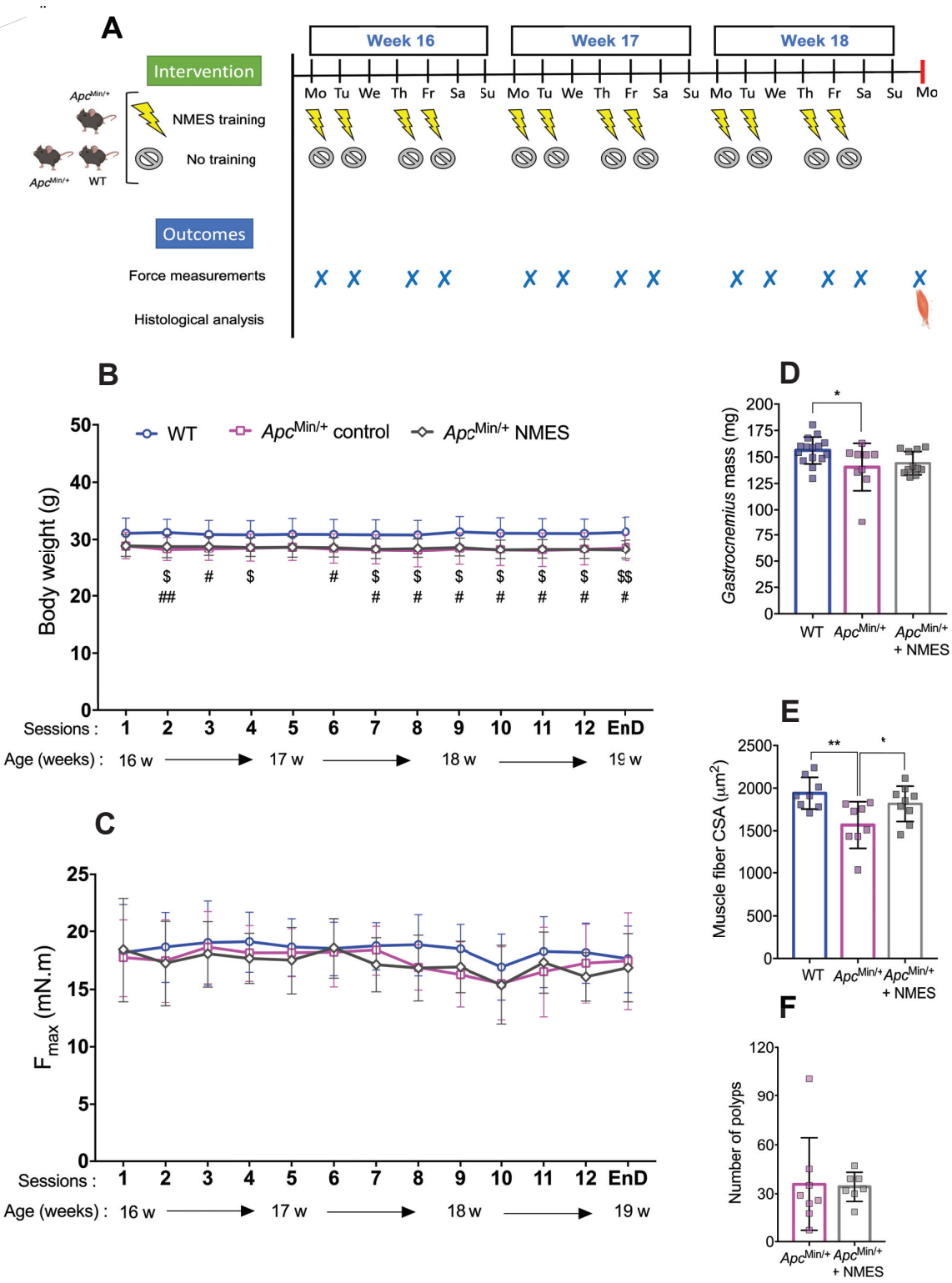
A
Week 16
Week 17
Week 18
Intervention
Mo Tu We Th Fr Sa Su Mo Tu We Th Fr Sa Su Mo Tu We Th Fr Sa Su Mo
NMES training
No training
Outcomes
Force measurements
Histological analysis
WT
B
WT
ApcMin/+ control
ApcMin/+ NMES
Body weight (g)
Sessions : 1 2 3 4 5 6 7 8 9 10 11 12 EnD
Age (weeks) : 16 w 17 w 18 w 19 w
C
Fmax (mN.m)
Sessions : 1 2 3 4 5 6 7 8 9 10 11 12 EnD
Age (weeks) : 16 w 17 w 18 w 19 w
D
Gastrocnemius mass (mg)
WT
ApcMin/+
ApcMin/+ + NMES
E
Muscle fiber CSA (µm2)
WT
ApcMin/+
ApcMin/+ + NMES
F
Number of polyps
ApcMin/+
ApcMin/+ + NMES

Figure 11

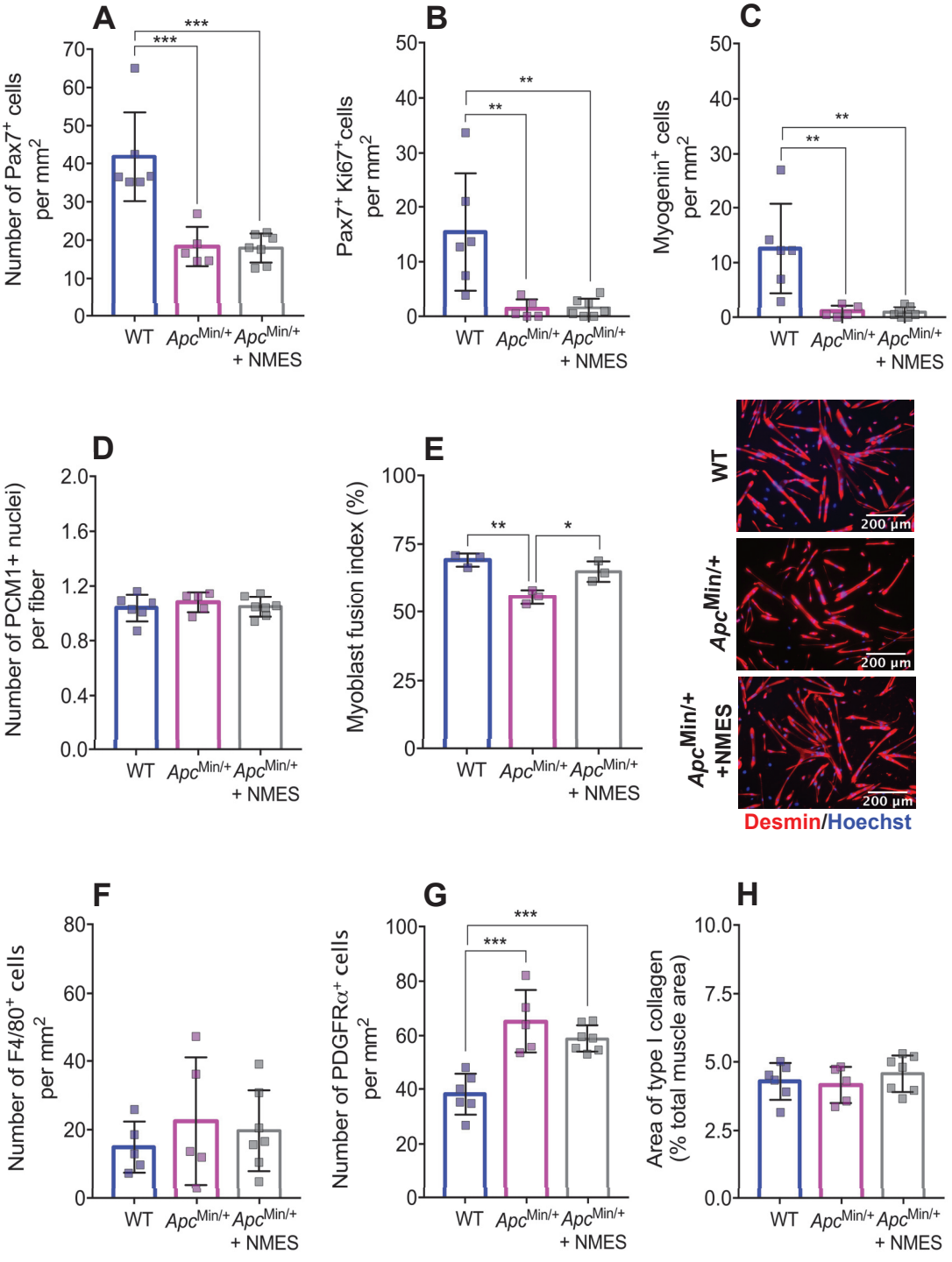
A
Number of Pax7+ cells per mm2
B
Pax7+ Ki67+cells per mm2
C
Myogenin+ cells per mm2
D
Number of PCM1+ nuclei) per fiber
E
Myoblast fusion index (%)
WT
ApcMin/+
ApcMin/+ +NMES
200 µm
Desmin/Hoechst
F
Number of F4/80+ cells per mm2
G
Number of PDGFRα+ cells per mm2
H
Area of type I collagen (% total muscle area)
WT
ApcMin/+
ApcMin/+ + NMES

Figure S1

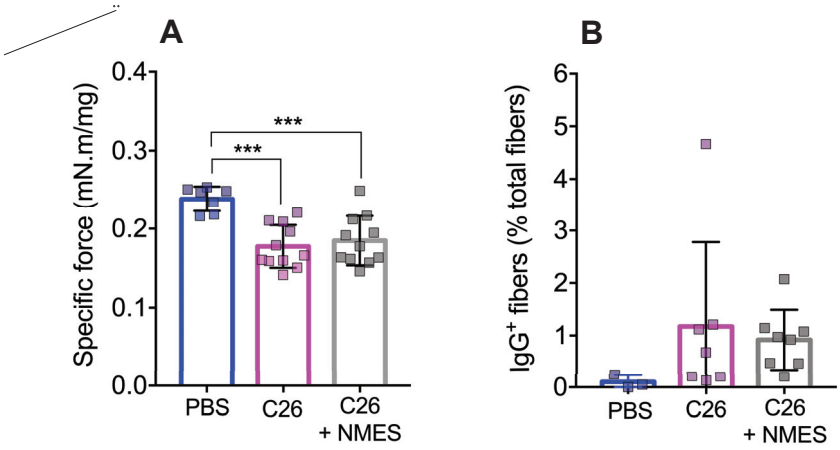
A
Specific force (mN.m/mg)
0.4
0.3
0.2
0.1
0.0
***
***
PBS
C26
C26
+ NMES
B
IgG+ fibers (% total fibers)
6
5
4
3
2
1
0
PBS
C26
C26
+ NMES

Figure S2

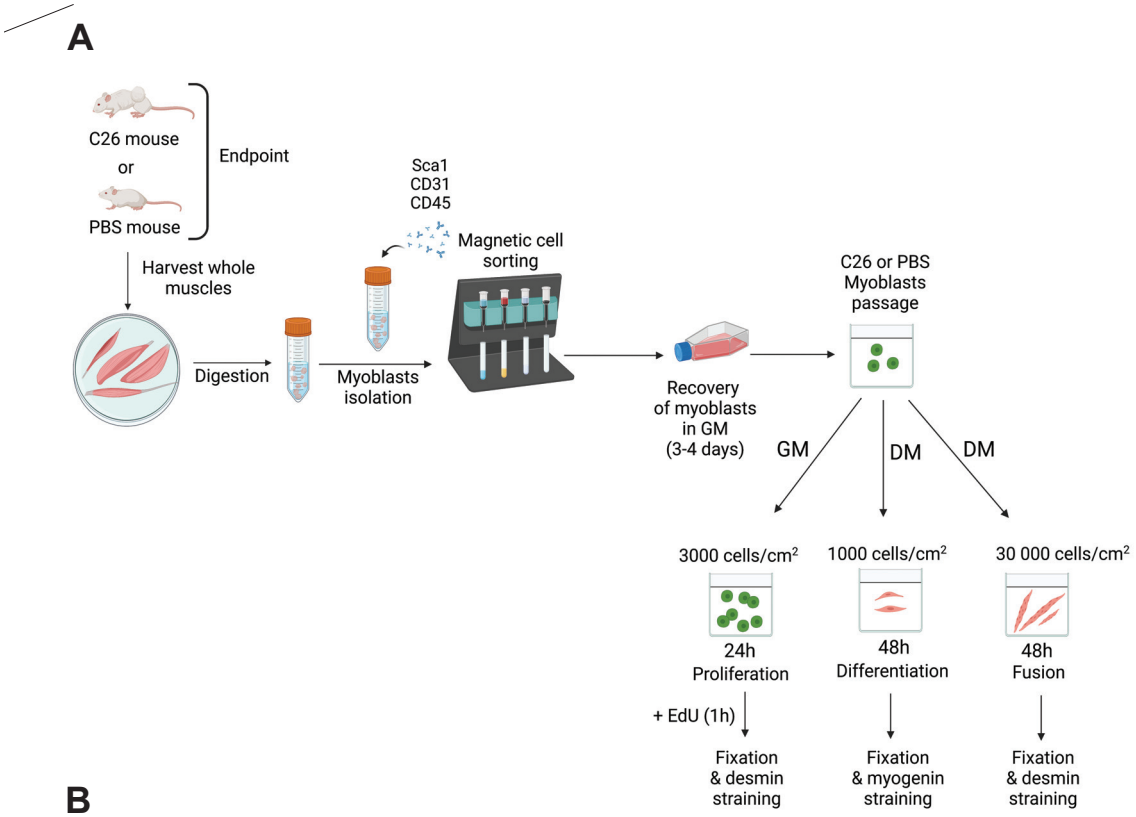
A
C26 mouse
or
PBS mouse
Endpoint
Harvest whole muscles
Digestion
Sca1
CD31
CD45
Magnetic cell sorting
Myoblasts isolation
Recovery of myoblasts in GM (3-4 days)
C26 or PBS Myoblasts passage
GM
DM
DM
3000 cells/cm²
1000 cells/cm²
30 000 cells/cm²
24h Proliferation
48h Differentiation
48h Fusion
+ EdU (1h)
Fixation & desmin straining
Fixation & myogenin straining
Fixation & desmin straining

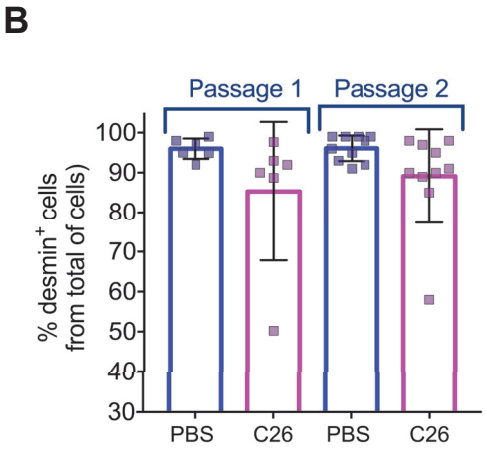
B
Passage 1
Passage 2
% desmin+ cells from total of cells)
100
90
80
70
60
50
40
30
PBS
C26
PBS
C26

Figure S3

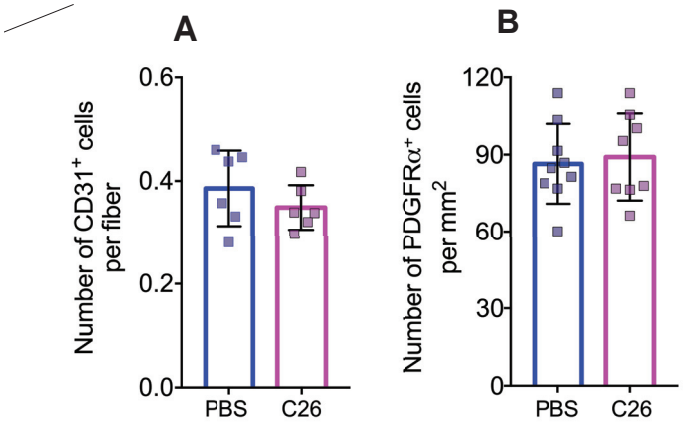
A
B
Number of CD31+ cells per fiber
0.6
0.4
0.2
0.0
PBS
C26
Number of PDGFRα+ cells per mm2
120
90
60
30
0
PBS
C26

Figure S4

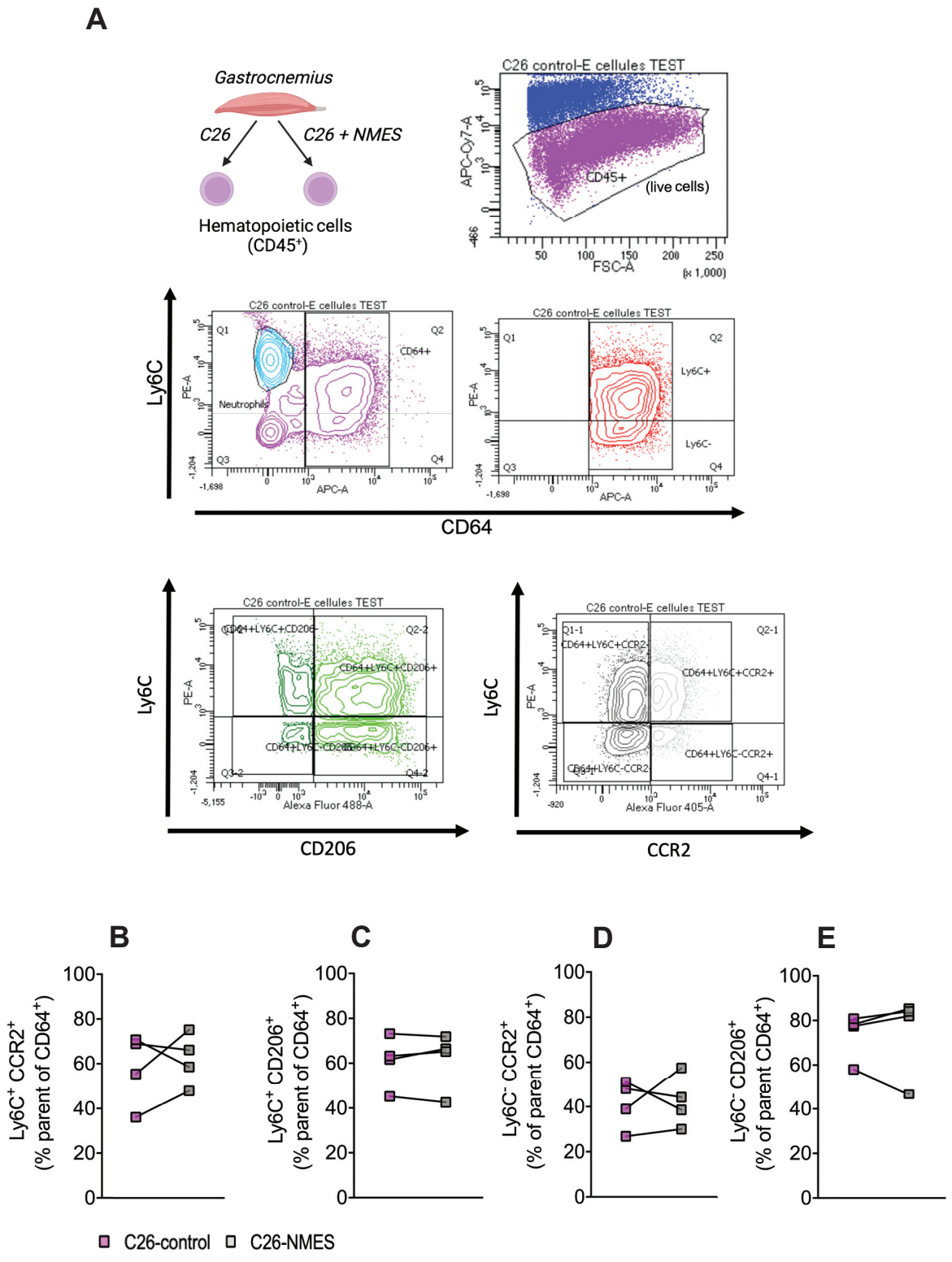
A
Gastrocnemius
C26
C26 + NMES
Hematopoietic cells
(CD45+)
C26 control-E cellules TEST
APC-Cy7-A
CD45+
(live cells)
FSC-A
(x 1,000)
Ly6C
CD64
Neutrophils
CD64+
Ly6C+
Ly6C-
APC-A
PE-A
CD206
CCR2
Alexa Fluor 488-A
Alexa Fluor 405-A
B
C
D
E
Ly6C+ CCR2+ (% parent of CD64+)
Ly6C+ CD206+ (% parent of CD64+)
Ly6C- CCR2+ (% of parent CD64+)
Ly6C- CD206+ (% of parent CD64+)
C26-control
C26-NMES

Figure S5

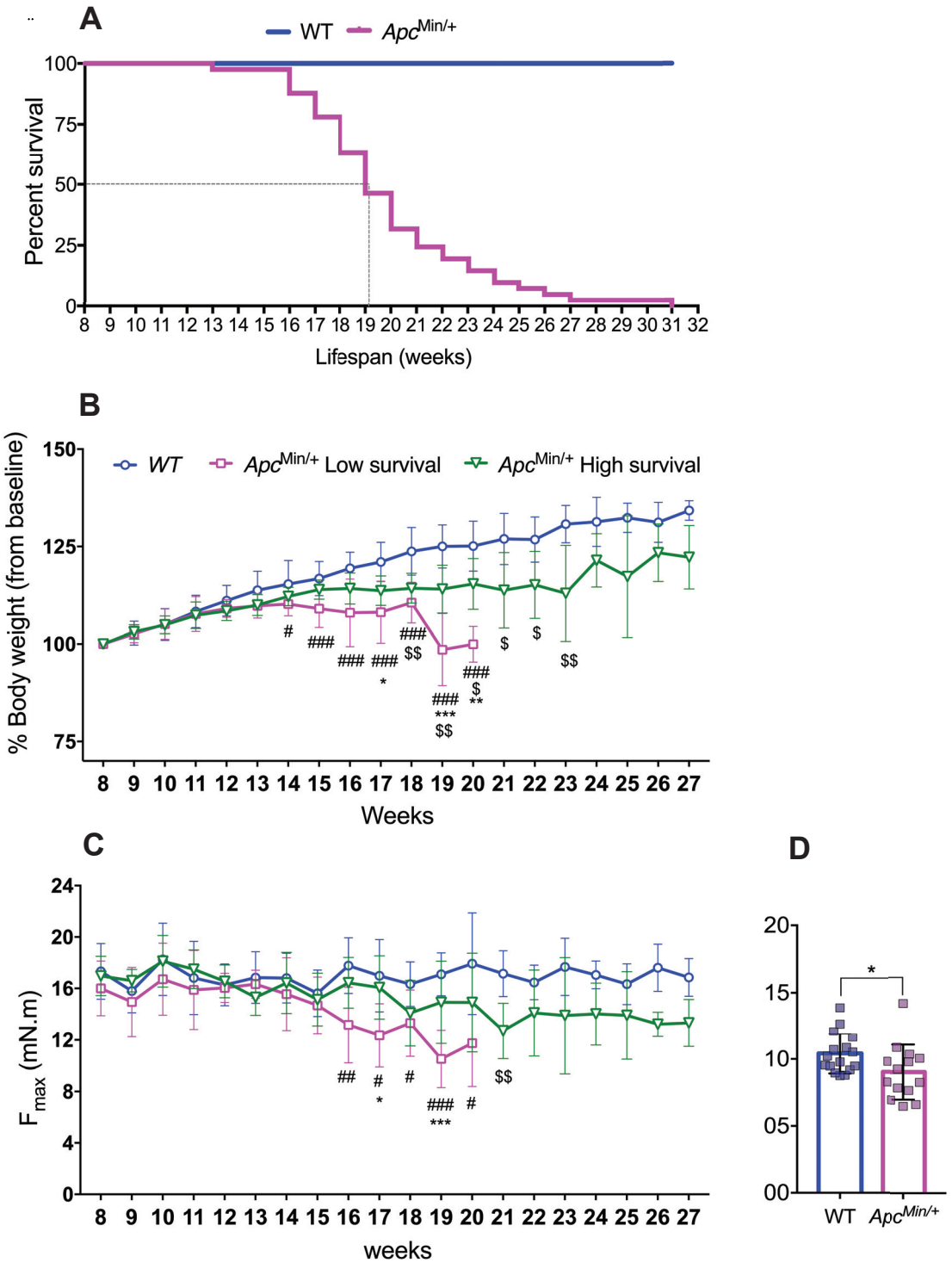
A
WT
ApcMin/+
Percent survival
Lifespan (weeks)
B
WT
ApcMin/+ Low survival
ApcMin/+ High survival
% Body weight (from baseline)
Weeks
C
Fmax (mN.m)
weeks
D
WT
ApcMin/+

Figure legends

Figure 1: Schematic representation of the experimental design for the C26 tumor-bearing mice. C26 mice were submitted either to an individualized NMES training protocol or a control intervention together with PBS mice from 7 to 14 days following C26 injection. Maximal force production was recorded before, at the beginning of each NMES or control interventions as well as at day 14. The animals were sacrificed at day 14 and either the right gastrocnemius muscle or muscles from two limbs were harvested.

Figure 2: NMES training in the C26 tumor-bearing mouse model prevents the loss of muscle force and mass without affecting tumor burden. A) Percentage of body weight relative to initial body weight (measured 2 days prior to C26 or PBS injection) during the experimental protocol, from PBS (n= 19), C26 (n=25) and C26+NMES (n=28) mice. B) Tumor weight from C26 (n=27) and C26+NMES (n=27) mice. C) Percentage of muscle maximal force relative to initial muscle force (measured 2 days prior to C26 injection) during the experimental protocol, from PBS (n=36), C26 (n=49) and C26+NMES (n=53) mice. D) Percentage of the muscle maximal force relative to baseline, obtained at the end of the experimental protocol from PBS (n=20), C26 (n= 36) and C26+NMES (n=39) mice. E) *Gastrocnemius* muscle weight of PBS (n=14), C26 (n=14) and C26+NMES (n=19) mice F) *Gastrocnemius* muscle fiber cross-sectional area of PBS (n=7), C26 (n=9), C26+NMES (n=8) mice and representative immunostainings. G) Proportion of muscle fibers positive for MyHC I, IIA, IIX and IIB in PBS (n=7), C26 (n=9), and C26+NMES (n=8) mice and representative image showing muscle fibers positive for MyHC type I in blue, MyHC type IIA in green, MyHC type IIX same as background color and MyHC type IIB in red. For A) and C) $^{\#}p < 0.05$, $^{\#\#}p < 0.01$ $^{\#\#\#}p < 0.001$ significantly different between C26 and PBS. $^{\$}p < 0.05$, $^{\$\$}p < 0.01$ $^{\$\$\$}p < 0.001$ significantly different between C26+NMES and PBS. $^{*}p < 0.05$, $^{**}p < 0.01$ $^{***}p < 0.001$ significantly different between C26 and C26+NMES. For the rest of graphs, significance of the differences: $^{*}p < 0.05$, $^{**}p < 0.01$, $^{***}p < 0.001$, values are reported as mean $\pm$ SD.

Figure 3: NMES training facilitate *in vivo* SC fusion with muscle fibers in the C26 mice. A) Quantification of SCs stained for Pax7 per muscle fiber and representative microscopy images of Laminin (red), Pax7 (green) and Hoechst (blue) immunostaining on *gastrocnemius* muscle section from PBS (n=8), C26 (n=9), and C26+NMES (n=7) mice. B) Quantification of myonuclei (nuclei with their geometric center within the inner rim of the laminin ring) *per* muscle fiber on *gastrocnemius* muscle section from PBS (n=7), C26 (n=9) and C26+NMES (n=10) mice. Quantification of myonuclei stained for PCM1 *per* muscle fiber and representative microscopy images of Laminin (red), PCM1 (green) and Hoechst (blue) immunostaining on *gastrocnemius* muscle section from PBS (n=4), C26 (n=4), and C26+NMES (n=4) mice. D) Quantification of proliferating SCs stained for Pax7 and Ki67 *per* mm^2 on *gastrocnemius* muscle section from PBS (n=3), C26 (n=3), and C26+NMES (n=3) mice. E) Quantification of differentiating myogenic cells stained for myogenin *per* mm^2 on *gastrocnemius* muscle section from PBS (n=3), C26 (n=3), and C26+NMES (n=3) mice. F) Percentage of proliferating myoblasts isolated from PBS (n=6) and C26 mice (n=6) determined by EdU uptake. G) Percentage of differentiating myoblasts isolated from PBS (n=4) and C26 mice (n=3) stained for myogenin. H) Percentage of fusion index (number of nuclei from myotubes > 2 nuclei/ total number of $desmin^+$ nuclei) of myoblasts isolated from PBS (n=6) and C26 mice (n=6) isolated and representative images showing myoblasts and myotubes stained for desmin (red) and Hoechst (blue). Significance of the differences: *p< 0.05, **p< 0.01, ***p< 0.001, values are reported as mean ± SD.

Figure 4: NMES induces macrophages to transition towards an anti-inflammatory state and decreases the proportion of neutrophils in the C26 mice. A) Quantification of total macrophages stained for F4/80 *per* mm^2 of muscle area and representative microscopy images of Laminin (green), F4/80 (red) and Hoechst (blue) immunostaining on *gastrocnemius* muscle section from PBS (n=7), C26 (n=8), and C26+NMES (n=9) mice. Quantification of B) $COX2^+$ macrophages C) $iNOS^+$ macrophages D) $CD206^+$ macrophages and E) IL-10^+ macrophages among the total number of macrophages ($F4/80^+$ cells) from *gastrocnemius* muscle sections of C26 (n= 5-10) and C26+NMES (n=5-8) mice. Analysis of flow cytometry showing the percentage of F) neutrophils G) total macrophages H) $Ly6C^+$ and I) $Ly6C^-$ macrophages relative to $CD45^+$ live cells (hematopoietic cells) isolated from C26 and

C26+NMES *gastrocnemius* muscles. Each square represents one flow cytometry experiment. For each experiment, 2 to 4 muscles were digested from each group. Significance of the differences: *p< 0.05, **p< 0.01, values are reported as mean ± SD.

Figure 5: Protein extracts from NMES-stimulated C26 muscles modulate macrophage activity to drive SC fate *in vitro*. A) Schematic representation of experimental setup B) Quantification of TNFα$^+$ BMDMs and C) of CD206$^+$ BMDMs among total BMDMs exposed to protein extracts (1 µg/ml) derived from PBS (n=2), C26 (n=2) and C26+NMES (n=2) *gastrocnemius* muscles and the representative images from TNFα and CD206 immunostainings of BMDMs *in vitro* culture. D) Proliferation E) Differentiation and F) Fusion index of control myoblasts cultured in growth or differentiation conditions using the conditioned medium of BMDMs previously polarized with muscle PBS, C26 or C26+NMES protein extracts (1µg/ml). Representative microscopy images for E) and F) showing differentiating myoblasts stained for myogenin (red) (up pannel) and myotubes stained for desmin (red) (down pannel), nuclei are labelled with Hoechst (blue). Each square represents one biological replicate. Values are reported as mean ± SD.

Figure 6: Regulation of SC fate by muscle protein extracts is not effective without macrophage activity in the C26 muscles following NMES. A) Schematic representation of experimental setup. Percentages of B) Proliferation, C) Differentiation and D) Fusion index of control myoblasts cultured in standard growth or differentiation medium supplied with protein extracts (1µg/ml) obtained from PBS, C26 or C26+NMES muscles. Each square represents one biological replicate.

Figure 7: Longitudinal analysis of body weight and muscle force decline in the *Apc*$^{Min/+}$ mouse model. A) Weekly measurement of body weight in the *Apc*$^{Min/+}$ and WT mice, body weight was normalized to initial body weight from each group (measured at 8 weeks of age, WT n=16 and *Apc*$^{Min/+}$ n=17) B) Weekly measurement of muscle maximal force in the *Apc*$^{Min/+}$ (n= 17) and WT (n=16) mice. C) Percentage of body weight at ethical endpoint from maximal body weight reached in WT (n=19) and *Apc*$^{Min/+}$ mice (n= 29). D) Percentage of

muscle maximal force at ethical endpoint from initial muscle maximal force (8 weeks) in WT (n=16) and *Apc*$^{Min/+}$ mice (n= 17). E) *Gastrocnemius* muscle weight of WT (n=28) and *Apc*$^{Min/+}$ (n=39) mice. F) Representative microscopy images showing the absence of muscle fibers positive for IgG in the WT and *Apc*$^{Min/+}$ mice. Four mice *per* group were assessed and no IgG^{+} muscle fibers were detected G) *Gastrocnemius* muscle fiber cross-sectional area of WT (n=6) and *Apc*$^{Min/+}$ (n=7) mice and representative immunostainings. H) Number of myonuclei *per* muscle fiber in WT (n=4) and *Apc*$^{Min/+}$ (n= 4) mice. Significance of the differences: *p< 0.05, **p< 0.01, ***p< 0.001, values are reported as mean ± SD.

Figure 8: Skeletal muscle of *Apc*$^{Min/+}$ mice displays altered level of SCs, macrophages and FAPs and increased amounts of collagen type I. A) Quantification of SCs stained for Pax7 *per* muscle fiber in WT (n=11) and *Apc*$^{Min/+}$ (n=11) mice B) Quantification of macrophages stained for F4/80 *per* mm^2 of muscle area and representative immunostainings showing F4/80^{+} cells in red, Laminin in green and nuclei in blue in WT (n=5) and *Apc*$^{Min/+}$ (n=5) mice C) Quantification of ECs stained for CD31 *per* muscle fiber in WT (n=6) and *Apc*$^{Min/+}$ (n=6) mice D) Quantification of FAPs stained for PDGFRα *per* mm^2 of muscle area and representative immunostainings showing PDGFRα $^{+}$ cells in green, Laminin in red and nuclei in blue in WT (n=5) and *Apc*$^{Min/+}$ (n=6) mice E) Percentage of type I collagen area from total muscle area in WT (n=6) and *Apc*$^{Min/+}$ (n=7) mice and the corresponding immunostainings of collagen type I of 3 distinct mice from each group. Significance of the differences: *p< 0.05, ***p< 0.001, values are reported as mean ± SD.

Figure 9: The intrinsic myogenic capacities of SCs are compromised only after the onset of CC and not before in the *Apc*$^{Min/+}$ mice. A) Percentage of proliferating myoblasts stained for EdU uptake, isolated from either WT or *Apc*$^{Min/+}$ mice at ethical endpoint. B) Percentage of differentiating myoblasts stained for myogenin and isolated from either WT or *Apc*$^{Min/+}$ mice at ethical endpoint (R= 16-23 weeks). C) Percentage of fusion index of myoblasts isolated from either WT or *Apc*$^{Min/+}$ mice at ethical endpoint. D) Proliferation E) Differentiation and F) Fusion index percentages of myoblasts isolated from WT and *Apc*$^{Min/+}$ mice at an early time point (8-9 weeks of age). Mice did not present any clinical sign of health degradation (*e.g.,* body weight or cage activity loss). Microscopy photos represent myoblasts

fusing into multinucleated myotubes stained for desmin in red and nuclei in blue, either isolated from WT and cachectic *Apc*$^{Min/+}$ mice at endpoint (upper panels) or from WT and non-cachectic *Apc*$^{Min/+}$ mice at an early time point (lower panels). Significance of the differences: *p< 0.05, values are reported as mean ± SD.

Figure 10: Long-term NMES training started at the onset of muscle weakness counteracts muscle atrophy in the *Apc*$^{Min/+}$ mice. A) Schematic representation of NMES training in *Apc*$^{Min/+}$ mice. *Apc*$^{Min/+}$ mice were either submitted to an individualized NMES training protocol or a control intervention together with WT mice from 16 weeks of age. In total 12 sessions of NMES were performed with 4 sessions/week at indicated days during 3 weeks. Mice were sacrificed on the third day after the last NMES session and the right *gastrocnemius* muscles were harvested for histological analysis. Longitudinal monitoring of B) The body weight and C) The maximal force production at the beginning of each NMES or control intervention. D) *Gastrocnemius* muscle weight of WT (n=15), *Apc*$^{Min/+}$ (n=9) and *Apc*$^{Min/+}$+NMES (n=11) mice. E) *Gastrocnemius* muscle fiber cross-sectional area of WT (n=8) *Apc*$^{Min/+}$ (n=8) and *Apc*$^{Min/+}$+NMES (n=9) mice. F) Number of polyps in *Apc*$^{Min/+}$ (n=8) and *Apc*$^{Min/+}$+NMES (n=7) mice. For B) and C) $^{\#}$p <0.05, $^{\#\#}$p <0.01 significantly different between *Apc*$^{Min/+}$ control and WT. $^{\$}$p <0.05, $^{\$\$}$p <0.01 significantly different between *Apc*$^{Min/+}$ +NMES and WT. For the rest of graphs, significance of the differences: *p< 0.05, **p< 0.01, values are reported as mean ± SD.

Figure 11: SC fate within the SC niche is not improved with NMES training in the *Apc*$^{Min/+}$ mice. A) Quantification of SCs (Pax7^{+}cells) B) of proliferating SCs (Pax7^{+}Ki67^{+} cells) and C) differentiating muscle precursor cells (Myogenin^{+} cells) *per* mm^2 of muscle area in WT (n=6), *Apc*$^{Min/+}$ (n=5) and *Apc*$^{Min/+}$+NMES (n=7) mice. D) Quantification of myonuclei (PCM1^{+} nuclei) in WT (n=6), *Apc*$^{Min/+}$ (n=5) and *Apc*$^{Min/+}$+NMES (n=7) mice. E) Percentage of Fusion of control myoblasts cultured in standard differentiation medium supplied with protein extracts (1µg/ml) obtained from WT, *Apc*$^{Min/+}$ or *Apc*$^{Min/+}$ +NMES muscles. Each square represents one biological replicate. F) Quantification of macrophages stained (F4/80^{+} cells) *per* mm^2 of muscle area in WT (n=5), *Apc*$^{Min/+}$ (n=5) and *Apc*$^{Min/+}$+NMES (n=7) mice G) Quantification of FAPs (PDGFRα^{+} cells) in WT (n=6), *Apc*$^{Min/+}$ (n=5) and *Apc*$^{Min/+}$+NMES (n=7) mice. H) Percentage of

type I collagen area from total muscle area in WT (n=6), *Apc*$^{Min/+}$ (n=6) mice and *Apc*$^{Min/+}$+NMES (n=7) mice. Significance of the differences: *p< 0.05, **p< 0.01, values are reported as mean ± SD.

Supplemental figure legends

Figure S1: A) Specific force expressed as the ratio of muscle maximal force to muscle mass for PBS (n=7), C26 (n=11) and C26+NMES (n=11) at the endpoint. B) Proportion of muscle fibers positive for IgG in PBS (n=3), C26 (n=7) and C26+NMES (n=8). Significance of the differences: ***p< 0.001, values are reported as mean ± SD.

Figure S2: A) Experimental setup of myoblasts isolation via MACS (Magnetic cell sorting) from PBS and C26 tumor-bearing mice. B) Purity of myoblasts (stained with desmin) *in vitro* at passage 1 and passage 2 isolated from PBS and C26 tumor-bearing mice.

Figure S3: A) Quantification of ECs (CD31$^+$ cells) and B) of FAPs (PDGFRα^+ cells) from PBS (n=6-9) and C26 mice (n=6-8) at the endpoint. Values are reported as mean ± SD.

Figure S4: A) Gating approach of macrophage phenotype characterization. Macrophages were analyzed using flow cytometry performed on hematopoietic cell suspension (CD45$^+$ cells) obtained from C26 and C26+NMES *gastrocnemius* muscles. CD45$^+$ viable cells were first gated according to the expression of CD64 pan-macrophage marker to identify macrophages and of inflammatory marker Ly6C to distinguish the pro-inflammatory macrophages from the anti-inflammatory ones. CD64$^+$Ly6C$^+$ and CD64$^+$Ly6C$^-$ macrophages were additionally gated according to CD206 anti-inflammatory and CCR2 pro-inflammatory markers. Percentages of B) Ly6C$^+$CCR2$^+$ C) Ly6C$^+$CD206$^+$ D) Ly6C$^-$CCR2$^+$ and E) Ly6C$^+$CD206$^-$ expressing macrophages from C26 and C26+NMES *gastrocnemius* muscles. Each square represents one flow cytometry experiment. For each experiment, 2 to 4 muscles were digested from each group.

Figure S5: A) Survival curve of *Apc*$^{Min/+}$. B) Weekly measurement of body weight in the WT, *Apc*$^{Min/+}$ low survival (≤ 20 weeks) and *Apc*$^{Min/+}$ high survival (>20 weeks) mice. Body weight

was normalized to initial body weight from each group (measured at 8 weeks of age, WT n=16, *Apc*$^{Min/+}$low survival n=8 and *Apc*$^{Min/+}$high survival n=9) C) Weekly measurement of muscle maximal force in the WT (n=16), *Apc*$^{Min/+}$ low survival ($\leq$ 20 weeks) (n=8) and *Apc*$^{Min/+}$ high survival (>20 weeks) (n=9) mice. D) Specific force expressed as the ratio of muscle maximal force to muscle mass for WT and *Apc*$^{Min/+}$ mice. For B) and C) $^{\#}$p <0.05, $^{\#\#}$p <0.01 $^{\#\#\#}$p <0.001 significantly different between *Apc*$^{Min/+}$ and WT. $^{\$}$p <0.05, $^{\$\$}$p <0.01 significantly different between *Apc*$^{Min/+}$ +NMES and WT. *p <0.05, **p <0.01 ***p <0.001 significantly different between *Apc*$^{Min/+}$ and *Apc*$^{Min/+}$ +NMES. For D) Significance of the differences: *p< 0.05, **p< 0.01, ***p< 0.001. Values are reported as mean $\pm$ SD.

Discussion

In the present study, we first sought to determine alterations in SC fate and in cellular interactions within the cachectic SC niche from 2 complementary mouse models of CC (*i.e.*, C26 and *Apc*$^{Min/+}$ mouse models). Subsequently, we indented to assess whether NMES, as a non-pharmacological strategy exerts positive effects on muscle mass and force by regulating the SC fate and its niche. The first model was the C26-colon tumor bearing mouse model, a widely used model in the field, which develops rapid and aggressive cachexia unlike the human experience but allowing to easily control our studies outcomes. In contrast, the second model was the *Apc*$^{Min/+}$ mouse model, carrying a mutation in the *Apc* gene that predisposes to intestinal adenoma formation and colon cancer and which reproduces more closely the characteristics of human CC. Our findings showed that NMES training improved muscle force and mass in the C26 mice and induced a shift from slow-twitch muscle fibers into fast-twitch ones. These functional, structural and metabolic changes occurred in association with improvement in SC fusion and a transition from a pro- towards an anti-inflammatory macrophage phenotype within the cachectic muscles. The present study also showed for the first time that cancer-induced muscle wasting and weakness in the *Apc*$^{Min/+}$ mice, are associated with a decrease in the number of SCs and in their ability to fuse as well as with an increase in the number of macrophages and FAPs. By contrast to C26 mice, the positive effects of NMES on *Apc*$^{Min/+}$ muscles occurred independently of SC fate regulation or its niche.

SCs and niche alterations in the C26 tumor-bearing and Apc$^{Min/+}$ mouse models

Earlier findings have revealed that SCs increase in number and accumulate in the cachectic muscles from human cancer patients and tumor-bearing mice[13,14,15,16]. As a result, SCs cannot properly differentiate and fuse, causing muscle wasting[13]. Consistently, in our study, increased numbers of SCs were observed in the C26 mice while they were significantly diminished in the *Apc*$^{Min/+}$ mice. A responsible factor for these differences could be the aggressiveness of tumor and cachexia severity which do not occur at the same extent in the two mouse models. Compared to *Apc*$^{Min/+}$ mice, in which cachexia develops progressively, C26 mice develop acute cachexia which may be far more detrimental to muscle homeostasis and instead cause SCs to become activated. Previous reports have shown muscle damage in the presence of tumor,

including disruptions to muscle fiber membranes and increased membrane permeability, from cachectic C26 mice[13,28] and from muscle biopsies of cancer patients[13] that could trigger SC activation. Surprisingly, we did not notice overt signs of muscle injury from any of the two mouse models of CC in the current study. Although, we do not dismiss the possibility that a variety of signals released by the tumor can slightly damage the muscle fibers and cause profound alterations in the muscle homeostasis. Variation in the number of SCs between the two mouse models of our study could also be attributable to the presence of *Apc* gene mutation in the SCs from *Apc*$^{Min/+}$ mice. *Apc* in SCs was shown to be required for SCs to promote their proper cell cycle entry and progression throughout myogenesis, by dampening the Wnt/β-catenin signaling[55]. Importantly, conditional genetic disruption of *Apc* in SCs from healthy mice resulted in inhibition of SC proliferation and self-renewal and to induction of SC apoptosis, which were all mediated by overactivation of β-catenin. In our study, the *Apc*$^{Min/+}$ mice carry a germline mutation in the *Apc* gene, resulting in the expression of a truncated protein in SCs which might consequently impact SC fate and survival independently of CC. We showed that the proliferation of SCs was decreased *in vivo* but their proliferative ability was preserved *in vitro*, suggesting that is not the *APC* gene mutation that causes the SC proliferation to decrease in the *Apc*$^{Min/+}$ mice, but rather is the cachectic muscle microenvironment. On the other hand, the differentiation and fusion abilities of SCs derived from severely cachectic Apc$^{Min/+}$ mice were impaired *in vitro*, suggesting dysfunction of intrinsic mechanisms regulating the SC in the Apc$^{Min/+}$ mice. A lower myogenic fusion index was detected in SCs from Apc$^{Min/+}$ mice at late-stage cachexia (~20 weeks) *versus* mice which did not yet recapitulate features of CC (~8 weeks), suggesting that intrinsic deficiency of fusion is caused by the cachectic muscle microenvironment rather than the constitutive inactivation of *Apc* gene.

Further we showed, that SCs from the C26 mice display normal proliferation, differentiation and fusion *in vitro* suggesting that the aberrant myogenic properties observed *in vivo* from C26 mice are induced by the presence of CC. Previous data have shown similarly that SCs from muscles of cachectic C26 tumor-bearing mice proliferate normally[24] or more[15] than those derived from control mice, *in vitro*. However, it should be emphasized that these studies did not accurately report the process on how SCs were cultured, thus lack of standardization among the different conditions *in vitro* can affect SC behavior.

Overall, our findings imply that the regulation of SC fate, in the C26 mouse model, is rather impacted by factors located in the SC niche, that act in conjunction with the SCs *(e.g.,* cell-to-cell interactions) to dysregulate myogenesis, than the SC itself. Conversely, impairment of SC fate in the *Apc*$^{Min/+}$ mice seems to be caused by external stimuli arising from the cachectic niche that disrupts the inner mechanisms of SC.

Until now, the number of macrophages within the muscle microenvironment in experimental CC has been poorly described, on top of that data between the existing studies are inconsistent due to methods used to characterize macrophages. Costamagna et al.[15] reported no changes regarding the number of macrophages in the C26 mice, by analyzing F4/80 and CD206 protein expression with western blot, which does not allow to quantify macrophage number accurately. In addition, small but significant changes in macrophage amounts might not be detectable with this method. Another study reported decreased number of macrophages at late-stage cachexia from histological muscle sections of C26 tumor-bearing mice by staining esterase uptake. However, this is a non-specific method for macrophage identification, as it stains also lymphocytes[57]. Other studies have found abnormally higher[25] or decreased[24] numbers of macrophages in muscles of tumor-bearing mice but these changes were induced only after muscle injury, which does not reflect the pathophysiology of CC. For the first time, our study allowed to visualize and to quantify macrophages from cachectic muscle sections using F4/80 immunostaining. Our histological analysis revealed increased number of total macrophages in muscles from both mouse models, indicating that CC induces muscle inflammation. Coherent findings were obtained from muscle sections immunostained with CD68 antibody from pancreatic cancer patients[26]. Macrophages interact with SCs to regulate myogenesis, in response to acute muscle injury. Indeed, pro-inflammatory macrophages support SC proliferation while the switch of pro- to anti-inflammatory is required for myogenic differentiation and fusion of SCs[53]. Hence the aberrant increase in SCs in the C26 mice, could be triggered by the presence of macrophages that are maintained in a pro-inflammatory status. We also showed, thanks to our *in vitro* analysis, that factors released by macrophages in the muscle microenvironment of C26 mice could negatively affect SC differentiation and fusion. Thus, our study shed light on possible alterations of the interactions between SCs and macrophages during CC.

With regards to FAPs, their number remained unchanged in the C26 mice, whereas FAPs were found to be increased in muscles from the *Apc*$^{Min/+}$ mice. Interestingly, the increase of FAPs

number in the the *Apc*$^{Min/+}$ muscles was associated with greater amounts of type I collagen, suggesting that muscle fibrosis occurs in the *Apc*$^{Min/+}$ mice. It is likely that the short life span of the C26 mouse model might not enable to see the long-term consequences on FAPs. Indeed, abnormal proliferation of FAPs has been observed in chronic muscle disease (*i.e.*, muscular dystrophy) which is associated with persistent muscle inflammation and in the final stage, with replacement of muscle fibers with fibrotic tissue[58,59]. The increase in FAPs population and collagen content along with infiltration of macrophages in the cachectic muscles of *Apc*$^{Min/+}$ mice is consistent with that observed in pancreatic cancer patients[26]. Muscles of pancreatic cancer patients, also exhibited upregulation in genes related to the activation of TGF-β signaling[26]. In chronic muscle disease, macrophages were shown to express high levels of TGF-β1 which induce the differentiation of FAPs into fibroblasts producing matrix components such as collagen type [60,61]. This indicates that the collagen deposition in the *Apc*$^{Min/+}$ mice could be mediated, at least in part, through the release of TGF-β by aberrant macrophages. Moreover, suppression of SC numbers[20] or SC proliferation[55] results in dysregulation of fibroblasts numbers and a dramatic increase in fibrosis during muscle regeneration in healthy mice. These findings strongly suggest that the reciprocal interactions between SCs, macrophages and FAPs are defective in the *Apc*$^{Min/+}$ mice and could be responsible for muscle weakness during CC.

ECs composing the blood vessels also play crucial roles within the muscle microenvironment. ECs are critical for controlling tissue perfusion, nutrient supply and immune cell infiltration[62]. During muscle regeneration, ECs stimulate SC proliferation[21,63] and SCs stimulate in turn EC-angiogenic properties[21,64]. Since we observed alterations in the numbers of macrophages and SCs from both models, we hypothesized that ECs numbers might also be altered. Unexpectedly, we did not observe changes regarding the numbers of ECs which reflected the number of vessels from any of the mouse models of CC. This strongly implies that neither acute nor gradual CC have an impact on muscle vascularization. These findings are not in line with a previous study that found an increased number of vessels from the muscles of C26 mice[29]. In contrast to our study, the authors used a different marker to identify vessels (*i.e.,* isolectin) and the number of vessels were reported *per* unit of muscle area. Therefore, in the absence of *de novo* angiogenesis, the increase in vessel numbers could be caused by lower muscle fiber width. Our findings were also surprising, considering that *Apc*$^{Min/+}$ mice suffer from anemia and whose muscles were poorly vascularized (*i.e.,* pale color) at the study's

endpoint. Nevertheless, it would be interesting to investigate EC function during CC, as we cannot rule out the possibility that ECs might be dysfunctional or have become more permeable to allow extravasation of inflammatory cells through the atrophied muscle.

Overall, it remains to be determined how these alterations in the SC niche relate to the development of tumor growth and to muscle functional impairment. In this context, our device would allow us to link the decrease in muscle force production from both models of CC with the alterations occurring in the SC niche over time. Future directions should allow to determine the signaling mediators responsible for the SC niche alterations. Factors released by the tumor were suggested to signal through distinct signaling pathways within the skeletal muscles such as the NF-κB[13] or ERK[14] signaling to inhibit SC commitment into myogenesis. Further, tumor factors reaching the muscles could also act on signaling pathways residing within macrophages or FAPs and in turn impact the SC function.

Beneficial effects of NMES in the C26 tumor-bearing and $Apc^{Min/+}$ mouse models

Pharmacological agents tested in clinical trials were ineffective at treating CC due to the multiple mechanisms involved in the pathogenesis of this syndrome[65]. Consequently, there is no curative treatment to fight CC at present. NMES can be used as a substitute for classic exercise by increasing muscle contractile activity. Thus, we wanted to determine whether NMES could serve as non-pharmacological therapy to improve skeletal muscle alterations in both models of CC.

Short term NMES protocol limited the loss of muscle force and mass in the C26 mice which were accompanied by a shift from MyHC-I towards MyHC-IIB muscle fibers, *i.e.,* a slow-to-fast transition. This is relatively unexpected since NMES was shown to conversely induce a slow-to-fast muscle fiber transition in muscles of healthy subjects[66]. A change from slow to fast muscle fiber type in cachectic muscles after NMES could lead to higher and faster force production which might be useful to overcome decline in muscle force. Muscle fiber switching following NMES could be induced by modifications in the pattern of neural stimulation and by variations in intracellular calcium induced by the nerve activity[67,68]. During muscle contractile activity, elevation in the intracellular calcium is mediated by calcium channels that act as voltage sensors and which can induce signaling pathways that regulate muscle fiber type[69]. Cav1.1, a voltage sensor, was proposed to control the release of intracellular ATP and

Ins(1,4,5)P_3 following electrostimulation, which in turn induces transcriptional changes that define muscle fiber phenotype[70]. Further, we saw that the improvement in muscle function and phenotypic switch was associated with increase in SC fusion. The addition of new nuclei *via* SC fusion into muscle fibers following NMES could serve, among others, to sustain transcriptional reprogramming of such muscle fiber phenotypic switch. Lately, Dos Santos et al.[71] demonstrated that most myonuclei within a specific type of muscle fiber are synchronized and co-express only one MyHC isoform together with selective panel of muscle-specific genes. Thus, addition of myonuclei following NMES in the C26 mice could be required to increase expression of MyHC protein isoforms that determine the new muscle fiber phenotype.

NMES was insufficient to reverse the decrease in muscle fiber size from cachectic C26 mice. One explanation is that increase in muscle fiber size might be a chronic physiological adaptation generated by NMES that cannot be seen due to the short lifespan of the C26 mouse model. Thus, NMES appears to preserve muscle force and mass in the C26 mice by providing the muscle fibers with new metabolic and contractile properties rather than increasing their size.

We saw that SCs numbers and possibly their function are impaired in the C26 mouse model. Here we demonstrated that NMES improved SC fate by positively regulating inflammation in the SC niche from C26 cachectic mice. Histological analysis from C26 muscles, revealed an increase in the proportion of macrophages expressing the anti-inflammatory IL-10 cytokine following NMES. IL-10 was shown to be crucial in the regulation of muscle macrophage switch from a pro-to anti-inflammatory phenotype during muscle regeneration[54]. Loss of IL-10 attenuates the shift of macrophage to the anti-inflammatory phenotype in injured muscle and slows down muscle regeneration[54] . Additionally, treatment with IL-10 cytokine was also shown to reduce activation of pro-inflammatory macrophages and modulate macrophage phenotype in dystrophic muscles[72]. The finding that the macrophages expressing IL-10 cytokine were increased following NMES led us to wonder whether NMES modulates macrophage activity by inducing a transition towards an anti-inflammatory phenotype. Using flow cytometry, we showed that NMES induces a reduction in the proportion of neutrophils and in macrophages expressing high levels of Ly6C, a marker used to define pro-inflammatory macrophages, while those expressing low levels of Ly6C were increased. Overall, our findings indicated that NMES lowered muscle inflammation by reducing the content in neutrophils and by inducing a shift of macrophage population from pro-to anti-inflammatory status.

In order to mimic the muscle microenvironment *in vitro*, we used muscle protein extracts in the presence or absence of macrophages to assess the impact on SC fate. Muscle extracts from C26 mice trained with NMES had no direct effect on SC fate defect. Macrophages in the presence of muscle protein extracts from C26 mice trained with NMES, seemed to be converted into anti-inflammatory and the factors released by these macrophages reversed the defect in SC fate. Thus, NMES appears to modulate macrophages within the cachectic muscles in order to guide SC fate. Likewise, recent research has demonstrated that myonuclear accretion in contracting muscle fibers after increased load was ascribed to macrophage recruitment within the muscles favored by the expression of the chemokines CCL3/CX3CL1[32]. Notably, macrophage depletion inhibited muscle fiber growth and reduced both the number and fusion of SCs[32], illustrating the role of macrophages in the fate of SC in response to muscle overload. Further, muscle fiber in response to overload can secrete various factors (*i.e.,* myokines) such as IL-6[34,73], IL-4[34], or RhoA[32] that can dynamically regulate the interactions between SCs, macrophages and FAPs to promote muscle growth. Thus, it remains necessary to determine the factors secreted from muscle fibers, SCs or macrophages that may be contribute to the beneficial effects of NMES.

The *Apc*$^{Min/+}$ mouse model provided a longer time window to study the therapeutical effects of NMES on muscle alterations during CC. In contrast to C26 mice, prolonged NMES training in cachectic *Apc*$^{Min/+}$ mice significantly increased muscle fiber size by 16% compared to non-trained *Apc*$^{Min/+}$ mice without rescuing muscle mass loss. Unexpectedly, muscle force reduction was not observed in non-trained *Apc*$^{Min/+}$mice. A limitation of our experimental design, is that repeated force measurements over an extended period of time might have minimized the muscle dysfunction in the non-stimulated *Apc*$^{Min/+}$mice. We next showed that NMES prevented muscle atrophy independently from regulation of SC fate in the *Apc*$^{Min/+}$mice. We did not observe myonuclear accretion after NMES like in the C26 mice, suggesting that NMES failed to improve the SC fusion in the *Apc*$^{Min/+}$mice. Interestingly, we demonstrated that protein extracts from muscles of cachectic Apc$^{Min/+}$ mice alter the ability of control myoblasts to fuse, while protein extracts from electrically stimulated muscles of the *Apc*$^{Min/+}$mice rescued the fusion defect of these myoblasts. This most likely implies that proteins are secreted in response to NMES and have positive effect on SC regulation but additional impairment within the SCs induced by the cachectic microenvironment from *Apc*$^{Min/+}$mice prevents their action. Proteomic and mass spectrometry methodologies would allow to analyze the secretome of

electrostimulated muscle cells from *Apc*$^{Min/+}$ mice and to identify the exact nature of proteins involved in the beneficial effects of NMES. However, another possibility to lack of SC fusion after NMES, is the drastic reduction of SC numbers that might occur before the start of NMES training in *Apc*$^{Min/+}$ mice. During CC, atrophy of skeletal muscle fiber is thought to arise from signaling pathways that regulate the muscle protein turnover. The excessive activation of the ubiquitin proteasome system, which promotes muscle protein breakdown and the reduced Akt and mTOR activities which decreases protein synthesis have mainly been described in the context of CC[74]. Cumulatively, we predict that the increase in muscle fiber size from *Apc*$^{Min/+}$ mice following NMES could derive from improvement in the signaling pathways muscle protein balance operating within the muscle fiber. Indeed, evidence that NMES stimulates skeletal muscle protein synthesis was shown in older patients with diabetes or during immobilization[75,76,77].

Finally, the beneficial effects of NMES were achieved without changes in tumor mass or in the number of polyps. A possible explanation to these observations is that NMES effects remain localized within the muscle. Although it has to be determined whether NMES affects the tumor composition or its secretory activity. Release of specific factors by the crosstalk of the host immune system and the polyps of *Apc*$^{Min/+}$ mice could retain SCs from fusing with NMES.

To conclude, throughout this study we have evidenced that SCs number and function as well as the other cell types composing the SC niche are altered during CC. Moreover, our study strongly suggests that the interactions between these cell types might be compromised and drive muscle weakness and wasting. To date, despite efforts in basic and clinical research, there are no approved therapies to prevent or treat CC. In our study, NMES application upon CC onset, improved muscle force, mass and SC fate and was able to impinge on muscle inflammation in cachectic mice. Thus, adopting a carefully controlled NMES protocol in CC patients appears promising to help improve muscle function and mass, although first it has to be validated in clinical studies.

References

1. Baracos, V. E., Martin, L., Korc, M., Guttridge, D. C. & Fearon, K. C. H. Cancer-associated cachexia. *Nat Rev Dis Primers* **4**, 17105 (2018).
2. von Haehling, S. & Anker, S. D. Cachexia as a major underestimated and unmet medical need: facts and numbers. *J Cachexia Sarcopenia Muscle* **1**, 1–5 (2010).
3. Ni, J. & Zhang, L. Cancer Cachexia: Definition, Staging, and Emerging Treatments. *Cancer Manag Res* **12**, 5597–5605 (2020).
4. Dewys, W. D. *et al.* Prognostic effect of weight loss prior to chemotherapy in cancer patients. Eastern Cooperative Oncology Group. *Am J Med* **69**, 491–497 (1980).
5. Tan, B. H. L. & Fearon, K. C. H. Cachexia: prevalence and impact in medicine. *Curr Opin Clin Nutr Metab Care* **11**, 400–407 (2008).
6. Deans, C. & Wigmore, S. J. Systemic inflammation, cachexia and prognosis in patients with cancer. *Curr Opin Clin Nutr Metab Care* **8**, 265–269 (2005).
7. Fang, Z., Shang, L. & Li, L. Impact of Low Skeletal Muscle Mass on Complications and Survival for Gastric Cancer: A Propensity Score Matching Analysis. *Front Surg* **9**, 901142 (2022).
8. Yang, W. *et al.* Molecular mechanisms of cancer cachexia-induced muscle atrophy (Review). *Mol Med Rep* **22**, 4967–4980 (2020).
9. Cole, C. L., Kleckner, I. R., Jatoi, A., Schwarz, E. M. & Dunne, R. F. The Role of Systemic Inflammation in Cancer-Associated Muscle Wasting and Rationale for Exercise as a Therapeutic Intervention. *JCSM Clin Rep* **3**, e00065 (2018).
10. Seale, P. *et al.* Pax7 is required for the specification of myogenic satellite cells. *Cell* **102**, 777–786 (2000).
11. Dumont, N. A., Bentzinger, C. F., Sincennes, M.-C. & Rudnicki, M. A. Satellite Cells and Skeletal Muscle Regeneration. *Compr Physiol* **5**, 1027–1059 (2015).
12. Chargé, S. B. P. & Rudnicki, M. A. Cellular and molecular regulation of muscle regeneration. *Physiol Rev* **84**, 209–238 (2004).
13. He, W. A. *et al.* NF-κB-mediated Pax7 dysregulation in the muscle microenvironment promotes cancer cachexia. *J Clin Invest* **123**, 4821–4835 (2013).
14. Penna, F. *et al.* Muscle wasting and impaired myogenesis in tumor bearing mice are prevented by ERK inhibition. *PLoS One* **5**, e13604 (2010).
15. Costamagna, D. *et al.* Interleukin-4 administration improves muscle function, adult myogenesis, and lifespan of colon carcinoma-bearing mice. *J Cachexia Sarcopenia Muscle* **11**, 783–801 (2020).
16. Brzeszczyńska, J. *et al.* Loss of oxidative defense and potential blockade of satellite cell maturation in the skeletal muscle of patients with cancer but not in the healthy elderly. *Aging (Albany NY)* **8**, 1690–1702 (2016).
17. Yang, W. & Hu, P. Skeletal muscle regeneration is modulated by inflammation. *J Orthop Translat* **13**, 25–32 (2018).
18. Schilling, J. D. Macrophages Fuel Skeletal Muscle Regeneration. *Immunometabolism* **3**, e210013 (2021).
19. Biferali, B., Proietti, D., Mozzetta, C. & Madaro, L. Fibro-Adipogenic Progenitors Cross-Talk in Skeletal Muscle: The Social Network. *Front Physiol* **10**, 1074 (2019).
20. Murphy, M. M., Lawson, J. A., Mathew, S. J., Hutcheson, D. A. & Kardon, G. Satellite cells, connective tissue fibroblasts and their interactions are crucial for muscle regeneration. *Development* **138**, 3625–3637 (2011).
21. Christov, C. *et al.* Muscle satellite cells and endothelial cells: close neighbors and privileged partners. *Mol Biol Cell* **18**, 1397–1409 (2007).
22. Mounier, R., Chrétien, F. & Chazaud, B. Blood vessels and the satellite cell niche.

Curr Top Dev Biol **96**, 121–138 (2011).
23. Berardi, E. *et al.* Skeletal muscle is enriched in hematopoietic stem cells and not inflammatory cells in cachectic mice. *Neurol Res* **30**, 160–169 (2008).
24. Inaba, S., Hinohara, A., Tachibana, M., Tsujikawa, K. & Fukada, S.-I. Muscle regeneration is disrupted by cancer cachexia without loss of muscle stem cell potential. *PLoS One* **13**, e0205467 (2018).
25. Coletti, D. *et al.* Spontaneous Physical Activity Downregulates Pax7 in Cancer Cachexia. *Stem Cells Int* **2016**, 6729268 (2016).
26. Judge, S. M. *et al.* Skeletal Muscle Fibrosis in Pancreatic Cancer Patients with Respect to Survival. *JNCI Cancer Spectr* **2**, pky043 (2018).
27. Shukla, S. K. *et al.* Macrophages potentiate STAT3 signaling in skeletal muscles and regulate pancreatic cancer cachexia. *Cancer Lett* **484**, 29–39 (2020).
28. Acharyya, S. *et al.* Dystrophin glycoprotein complex dysfunction: a regulatory link between muscular dystrophy and cancer cachexia. *Cancer Cell* **8**, 421–432 (2005).
29. Hiroux, C., Dalle, S., Koppo, K. & Hespel, P. Voluntary exercise does not improve muscular properties or functional capacity during C26-induced cancer cachexia in mice. *J Muscle Res Cell Motil* **42**, 169–181 (2021).
30. Tanaka, M. *et al.* Preventive effects of low-intensity exercise on cancer cachexia-induced muscle atrophy. *FASEB J* **33**, 7852–7862 (2019).
31. Tanaka, M. *et al.* Differential effects of pre-exercise on cancer cachexia-induced muscle atrophy in fast- and slow-twitch muscles. *FASEB J* **34**, 14389–14406 (2020).
32. Noviello, C. *et al.* RhoA within myofibers controls satellite cell microenvironment to allow hypertrophic growth. *iScience* **25**, 103616 (2022).
33. Kaneshige, A. *et al.* Relayed signaling between mesenchymal progenitors and muscle stem cells ensures adaptive stem cell response to increased mechanical load. *Cell Stem Cell* **29**, 265-280.e6 (2022).
34. Guerci, A. *et al.* Srf-dependent paracrine signals produced by myofibers control satellite cell-mediated skeletal muscle hypertrophy. *Cell Metab* **15**, 25–37 (2012).
35. Peck, B. D. *et al.* A muscle cell-macrophage axis involving matrix metalloproteinase 14 facilitates extracellular matrix remodeling with mechanical loading. *FASEB J* **36**, e22155 (2022).
36. Murach, K. A. *et al.* Early satellite cell communication creates a permissive environment for long-term muscle growth. *iScience* **24**, 102372 (2021).
37. Saito, Y., Chikenji, T. S., Matsumura, T., Nakano, M. & Fujimiya, M. Exercise enhances skeletal muscle regeneration by promoting senescence in fibro-adipogenic progenitors. *Nat Commun* **11**, 889 (2020).
38. Murach, K. A., Fry, C. S., Dupont-Versteegden, E. E., McCarthy, J. J. & Peterson, C. A. Fusion and beyond: Satellite cell contributions to loading-induced skeletal muscle adaptation. *FASEB J* **35**, e21893 (2021).
39. Goh, Q. *et al.* Myonuclear accretion is a determinant of exercise-induced remodeling in skeletal muscle. *Elife* **8**, e44876 (2019).
40. Walton, R. G. *et al.* Human skeletal muscle macrophages increase following cycle training and are associated with adaptations that may facilitate growth. *Sci Rep* **9**, 969 (2019).
41. Zuo, Q., Wang, S.-C., Yu, X.-K. & Chao, W.-W. Response of macrophages in rat skeletal muscle after eccentric exercise. *Chin J Traumatol* **21**, 88–95 (2018).
42. Zavoriti, A. *et al. Individualized isometric neuromuscular electrical stimulation training promotes myonuclear accretion in mouse skeletal muscle*. http://biorxiv.org/lookup/doi/10.1101/2021.12.14.472254 (2021) doi:10.1101/2021.12.14.472254.
43. Maddocks, M. *et al.* Randomized controlled pilot study of neuromuscular electrical

stimulation of the quadriceps in patients with non-small cell lung cancer. *J Pain Symptom Manage* **38**, 950–956 (2009).
44. Maddocks, M. *et al.* Neuromuscular electrical stimulation of the quadriceps in patients with non-small cell lung cancer receiving palliative chemotherapy: a randomized phase II study. *PLoS One* **8**, e86059 (2013).
45. O'Connor, D., Caulfield, B. & Lennon, O. The efficacy and prescription of neuromuscular electrical stimulation (NMES) in adult cancer survivors: a systematic review and meta-analysis. *Support Care Cancer* **26**, 3985–4000 (2018).
46. Maffiuletti, N. A. Physiological and methodological considerations for the use of neuromuscular electrical stimulation. *Eur J Appl Physiol* **110**, 223–234 (2010).
47. Bruusgaard, J. C., Johansen, I. B., Egner, I. M., Rana, Z. A. & Gundersen, K. Myonuclei acquired by overload exercise precede hypertrophy and are not lost on detraining. *Proc Natl Acad Sci U S A* **107**, 15111–15116 (2010).
48. Bruusgaard, J. C. *et al.* No change in myonuclear number during muscle unloading and reloading. *J Appl Physiol (1985)* **113**, 290–296 (2012).
49. Winje, I. M. *et al.* Specific labelling of myonuclei by an antibody against pericentriolar material 1 on skeletal muscle tissue sections. *Acta Physiol (Oxf)* **223**, e13034 (2018).
50. Desgeorges, T. *et al.* Open-CSAM, a new tool for semi-automated analysis of myofiber cross-sectional area in regenerating adult skeletal muscle. *Skelet Muscle* **9**, 2 (2019).
51. Espigat-Georger, A., Dyachuk, V., Chemin, C., Emorine, L. & Merdes, A. Nuclear alignment in myotubes requires centrosome proteins recruited by nesprin-1. *J Cell Sci* **129**, 4227–4237 (2016).
52. Srsen, V., Fant, X., Heald, R., Rabouille, C. & Merdes, A. Centrosome proteins form an insoluble perinuclear matrix during muscle cell differentiation. *BMC Cell Biol* **10**, 28 (2009).
53. Chazaud, B. Inflammation and Skeletal Muscle Regeneration: Leave It to the Macrophages! *Trends Immunol* **41**, 481–492 (2020).
54. Deng, B., Wehling-Henricks, M., Villalta, S. A., Wang, Y. & Tidball, J. G. IL-10 triggers changes in macrophage phenotype that promote muscle growth and regeneration. *J Immunol* **189**, 3669–3680 (2012).
55. Parisi, A. *et al.* APC is required for muscle stem cell proliferation and skeletal muscle tissue repair. *J Cell Biol* **210**, 717–726 (2015).
56. Martin, A. *et al.* Hypothalamic-pituitary-adrenal axis activation and glucocorticoid-responsive gene expression in skeletal muscle and liver of Apc mice. *J Cachexia Sarcopenia Muscle* **13**, 1686–1703 (2022).
57. Manconi, P. E. *et al.* Alpha-naphthyl acetate esterase activity in mouse thymus and other lymphoid organs. *Thymus* **4**, 135–146 (1982).
58. Mann, C. J. *et al.* Aberrant repair and fibrosis development in skeletal muscle. *Skelet Muscle* **1**, 21 (2011).
59. Kharraz, Y., Guerra, J., Pessina, P., Serrano, A. L. & Muñoz-Cánoves, P. Understanding the process of fibrosis in Duchenne muscular dystrophy. *Biomed Res Int* **2014**, 965631 (2014).
60. Juban, G. *et al.* AMPK Activation Regulates LTBP4-Dependent TGF-β1 Secretion by Pro-inflammatory Macrophages and Controls Fibrosis in Duchenne Muscular Dystrophy. *Cell Rep* **25**, 2163-2176.e6 (2018).
61. Lemos, D. R. *et al.* Nilotinib reduces muscle fibrosis in chronic muscle injury by promoting TNF-mediated apoptosis of fibro/adipogenic progenitors. *Nat Med* **21**, 786–794 (2015).
62. Amersfoort, J., Eelen, G. & Carmeliet, P. Immunomodulation by endothelial cells -

partnering up with the immune system? *Nat Rev Immunol* **22**, 576–588 (2022).
63. Bryan, B. A. *et al.* Coordinated vascular endothelial growth factor expression and signaling during skeletal myogenic differentiation. *Mol Biol Cell* **19**, 994–1006 (2008).
64. Germani, A. *et al.* Vascular endothelial growth factor modulates skeletal myoblast function. *Am J Pathol* **163**, 1417–1428 (2003).
65. Naito, T. Emerging Treatment Options For Cancer-Associated Cachexia: A Literature Review. *Ther Clin Risk Manag* **15**, 1253–1266 (2019).
66. Gondin, J. *et al.* Neuromuscular electrical stimulation training induces atypical adaptations of the human skeletal muscle phenotype: a functional and proteomic analysis. *J Appl Physiol (1985)* **110**, 433–450 (2011).
67. Ausoni, S., Gorza, L., Schiaffino, S., Gundersen, K. & Lømo, T. Expression of myosin heavy chain isoforms in stimulated fast and slow rat muscles. *J Neurosci* **10**, 153–160 (1990).
68. Blaauw, B., Schiaffino, S. & Reggiani, C. Mechanisms modulating skeletal muscle phenotype. *Compr Physiol* **3**, 1645–1687 (2013).
69. Gundersen, K. Excitation-transcription coupling in skeletal muscle: the molecular pathways of exercise. *Biol Rev Camb Philos Soc* **86**, 564–600 (2011).
70. Jorquera, G. *et al.* Cav1.1 controls frequency-dependent events regulating adult skeletal muscle plasticity. *J Cell Sci* **126**, 1189–1198 (2013).
71. Dos Santos, M. *et al.* Single-nucleus RNA-seq and FISH identify coordinated transcriptional activity in mammalian myofibers. *Nat Commun* **11**, 5102 (2020).
72. Villalta, S. A. *et al.* Interleukin-10 reduces the pathology of mdx muscular dystrophy by deactivating M1 macrophages and modulating macrophage phenotype. *Hum Mol Genet* **20**, 790–805 (2011).
73. Serrano, A. L., Baeza-Raja, B., Perdiguero, E., Jardí, M. & Muñoz-Cánoves, P. Interleukin-6 is an essential regulator of satellite cell-mediated skeletal muscle hypertrophy. *Cell Metab* **7**, 33–44 (2008).
74. Glass, D. J. Signaling pathways perturbing muscle mass. *Curr Opin Clin Nutr Metab Care* **13**, 225–229 (2010).
75. Wall, B. T. *et al.* Neuromuscular electrical stimulation increases muscle protein synthesis in elderly type 2 diabetic men. *Am J Physiol Endocrinol Metab* **303**, E614-623 (2012).
76. Gibson, J. N., Smith, K. & Rennie, M. J. Prevention of disuse muscle atrophy by means of electrical stimulation: maintenance of protein synthesis. *Lancet* **2**, 767–770 (1988).
77. Dirks, M. L., Hansen, D., Van Assche, A., Dendale, P. & Van Loon, L. J. C. Neuromuscular electrical stimulation prevents muscle wasting in critically ill comatose patients. *Clin Sci (Lond)* **128**, 357–365 (2015).

GENERAL DISCUSSION

During my thesis, we sought to evaluate the effects of muscle overload induced by NMES on muscle strength, size as well as on SC fate in a physiological setting. Then, we aimed to determine alterations of SCs and their cellular interactions within the cachectic niche from 2 complementary mouse models of CC (*i.e.*, C26 and *Apc*$^{Min/+}$ mouse models). Finally, we wanted to assess whether the NMES could counteract muscle wasting and weakness during CC and whether the benefits of NMES occur through improvement of SC fate and niche.

We have developed a protocol of NMES that allows to increase muscle contractile activity based on its ability to produce force in response to electrical stimuli. Our NMES training protocol was shown to regulate the SC fate by increasing the SC content and fusion (*i.e.*, myonuclear accretion) and induced muscle hypertrophy in the absence of muscle damage/regeneration in healthy mice. This result is novel because, up until now, myonuclear accretion was demonstrated using non-physiological models of increased mechanical loading such as synergist ablation or tenotomy models that lead to rapid muscle hypertrophy and damage[495,496,478]. Therefore, it was unclear to what extent muscle loading alone influences SC activation and fusion aside from muscle damage/regeneration process. Myonuclear accretion and muscle hypertrophy mediated through the NMES protocol would be useful at identifying the cellular and molecular mechanisms governing the SC fate in response to mechanical overload. For instance, Goh et Millay[479], have shown that myomaker, a muscle specific membrane protein, specifically activated in SCs and not in muscle fibers, is involved in muscle growth by promoting SC fusion in response to muscle overload. Further, NMES would allow to decipher the differences between muscle regeneration and overload regarding SC dynamics. Fukuda et al.[483] have shown that SCs can proliferate in the absence of detectable MyoD expression, unlike in regenerating muscle, by expressing HeyL in overloaded muscle. Additionally in their study, the kinetics and location of SC proliferation differ in comparison to regenerating muscle. These findings indicate that SCs adopt distinct behaviors in regenerating and overloaded muscles. NMES could also allow to decipher the role of cell-to cell interactions and the factors expressed by the other cell components of the SC niche that regulate muscle growth in a physiological context. Peck et al.[646] discovered that macrophages enhance remodeling of the extracellular matrix by secreting Mmp14 (matrix metallopeptidase 14), and they suggested that LIF cytokine (leukemia inhibitory factor) expressed by the muscle fibers stimulates Mp14 expression in macrophages, in response to mechanical loading. Moreover, Noviello et al.[494] demonstrated that mechanosensitive RhoA pathway in overloaded muscle

fibers induces the expression of the chemokine Ccl3/Cx3c11, which results in macrophage recruitment into the muscle. They also showed that macrophage depletion by clodronate liposomes inhibits muscle growth, suggesting an essential role of macrophages in muscle hypertrophy. These data also strongly implicate a potential role of macrophages in ECM remodeling and collagen during muscle increased load[646,494,755], a role that could be sustained through interaction with mesenchymal stromal cells (*e.g.,* FAPs), as these cells are the primary source of collagen. Overall, our NMES training protocol could allow to improve our understanding of the role of macrophages and their interactions with neighboring cells and muscle fibers in the regulation of muscle growth. Finally, use of our NMES program may be helpful for expanding our comprehension on the role of muscle memory in the context of muscle adaptations. For instance, to assess whether myonuclei acquired during muscle hypertrophy are retained or lost during detraining. Gundersen and colleagues[756] have demonstrated that the increased number of myonuclei acquired from anabolic steroids- or synergist ablation-mediated skeletal muscle hypertrophy might be long-lasting or permanent and could lead to faster muscle growth during the following overload trainings. However, other animal experiments have shown contradictory results regarding the retention of myonuclei during detraining, possibly due to differences in age and species, in the protocol of training and in methods of analysis[496,757]. In addition, an attempt to decipher whether a long-lasting muscle memory exists in humans was performed by Psilander et al.[758], but in their study the program of strength training did not induce myonculear accretion. Thus, our NMES protocol could allow to assess whether myonuclei acquired by previous NMES training are maintained during a detraining period and whether an additional training protocol results in faster muscle growth. Our NMES training protocol can further extend the notion of muscle memory in muscle atrophy during CC. Finally, we demonstrated that SCs are able to sense subtle changes in muscle activity highlighting the readiness of SCs to assist muscle demands at any degree of stimulus.

The second purpose of my PhD work, was to find out alterations in SCs and their cellular interactions within the cachectic SC niche from two mouse models of CC (i.e., C26 and *Apc*$^{Min/+}$) and if enhanced muscle contractile activity induced by our NMES protocol can minimize loss of muscle mass and function and the alterations of SCs and its niche. We first monitored the decline in muscle force throughout CC using our original device that allows for non-invasive

muscle force measurements in response to electrical stimuli. We were able to determine the time course of skeletal muscle force decline from both models of CC. Indeed, kinetics of the maximal force produced by the muscle contraction throughout progression of CC has never been reported previously from cancerous mouse models. Indeed, grip strength from cancerous mice and humans has been assessed but is not sufficiently accurate to predict the maximum strength of muscle. Muscle wasting and weakness from both C26 and *Apc*$^{Min/+}$ mice at the study's endpoint were associated with alterations in the number of SCs in the absence of overt signs of muscle damage. The increase in the number of SCs that we observed from the C26 model is consistent with the literature[506,259,174,500,173] from cancer patients and tumor-bearing mice. In particular He et al.[259] showed that CC, from both cancer patients and tumor-bearing mice, was associated with a certain type of muscle damage resulting in aberrant activation of SCs and to deficient myogenesis. In contrast, we are the first to report a decrease in the number of SCs in the cachectic *Apc*$^{Min/+}$ mice. Recently, upregulation of the transcription factor C/EBPβ (CCAAT/enhancer binding protein beta) in SCs was proposed to be responsible for their myogenic failure in cachectic tumor-bearing animals through inhibition of SC apoptosis[759]. Indeed, knockout animals lacking C/EBPβ in SCs display reduced SC compartment due to increase of apoptosis accompanied by impairment in muscle regeneration. Therefore, in contrast to the C26-tumor bearing mouse model, the decrease in SCs from the *Apc*$^{Min/+}$ mouse model, could occur progressively through apoptosis because SCs exhibit downregulation of C/EBPβ. Thanks to the determination of the time-point at which muscle weakness begins in *Apc*$^{Min/+}$ mice, we can assess SC apoptosis prior to and throughout muscle weakness using TUNEL staining[760]. Additionally, differences among the two mouse models used, could result from the location and type of tumor. Most of the time, SCs alterations in experimental CC have been shown in tumor-bearing animals and especially with colon cancer. Using an additional mouse model to *Apc*$^{Min/+,}$ that likewise recapitulates the features of CC such as in humans, will be useful to bring clarity in the variations of SC content during CC in a more physiological context. Such model could be the KPP mouse model, which is engineered to develop PDA cancer[191]. This is of particular importance given that pancreatic cancer shows the highest prevalence of cachexia[761].

Previous studies that have assessed myogenesis *in vitro*, did not used standardized cell culture protocols. For instance, the number of cells or the duration of assays were not controlled. By establishing the cell density and kinetic for each step of myogenesis *in vitro*, we pertinently

evidenced an intrinsic defect in the fusion ability of SCs from the *Apc*$^{Min/+}$ mice while that was not the case in SCs from the C26 mice. Our studies suggested that the cachectic muscle microenvironment induced intrinsic alterations to SCs in the *Apc*$^{Min/+}$ mice. On the contrary, the myogenic defect in SCs from the C26 mice originate from exogenous factors within the cachectic SC niche. Interestingly the decrease in the number of SCs and the defect in their ability to fuse did not impact the number of myonuclei *per* muscle fiber, indicating that myonuclei remain constant during CC even in the presence of reduced SC numbers. Consistently, Winje et al.[762] have previously demonstrated that cachexia does not induce loss of myonuclei from the muscle fibers in xenografted prostate cancer in mice. These findings point to an extremely strict regulation of myonuclei survival when facing the tumor assaults within the muscle.

Using immunofluorescence techniques combined to specific markers we thoroughly investigated the SC niche cellular content. For the first time, we find out increased accumulation of macrophages in the muscles of C26 mice and *Apc*$^{Min/+}$ mice which in the latter was associated with increase in FAPs and collagen content. However, it is still unclear whether these cellular alterations of the SC niche drive muscle wasting or occur subsequently to it during CC. Our *in vitro* experiments showed that the cachectic niche in the C26 mice promote pro-inflammatory activity of macrophages that could alter SC function, suggesting for the first-time compromised interaction between macrophages and SCs in the setting of CC. *Apc*$^{Min/+}$ mice displayed high levels of macrophages and FAPs which were associated with increased collagen content, suggesting inflammation and fibrosis. Fibrosis in the cachectic muscle of *Apc*$^{Min/+}$ mice could result from impairment in the interactions between the SCs, macrophages and FAPs. Similarly, Judge et al.[261] reported increased infiltration of CD68^{+} macrophages and collagen deposition in muscles of pancreatic cancer patients, while the number of SCs were not assessed in this study. In particular, the increased collagen content correlated with reduced survival in these patients. Recent findings indicate that macrophage derived TGFβ signaling plays a key role in the survival and fibrogenic differentiation of FAPs and consequent collagen deposition in muscular dystrophy[530,543]. Future studies regarding the interactions between the SCs and macrophages or between the SCs and FAPs will allow for the identification of dysfunctional signaling pathways or factors released by these cell types during CC to be able to propose relevant therapies. Proteomics or single-cell RNA sequencing of the whole muscles could be used to determine the proteins produced or the distinct gene

expression profiles respectively from each cell population and the corresponding signaling pathways responsible for the altered alterations during CC. Further, flow cytometry approach could allow to characterize the inflammatory phenotype of macrophages infiltrating the muscles of the *Apc*$^{Min/+}$ mice. *In vitro* studies using conditioned-medium from macrophages or FAPs exposed prior to muscle protein extracts from the *Apc*$^{Min/+}$ mice would allow to assess their potential impact on the SC fate. Such experiments could further extent understanding on the mechanisms that alter the interactions of macrophage/SC/FAP leading to collagen accumulation during CC. Based on these data, establishing approaches to counteract the alterations in the SC niche such as muscle fibrosis can improve outcomes of cachectic cancer patients[261].

Due to pathophysiological complexity and multifactorial characteristics of CC, to date no curative therapies exist for CC. More Importantly, muscle wasting has been shown to have negative impact on cancer patient's overall survival[155,152]. Our individualized and carefully-controlled NMES training protocol was used in the perspective of therapy to minimize the muscle alterations during experimental CC. NMES limited loss of muscle force and mass in the C26 mice while NMES increased muscle fiber size in the *Apc*$^{Min/+}$ mice. Studies that aimed at assessing NMES usefulness in cancer patients are quite limited and have shown conflicting results. Two studies[750,751] aimed to assess advantages of NMES in cancer patients but they did not use muscle strength, mass or muscle fiber size as outcomes of NMES efficiency. Two other studies[753,752] showed improvements in muscle strength or mass with NMES in cancer patients but were statistically not significant. O'connor et al.[754] point out methodological limitations regarding the use of NMES is cancer patients such as lack of standardization among the NMES protocols (*e.g.,* uncontrolled application, timing of intervention, size sample). Most importantly, the muscle force produced in response to the stimulation, which is the main determinant of NMES effectiveness, has never been monitored in cachectic patients[705]. To our knowledge, we are the first to evaluate the effects of a controlled NMES protocol in CC. The benefits observed in muscle force and mass following NMES from our cachectic tumor-bearing animals were achieved using a training intensity corresponding to only ∼15% of maximal muscle force to avoid muscle damage. Similarly, in patients with chronic obstructive pulmonary disease, NMES contractions equivalent to 15-25% of muscle maximal voluntary contraction led to significant increase in muscle function and mass[728]. Thus, our current evidence supports the use of NMES as an effective strategy for improving muscle strength and

mass in cancer patients. Increasing muscle force and mass holds the greatest potential to increase quality of life and survival in cancer patients and may encourage patients getting back to voluntary physical activities.

The beneficial effects of NMES seem to involve distinct mechanisms between the C26 and the *Apc*$^{Min/+}$ mouse models. In the former, the increase in muscle force/mass occurred in conjunction with improved SC fate and its niche, whereas in the latter, increase in muscle fiber size was not accompanied by improvement in SC fate and its niche. Improvement of SC fate in the C26 mice seem to depend upon switch of macrophage from pro-inflammatory to anti-inflammatory phenotype which was validated by both *in vivo* and *in* vitro analyzes. Indeed, histological muscle sections from C26 mice showed increased proportion of macrophages secreting IL-10 cytokine following NMES, a cytokine with anti-inflammatory properties required for macrophage phenotype switch during muscle regeneration[534]. IL-10 decreases activation of pro-inflammatory macrophage as much as inhibits the release of pro-inflammatory cytokines such as TNFα[763,764]. We could test *in vitro* whether control macrophages secrete this molecule when they are in contact with protein extracts from C26 stimulated muscles or directly treat macrophages with IL-10 cytokine. Further we could use C26 tumor-bearing mice (IL-10 -/-) carrying IL-10 knock out gene expression, as previously described in healthy mice[534], and see if they still retain the advantages offered from NMES training (*e.g.,* macrophage phenotype switch or myonuclear accretion). In the *Apc*$^{Min/+}$ mice, NMES did not improve SC fate. Possibly either because SCs were affected by intrinsic alterations induced by the cachectic microenvironment that prevented them to respond to NMES or because SC numbers were decreased thus not being available to fuse. To extend our knowledge on the different mechanisms carried out by SCs and muscle fibers in response to NMES between the C26 and the *Apc*$^{Min/+}$ mice, we could perform gene expression analysis or metabolomics to determine their metabolic profiles[765]. The latter would allow to decipher metabolite signals that activate paracrine processes, within the cachectic microenvironment in response to NMES, originating either from the contracting cachectic muscle or the SCs. Metabolomics have already been performed previously to determine potential metabolites released in the local extracellular milieu that promote muscle remodeling in the setting of exercise[766]. The aforementioned techniques allow to identify specific molecules regulated by NMES that could serve to ameliorate SC fate in the cachectic muscle, yet pharmacological or

genetic overexpression/downregulation approaches of such factors in the muscle, will confirm whether NMES requires this molecule to improve SC fate in cachectic mice.

Generally, the degree of muscle wasting is dependent on tumor growth and spreading[767] indicating that tumor and muscles communicate with each other. It is now well established that tumor-released factors induce muscle wasting[259,768]. In our study, tumor mass or polyp number were not affected by NMES. Although it is possible that NMES could affect tumor's microenvironment (*e.g.,* immune cell content) or its secretory activity and in turn induce positive changes in the muscles. Recently, Kurtz et al.[769] showed that low-intensity exercise induces inhibitory effect on murine PDA tumor growth by modulation of systemic and intra-tumoral immunity in a IL-15 dependent manner. The study by Kurz et al. demonstrates that exercise impact cellular immunity of cancer *via* the release of IL-15 myokine. Myokines, are expressed in the skeletal muscle when muscle contracts during exercise, released into circulation and can modulate the muscle/tumor crosstalk in CC[770]. In that regard, musclin a myokine released during exercise was shown to delay muscle wasting during CC in mice[771]. Exogenous expression of musclin partially preserved muscle fiber area during C26 tumor growth in mice. Therefore, it would be interesting to study tumor's composition after NMES in the cachectic mice *via* proteomic approach to determine potential targets of NMES that can inhibit CC.

Altogether, determination of the mechanisms that alter the cachectic SC niche and of factors released in response to NMES would allow to design possible drugs to counteract muscle wasting in CC.

REFERENCES

1. GBD 2015 Mortality and Causes of Death Collaborators. Global, regional, and national life expectancy, all-cause mortality, and cause-specific mortality for 249 causes of death, 1980-2015: a systematic analysis for the Global Burden of Disease Study 2015. *Lancet* **388**, 1459–1544 (2016).
2. Ferlay, J. *et al.* Cancer statistics for the year 2020: An overview. *Int J Cancer* (2021) doi:10.1002/ijc.33588.
3. Keum, N. & Giovannucci, E. Global burden of colorectal cancer: emerging trends, risk factors and prevention strategies. *Nat Rev Gastroenterol Hepatol* **16**, 713–732 (2019).
4. World Health Organization. Global Health Observatory. Geneva: World Health Organization; 2018.
5. Torre, L. A., Siegel, R. L., Ward, E. M. & Jemal, A. Global Cancer Incidence and Mortality Rates and Trends--An Update. *Cancer Epidemiol Biomarkers Prev* **25**, 16–27 (2016).
6. Kingham, T. P. *et al.* Treatment of cancer in sub-Saharan Africa. *Lancet Oncol* **14**, e158-167 (2013).
7. Atun, R. *et al.* Expanding global access to radiotherapy. *Lancet Oncol* **16**, 1153–1186 (2015).
8. Shah, S. C., Kayamba, V., Peek, R. M. & Heimburger, D. Cancer Control in Low- and Middle-Income Countries: Is It Time to Consider Screening? *J Glob Oncol* **5**, 1–8 (2019).
9. Siegel, R. L., Miller, K. D. & Jemal, A. Cancer statistics, 2018. *CA Cancer J Clin* **68**, 7–30 (2018).
10. Pilleron, S. *et al.* Global cancer incidence in older adults, 2012 and 2035: A population-based study. *Int J Cancer* **144**, 49–58 (2019).
11. Pilleron, S. *et al.* Estimated global cancer incidence in the oldest adults in 2018 and projections to 2050. *Int J Cancer* **148**, 601–608 (2021).
12. GBD 2019 Cancer Risk Factors Collaborators. The global burden of cancer attributable to risk factors, 2010-19: a systematic analysis for the Global Burden of Disease Study 2019. *Lancet* **400**, 563–591 (2022).
13. Davis, M. P. & Dickerson, D. Cachexia and anorexia: cancer's covert killer. *Support Care Cancer* **8**, 180–187 (2000).
14. Prado, C. M. M. *et al.* Prevalence and clinical implications of sarcopenic obesity in patients with solid tumours of the respiratory and gastrointestinal tracts: a population-based study. *Lancet Oncol* **9**, 629–635 (2008).
15. Moley, J. F., Aamodt, R., Rumble, W., Kaye, W. & Norton, J. A. Body cell mass in cancer-bearing and anorexic patients. *JPEN J Parenter Enteral Nutr* **11**, 219–222 (1987).
16. Tisdale, M. J. Cancer anorexia and cachexia. *Nutrition* **17**, 438–442 (2001).
17. Jeejeebhoy, K. N. Malnutrition, fatigue, frailty, vulnerability, sarcopenia and cachexia: overlap of clinical features. *Curr Opin Clin Nutr Metab Care* **15**, 213–219 (2012).
18. Strasser, F. Diagnostic criteria of cachexia and their assessment: decreased muscle strength and fatigue. *Curr Opin Clin Nutr Metab Care* **11**, 417–421 (2008).
19. Evans, W. J. *et al.* Cachexia: a new definition. *Clin Nutr* **27**, 793–799 (2008).
20. Fearon, K. *et al.* Definition and classification of cancer cachexia: an international consensus. *Lancet Oncol* **12**, 489–495 (2011).
21. Oken, M. M. *et al.* Toxicity and response criteria of the Eastern Cooperative Oncology Group. *Am J Clin Oncol* **5**, 649–655 (1982).
22. Blum, D. *et al.* Validation of the Consensus-Definition for Cancer Cachexia and evaluation of a classification model--a study based on data from an international multicentre project (EPCRC-CSA). *Ann Oncol* **25**, 1635–1642 (2014).
23. von Haehling, S., Anker, M. S. & Anker, S. D. Prevalence and clinical impact of

cachexia in chronic illness in Europe, USA, and Japan: facts and numbers update 2016. *J Cachexia Sarcopenia Muscle* **7**, 507–509 (2016).
24. Pressoir, M. *et al.* Prevalence, risk factors and clinical implications of malnutrition in French Comprehensive Cancer Centres. *Br J Cancer* **102**, 966–971 (2010).
25. Bozzetti, F. & SCRINIO Working Group. Screening the nutritional status in oncology: a preliminary report on 1,000 outpatients. *Support Care Cancer* **17**, 279–284 (2009).
26. Segura, A. *et al.* An epidemiological evaluation of the prevalence of malnutrition in Spanish patients with locally advanced or metastatic cancer. *Clin Nutr* **24**, 801–814 (2005).
27. Hébuterne, X. *et al.* Prevalence of malnutrition and current use of nutrition support in patients with cancer. *JPEN J Parenter Enteral Nutr* **38**, 196–204 (2014).
28. Muscaritoli, M. *et al.* Prevalence of malnutrition in patients at first medical oncology visit: the PreMiO study. *Oncotarget* **8**, 79884–79896 (2017).
29. Fearon, K. C. H., Glass, D. J. & Guttridge, D. C. Cancer cachexia: mediators, signaling, and metabolic pathways. *Cell Metab* **16**, 153–166 (2012).
30. Onesti, J. K. & Guttridge, D. C. Inflammation based regulation of cancer cachexia. *Biomed Res Int* **2014**, 168407 (2014).
31. Dewys, W. D. *et al.* Prognostic effect of weight loss prior to chemotherapy in cancer patients. Eastern Cooperative Oncology Group. *Am J Med* **69**, 491–497 (1980).
32. Baracos, V. E., Martin, L., Korc, M., Guttridge, D. C. & Fearon, K. C. H. Cancer-associated cachexia. *Nat Rev Dis Primers* **4**, 17105 (2018).
33. Stojcev, Z., Matysiak, K., Duszewski, M. & Banasiewicz, T. The role of dietary nutrition in stomach cancer. *Contemp Oncol (Pozn)* **17**, 343–345 (2013).
34. Utech, A. E., Tadros, E. M., Hayes, T. G. & Garcia, J. M. Predicting survival in cancer patients: the role of cachexia and hormonal, nutritional and inflammatory markers. *J Cachexia Sarcopenia Muscle* **3**, 245–251 (2012).
35. Farkas, J. *et al.* Cachexia as a major public health problem: frequent, costly, and deadly. *J Cachexia Sarcopenia Muscle* **4**, 173–178 (2013).
36. Andreyev, H. J., Norman, A. R., Oates, J. & Cunningham, D. Why do patients with weight loss have a worse outcome when undergoing chemotherapy for gastrointestinal malignancies? *Eur J Cancer* **34**, 503–509 (1998).
37. Wakahara, T. *et al.* Nutritional screening with Subjective Global Assessment predicts hospital stay in patients with digestive diseases. *Nutrition* **23**, 634–639 (2007).
38. Khalid, U. *et al.* Symptoms and weight loss in patients with gastrointestinal and lung cancer at presentation. *Support Care Cancer* **15**, 39–46 (2007).
39. Persson, C., Sjödén, P. O. & Glimelius, B. The Swedish version of the patient-generated subjective global assessment of nutritional status: gastrointestinal vs urological cancers. *Clin Nutr* **18**, 71–77 (1999).
40. Tisdale, M. J. Mechanisms of cancer cachexia. *Physiol Rev* **89**, 381–410 (2009).
41. Argilés, J. M. Cancer-associated malnutrition. *Eur J Oncol Nurs* **9 Suppl 2**, S39-50 (2005).
42. von Haehling, S. & Anker, S. D. Cachexia as a major underestimated and unmet medical need: facts and numbers. *J Cachexia Sarcopenia Muscle* **1**, 1–5 (2010).
43. Smith, B. D., Smith, G. L., Hurria, A., Hortobagyi, G. N. & Buchholz, T. A. Future of cancer incidence in the United States: burdens upon an aging, changing nation. *J Clin Oncol* **27**, 2758–2765 (2009).
44. Windsor, J. A. & Hill, G. L. Risk factors for postoperative pneumonia. The importance of protein depletion. *Ann Surg* **208**, 209–214 (1988).
45. Tian, M. *et al.* Cardiac alterations in cancer-induced cachexia in mice. *Int J Oncol* **37**, 347–353 (2010).
46. Johns, N. *et al.* Clinical classification of cancer cachexia: phenotypic correlates in

human skeletal muscle. *PLoS One* **9**, e83618 (2014).
47. Tan, B. H. L. *et al.* Identification of possible genetic polymorphisms involved in cancer cachexia: a systematic review. *J Genet* **90**, 165–177 (2011).
48. Tan, B. H. L. & Fearon, K. C. H. Cytokine gene polymorphisms and susceptibility to cachexia. *Curr Opin Support Palliat Care* **4**, 243–248 (2010).
49. Martignoni, M. E. *et al.* Role of mononuclear cells and inflammatory cytokines in pancreatic cancer-related cachexia. *Clin Cancer Res* **11**, 5802–5808 (2005).
50. Deans, D. A. C. *et al.* Cancer cachexia is associated with the IL10 -1082 gene promoter polymorphism in patients with gastroesophageal malignancy. *Am J Clin Nutr* **89**, 1164–1172 (2009).
51. Sun, F. *et al.* Interleukin-10 gene polymorphisms influence susceptibility to cachexia in patients with low-third gastric cancer in a Chinese population. *Mol Diagn Ther* **14**, 95–100 (2010).
52. Robert, F. *et al.* Targeting protein synthesis in a Myc/mTOR-driven model of anorexia-cachexia syndrome delays its onset and prolongs survival. *Cancer Res* **72**, 747–756 (2012).
53. Shibata, M. *et al.* Serum levels of interleukin-10 and interleukin-12 in patients with colorectal cancer. *Ann N Y Acad Sci* **795**, 410–412 (1996).
54. Tan, B. H. L. *et al.* P-selectin genotype is associated with the development of cancer cachexia. *EMBO Mol Med* **4**, 462–471 (2012).
55. Johns, N. *et al.* New genetic signatures associated with cancer cachexia as defined by low skeletal muscle index and weight loss. *J Cachexia Sarcopenia Muscle* **8**, 122–130 (2017).
56. Avan, A. *et al.* AKT1 and SELP polymorphisms predict the risk of developing cachexia in pancreatic cancer patients. *PLoS One* **9**, e108057 (2014).
57. Yehia, R. *et al.* Impact of TNF-α Gene Polymorphisms on Pancreatic and Non-Small Cell Lung Cancer-Induced Cachexia in Adult Egyptian Patients: A Focus on Pathogenic Trajectories. *Front Oncol* **11**, 783231 (2021).
58. Geppert, J. *et al.* Aging Aggravates Cachexia in Tumor-Bearing Mice. *Cancers (Basel)* **14**, 90 (2021).
59. Lacau St Guily, J. *et al.* NutriCancer: A French observational multicentre cross-sectional study of malnutrition in elderly patients with cancer. *J Geriatr Oncol* **9**, 74–80 (2018).
60. Dunne, R. F. *et al.* Characterizing cancer cachexia in the geriatric oncology population. *J Geriatr Oncol* **10**, 415–419 (2019).
61. Williams, G. R., Rier, H. N., McDonald, A. & Shachar, S. S. Sarcopenia & aging in cancer. *J Geriatr Oncol* **10**, 374–377 (2019).
62. Ali, S. & Garcia, J. M. Sarcopenia, cachexia and aging: diagnosis, mechanisms and therapeutic options - a mini-review. *Gerontology* **60**, 294–305 (2014).
63. Rosa-Caldwell, M. E. & Greene, N. P. Muscle metabolism and atrophy: let's talk about sex. *Biol Sex Differ* **10**, 43 (2019).
64. Zhong, X. *et al.* Sex specificity of pancreatic cancer cachexia phenotypes, mechanisms, and treatment in mice and humans: role of Activin. *J Cachexia Sarcopenia Muscle* **13**, 2146–2161 (2022).
65. Baracos, V. E., Reiman, T., Mourtzakis, M., Gioulbasanis, I. & Antoun, S. Body composition in patients with non-small cell lung cancer: a contemporary view of cancer cachexia with the use of computed tomography image analysis. *Am J Clin Nutr* **91**, 1133S-1137S (2010).
66. Wallengren, O., Iresjö, B.-M., Lundholm, K. & Bosaeus, I. Loss of muscle mass in the end of life in patients with advanced cancer. *Support Care Cancer* **23**, 79–86 (2015).
67. Skipworth, R. J. E. *et al.* Interaction of gonadal status with systemic inflammation and

opioid use in determining nutritional status and prognosis in advanced pancreatic cancer. *Support Care Cancer* **19**, 391–401 (2011).
68. Hetzler, K. L. *et al.* Sex differences in the relationship of IL-6 signaling to cancer cachexia progression. *Biochim Biophys Acta* **1852**, 816–825 (2015).
69. Sasaki, S. *et al.* Skeletal muscle loss during systemic chemotherapy for colorectal cancer indicates treatment response: a pooled analysis of a multicenter clinical trial (KSCC 1605-A). *Int J Clin Oncol* **24**, 1204–1213 (2019).
70. Howarth, F. C., Calaghan, S. C., Boyett, M. R. & White, E. Effect of the microtubule polymerizing agent taxol on contraction, Ca2+ transient and L-type Ca2+ current in rat ventricular myocytes. *J Physiol* **516 (Pt 2)**, 409–419 (1999).
71. Konishi, S. & Kishida, S. Studies on the morphological changes of skeletal muscle induced by vincristine, vinblastine and colchicine. *Bull Osaka Med Sch* **30**, 19–40 (1984).
72. Del Fabbro, E. *et al.* The relationship between body composition and response to neoadjuvant chemotherapy in women with operable breast cancer. *Oncologist* **17**, 1240–1245 (2012).
73. Dalal, S. *et al.* Relationships among body mass index, longitudinal body composition alterations, and survival in patients with locally advanced pancreatic cancer receiving chemoradiation: a pilot study. *J Pain Symptom Manage* **44**, 181–191 (2012).
74. Mir, O. *et al.* Sarcopenia predicts early dose-limiting toxicities and pharmacokinetics of sorafenib in patients with hepatocellular carcinoma. *PLoS One* **7**, e37563 (2012).
75. Antoun, S. *et al.* Association of skeletal muscle wasting with treatment with sorafenib in patients with advanced renal cell carcinoma: results from a placebo-controlled study. *J Clin Oncol* **28**, 1054–1060 (2010).
76. Aversa, Z., Costelli, P. & Muscaritoli, M. Cancer-induced muscle wasting: latest findings in prevention and treatment. *Ther Adv Med Oncol* **9**, 369–382 (2017).
77. Imai, K. *et al.* Rapid Depletions of Subcutaneous Fat Mass and Skeletal Muscle Mass Predict Worse Survival in Patients with Hepatocellular Carcinoma Treated with Sorafenib. *Cancers (Basel)* **11**, E1206 (2019).
78. Barreto, R. *et al.* Cancer and Chemotherapy Contribute to Muscle Loss by Activating Common Signaling Pathways. *Front Physiol* **7**, 472 (2016).
79. Barreto, R. *et al.* Chemotherapy-related cachexia is associated with mitochondrial depletion and the activation of ERK1/2 and p38 MAPKs. *Oncotarget* **7**, 43442–43460 (2016).
80. Grossberg, A. J., Mohamed, A. S. R. & Fuller, C. D. Cachexia in Radiotherapy-Treated Patients With Head and Neck Cancer-Reply. *JAMA Oncol* **2**, 831–832 (2016).
81. Canada, J. M. *et al.* Determinants of Cardiorespiratory Fitness Following Thoracic Radiotherapy in Lung or Breast Cancer Survivors. *Am J Cardiol* **125**, 988–996 (2020).
82. Mitsunaga, S., Kasamatsu, E. & Machii, K. Incidence and frequency of cancer cachexia during chemotherapy for advanced pancreatic ductal adenocarcinoma. *Support Care Cancer* **28**, 5271–5279 (2020).
83. Awad, S. *et al.* Marked changes in body composition following neoadjuvant chemotherapy for oesophagogastric cancer. *Clin Nutr* **31**, 74–77 (2012).
84. Yip, C. *et al.* Assessment of sarcopenia and changes in body composition after neoadjuvant chemotherapy and associations with clinical outcomes in oesophageal cancer. *Eur Radiol* **24**, 998–1005 (2014).
85. Martin, L. *et al.* Diagnostic criteria for the classification of cancer-associated weight loss. *J Clin Oncol* **33**, 90–99 (2015).
86. Fonseca, G. W. P. da, Farkas, J., Dora, E., von Haehling, S. & Lainscak, M. Cancer Cachexia and Related Metabolic Dysfunction. *Int J Mol Sci* **21**, E2321 (2020).
87. Sun, X. *et al.* Fat Wasting Is Damaging: Role of Adipose Tissue in Cancer-Associated Cachexia. *Front Cell Dev Biol* **8**, 33 (2020).

88. Vaitkus, J. A. & Celi, F. S. The role of adipose tissue in cancer-associated cachexia. *Exp Biol Med (Maywood)* **242**, 473–481 (2017).
89. Divella, R., Gadaleta Caldarola, G. & Mazzocca, A. Chronic Inflammation in Obesity and Cancer Cachexia. *J Clin Med* **11**, 2191 (2022).
90. Hendifar, A. E., Chang, J. I., Huang, B. Z., Tuli, R. & Wu, B. U. Cachexia, and not obesity, prior to pancreatic cancer diagnosis worsens survival and is negated by chemotherapy. *J Gastrointest Oncol* **9**, 17–23 (2018).
91. Martin, L. *et al.* Cancer cachexia in the age of obesity: skeletal muscle depletion is a powerful prognostic factor, independent of body mass index. *J Clin Oncol* **31**, 1539–1547 (2013).
92. Roeland, E. J. *et al.* Weight loss versus muscle loss: re-evaluating inclusion criteria for future cancer cachexia interventional trials. *Support Care Cancer* **25**, 365–369 (2017).
93. Nishikawa, H., Enomoto, H., Nishiguchi, S. & Iijima, H. Sarcopenic Obesity in Liver Cirrhosis: Possible Mechanism and Clinical Impact. *Int J Mol Sci* **22**, 1917 (2021).
94. Baumgartner, R. N. *et al.* Epidemiology of sarcopenia among the elderly in New Mexico. *Am J Epidemiol* **147**, 755–763 (1998).
95. Heymsfield, S. B. *et al.* Body composition of humans: comparison of two improved four-compartment models that differ in expense, technical complexity, and radiation exposure. *Am J Clin Nutr* **52**, 52–58 (1990).
96. Shiel, F. *et al.* Dual energy X-ray absorptiometry positioning protocols in assessing body composition: A systematic review of the literature. *J Sci Med Sport* **21**, 1038–1044 (2018).
97. Ellis, K. J. *et al.* Z score prediction model for assessment of bone mineral content in pediatric diseases. *J Bone Miner Res* **16**, 1658–1664 (2001).
98. Guglielmi, G. *et al.* The role of DXA in sarcopenia. *Aging Clin Exp Res* **28**, 1047–1060 (2016).
99. Prado, C. M. M. & Heymsfield, S. B. Lean tissue imaging: a new era for nutritional assessment and intervention. *JPEN J Parenter Enteral Nutr* **38**, 940–953 (2014).
100. Trutschnigg, B. *et al.* Precision and reliability of strength (Jamar vs. Biodex handgrip) and body composition (dual-energy X-ray absorptiometry vs. bioimpedance analysis) measurements in advanced cancer patients. *Appl Physiol Nutr Metab* **33**, 1232–1239 (2008).
101. Coin, A. *et al.* Prevalence of sarcopenia based on different diagnostic criteria using DEXA and appendicular skeletal muscle mass reference values in an Italian population aged 20 to 80. *J Am Med Dir Assoc* **14**, 507–512 (2013).
102. Cruz-Jentoft, A. J. *et al.* Sarcopenia: European consensus on definition and diagnosis: Report of the European Working Group on Sarcopenia in Older People. *Age Ageing* **39**, 412–423 (2010).
103. Cruz-Jentoft, A. J. *et al.* Sarcopenia: revised European consensus on definition and diagnosis. *Age Ageing* **48**, 16–31 (2019).
104. Kim, K. M., Jang, H. C. & Lim, S. Differences among skeletal muscle mass indices derived from height-, weight-, and body mass index-adjusted models in assessing sarcopenia. *Korean J Intern Med* **31**, 643–650 (2016).
105. Fuggle, N., Shaw, S., Dennison, E. & Cooper, C. Sarcopenia. *Best Pract Res Clin Rheumatol* **31**, 218–242 (2017).
106. Kim, H. *et al.* Sarcopenia: Prevalence and associated factors based on different suggested definitions in community-dwelling older adults. *Geriatr Gerontol Int* **16 Suppl 1**, 110–122 (2016).
107. Kim, E. Y. *et al.* Prognostic Significance of CT-Determined Sarcopenia in Patients with Small-Cell Lung Cancer. *J Thorac Oncol* **10**, 1795–1799 (2015).
108. Prado, C. M. M., Birdsell, L. A. & Baracos, V. E. The emerging role of computerized

tomography in assessing cancer cachexia. *Curr Opin Support Palliat Care* **3**, 269–275 (2009).
109. Faron, A. *et al.* Quantification of fat and skeletal muscle tissue at abdominal computed tomography: associations between single-slice measurements and total compartment volumes. *Abdom Radiol (NY)* **44**, 1907–1916 (2019).
110. Shen, W. *et al.* Total body skeletal muscle and adipose tissue volumes: estimation from a single abdominal cross-sectional image. *J Appl Physiol (1985)* **97**, 2333–2338 (2004).
111. Lieffers, J. R., Bathe, O. F., Fassbender, K., Winget, M. & Baracos, V. E. Sarcopenia is associated with postoperative infection and delayed recovery from colorectal cancer resection surgery. *Br J Cancer* **107**, 931–936 (2012).
112. Prado, C. M. M. *et al.* Body composition as an independent determinant of 5-fluorouracil-based chemotherapy toxicity. *Clin Cancer Res* **13**, 3264–3268 (2007).
113. Su, H., Ruan, J., Chen, T., Lin, E. & Shi, L. CT-assessed sarcopenia is a predictive factor for both long-term and short-term outcomes in gastrointestinal oncology patients: a systematic review and meta-analysis. *Cancer Imaging* **19**, 82 (2019).
114. Brenner, D. J. & Hall, E. J. Computed tomography--an increasing source of radiation exposure. *N Engl J Med* **357**, 2277–2284 (2007).
115. Coelen, R. J. S. *et al.* Preoperative computed tomography assessment of skeletal muscle mass is valuable in predicting outcomes following hepatectomy for perihilar cholangiocarcinoma. *HPB (Oxford)* **17**, 520–528 (2015).
116. Mourtzakis, M. *et al.* A practical and precise approach to quantification of body composition in cancer patients using computed tomography images acquired during routine care. *Appl Physiol Nutr Metab* **33**, 997–1006 (2008).
117. Kyle, U. G. *et al.* Bioelectrical impedance analysis--part I: review of principles and methods. *Clin Nutr* **23**, 1226–1243 (2004).
118. Gonzalez, M. C. & Heymsfield, S. B. Bioelectrical impedance analysis for diagnosing sarcopenia and cachexia: what are we really estimating? *J Cachexia Sarcopenia Muscle* **8**, 187–189 (2017).
119. Yamada, Y. *et al.* Developing and Validating an Age-Independent Equation Using Multi-Frequency Bioelectrical Impedance Analysis for Estimation of Appendicular Skeletal Muscle Mass and Establishing a Cutoff for Sarcopenia. *Int J Environ Res Public Health* **14**, E809 (2017).
120. Sergi, G. *et al.* Assessing appendicular skeletal muscle mass with bioelectrical impedance analysis in free-living Caucasian older adults. *Clin Nutr* **34**, 667–673 (2015).
121. Chen, L.-K. *et al.* Sarcopenia in Asia: consensus report of the Asian Working Group for Sarcopenia. *J Am Med Dir Assoc* **15**, 95–101 (2014).
122. Fukuta, A. *et al.* Impact of preoperative cachexia on postoperative length of stay in elderly patients with gastrointestinal cancer. *Nutrition* **58**, 65–68 (2019).
123. Chen, X. *et al.* Preoperative Cachexia predicts poor outcomes in young rather than elderly gastric cancer patients: a prospective study. *Cancer Manag Res* **11**, 8101–8110 (2019).
124. Ræder, H. *et al.* Validity of bioelectrical impedance analysis in estimation of fat-free mass in colorectal cancer patients. *Clin Nutr* **37**, 292–300 (2018).
125. Nishikawa, H. *et al.* Clinical utility of bioimpedance analysis in liver cirrhosis. *J Hepatobiliary Pancreat Sci* **24**, 409–416 (2017).
126. Grossi, M. & Riccò, B. Electrical impedance spectroscopy (EIS) for biological analysis and food characterization: a review. *J. Sens. Sens. Syst.* **6**, 303–325 (2017).
127. Drescher, C., Konishi, M., Ebner, N. & Springer, J. Loss of muscle mass: current developments in cachexia and sarcopenia focused on biomarkers and treatment. *J Cachexia Sarcopenia Muscle* **6**, 303–311 (2015).
128. Chen, L.-K. *et al.* Asian Working Group for Sarcopenia: 2019 Consensus Update on

Sarcopenia Diagnosis and Treatment. *J Am Med Dir Assoc* **21**, 300-307.e2 (2020).
129. Walowski, C. O. *et al.* Reference Values for Skeletal Muscle Mass - Current Concepts and Methodological Considerations. *Nutrients* **12**, E755 (2020).
130. Jensen, B. *et al.* Ethnic differences in fat and muscle mass and their implication for interpretation of bioelectrical impedance vector analysis. *Appl Physiol Nutr Metab* **44**, 619–626 (2019).
131. Silva, A. M. *et al.* Ethnicity-related skeletal muscle differences across the lifespan. *Am J Hum Biol* **22**, 76–82 (2010).
132. Couch, M. E. *et al.* Cancer cachexia update in head and neck cancer: Pathophysiology and treatment. *Head Neck* **37**, 1057–1072 (2015).
133. Fearon, K. C., Voss, A. C., Hustead, D. S., & Cancer Cachexia Study Group. Definition of cancer cachexia: effect of weight loss, reduced food intake, and systemic inflammation on functional status and prognosis. *Am J Clin Nutr* **83**, 1345–1350 (2006).
134. Vanhoutte, G. *et al.* Cachexia in cancer: what is in the definition? *BMJ Open Gastroenterol* **3**, e000097 (2016).
135. Huang, D.-D. *et al.* Sarcopenia, as defined by low muscle mass, strength and physical performance, predicts complications after surgery for colorectal cancer. *Colorectal Dis* **17**, O256-264 (2015).
136. Weber, M.-A. *et al.* Morphology, metabolism, microcirculation, and strength of skeletal muscles in cancer-related cachexia. *Acta Oncol* **48**, 116–124 (2009).
137. Toledo, M. *et al.* Cancer cachexia: physical activity and muscle force in tumour-bearing rats. *Oncol Rep* **25**, 189–193 (2011).
138. Baltgalvis, K. A. *et al.* Muscle wasting and interleukin-6-induced atrogin-I expression in the cachectic Apc (Min/+) mouse. *Pflugers Arch* **457**, 989–1001 (2009).
139. Aulino, P. *et al.* Molecular, cellular and physiological characterization of the cancer cachexia-inducing C26 colon carcinoma in mouse. *BMC Cancer* **10**, 363 (2010).
140. Fearon, K. C. H. Cancer cachexia: developing multimodal therapy for a multidimensional problem. *Eur J Cancer* **44**, 1124–1132 (2008).
141. LeBlanc, T. W. *et al.* Correlation between the international consensus definition of the Cancer Anorexia-Cachexia Syndrome (CACS) and patient-centered outcomes in advanced non-small cell lung cancer. *J Pain Symptom Manage* **49**, 680–689 (2015).
142. Jeffery, E. *et al.* Body composition and nutritional status in malignant pleural mesothelioma: implications for activity levels and quality of life. *Eur J Clin Nutr* **73**, 1412–1421 (2019).
143. Naito, T. *et al.* Unfavorable impact of cancer cachexia on activity of daily living and need for inpatient care in elderly patients with advanced non-small-cell lung cancer in Japan: a prospective longitudinal observational study. *BMC Cancer* **17**, 800 (2017).
144. Arthur, S. T. *et al.* Cachexia among US cancer patients. *J Med Econ* **19**, 874–880 (2016).
145. Wallengren, O., Lundholm, K. & Bosaeus, I. Diagnostic criteria of cancer cachexia: relation to quality of life, exercise capacity and survival in unselected palliative care patients. *Support Care Cancer* **21**, 1569–1577 (2013).
146. Ross, P. J. *et al.* Do patients with weight loss have a worse outcome when undergoing chemotherapy for lung cancers? *Br J Cancer* **90**, 1905–1911 (2004).
147. Kimura, M. *et al.* Prognostic impact of cancer cachexia in patients with advanced non-small cell lung cancer. *Support Care Cancer* **23**, 1699–1708 (2015).
148. Takayama, K. *et al.* Quality of life and survival survey of cancer cachexia in advanced non-small cell lung cancer patients-Japan nutrition and QOL survey in patients with advanced non-small cell lung cancer study. *Support Care Cancer* **24**, 3473–3480 (2016).
149. Bachmann, J. *et al.* Cachexia worsens prognosis in patients with resectable pancreatic

cancer. *J Gastrointest Surg* **12**, 1193–1201 (2008).
150. Kasvis, P., Vigano, M. & Vigano, A. Health-related quality of life across cancer cachexia stages. *Ann Palliat Med* **8**, 33–42 (2019).
151. McClement, S. Cancer anorexia-cachexia syndrome: psychological effect on the patient and family. *J Wound Ostomy Continence Nurs* **32**, 264–268 (2005).
152. Fang, Z., Shang, L. & Li, L. Impact of Low Skeletal Muscle Mass on Complications and Survival for Gastric Cancer: A Propensity Score Matching Analysis. *Front Surg* **9**, 901142 (2022).
153. Jeffery, E. *et al.* Changes in body composition in patients with malignant pleural mesothelioma and the relationship with activity levels and dietary intake. *Eur J Clin Nutr* **76**, 979–986 (2022).
154. Cho, K.-M. *et al.* Skeletal muscle depletion predicts survival of patients with advanced biliary tract cancer undergoing palliative chemotherapy. *Oncotarget* **8**, 79441–79452 (2017).
155. Iritani, S. *et al.* Skeletal muscle depletion is an independent prognostic factor for hepatocellular carcinoma. *J Gastroenterol* **50**, 323–332 (2015).
156. Huang, C.-Y. *et al.* Muscle loss during primary debulking surgery and chemotherapy predicts poor survival in advanced-stage ovarian cancer. *J Cachexia Sarcopenia Muscle* **11**, 534–546 (2020).
157. Vermaete, N., Wolter, P., Verhoef, G. & Gosselink, R. Physical activity and physical fitness in lymphoma patients before, during, and after chemotherapy: a prospective longitudinal study. *Ann Hematol* **93**, 411–424 (2014).
158. Prado, C. M. M. *et al.* Sarcopenia as a determinant of chemotherapy toxicity and time to tumor progression in metastatic breast cancer patients receiving capecitabine treatment. *Clin Cancer Res* **15**, 2920–2926 (2009).
159. Prado, C. M. M. *et al.* An exploratory study of body composition as a determinant of epirubicin pharmacokinetics and toxicity. *Cancer Chemother Pharmacol* **67**, 93–101 (2011).
160. Antoun, S., Baracos, V. E., Birdsell, L., Escudier, B. & Sawyer, M. B. Low body mass index and sarcopenia associated with dose-limiting toxicity of sorafenib in patients with renal cell carcinoma. *Ann Oncol* **21**, 1594–1598 (2010).
161. da Rocha, I. M. G. *et al.* Is cachexia associated with chemotherapy toxicities in gastrointestinal cancer patients? A prospective study. *J Cachexia Sarcopenia Muscle* **10**, 445–454 (2019).
162. Jung, H.-W. *et al.* Effect of muscle mass on toxicity and survival in patients with colon cancer undergoing adjuvant chemotherapy. *Support Care Cancer* **23**, 687–694 (2015).
163. Gusella, M., Toso, S., Ferrazzi, E., Ferrari, M. & Padrini, R. Relationships between body composition parameters and fluorouracil pharmacokinetics. *Br J Clin Pharmacol* **54**, 131–139 (2002).
164. Bozzetti, F. Forcing the vicious circle: sarcopenia increases toxicity, decreases response to chemotherapy and worsens with chemotherapy. *Ann Oncol* **28**, 2107–2118 (2017).
165. Janssen, I., Heymsfield, S. B., Wang, Z. M. & Ross, R. Skeletal muscle mass and distribution in 468 men and women aged 18-88 yr. *J Appl Physiol (1985)* **89**, 81–88 (2000).
166. Frontera, W. R. & Ochala, J. Skeletal muscle: a brief review of structure and function. *Calcif Tissue Int* **96**, 183–195 (2015).
167. Listrat, A. *et al.* How Muscle Structure and Composition Influence Meat and Flesh Quality. *ScientificWorldJournal* **2016**, 3182746 (2016).
168. Sandow, A. Excitation-contraction coupling in muscular response. *Yale J Biol Med* **25**, 176–201 (1952).
169. Schiaffino, S. & Reggiani, C. Fiber types in mammalian skeletal muscles. *Physiol Rev* **91**, 1447–1531 (2011).

170. Soukup, T., Zacharová, G. & Smerdu, V. Fibre type composition of soleus and extensor digitorum longus muscles in normal female inbred Lewis rats. *Acta Histochem* **104**, 399–405 (2002).
171. Talbot, J. & Maves, L. Skeletal muscle fiber type: using insights from muscle developmental biology to dissect targets for susceptibility and resistance to muscle disease. *Wiley Interdiscip Rev Dev Biol* **5**, 518–534 (2016).
172. Zhou, X. *et al.* Reversal of cancer cachexia and muscle wasting by ActRIIB antagonism leads to prolonged survival. *Cell* **142**, 531–543 (2010).
173. Coletti, D. *et al.* Spontaneous Physical Activity Downregulates Pax7 in Cancer Cachexia. *Stem Cells Int* **2016**, 6729268 (2016).
174. Penna, F. *et al.* Muscle wasting and impaired myogenesis in tumor bearing mice are prevented by ERK inhibition. *PLoS One* **5**, e13604 (2010).
175. Pin, F., Barreto, R., Couch, M. E., Bonetto, A. & O'Connell, T. M. Cachexia induced by cancer and chemotherapy yield distinct perturbations to energy metabolism. *J Cachexia Sarcopenia Muscle* **10**, 140–154 (2019).
176. Murphy, K. T., Chee, A., Trieu, J., Naim, T. & Lynch, G. S. Importance of functional and metabolic impairments in the characterization of the C-26 murine model of cancer cachexia. *Dis Model Mech* **5**, 533–545 (2012).
177. van Norren, K. *et al.* Dietary supplementation with a specific combination of high protein, leucine, and fish oil improves muscle function and daily activity in tumour-bearing cachectic mice. *Br J Cancer* **100**, 713–722 (2009).
178. Pin, F. *et al.* Interference with Ca2+-Dependent Proteolysis Does Not Alter the Course of Muscle Wasting in Experimental Cancer Cachexia. *Front Physiol* **8**, 213 (2017).
179. Lima, M., Sato, S., Enos, R. T., Baynes, J. W. & Carson, J. A. Development of an UPLC mass spectrometry method for measurement of myofibrillar protein synthesis: application to analysis of murine muscles during cancer cachexia. *J Appl Physiol (1985)* **114**, 824–828 (2013).
180. Mehl, K. A., Davis, J. M., Berger, F. G. & Carson, J. A. Myofiber degeneration/regeneration is induced in the cachectic ApcMin/+ mouse. *J Appl Physiol (1985)* **99**, 2379–2387 (2005).
181. Counts, B. R., Fix, D. K., Hetzler, K. L. & Carson, J. A. The Effect of Estradiol Administration on Muscle Mass Loss and Cachexia Progression in Female Apc Min/+ Mice. *Front Endocrinol (Lausanne)* **10**, 720 (2019).
182. Velázquez, K. T. *et al.* Quercetin supplementation attenuates the progression of cancer cachexia in ApcMin/+ mice. *J Nutr* **144**, 868–875 (2014).
183. VanderVeen, B. N., Hardee, J. P., Fix, D. K. & Carson, J. A. Skeletal muscle function during the progression of cancer cachexia in the male ApcMin/+ mouse. *J Appl Physiol (1985)* **124**, 684–695 (2018).
184. White, J. P. *et al.* Muscle oxidative capacity during IL-6-dependent cancer cachexia. *Am J Physiol Regul Integr Comp Physiol* **300**, R201-211 (2011).
185. Brown, J. L. *et al.* Cancer cachexia in a mouse model of oxidative stress. *J Cachexia Sarcopenia Muscle* **11**, 1688–1704 (2020).
186. Paul, P. K. *et al.* Targeted ablation of TRAF6 inhibits skeletal muscle wasting in mice. *J Cell Biol* **191**, 1395–1411 (2010).
187. Penna, F. *et al.* Combined approach to counteract experimental cancer cachexia: eicosapentaenoic acid and training exercise. *J Cachexia Sarcopenia Muscle* **2**, 95–104 (2011).
188. Costelli, P. *et al.* IGF-1 is downregulated in experimental cancer cachexia. *Am J Physiol Regul Integr Comp Physiol* **291**, R674-683 (2006).
189. Baracos, V. E., DeVivo, C., Hoyle, D. H. & Goldberg, A. L. Activation of the ATP-ubiquitin-proteasome pathway in skeletal muscle of cachectic rats bearing a hepatoma. *Am J*

Physiol **268**, E996-1006 (1995).
190. Costelli, P. *et al.* Muscle myostatin signalling is enhanced in experimental cancer cachexia. *Eur J Clin Invest* **38**, 531–538 (2008).
191. Talbert, E. E. *et al.* Modeling Human Cancer-induced Cachexia. *Cell Rep* **28**, 1612-1622.e4 (2019).
192. White, J. P. *et al.* The regulation of skeletal muscle protein turnover during the progression of cancer cachexia in the Apc(Min/+) mouse. *PLoS One* **6**, e24650 (2011).
193. Baltgalvis, K. A. *et al.* Activity level, apoptosis, and development of cachexia in Apc(Min/+) mice. *J Appl Physiol (1985)* **109**, 1155–1161 (2010).
194. Smith, K. L. & Tisdale, M. J. Increased protein degradation and decreased protein synthesis in skeletal muscle during cancer cachexia. *Br J Cancer* **67**, 680–685 (1993).
195. Khal, J., Wyke, S. M., Russell, S. T., Hine, A. V. & Tisdale, M. J. Expression of the ubiquitin-proteasome pathway and muscle loss in experimental cancer cachexia. *Br J Cancer* **93**, 774–780 (2005).
196. Aversa, Z. *et al.* Autophagy is induced in the skeletal muscle of cachectic cancer patients. *Sci Rep* **6**, 30340 (2016).
197. DeJong, C. H. C. *et al.* Systemic inflammation correlates with increased expression of skeletal muscle ubiquitin but not uncoupling proteins in cancer cachexia. *Oncol Rep* **14**, 257–263 (2005).
198. Tardif, N., Klaude, M., Lundell, L., Thorell, A. & Rooyackers, O. Autophagic-lysosomal pathway is the main proteolytic system modified in the skeletal muscle of esophageal cancer patients. *Am J Clin Nutr* **98**, 1485–1492 (2013).
199. Lerner, L. *et al.* Plasma growth differentiation factor 15 is associated with weight loss and mortality in cancer patients. *J Cachexia Sarcopenia Muscle* **6**, 317–324 (2015).
200. Op den Kamp, C. M. *et al.* Preserved muscle oxidative metabolic phenotype in newly diagnosed non-small cell lung cancer cachexia. *J Cachexia Sarcopenia Muscle* **6**, 164–173 (2015).
201. Op den Kamp, C. M. *et al.* Nuclear transcription factor κ B activation and protein turnover adaptations in skeletal muscle of patients with progressive stages of lung cancer cachexia. *Am J Clin Nutr* **98**, 738–748 (2013).
202. Stephens, N. A. *et al.* Sexual dimorphism modulates the impact of cancer cachexia on lower limb muscle mass and function. *Clin Nutr* **31**, 499–505 (2012).
203. Weber, M.-A. *et al.* Myoglobin plasma level related to muscle mass and fiber composition: a clinical marker of muscle wasting? *J Mol Med (Berl)* **85**, 887–896 (2007).
204. Narasimhan, A., Greiner, R., Bathe, O. F., Baracos, V. & Damaraju, S. Differentially expressed alternatively spliced genes in skeletal muscle from cancer patients with cachexia. *J Cachexia Sarcopenia Muscle* **9**, 60–70 (2018).
205. Lee, J. *et al.* Longitudinal changes in skeletal muscle mass in patients with advanced squamous cell lung cancer. *Thorac Cancer* **12**, 1662–1667 (2021).
206. Loumaye, A. *et al.* Role of Activin A and myostatin in human cancer cachexia. *J Clin Endocrinol Metab* **100**, 2030–2038 (2015).
207. Zhang, Y. *et al.* The autophagic-lysosomal and ubiquitin proteasome systems are simultaneously activated in the skeletal muscle of gastric cancer patients with cachexia. *Am J Clin Nutr* **111**, 570–579 (2020).
208. Talbert, E. E., Metzger, G. A., He, W. A. & Guttridge, D. C. Modeling human cancer cachexia in colon 26 tumor-bearing adult mice. *J Cachexia Sarcopenia Muscle* **5**, 321–328 (2014).
209. Liu, D. *et al.* IMB0901 inhibits muscle atrophy induced by cancer cachexia through MSTN signaling pathway. *Skelet Muscle* **9**, 8 (2019).
210. Tseng, Y.-C. *et al.* Preclinical Investigation of the Novel Histone Deacetylase

Inhibitor AR-42 in the Treatment of Cancer-Induced Cachexia. *J Natl Cancer Inst* **107**, djv274 (2015).
211. Hall, D. T. *et al.* The AMPK agonist 5-aminoimidazole-4-carboxamide ribonucleotide (AICAR), but not metformin, prevents inflammation-associated cachectic muscle wasting. *EMBO Mol Med* **10**, e8307 (2018).
212. Zhang, G. *et al.* Tumor induces muscle wasting in mice through releasing extracellular Hsp70 and Hsp90. *Nat Commun* **8**, 589 (2017).
213. Penna, F. *et al.* Muscle atrophy in experimental cancer cachexia: is the IGF-1 signaling pathway involved? *Int J Cancer* **127**, 1706–1717 (2010).
214. Bohnert, K. R. *et al.* Inhibition of ER stress and unfolding protein response pathways causes skeletal muscle wasting during cancer cachexia. *FASEB J* **30**, 3053–3068 (2016).
215. Assi, M., Derbré, F., Lefeuvre-Orfila, L. & Rébillard, A. Antioxidant supplementation accelerates cachexia development by promoting tumor growth in C26 tumor-bearing mice. *Free Radic Biol Med* **91**, 204–214 (2016).
216. Hardee, J. P. *et al.* Eccentric contraction-induced myofiber growth in tumor-bearing mice. *J Appl Physiol (1985)* **120**, 29–37 (2016).
217. Padilha, C. S. *et al.* Resistance exercise attenuates skeletal muscle oxidative stress, systemic pro-inflammatory state, and cachexia in Walker-256 tumor-bearing rats. *Appl Physiol Nutr Metab* **42**, 916–923 (2017).
218. Antunes, D. *et al.* Molecular insights into mitochondrial dysfunction in cancer-related muscle wasting. *Biochim Biophys Acta* **1841**, 896–905 (2014).
219. Fontes-Oliveira, C. C. *et al.* Mitochondrial and sarcoplasmic reticulum abnormalities in cancer cachexia: altered energetic efficiency? *Biochim Biophys Acta* **1830**, 2770–2778 (2013).
220. Murphy, K. T., Struk, A., Malcontenti-Wilson, C., Christophi, C. & Lynch, G. S. Physiological characterization of a mouse model of cachexia in colorectal liver metastases. *Am J Physiol Regul Integr Comp Physiol* **304**, R854-864 (2013).
221. Roberts, B. M. *et al.* Diaphragm and ventilatory dysfunction during cancer cachexia. *FASEB J* **27**, 2600–2610 (2013).
222. Goncalves, M. D. *et al.* Fenofibrate prevents skeletal muscle loss in mice with lung cancer. *Proc Natl Acad Sci U S A* **115**, E743–E752 (2018).
223. Salazar-Degracia, A. *et al.* Effects of the beta2 agonist formoterol on atrophy signaling, autophagy, and muscle phenotype in respiratory and limb muscles of rats with cancer-induced cachexia. *Biochimie* **149**, 79–91 (2018).
224. Chacon-Cabrera, A. *et al.* Pharmacological strategies in lung cancer-induced cachexia: effects on muscle proteolysis, autophagy, structure, and weakness. *J Cell Physiol* **229**, 1660–1672 (2014).
225. Banduseela, V., Ochala, J., Lamberg, K., Kalimo, H. & Larsson, L. Muscle paralysis and myosin loss in a patient with cancer cachexia. *Acta Myol* **26**, 136–144 (2007).
226. Roberts, B. M., Frye, G. S., Ahn, B., Ferreira, L. F. & Judge, A. R. Cancer cachexia decreases specific force and accelerates fatigue in limb muscle. *Biochem Biophys Res Commun* **435**, 488–492 (2013).
227. Diffee, G. M., Kalfas, K., Al-Majid, S. & McCarthy, D. O. Altered expression of skeletal muscle myosin isoforms in cancer cachexia. *Am J Physiol Cell Physiol* **283**, C1376-1382 (2002).
228. Marin-Corral, J. *et al.* Redox balance and carbonylated proteins in limb and heart muscles of cachectic rats. *Antioxid Redox Signal* **12**, 365–380 (2010).
229. Chacon-Cabrera, A. *et al.* Role of PARP activity in lung cancer-induced cachexia: Effects on muscle oxidative stress, proteolysis, anabolic markers, and phenotype. *J Cell Physiol* **232**, 3744–3761 (2017).

230. Salazar-Degracia, A. *et al.* Phenotypic and metabolic features of mouse diaphragm and gastrocnemius muscles in chronic lung carcinogenesis: influence of underlying emphysema. *J Transl Med* **14**, 244 (2016).
231. Murphy, K. T. *et al.* Antibody-directed myostatin inhibition enhances muscle mass and function in tumor-bearing mice. *Am J Physiol Regul Integr Comp Physiol* **301**, R716-726 (2011).
232. Ham, D. J., Murphy, K. T., Chee, A., Lynch, G. S. & Koopman, R. Glycine administration attenuates skeletal muscle wasting in a mouse model of cancer cachexia. *Clin Nutr* **33**, 448–458 (2014).
233. Puig-Vilanova, E. *et al.* Oxidative stress, redox signaling pathways, and autophagy in cachectic muscles of male patients with advanced COPD and lung cancer. *Free Radic Biol Med* **79**, 91–108 (2015).
234. Schmitt, T. L. *et al.* Activity of the Akt-dependent anabolic and catabolic pathways in muscle and liver samples in cancer-related cachexia. *J Mol Med (Berl)* **85**, 647–654 (2007).
235. Taskin, S. *et al.* Motor protein function in skeletal abdominal muscle of cachectic cancer patients. *J Cell Mol Med* **18**, 69–79 (2014).
236. Choi, E. *et al.* Concurrent muscle and bone deterioration in a murine model of cancer cachexia. *Physiol Rep* **1**, e00144 (2013).
237. Winbanks, C. E. *et al.* Smad7 gene delivery prevents muscle wasting associated with cancer cachexia in mice. *Sci Transl Med* **8**, 348ra98 (2016).
238. Puppa, M. J., Murphy, E. A., Fayad, R., Hand, G. A. & Carson, J. A. Cachectic skeletal muscle response to a novel bout of low-frequency stimulation. *J Appl Physiol (1985)* **116**, 1078–1087 (2014).
239. Bonetto, A. *et al.* Deacetylase inhibitors modulate the myostatin/follistatin axis without improving cachexia in tumor-bearing mice. *Curr Cancer Drug Targets* **9**, 608–616 (2009).
240. Shakri, A. R. *et al.* Upregulation of ZIP14 and Altered Zinc Homeostasis in Muscles in Pancreatic Cancer Cachexia. *Cancers (Basel)* **12**, E3 (2019).
241. Zhuang, P. *et al.* Reversal of muscle atrophy by Zhimu and Huangbai herb pair via activation of IGF-1/Akt and autophagy signal in cancer cachexia. *Support Care Cancer* **24**, 1189–1198 (2016).
242. Wang, G. *et al.* Metastatic cancers promote cachexia through ZIP14 upregulation in skeletal muscle. *Nat Med* **24**, 770–781 (2018).
243. Pin, F. *et al.* Combination of exercise training and erythropoietin prevents cancer-induced muscle alterations. *Oncotarget* **6**, 43202–43215 (2015).
244. Fermoselle, C. *et al.* Mitochondrial dysfunction and therapeutic approaches in respiratory and limb muscles of cancer cachectic mice: Mitochondrial respiratory chain dysfunction in cachexia. *Experimental Physiology* **98**, 1349–1365 (2013).
245. Penna, F. *et al.* Autophagy Exacerbates Muscle Wasting in Cancer Cachexia and Impairs Mitochondrial Function. *J Mol Biol* **431**, 2674–2686 (2019).
246. Toledo, M. *et al.* Complete reversal of muscle wasting in experimental cancer cachexia: Additive effects of activin type II receptor inhibition and β-2 agonist. *Int J Cancer* **138**, 2021–2029 (2016).
247. Bae, T. *et al.* Paeonia lactiflora root extract suppresses cancer cachexia by down-regulating muscular NF-κB signalling and muscle-specific E3 ubiquitin ligases in cancer-bearing mice. *J Ethnopharmacol* **246**, 112222 (2020).
248. Busquets, S. *et al.* Formoterol and cancer muscle wasting in rats: Effects on muscle force and total physical activity. *Exp Ther Med* **2**, 731–735 (2011).
249. Busquets, S. *et al.* Myostatin blockage using actRIIB antagonism in mice bearing the Lewis lung carcinoma results in the improvement of muscle wasting and physical

performance. *J Cachexia Sarcopenia Muscle* **3**, 37–43 (2012).
250. Levolger, S. *et al.* Inhibition of activin-like kinase 4/5 attenuates cancer cachexia associated muscle wasting. *Sci Rep* **9**, 9826 (2019).
251. Parajuli, P. *et al.* Twist1 Activation in Muscle Progenitor Cells Causes Muscle Loss Akin to Cancer Cachexia. *Dev Cell* **45**, 712-725.e6 (2018).
252. Penna, F., Busquets, S. & Argilés, J. M. Experimental cancer cachexia: Evolving strategies for getting closer to the human scenario. *Semin Cell Dev Biol* **54**, 20–27 (2016).
253. Kir, S. *et al.* PTH/PTHrP Receptor Mediates Cachexia in Models of Kidney Failure and Cancer. *Cell Metab* **23**, 315–323 (2016).
254. Counts, B. R. *et al.* Cachexia Disrupts Diurnal Regulation of Activity, Feeding, and Muscle Mechanistic Target of Rapamycin Complex 1 in Mice. *Med Sci Sports Exerc* **52**, 577–587 (2020).
255. Maddocks, M. *et al.* Physical activity level as an outcome measure for use in cancer cachexia trials: a feasibility study. *Support Care Cancer* **18**, 1539–1544 (2010).
256. Boehm, I. *et al.* Neuromuscular junctions are stable in patients with cancer cachexia. *J Clin Invest* **130**, 1461–1465 (2020).
257. Daou, N. *et al.* Displaced Myonuclei in Cancer Cachexia Suggest Altered Innervation. *Int J Mol Sci* **21**, E1092 (2020).
258. Sartori, R. *et al.* Perturbed BMP signaling and denervation promote muscle wasting in cancer cachexia. *Sci Transl Med* **13**, eaay9592 (2021).
259. He, W. A. *et al.* NF-κB-mediated Pax7 dysregulation in the muscle microenvironment promotes cancer cachexia. *J Clin Invest* **123**, 4821–4835 (2013).
260. Acharyya, S. *et al.* Dystrophin glycoprotein complex dysfunction: a regulatory link between muscular dystrophy and cancer cachexia. *Cancer Cell* **8**, 421–432 (2005).
261. Judge, S. M. *et al.* Skeletal Muscle Fibrosis in Pancreatic Cancer Patients with Respect to Survival. *JNCI Cancer Spectr* **2**, pky043 (2018).
262. Bossola, M., Marzetti, E., Rosa, F. & Pacelli, F. Skeletal muscle regeneration in cancer cachexia. *Clin Exp Pharmacol Physiol* **43**, 522–527 (2016).
263. Shum, A. M. Y. *et al.* Disruption of MEF2C signaling and loss of sarcomeric and mitochondrial integrity in cancer-induced skeletal muscle wasting. *Aging (Albany NY)* **4**, 133–143 (2012).
264. Tzika, A. A. *et al.* Skeletal muscle mitochondrial uncoupling in a murine cancer cachexia model. *Int J Oncol* **43**, 886–894 (2013).
265. Shum, A. M. Y. *et al.* Proteomic profiling of skeletal and cardiac muscle in cancer cachexia: alterations in sarcomeric and mitochondrial protein expression. *Oncotarget* **9**, 22001–22022 (2018).
266. Toth, M. J. *et al.* Molecular mechanisms underlying skeletal muscle weakness in human cancer: reduced myosin-actin cross-bridge formation and kinetics. *J Appl Physiol (1985)* **114**, 858–868 (2013).
267. Marin, O. S. & Denny-Brown, D. Changes in skeletal muscle associated with cachexia. *Am J Pathol* **41**, 23–39 (1962).
268. Mendell, J. R. & Engel, W. K. The fine structure of type II muscle fiber atrophy. *Neurology* **21**, 358–365 (1971).
269. Fontes-Oliveira, C. C. *et al.* A differential pattern of gene expression in skeletal muscle of tumor-bearing rats reveals dysregulation of excitation–contraction coupling together with additional muscle alterations. *Muscle Nerve* **49**, 233–248 (2014).
270. Gissel, H. The role of Ca2+ in muscle cell damage. *Ann N Y Acad Sci* **1066**, 166–180 (2005).
271. Rossi, A. E., Boncompagni, S. & Dirksen, R. T. Sarcoplasmic reticulum-mitochondrial symbiosis: bidirectional signaling in skeletal muscle. *Exerc Sport Sci Rev* **37**,

29–35 (2009).
272. de Castro, G. S. *et al.* Human Cachexia Induces Changes in Mitochondria, Autophagy and Apoptosis in the Skeletal Muscle. *Cancers (Basel)* **11**, E1264 (2019).
273. White, J. P. *et al.* IL-6 regulation on skeletal muscle mitochondrial remodeling during cancer cachexia in the ApcMin/+ mouse. *Skelet Muscle* **2**, 14 (2012).
274. Constantinou, C. *et al.* Nuclear magnetic resonance in conjunction with functional genomics suggests mitochondrial dysfunction in a murine model of cancer cachexia. *Int J Mol Med* **27**, 15–24 (2011).
275. VanderVeen, B. N., Fix, D. K. & Carson, J. A. Disrupted Skeletal Muscle Mitochondrial Dynamics, Mitophagy, and Biogenesis during Cancer Cachexia: A Role for Inflammation. *Oxid Med Cell Longev* **2017**, 3292087 (2017).
276. Neyroud, D., Nosacka, R. L., Judge, A. R. & Hepple, R. T. Colon 26 adenocarcinoma (C26)-induced cancer cachexia impairs skeletal muscle mitochondrial function and content. *J Muscle Res Cell Motil* **40**, 59–65 (2019).
277. Brown, J. L. *et al.* Mitochondrial degeneration precedes the development of muscle atrophy in progression of cancer cachexia in tumour-bearing mice. *J Cachexia Sarcopenia Muscle* **8**, 926–938 (2017).
278. Malva, A. della *et al.* Methods for Extraction of Muscle Proteins from Meat and Fish Using Denaturing and Nondenaturing Solutions. *Journal of Food Quality* **2018**, 1–9 (2018).
279. Giordano, A. *et al.* Skeletal muscle metabolism in physiology and in cancer disease. *J Cell Biochem* **90**, 170–186 (2003).
280. Dworzak, F., Ferrari, P., Gavazzi, C., Maiorana, C. & Bozzetti, F. Effects of cachexia due to cancer on whole body and skeletal muscle protein turnover. *Cancer* **82**, 42–48 (1998).
281. Acharyya, S. *et al.* Cancer cachexia is regulated by selective targeting of skeletal muscle gene products. *J Clin Invest* **114**, 370–378 (2004).
282. Tisdale, M. J. Loss of skeletal muscle in cancer: biochemical mechanisms. *Front Biosci* **6**, D164-174 (2001).
283. Eley, H. L., Skipworth, R. J. E., Deans, D. a. C., Fearon, K. C. H. & Tisdale, M. J. Increased expression of phosphorylated forms of RNA-dependent protein kinase and eukaryotic initiation factor 2alpha may signal skeletal muscle atrophy in weight-losing cancer patients. *Br J Cancer* **98**, 443–449 (2008).
284. Cohen, S., Nathan, J. A. & Goldberg, A. L. Muscle wasting in disease: molecular mechanisms and promising therapies. *Nat Rev Drug Discov* **14**, 58–74 (2015).
285. Lecker, S. H., Solomon, V., Mitch, W. E. & Goldberg, A. L. Muscle protein breakdown and the critical role of the ubiquitin-proteasome pathway in normal and disease states. *J Nutr* **129**, 227S-237S (1999).
286. Rock, K. L. *et al.* Inhibitors of the proteasome block the degradation of most cell proteins and the generation of peptides presented on MHC class I molecules. *Cell* **78**, 761–771 (1994).
287. Hershko, A. & Ciechanover, A. The ubiquitin system. *Annu Rev Biochem* **67**, 425–479 (1998).
288. Hershko, A. & Ciechanover, A. Mechanisms of intracellular protein breakdown. *Annu Rev Biochem* **51**, 335–364 (1982).
289. Haas, A. L. & Rose, I. A. The mechanism of ubiquitin activating enzyme. A kinetic and equilibrium analysis. *J Biol Chem* **257**, 10329–10337 (1982).
290. Hershko, A., Heller, H., Elias, S. & Ciechanover, A. Components of ubiquitin-protein ligase system. Resolution, affinity purification, and role in protein breakdown. *J Biol Chem* **258**, 8206–8214 (1983).
291. Hershko, A. The ubiquitin pathway for protein degradation. *Trends Biochem Sci* **16**, 265–268 (1991).

292. Voges, D., Zwickl, P. & Baumeister, W. The 26S proteasome: a molecular machine designed for controlled proteolysis. *Annu Rev Biochem* **68**, 1015–1068 (1999).
293. Rom, O. & Reznick, A. Z. The role of E3 ubiquitin-ligases MuRF-1 and MAFbx in loss of skeletal muscle mass. *Free Radic Biol Med* **98**, 218–230 (2016).
294. Kwak, K. S. *et al.* Regulation of protein catabolism by muscle-specific and cytokine-inducible ubiquitin ligase E3alpha-II during cancer cachexia. *Cancer Res* **64**, 8193–8198 (2004).
295. Yuan, L. *et al.* Muscle-specific E3 ubiquitin ligases are involved in muscle atrophy of cancer cachexia: an in vitro and in vivo study. *Oncol Rep* **33**, 2261–2268 (2015).
296. Doss, H. M., Kim, J. Y. & Kim, K. S. Taurine Supplementation Inhibits the Expression of Atrogin-1 and MURF-1, Protein Degradation Marker Genes, in Skeletal Muscle of C26-Induced Cachexia Mouse Model. *Adv Exp Med Biol* **1370**, 129–136 (2022).
297. Henderson, S. E. *et al.* Suppression of Tumor Growth and Muscle Wasting in a Transgenic Mouse Model of Pancreatic Cancer by the Novel Histone Deacetylase Inhibitor AR-42. *Neoplasia* **18**, 765–774 (2016).
298. Greco, S. H. *et al.* TGF-β Blockade Reduces Mortality and Metabolic Changes in a Validated Murine Model of Pancreatic Cancer Cachexia. *PLoS One* **10**, e0132786 (2015).
299. Penedo-Vázquez, A., Duran, X., Mateu, J., López-Postigo, A. & Barreiro, E. Curcumin and Resveratrol Improve Muscle Function and Structure through Attenuation of Proteolytic Markers in Experimental Cancer-Induced Cachexia. *Molecules* **26**, 4904 (2021).
300. Llovera, M. *et al.* Protein turnover in skeletal muscle of tumour-bearing transgenic mice overexpressing the soluble TNF receptor-1. *Cancer Lett* **130**, 19–27 (1998).
301. Fujita, J. *et al.* Anti-interleukin-6 receptor antibody prevents muscle atrophy in colon-26 adenocarcinoma-bearing mice with modulation of lysosomal and ATP-ubiquitin-dependent proteolytic pathways. *Int J Cancer* **68**, 637–643 (1996).
302. Attaix, D., Combaret, L., Tilignac, T. & Taillandier, D. Adaptation of the ubiquitin-proteasome proteolytic pathway in cancer cachexia. *Mol Biol Rep* **26**, 77–82 (1999).
303. Lazarus, D. D. *et al.* A new model of cancer cachexia: contribution of the ubiquitin-proteasome pathway. *Am J Physiol* **277**, E332-341 (1999).
304. Op den Kamp, C. M. *et al.* Pre-cachexia in patients with stages I-III non-small cell lung cancer: systemic inflammation and functional impairment without activation of skeletal muscle ubiquitin proteasome system. *Lung Cancer* **76**, 112–117 (2012).
305. Stephens, N. A. *et al.* Using transcriptomics to identify and validate novel biomarkers of human skeletal muscle cancer cachexia. *Genome Med* **2**, 1 (2010).
306. Bossola, M. *et al.* Increased muscle ubiquitin mRNA levels in gastric cancer patients. *Am J Physiol Regul Integr Comp Physiol* **280**, R1518-1523 (2001).
307. Bossola, M. *et al.* Increased muscle proteasome activity correlates with disease severity in gastric cancer patients. *Ann Surg* **237**, 384–389 (2003).
308. Williams, A., Sun, X., Fischer, J. E. & Hasselgren, P. O. The expression of genes in the ubiquitin-proteasome proteolytic pathway is increased in skeletal muscle from patients with cancer. *Surgery* **126**, 744–749; discussion 749-750 (1999).
309. Glick, D., Barth, S. & Macleod, K. F. Autophagy: cellular and molecular mechanisms. *J Pathol* **221**, 3–12 (2010).
310. Masiero, E. *et al.* Autophagy is required to maintain muscle mass. *Cell Metab* **10**, 507–515 (2009).
311. Bonaldo, P. & Sandri, M. Cellular and molecular mechanisms of muscle atrophy. *Dis Model Mech* **6**, 25–39 (2013).
312. Penna, F., Baccino, F. M. & Costelli, P. Coming back: autophagy in cachexia. *Curr Opin Clin Nutr Metab Care* **17**, 241–246 (2014).
313. Funderburk, S. F., Wang, Q. J. & Yue, Z. The Beclin 1-VPS34 complex--at the

crossroads of autophagy and beyond. *Trends Cell Biol* **20**, 355–362 (2010).
314. Tanida, I., Ueno, T. & Kominami, E. LC3 and Autophagy. *Methods Mol Biol* **445**, 77–88 (2008).
315. Singh, R. Hypothalamic lipophagy and energetic balance. *Aging (Albany NY)* **3**, 934–942 (2011).
316. Pigna, E. *et al.* Aerobic Exercise and Pharmacological Treatments Counteract Cachexia by Modulating Autophagy in Colon Cancer. *Sci Rep* **6**, 26991 (2016).
317. Asp, M. L., Tian, M., Wendel, A. A. & Belury, M. A. Evidence for the contribution of insulin resistance to the development of cachexia in tumor-bearing mice. *Int J Cancer* **126**, 756–763 (2010).
318. Lokireddy, S. *et al.* 1) Myostatin is a novel tumoral factor that induces cancer cachexia. *Biochem J* **466**, 201 (2015).
319. Penna, F. *et al.* Autophagic degradation contributes to muscle wasting in cancer cachexia. *Am J Pathol* **182**, 1367–1378 (2013).
320. Stephens, N. A. *et al.* Evaluating potential biomarkers of cachexia and survival in skeletal muscle of upper gastrointestinal cancer patients. *J Cachexia Sarcopenia Muscle* **6**, 53–61 (2015).
321. Bennani-Baiti, N. & Walsh, D. Animal models of the cancer anorexia-cachexia syndrome. *Support Care Cancer* **19**, 1451–1463 (2011).
322. Dj, G. PI3 kinase regulation of skeletal muscle hypertrophy and atrophy. *Current topics in microbiology and immunology* **346**, (2010).
323. Calnan, D. R. & Brunet, A. The FoxO code. *Oncogene* **27**, 2276–2288 (2008).
324. Sandri, M. *et al.* Foxo transcription factors induce the atrophy-related ubiquitin ligase atrogin-1 and cause skeletal muscle atrophy. *Cell* **117**, 399–412 (2004).
325. Latres, E. *et al.* Insulin-like growth factor-1 (IGF-1) inversely regulates atrophy-induced genes via the phosphatidylinositol 3-kinase/Akt/mammalian target of rapamycin (PI3K/Akt/mTOR) pathway. *J Biol Chem* **280**, 2737–2744 (2005).
326. Zhao, J. *et al.* FoxO3 coordinately activates protein degradation by the autophagic/lysosomal and proteasomal pathways in atrophying muscle cells. *Cell Metab* **6**, 472–483 (2007).
327. Mammucari, C. *et al.* FoxO3 controls autophagy in skeletal muscle in vivo. *Cell Metab* **6**, 458–471 (2007).
328. Castets, P. *et al.* Sustained activation of mTORC1 in skeletal muscle inhibits constitutive and starvation-induced autophagy and causes a severe, late-onset myopathy. *Cell Metab* **17**, 731–744 (2013).
329. Short-term pyrrolidine dithiocarbamate administration attenuates cachexia-induced alterations to muscle and liver in ApcMin/+ mice - PubMed. https://pubmed.ncbi.nlm.nih.gov/27449092/.
330. Lopes, M. N., Black, P., Ashford, A. J. & Pain, V. M. Protein metabolism in the tumour-bearing mouse. Rates of protein synthesis in host tissues and in an Ehrlich ascites tumour at different stages in tumour growth. *Biochem J* **264**, 713–719 (1989).
331. White, J. P. *et al.* Muscle mTORC1 suppression by IL-6 during cancer cachexia: a role for AMPK. *Am J Physiol Endocrinol Metab* **304**, E1042-1052 (2013).
332. Emery, P. W., Edwards, R. H., Rennie, M. J., Souhami, R. L. & Halliday, D. Protein synthesis in muscle measured in vivo in cachectic patients with cancer. *Br Med J (Clin Res Ed)* **289**, 584–586 (1984).
333. Tisdale, M. J. Cachexia in cancer patients. *Nat Rev Cancer* **2**, 862–871 (2002).
334. MacDonald, A. J. *et al.* Habitual Myofibrillar Protein Synthesis Is Normal in Patients with Upper GI Cancer Cachexia. *Clin Cancer Res* **21**, 1734–1740 (2015).
335. Combaret, L., Rallière, C., Taillandier, D., Tanaka, K. & Attaix, D. Manipulation of

the ubiquitin-proteasome pathway in cachexia: pentoxifylline suppresses the activation of 20S and 26S proteasomes in muscles from tumor-bearing rats. *Mol Biol Rep* **26**, 95–101 (1999).
336. Emery, P. W., Lovell, L. & Rennie, M. J. Protein synthesis measured in vivo in muscle and liver of cachectic tumor-bearing mice. *Cancer Res* **44**, 2779–2784 (1984).
337. Rennie, M. J. *et al.* Depressed protein synthesis is the dominant characteristic of muscle wasting and cachexia. *Clin Physiol* **3**, 387–398 (1983).
338. Egerman, M. A. & Glass, D. J. Signaling pathways controlling skeletal muscle mass. *Crit Rev Biochem Mol Biol* **49**, 59–68 (2014).
339. Argilés, J. M., Busquets, S., Toledo, M. & López-Soriano, F. J. The role of cytokines in cancer cachexia. *Curr Opin Support Palliat Care* **3**, 263–268 (2009).
340. Ta, Z., Ml, F. & A, B. STAT3 in the systemic inflammation of cancer cachexia. *Seminars in cell & developmental biology* **54**, (2016).
341. Llovera, M. *et al.* Role of TNF receptor 1 in protein turnover during cancer cachexia using gene knockout mice. *Mol Cell Endocrinol* **142**, 183–189 (1998).
342. Li, Y. P., Schwartz, R. J., Waddell, I. D., Holloway, B. R. & Reid, M. B. Skeletal muscle myocytes undergo protein loss and reactive oxygen-mediated NF-kappaB activation in response to tumor necrosis factor alpha. *FASEB J* **12**, 871–880 (1998).
343. Cai, D. *et al.* IKKbeta/NF-kappaB activation causes severe muscle wasting in mice. *Cell* **119**, 285–298 (2004).
344. Gomes, M. D., Lecker, S. H., Jagoe, R. T., Navon, A. & Goldberg, A. L. Atrogin-1, a muscle-specific F-box protein highly expressed during muscle atrophy. *Proc Natl Acad Sci U S A* **98**, 14440–14445 (2001).
345. Llovera, M., García-Martínez, C., Agell, N., López-Soriano, F. J. & Argilés, J. M. TNF can directly induce the expression of ubiquitin-dependent proteolytic system in rat soleus muscles. *Biochem Biophys Res Commun* **230**, 238–241 (1997).
346. DeBoer, M. D. *et al.* Increases in IGF-1 After Anti-TNF-α Therapy Are Associated With Bone and Muscle Accrual in Pediatric Crohn Disease. *J Clin Endocrinol Metab* **103**, 936–945 (2018).
347. Anwar, A., Zahid, A. A., Scheidegger, K. J., Brink, M. & Delafontaine, P. Tumor necrosis factor-alpha regulates insulin-like growth factor-1 and insulin-like growth factor binding protein-3 expression in vascular smooth muscle. *Circulation* **105**, 1220–1225 (2002).
348. Moore-Carrasco, R. *et al.* The AP-1/NF-kappaB double inhibitor SP100030 can revert muscle wasting during experimental cancer cachexia. *Int J Oncol* **30**, 1239–1245 (2007).
349. Mittal, A. *et al.* The TWEAK-Fn14 system is a critical regulator of denervation-induced skeletal muscle atrophy in mice. *J Cell Biol* **188**, 833–849 (2010).
350. Sato, S., Ogura, Y., Tajrishi, M. M. & Kumar, A. Elevated levels of TWEAK in skeletal muscle promote visceral obesity, insulin resistance, and metabolic dysfunction. *FASEB J* **29**, 988–1002 (2015).
351. Johnston, A. J. *et al.* Targeting of Fn14 Prevents Cancer-Induced Cachexia and Prolongs Survival. *Cell* **162**, 1365–1378 (2015).
352. Kumari, N., Dwarakanath, B. S., Das, A. & Bhatt, A. N. Role of interleukin-6 in cancer progression and therapeutic resistance. *Tumour Biol* **37**, 11553–11572 (2016).
353. Nozawa, H., Chiu, C. & Hanahan, D. Infiltrating neutrophils mediate the initial angiogenic switch in a mouse model of multistage carcinogenesis. *Proc Natl Acad Sci U S A* **103**, 12493–12498 (2006).
354. Nagasaki, T. *et al.* Interleukin-6 released by colon cancer-associated fibroblasts is critical for tumour angiogenesis: anti-interleukin-6 receptor antibody suppressed angiogenesis and inhibited tumour-stroma interaction. *Br J Cancer* **110**, 469–478 (2014).
355. Bournazou, E. & Bromberg, J. Targeting the tumor microenvironment: JAK-STAT3 signaling. *JAKSTAT* **2**, e23828 (2013).

356. McCart, A. E., Vickaryous, N. K. & Silver, A. Apc mice: models, modifiers and mutants. *Pathol Res Pract* **204**, 479–490 (2008).
357. Strassmann, G., Fong, M., Kenney, J. S. & Jacob, C. O. Evidence for the involvement of interleukin 6 in experimental cancer cachexia. *J Clin Invest* **89**, 1681–1684 (1992).
358. Soda, K., Kawakami, M., Kashii, A. & Miyata, M. Manifestations of cancer cachexia induced by colon 26 adenocarcinoma are not fully ascribable to interleukin-6. *Int J Cancer* **62**, 332–336 (1995).
359. G, S. *et al.* Suramin interferes with interleukin-6 receptor binding in vitro and inhibits colon-26-mediated experimental cancer cachexia in vivo. *The Journal of clinical investigation* **92**, (1993).
360. Tamura, S. *et al.* Involvement of human interleukin 6 in experimental cachexia induced by a human uterine cervical carcinoma xenograft. *Clin Cancer Res* **1**, 1353–1358 (1995).
361. Ando, K. *et al.* Possible role for tocilizumab, an anti-interleukin-6 receptor antibody, in treating cancer cachexia. *J Clin Oncol* **31**, e69-72 (2013).
362. Ando, K. *et al.* Tocilizumab, a proposed therapy for the cachexia of Interleukin6-expressing lung cancer. *PLoS One* **9**, e102436 (2014).
363. Ohe, Y. *et al.* Interleukin-6 cDNA transfected Lewis lung carcinoma cells show unaltered net tumour growth rate but cause weight loss and shortened survival in syngeneic mice. *Br J Cancer* **67**, 939–944 (1993).
364. Zhang, L. *et al.* Stat3 activation links a C/EBPδ to myostatin pathway to stimulate loss of muscle mass. *Cell Metab* **18**, 368–379 (2013).
365. Silva, K. A. S. *et al.* Inhibition of Stat3 activation suppresses caspase-3 and the ubiquitin-proteasome system, leading to preservation of muscle mass in cancer cachexia. *J Biol Chem* **290**, 11177–11187 (2015).
366. Eskiler, G. G. *et al.* IL-6 mediated JAK/STAT3 signaling pathway in cancer patients with cachexia. *Bratisl Lek Listy* **66**, 819–826 (2019).
367. Bonetto, A. *et al.* JAK/STAT3 pathway inhibition blocks skeletal muscle wasting downstream of IL-6 and in experimental cancer cachexia. *Am J Physiol Endocrinol Metab* **303**, E410-421 (2012).
368. Bonetto, A. *et al.* STAT3 activation in skeletal muscle links muscle wasting and the acute phase response in cancer cachexia. *PLoS One* **6**, e22538 (2011).
369. Kandarian, S. C. *et al.* Tumour-derived leukaemia inhibitory factor is a major driver of cancer cachexia and morbidity in C26 tumour-bearing mice. *J Cachexia Sarcopenia Muscle* **9**, 1109–1120 (2018).
370. Seto, D. N., Kandarian, S. C. & Jackman, R. W. A Key Role for Leukemia Inhibitory Factor in C26 Cancer Cachexia. *J Biol Chem* **290**, 19976–19986 (2015).
371. Gelfo, V. *et al.* Roles of IL-1 in Cancer: From Tumor Progression to Resistance to Targeted Therapies. *Int J Mol Sci* **21**, E6009 (2020).
372. Huang, N. *et al.* Deletion of Nlrp3 protects from inflammation-induced skeletal muscle atrophy. *Intensive Care Med Exp* **5**, 3 (2017).
373. Brigelius-Flohé, R., Banning, A., Kny, M. & Böl, G.-F. Redox events in interleukin-1 signaling. *Arch Biochem Biophys* **423**, 66–73 (2004).
374. Central nervous system inflammation induces muscle atrophy via activation of the hypothalamic-pituitary-adrenal axis - PubMed. https://pubmed.ncbi.nlm.nih.gov/22084407/.
375. Cannon, T. *et al.* Immunocompetent murine model of cancer cachexia for head and neck squamous cell carcinoma. *Head Neck* **30**, 320–326 (2008).
376. Dobierzewska, A., Shi, L., Karakashian, A. A. & Nikolova-Karakashian, M. N. Interleukin 1β regulation of FoxO1 protein content and localization: evidence for a novel ceramide-dependent mechanism. *J Biol Chem* **287**, 44749–44760 (2012).

377. Effect of central administration of interleukin-1 receptor antagonist on protein synthesis in skeletal muscle, kidney, and liver during sepsis - PubMed. https://pubmed.ncbi.nlm.nih.gov/14506630/.
378. Burfeind, K. G., Michaelis, K. A. & Marks, D. L. The central role of hypothalamic inflammation in the acute illness response and cachexia. *Semin Cell Dev Biol* **54**, 42–52 (2016).
379. Ikushima, H. & Miyazono, K. TGFbeta signalling: a complex web in cancer progression. *Nat Rev Cancer* **10**, 415–424 (2010).
380. Johnen, H. *et al.* Tumor-induced anorexia and weight loss are mediated by the TGF-beta superfamily cytokine MIC-1. *Nat Med* **13**, 1333–1340 (2007).
381. Penafuerte, C. A. *et al.* Identification of neutrophil-derived proteases and angiotensin II as biomarkers of cancer cachexia. *Br J Cancer* **114**, 680–687 (2016).
382. Tobin, J. F. & Celeste, A. J. Myostatin, a negative regulator of muscle mass: implications for muscle degenerative diseases. *Curr Opin Pharmacol* **5**, 328–332 (2005).
383. Latres, E. *et al.* Activin A more prominently regulates muscle mass in primates than does GDF8. *Nat Commun* **8**, 15153 (2017).
384. Mathews, L. S. & Vale, W. W. Expression cloning of an activin receptor, a predicted transmembrane serine kinase. *Cell* **65**, 973–982 (1991).
385. Attisano, L., Wrana, J. L., Cheifetz, S. & Massagué, J. Novel activin receptors: distinct genes and alternative mRNA splicing generate a repertoire of serine/threonine kinase receptors. *Cell* **68**, 97–108 (1992).
386. Oh, S. P. & Li, E. The signaling pathway mediated by the type IIB activin receptor controls axial patterning and lateral asymmetry in the mouse. *Genes Dev* **11**, 1812–1826 (1997).
387. Lodberg, A. Principles of the activin receptor signaling pathway and its inhibition. *Cytokine Growth Factor Rev* **60**, 1–17 (2021).
388. El Shafey, N. *et al.* Inhibition of the myostatin/Smad signaling pathway by short decorin-derived peptides. *Exp Cell Res* **341**, 187–195 (2016).
389. Trendelenburg, A. U. *et al.* Myostatin reduces Akt/TORC1/p70S6K signaling, inhibiting myoblast differentiation and myotube size. *Am J Physiol Cell Physiol* **296**, C1258-1270 (2009).
390. Amirouche, A. *et al.* Down-regulation of Akt/mammalian target of rapamycin signaling pathway in response to myostatin overexpression in skeletal muscle. *Endocrinology* **150**, 286–294 (2009).
391. Chen, J. L. *et al.* Elevated expression of activins promotes muscle wasting and cachexia. *FASEB J* **28**, 1711–1723 (2014).
392. InACTIVatINg cancer cachexia - PubMed. https://pubmed.ncbi.nlm.nih.gov/21372048/.
393. Tisdale, M. J. Reversing cachexia. *Cell* **142**, 511–512 (2010).
394. E, B. *et al.* Activin A in Mammalian Physiology. *Physiological reviews* **99**, (2019).
395. Pettersen, K. *et al.* Autocrine activin A signalling in ovarian cancer cells regulates secretion of interleukin 6, autophagy, and cachexia. *J Cachexia Sarcopenia Muscle* **11**, 195–207 (2020).
396. Harada, K. *et al.* Serum immunoreactive activin A levels in normal subjects and patients with various diseases. *J Clin Endocrinol Metab* **81**, 2125–2130 (1996).
397. Leto, G. *et al.* Activin A circulating levels in patients with bone metastasis from breast or prostate cancer. *Clin Exp Metastasis* **23**, 117–122 (2006).
398. Lee, S.-J. Regulation of muscle mass by myostatin. *Annu Rev Cell Dev Biol* **20**, 61–86 (2004).
399. Schuelke, M. *et al.* Myostatin mutation associated with gross muscle hypertrophy in a

child. *N Engl J Med* **350**, 2682–2688 (2004).
400. Mosher, D. S. *et al.* A mutation in the myostatin gene increases muscle mass and enhances racing performance in heterozygote dogs. *PLoS Genet* **3**, e79 (2007).
401. George, I. *et al.* Myostatin activation in patients with advanced heart failure and after mechanical unloading. *Eur J Heart Fail* **12**, 444–453 (2010).
402. Padrão, A. I. *et al.* Bladder cancer-induced skeletal muscle wasting: disclosing the role of mitochondria plasticity. *Int J Biochem Cell Biol* **45**, 1399–1409 (2013).
403. Gallot, Y. S. *et al.* Myostatin gene inactivation prevents skeletal muscle wasting in cancer. *Cancer Res* **74**, 7344–7356 (2014).
404. Benny Klimek, M. E. *et al.* Acute inhibition of myostatin-family proteins preserves skeletal muscle in mouse models of cancer cachexia. *Biochem Biophys Res Commun* **391**, 1548–1554 (2010).
405. Smith, R. C. *et al.* Myostatin Neutralization Results in Preservation of Muscle Mass and Strength in Preclinical Models of Tumor-Induced Muscle Wasting. *Mol Cancer Ther* **14**, 1661–1670 (2015).
406. Waning, D. L. *et al.* Excess TGF-β mediates muscle weakness associated with bone metastases in mice. *Nat Med* **21**, 1262–1271 (2015).
407. Snezhkina, A. V. *et al.* ROS Generation and Antioxidant Defense Systems in Normal and Malignant Cells. *Oxid Med Cell Longev* **2019**, 6175804 (2019).
408. Bedard, K. & Krause, K.-H. The NOX family of ROS-generating NADPH oxidases: physiology and pathophysiology. *Physiol Rev* **87**, 245–313 (2007).
409. Powers, S. K., Morton, A. B., Ahn, B. & Smuder, A. J. Redox control of skeletal muscle atrophy. *Free Radic Biol Med* **98**, 208–217 (2016).
410. Powers, S. K., DeCramer, M., Gayan-Ramirez, G. & Levine, S. Pressure support ventilation attenuates ventilator-induced protein modifications in the diaphragm. *Crit Care* **12**, 191 (2008).
411. Mastrocola, R. *et al.* Muscle wasting in diabetic and in tumor-bearing rats: role of oxidative stress. *Free Radic Biol Med* **44**, 584–593 (2008).
412. Sullivan-Gunn, M. J., Campbell-O'Sullivan, S. P., Tisdale, M. J. & Lewandowski, P. A. Decreased NADPH oxidase expression and antioxidant activity in cachectic skeletal muscle. *J Cachexia Sarcopenia Muscle* **2**, 181–188 (2011).
413. Gomes-Marcondes, M. C. C. & Tisdale, M. J. Induction of protein catabolism and the ubiquitin-proteasome pathway by mild oxidative stress. *Cancer Lett* **180**, 69–74 (2002).
414. Ballarò, R. *et al.* Moderate Exercise Improves Experimental Cancer Cachexia by Modulating the Redox Homeostasis. *Cancers (Basel)* **11**, E285 (2019).
415. Derbré, F. *et al.* Antioxidants and muscle atrophy in colon cancer: beneficial or deleterious effects? *Free Radic Biol Med* **75 Suppl 1**, S22 (2014).
416. Barreiro, E. *et al.* Both oxidative and nitrosative stress are associated with muscle wasting in tumour-bearing rats. *FEBS Lett* **579**, 1646–1652 (2005).
417. T, X. *et al.* Pyrroloquinoline quinone attenuates cachexia-induced muscle atrophy via suppression of reactive oxygen species. *Journal of thoracic disease* **10**, (2018).
418. Gelin, J. *et al.* Role of endogenous tumor necrosis factor alpha and interleukin 1 for experimental tumor growth and the development of cancer cachexia. *Cancer Res* **51**, 415–421 (1991).
419. Mantovani, G. *et al.* Cytokine activity in cancer-related anorexia/cachexia: role of megestrol acetate and medroxyprogesterone acetate. *Semin Oncol* **25**, 45–52 (1998).
420. Smith, H. J. & Tisdale, M. J. Signal transduction pathways involved in proteolysis-inducing factor induced proteasome expression in murine myotubes. *Br J Cancer* **89**, 1783–1788 (2003).
421. Cytotoxic activity of tumor necrosis factor is mediated by early damage of

mitochondrial functions. Evidence for the involvement of mitochondrial radical generation - PubMed. https://pubmed.ncbi.nlm.nih.gov/1312087/.
422. Abrigo, J., Rivera, J. C., Simon, F., Cabrera, D. & Cabello-Verrugio, C. Transforming growth factor type beta (TGF-β) requires reactive oxygen species to induce skeletal muscle atrophy. *Cell Signal* **28**, 366–376 (2016).
423. McClung, J. M., Judge, A. R., Talbert, E. E. & Powers, S. K. Calpain-1 is required for hydrogen peroxide-induced myotube atrophy. *Am J Physiol Cell Physiol* **296**, C363-371 (2009).
424. Dargelos, E. *et al.* Up-regulation of calcium-dependent proteolysis in human myoblasts under acute oxidative stress. *Exp Cell Res* **316**, 115–125 (2010).
425. Whidden, M. A. *et al.* Oxidative stress is required for mechanical ventilation-induced protease activation in the diaphragm. *J Appl Physiol (1985)* **108**, 1376–1382 (2010).
426. Gg, R., R, P. & R, A.-Z. Redox regulation of autophagy in skeletal muscle. *Free radical biology & medicine* **98**, (2016).
427. Li, Y.-P., Chen, Y., Li, A. S. & Reid, M. B. Hydrogen peroxide stimulates ubiquitin-conjugating activity and expression of genes for specific E2 and E3 proteins in skeletal muscle myotubes. *Am J Physiol Cell Physiol* **285**, C806-812 (2003).
428. Mallard, J. *et al.* Chemotherapy impairs skeletal muscle mitochondrial homeostasis in early breast cancer patients. *J Cachexia Sarcopenia Muscle* **13**, 1896–1907 (2022).
429. Gouspillou, G. *et al.* Anthracycline-containing chemotherapy causes long-term impairment of mitochondrial respiration and increased reactive oxygen species release in skeletal muscle. *Sci Rep* **5**, 8717 (2015).
430. Hiensch, A. E. *et al.* Doxorubicin-induced skeletal muscle atrophy: Elucidating the underlying molecular pathways. *Acta Physiol (Oxf)* **229**, e13400 (2020).
431. Boveris, A. Determination of the production of superoxide radicals and hydrogen peroxide in mitochondria. *Methods Enzymol* **105**, 429–435 (1984).
432. Ji, L. L., Yeo, D., Kang, C. & Zhang, T. The role of mitochondria in redox signaling of muscle homeostasis. *J Sport Health Sci* **9**, 386–393 (2020).
433. Andreyev, A. Y., Kushnareva, Y. E. & Starkov, A. A. Mitochondrial metabolism of reactive oxygen species. *Biochemistry (Mosc)* **70**, 200–214 (2005).
434. Muller, F. The nature and mechanism of superoxide production by the electron transport chain: Its relevance to aging. *J Am Aging Assoc* **23**, 227–253 (2000).
435. Dröge, W. Free radicals in the physiological control of cell function. *Physiol Rev* **82**, 47–95 (2002).
436. Boveris, A. & Chance, B. The mitochondrial generation of hydrogen peroxide. General properties and effect of hyperbaric oxygen. *Biochem J* **134**, 707–716 (1973).
437. Julienne, C. M. *et al.* Cancer cachexia is associated with a decrease in skeletal muscle mitochondrial oxidative capacities without alteration of ATP production efficiency. *J Cachexia Sarcopenia Muscle* **3**, 265–275 (2012).
438. Mauro, A. Satellite cell of skeletal muscle fibers. *J Biophys Biochem Cytol* **9**, 493–495 (1961).
439. Allbrook, D. B., Han, M. F. & Hellmuth, A. E. Population of muscle satellite cells in relation to age and mitotic activity. *Pathology* **3**, 223–243 (1971).
440. Schultz, E. A quantitative study of the satellite cell population in postnatal mouse lumbrical muscle. *Anat Rec* **180**, 589–595 (1974).
441. Chargé, S. B. P. & Rudnicki, M. A. Cellular and molecular regulation of muscle regeneration. *Physiol Rev* **84**, 209–238 (2004).
442. Sambasivan, R. *et al.* Pax7-expressing satellite cells are indispensable for adult skeletal muscle regeneration. *Development* **138**, 3647–3656 (2011).
443. Chen, J. C. J. & Goldhamer, D. J. Skeletal muscle stem cells. *Reprod Biol Endocrinol*

1, 101 (2003).
444. Pallafacchina, G., Blaauw, B. & Schiaffino, S. Role of satellite cells in muscle growth and maintenance of muscle mass. *Nutr Metab Cardiovasc Dis* **23 Suppl 1**, S12-18 (2013).
445. Bazgir, B., Fathi, R., Rezazadeh Valojerdi, M., Mozdziak, P. & Asgari, A. Satellite Cells Contribution to Exercise Mediated Muscle Hypertrophy and Repair. *Cell J* **18**, 473–484 (2017).
446. Garry, D. J. *et al.* Myogenic stem cell function is impaired in mice lacking the forkhead/winged helix protein MNF. *Proc Natl Acad Sci U S A* **97**, 5416–5421 (2000).
447. Seale, P. *et al.* Pax7 is required for the specification of myogenic satellite cells. *Cell* **102**, 777–786 (2000).
448. Nicolas, N., Marazzi, G., Kelley, K. & Sassoon, D. Embryonic deregulation of muscle stress signaling pathways leads to altered postnatal stem cell behavior and a failure in postnatal muscle growth. *Dev Biol* **281**, 171–183 (2005).
449. Giordani, L., Parisi, A. & Le Grand, F. Satellite Cell Self-Renewal. *Curr Top Dev Biol* **126**, 177–203 (2018).
450. Schultz, E., Gibson, M. C. & Champion, T. Satellite cells are mitotically quiescent in mature mouse muscle: an EM and radioautographic study. *J Exp Zool* **206**, 451–456 (1978).
451. Floss, T., Arnold, H. H. & Braun, T. A role for FGF-6 in skeletal muscle regeneration. *Genes Dev* **11**, 2040–2051 (1997).
452. White, T. P. & Esser, K. A. Satellite cell and growth factor involvement in skeletal muscle growth. *Med Sci Sports Exerc* **21**, S158-163 (1989).
453. Hasty, P. *et al.* Muscle deficiency and neonatal death in mice with a targeted mutation in the myogenin gene. *Nature* **364**, 501–506 (1993).
454. Nabeshima, Y. *et al.* Myogenin gene disruption results in perinatal lethality because of severe muscle defect. *Nature* **364**, 532–535 (1993).
455. Megeney, L. A., Kablar, B., Garrett, K., Anderson, J. E. & Rudnicki, M. A. MyoD is required for myogenic stem cell function in adult skeletal muscle. *Genes Dev* **10**, 1173–1183 (1996).
456. Ogawa, R. *et al.* Doublecortin marks a new population of transiently amplifying muscle progenitor cells and is required for myofiber maturation during skeletal muscle regeneration. *Development* **142**, 51–61 (2015).
457. Gros, J., Manceau, M., Thomé, V. & Marcelle, C. A common somitic origin for embryonic muscle progenitors and satellite cells. *Nature* **435**, 954–958 (2005).
458. Tapscott, S. J. The circuitry of a master switch: Myod and the regulation of skeletal muscle gene transcription. *Development* **132**, 2685–2695 (2005).
459. Dumont, N. A., Bentzinger, C. F., Sincennes, M.-C. & Rudnicki, M. A. Satellite Cells and Skeletal Muscle Regeneration. *Compr Physiol* **5**, 1027–1059 (2015).
460. von Maltzahn, J., Jones, A. E., Parks, R. J. & Rudnicki, M. A. Pax7 is critical for the normal function of satellite cells in adult skeletal muscle. *Proc Natl Acad Sci U S A* **110**, 16474–16479 (2013).
461. Olguin, H. C. & Olwin, B. B. Pax-7 up-regulation inhibits myogenesis and cell cycle progression in satellite cells: a potential mechanism for self-renewal. *Dev Biol* **275**, 375–388 (2004).
462. Oustanina, S., Hause, G. & Braun, T. Pax7 directs postnatal renewal and propagation of myogenic satellite cells but not their specification. *EMBO J* **23**, 3430–3439 (2004).
463. Zammit, P. S. *et al.* Muscle satellite cells adopt divergent fates: a mechanism for self-renewal? *J Cell Biol* **166**, 347–357 (2004).
464. Lepper, C., Partridge, T. A. & Fan, C.-M. An absolute requirement for Pax7-positive satellite cells in acute injury-induced skeletal muscle regeneration. *Development* **138**, 3639–3646 (2011).

465. Murphy, M. M., Lawson, J. A., Mathew, S. J., Hutcheson, D. A. & Kardon, G. Satellite cells, connective tissue fibroblasts and their interactions are crucial for muscle regeneration. *Development* **138**, 3625–3637 (2011).
466. Yablonka-Reuveni, Z. *et al.* The transition from proliferation to differentiation is delayed in satellite cells from mice lacking MyoD. *Dev Biol* **210**, 440–455 (1999).
467. B, G.-M. *et al.* A role for the myogenic determination gene Myf5 in adult regenerative myogenesis. *Developmental biology* **312**, (2007).
468. Cooper, R. N. *et al.* In vivo satellite cell activation via Myf5 and MyoD in regenerating mouse skeletal muscle. *J Cell Sci* **112 (Pt 17)**, 2895–2901 (1999).
469. Ustanina, S., Carvajal, J., Rigby, P. & Braun, T. The myogenic factor Myf5 supports efficient skeletal muscle regeneration by enabling transient myoblast amplification. *Stem Cells* **25**, 2006–2016 (2007).
470. Olguin, H. C., Yang, Z., Tapscott, S. J. & Olwin, B. B. Reciprocal inhibition between Pax7 and muscle regulatory factors modulates myogenic cell fate determination. *J Cell Biol* **177**, 769–779 (2007).
471. Wang, Y. X. & Rudnicki, M. A. Satellite cells, the engines of muscle repair. *Nat Rev Mol Cell Biol* **13**, 127–133 (2011).
472. Z, Y.-R. & Aj, R. Temporal expression of regulatory and structural muscle proteins during myogenesis of satellite cells on isolated adult rat fibers. *Developmental biology* **164**, (1994).
473. Cornelison, D. D. & Wold, B. J. Single-cell analysis of regulatory gene expression in quiescent and activated mouse skeletal muscle satellite cells. *Dev Biol* **191**, 270–283 (1997).
474. Cornelison, D. D., Olwin, B. B., Rudnicki, M. A. & Wold, B. J. MyoD(-/-) satellite cells in single-fiber culture are differentiation defective and MRF4 deficient. *Dev Biol* **224**, 122–137 (2000).
475. Sacco, A., Doyonnas, R., Kraft, P., Vitorovic, S. & Blau, H. M. Self-renewal and expansion of single transplanted muscle stem cells. *Nature* **456**, 502–506 (2008).
476. Collins, C. A. *et al.* Stem cell function, self-renewal, and behavioral heterogeneity of cells from the adult muscle satellite cell niche. *Cell* **122**, 289–301 (2005).
477. Ganassi, M., Badodi, S., Wanders, K., Zammit, P. S. & Hughes, S. M. Myogenin is an essential regulator of adult myofibre growth and muscle stem cell homeostasis. *Elife* **9**, e60445 (2020).
478. Goh, Q. *et al.* Myonuclear accretion is a determinant of exercise-induced remodeling in skeletal muscle. *Elife* **8**, e44876 (2019).
479. Goh, Q. & Millay, D. P. Requirement of myomaker-mediated stem cell fusion for skeletal muscle hypertrophy. *Elife* **6**, e20007 (2017).
480. Randrianarison-Huetz, V. *et al.* Srf controls satellite cell fusion through the maintenance of actin architecture. *J Cell Biol* **217**, 685–700 (2018).
481. Murach, K. A. *et al.* Differential requirement for satellite cells during overload-induced muscle hypertrophy in growing versus mature mice. *Skelet Muscle* **7**, 14 (2017).
482. Fry, C. S. *et al.* Regulation of the muscle fiber microenvironment by activated satellite cells during hypertrophy. *FASEB J* **28**, 1654–1665 (2014).
483. Fukuda, S. *et al.* Sustained expression of HeyL is critical for the proliferation of muscle stem cells in overloaded muscle. *Elife* **8**, e48284 (2019).
484. Masschelein, E. *et al.* Exercise promotes satellite cell contribution to myofibers in a load-dependent manner. *Skelet Muscle* **10**, 21 (2020).
485. Murach, K. A., Fry, C. S., Dupont-Versteegden, E. E., McCarthy, J. J. & Peterson, C. A. Fusion and beyond: Satellite cell contributions to loading-induced skeletal muscle adaptation. *FASEB J* **35**, e21893 (2021).
486. Roth, S. M. *et al.* Skeletal muscle satellite cell characteristics in young and older men

and women after heavy resistance strength training. *J Gerontol A Biol Sci Med Sci* **56**, B240-247 (2001).
487. Kadi, F. & Thornell, L. E. Concomitant increases in myonuclear and satellite cell content in female trapezius muscle following strength training. *Histochem Cell Biol* **113**, 99–103 (2000).
488. Charifi, N., Kadi, F., Féasson, L. & Denis, C. Effects of endurance training on satellite cell frequency in skeletal muscle of old men. *Muscle Nerve* **28**, 87–92 (2003).
489. Murach, K. A. *et al.* Cycle training modulates satellite cell and transcriptional responses to a bout of resistance exercise. *Physiol Rep* **4**, e12973 (2016).
490. Egner, I. M., Bruusgaard, J. C. & Gundersen, K. Satellite cell depletion prevents fiber hypertrophy in skeletal muscle. *Development* **143**, 2898–2906 (2016).
491. McCarthy, J. J. *et al.* Effective fiber hypertrophy in satellite cell-depleted skeletal muscle. *Development* **138**, 3657–3666 (2011).
492. Moss, F. P. & Leblond, C. P. Nature of dividing nuclei in skeletal muscle of growing rats. *J Cell Biol* **44**, 459–462 (1970).
493. Guerci, A. *et al.* Srf-dependent paracrine signals produced by myofibers control satellite cell-mediated skeletal muscle hypertrophy. *Cell Metab* **15**, 25–37 (2012).
494. Noviello, C. *et al.* RhoA within myofibers controls satellite cell microenvironment to allow hypertrophic growth. *iScience* **25**, 103616 (2022).
495. Fukada, S.-I., Akimoto, T. & Sotiropoulos, A. Role of damage and management in muscle hypertrophy: Different behaviors of muscle stem cells in regeneration and hypertrophy. *Biochim Biophys Acta Mol Cell Res* **1867**, 118742 (2020).
496. Dungan, C. M. *et al.* Elevated myonuclear density during skeletal muscle hypertrophy in response to training is reversed during detraining. *Am J Physiol Cell Physiol* **316**, C649–C654 (2019).
497. Murach, K. A., Englund, D. A., Dupont-Versteegden, E. E., McCarthy, J. J. & Peterson, C. A. Myonuclear Domain Flexibility Challenges Rigid Assumptions on Satellite Cell Contribution to Skeletal Muscle Fiber Hypertrophy. *Front Physiol* **9**, 635 (2018).
498. Schwarzkopf, M., Coletti, D., Sassoon, D. & Marazzi, G. Muscle cachexia is regulated by a p53-PW1/Peg3-dependent pathway. *Genes Dev* **20**, 3440–3452 (2006).
499. Talbert, E. E. & Guttridge, D. C. Impaired regeneration: A role for the muscle microenvironment in cancer cachexia. *Semin Cell Dev Biol* **54**, 82–91 (2016).
500. Costamagna, D. *et al.* Interleukin-4 administration improves muscle function, adult myogenesis, and lifespan of colon carcinoma-bearing mice. *J Cachexia Sarcopenia Muscle* **11**, 783–801 (2020).
501. Brzeszczyńska, J. *et al.* Loss of oxidative defense and potential blockade of satellite cell maturation in the skeletal muscle of patients with cancer but not in the healthy elderly. *Aging (Albany NY)* **8**, 1690–1702 (2016).
502. Fernandez, G. J. *et al.* MicroRNA-mRNA Co-sequencing Identifies Transcriptional and Post-transcriptional Regulatory Networks Underlying Muscle Wasting in Cancer Cachexia. *Front Genet* **11**, 541 (2020).
503. Nosacka, R. L. *et al.* Distinct cachexia profiles in response to human pancreatic tumours in mouse limb and respiratory muscle. *J Cachexia Sarcopenia Muscle* **11**, 820–837 (2020).
504. Inaba, S., Hinohara, A., Tachibana, M., Tsujikawa, K. & Fukada, S.-I. Muscle regeneration is disrupted by cancer cachexia without loss of muscle stem cell potential. *PLoS One* **13**, e0205467 (2018).
505. Zampieri, S. *et al.* Subclinical myopathy in patients affected with newly diagnosed colorectal cancer at clinical onset of disease: evidence from skeletal muscle biopsies. *Neurol Res* **32**, 20–25 (2010).

506. P, P. *et al.* Skeletal muscle of gastric cancer patients expresses genes involved in muscle regeneration. *Oncology reports* **24**, (2010).
507. Cerquone Perpetuini, A. *et al.* Group I Paks support muscle regeneration and counteract cancer-associated muscle atrophy. *J Cachexia Sarcopenia Muscle* **9**, 727–746 (2018).
508. Schmidt, M., Poser, C. & von Maltzahn, J. Wnt7a Counteracts Cancer Cachexia. *Mol Ther Oncolytics* **16**, 134–146 (2020).
509. Farhang-Sardroodi, S. & Wilkie, K. P. Mathematical Model of Muscle Wasting in Cancer Cachexia. *J Clin Med* **9**, E2029 (2020).
510. McCroskery, S., Thomas, M., Maxwell, L., Sharma, M. & Kambadur, R. Myostatin negatively regulates satellite cell activation and self-renewal. *J Cell Biol* **162**, 1135–1147 (2003).
511. Kovanen, V. Intramuscular extracellular matrix: complex environment of muscle cells. *Exerc Sport Sci Rev* **30**, 20–25 (2002).
512. Yin, H., Price, F. & Rudnicki, M. A. Satellite cells and the muscle stem cell niche. *Physiol Rev* **93**, 23–67 (2013).
513. Plasticity of the Muscle Stem Cell Microenvironment - PubMed. https://pubmed.ncbi.nlm.nih.gov/29204832/.
514. Mashinchian, O., Pisconti, A., Le Moal, E. & Bentzinger, C. F. The Muscle Stem Cell Niche in Health and Disease. *Curr Top Dev Biol* **126**, 23–65 (2018).
515. Pannérec, A., Marazzi, G. & Sassoon, D. Stem cells in the hood: the skeletal muscle niche. *Trends Mol Med* **18**, 599–606 (2012).
516. Bentzinger, C. F., Wang, Y. X., Dumont, N. A. & Rudnicki, M. A. Cellular dynamics in the muscle satellite cell niche. *EMBO Rep* **14**, 1062–1072 (2013).
517. Sciorati, C., Rigamonti, E., Manfredi, A. A. & Rovere-Querini, P. Cell death, clearance and immunity in the skeletal muscle. *Cell Death Differ* **23**, 927–937 (2016).
518. Fielding, R. A. *et al.* Acute phase response in exercise. III. Neutrophil and IL-1 beta accumulation in skeletal muscle. *Am J Physiol* **265**, R166-172 (1993).
519. Tidball, J. G., Berchenko, E. & Frenette, J. Macrophage invasion does not contribute to muscle membrane injury during inflammation. *J Leukoc Biol* **65**, 492–498 (1999).
520. Warren, G. L. *et al.* Chemokine receptor CCR2 involvement in skeletal muscle regeneration. *FASEB J* **19**, 413–415 (2005).
521. Contreras-Shannon, V. *et al.* Fat accumulation with altered inflammation and regeneration in skeletal muscle of CCR2-/- mice following ischemic injury. *Am J Physiol Cell Physiol* **292**, C953-967 (2007).
522. Zhang, J. *et al.* CD8 T cells are involved in skeletal muscle regeneration through facilitating MCP-1 secretion and Gr1(high) macrophage infiltration. *J Immunol* **193**, 5149–5160 (2014).
523. Juban, G. & Chazaud, B. Efferocytosis during Skeletal Muscle Regeneration. *Cells* **10**, 3267 (2021).
524. Baht, G. S. *et al.* Meteorin-like facilitates skeletal muscle repair through a Stat3/IGF-1 mechanism. *Nat Metab* **2**, 278–289 (2020).
525. Lu, H. *et al.* Macrophages recruited via CCR2 produce insulin-like growth factor-1 to repair acute skeletal muscle injury. *FASEB J* **25**, 358–369 (2011).
526. Ratnayake, D. *et al.* Macrophages provide a transient muscle stem cell niche via NAMPT secretion. *Nature* **591**, 281–287 (2021).
527. Macrophage-derived glutamine boosts satellite cells and muscle regeneration - PubMed. https://pubmed.ncbi.nlm.nih.gov/33116312/.
528. Tonkin, J. *et al.* Monocyte/Macrophage-derived IGF-1 Orchestrates Murine Skeletal Muscle Regeneration and Modulates Autocrine Polarization. *Mol Ther* **23**, 1189–1200 (2015).

529. Cantini, M. *et al.* Macrophages regulate proliferation and differentiation of satellite cells. *Biochem Biophys Res Commun* **202**, 1688–1696 (1994).
530. Lemos, D. R. *et al.* Nilotinib reduces muscle fibrosis in chronic muscle injury by promoting TNF-mediated apoptosis of fibro/adipogenic progenitors. *Nat Med* **21**, 786–794 (2015).
531. Varga, T. *et al.* Highly Dynamic Transcriptional Signature of Distinct Macrophage Subsets during Sterile Inflammation, Resolution, and Tissue Repair. *J Immunol* **196**, 4771–4782 (2016).
532. Giannakis, N. *et al.* Dynamic changes to lipid mediators support transitions among macrophage subtypes during muscle regeneration. *Nat Immunol* **20**, 626–636 (2019).
533. Varga, T. *et al.* Tissue LyC6- macrophages are generated in the absence of circulating LyC6- monocytes and Nur77 in a model of muscle regeneration. *J Immunol* **191**, 5695–5701 (2013).
534. Deng, B., Wehling-Henricks, M., Villalta, S. A., Wang, Y. & Tidball, J. G. IL-10 triggers changes in macrophage phenotype that promote muscle growth and regeneration. *J Immunol* **189**, 3669–3680 (2012).
535. Welc, S. S. *et al.* Differential Effects of Myeloid Cell PPARδ and IL-10 in Regulating Macrophage Recruitment, Phenotype, and Regeneration following Acute Muscle Injury. *J Immunol* **205**, 1664–1677 (2020).
536. Arnold, L. *et al.* Inflammatory monocytes recruited after skeletal muscle injury switch into antiinflammatory macrophages to support myogenesis. *J Exp Med* **204**, 1057–1069 (2007).
537. Saclier, M. *et al.* Differentially activated macrophages orchestrate myogenic precursor cell fate during human skeletal muscle regeneration. *Stem Cells* **31**, 384–396 (2013).
538. Zhao, W., Lu, H., Wang, X., Ransohoff, R. M. & Zhou, L. CX3CR1 deficiency delays acute skeletal muscle injury repair by impairing macrophage functions. *FASEB J* **30**, 380–393 (2016).
539. Varga, T. *et al.* Macrophage PPARγ, a Lipid Activated Transcription Factor Controls the Growth Factor GDF3 and Skeletal Muscle Regeneration. *Immunity* **45**, 1038–1051 (2016).
540. Juban, G. & Chazaud, B. Metabolic regulation of macrophages during tissue repair: insights from skeletal muscle regeneration. *FEBS Lett* **591**, 3007–3021 (2017).
541. Wang, H. *et al.* Altered macrophage phenotype transition impairs skeletal muscle regeneration. *Am J Pathol* **184**, 1167–1184 (2014).
542. Latroche, C. *et al.* Coupling between Myogenesis and Angiogenesis during Skeletal Muscle Regeneration Is Stimulated by Restorative Macrophages. *Stem Cell Reports* **9**, 2018–2033 (2017).
543. Juban, G. *et al.* AMPK Activation Regulates LTBP4-Dependent TGF-β1 Secretion by Pro-inflammatory Macrophages and Controls Fibrosis in Duchenne Muscular Dystrophy. *Cell Rep* **25**, 2163-2176.e6 (2018).
544. Panci, G. & Chazaud, B. Inflammation during post-injury skeletal muscle regeneration. *Semin Cell Dev Biol* **119**, 32–38 (2021).
545. Singh, P. & Chazaud, B. Benefits and pathologies associated with the inflammatory response. *Exp Cell Res* **409**, 112905 (2021).
546. Liu, X. *et al.* Macrophage depletion impairs skeletal muscle regeneration: The roles of regulatory factors for muscle regeneration. *Cell Biol Int* **41**, 228–238 (2017).
547. Segawa, M. *et al.* Suppression of macrophage functions impairs skeletal muscle regeneration with severe fibrosis. *Exp Cell Res* **314**, 3232–3244 (2008).
548. Theret, M. *et al.* Elevated numbers of infiltrating eosinophils accelerate the progression of Duchenne muscular dystrophy pathology in mdx mice. *Development* **149**, dev200112 (2022).

549. Heredia, J. E. *et al.* Type 2 innate signals stimulate fibro/adipogenic progenitors to facilitate muscle regeneration. *Cell* **153**, 376–388 (2013).
550. Gundra, U. M. *et al.* Alternatively activated macrophages derived from monocytes and tissue macrophages are phenotypically and functionally distinct. *Blood* **123**, e110-122 (2014).
551. Van Dyken, S. J. & Locksley, R. M. Interleukin-4- and interleukin-13-mediated alternatively activated macrophages: roles in homeostasis and disease. *Annu Rev Immunol* **31**, 317–343 (2013).
552. Berardi, E. *et al.* Skeletal muscle is enriched in hematopoietic stem cells and not inflammatory cells in cachectic mice. *Neurol Res* **30**, 160–169 (2008).
553. Ennist, D. L. & Jones, K. H. Rapid method for identification of macrophages in suspension by acid alpha-naphthyl acetate esterase activity. *J Histochem Cytochem* **31**, 960–963 (1983).
554. Dhingra, V. K., Gupta, R. K. & Sadana, J. R. Demonstration of acid alpha naphthyl acetate esterase activity in bovine lymphocytes and monocytes or macrophages. *Res Vet Sci* **33**, 26–30 (1982).
555. Shukla, S. K. *et al.* Macrophages potentiate STAT3 signaling in skeletal muscles and regulate pancreatic cancer cachexia. *Cancer Lett* **484**, 29–39 (2020).
556. Contreras, O., Rossi, F. M. V. & Theret, M. Origins, potency, and heterogeneity of skeletal muscle fibro-adipogenic progenitors-time for new definitions. *Skelet Muscle* **11**, 16 (2021).
557. Giordani, L. *et al.* High-Dimensional Single-Cell Cartography Reveals Novel Skeletal Muscle-Resident Cell Populations. *Mol Cell* **74**, 609-621.e6 (2019).
558. Joe, A. W. B. *et al.* Muscle injury activates resident fibro/adipogenic progenitors that facilitate myogenesis. *Nat Cell Biol* **12**, 153–163 (2010).
559. Uezumi, A., Fukada, S., Yamamoto, N., Takeda, S. & Tsuchida, K. Mesenchymal progenitors distinct from satellite cells contribute to ectopic fat cell formation in skeletal muscle. *Nat Cell Biol* **12**, 143–152 (2010).
560. Scott, R. W., Arostegui, M., Schweitzer, R., Rossi, F. M. V. & Underhill, T. M. Hic1 Defines Quiescent Mesenchymal Progenitor Subpopulations with Distinct Functions and Fates in Skeletal Muscle Regeneration. *Cell Stem Cell* **25**, 797-813.e9 (2019).
561. Wosczyna, M. N. *et al.* Mesenchymal Stromal Cells Are Required for Regeneration and Homeostatic Maintenance of Skeletal Muscle. *Cell Rep* **27**, 2029-2035.e5 (2019).
562. Roberts, E. W. *et al.* Depletion of stromal cells expressing fibroblast activation protein-α from skeletal muscle and bone marrow results in cachexia and anemia. *J Exp Med* **210**, 1137–1151 (2013).
563. Petrilli, L. L. *et al.* High-Dimensional Single-Cell Quantitative Profiling of Skeletal Muscle Cell Population Dynamics during Regeneration. *Cells* **9**, E1723 (2020).
564. De Micheli, A. J. *et al.* Single-Cell Analysis of the Muscle Stem Cell Hierarchy Identifies Heterotypic Communication Signals Involved in Skeletal Muscle Regeneration. *Cell Rep* **30**, 3583-3595.e5 (2020).
565. Oprescu, S. N., Yue, F., Qiu, J., Brito, L. F. & Kuang, S. Temporal Dynamics and Heterogeneity of Cell Populations during Skeletal Muscle Regeneration. *iScience* **23**, 100993 (2020).
566. Lemos, D. R. *et al.* Functionally convergent white adipogenic progenitors of different lineages participate in a diffused system supporting tissue regeneration. *Stem Cells* **30**, 1152–1162 (2012).
567. Chang, H. Y. *et al.* Diversity, topographic differentiation, and positional memory in human fibroblasts. *Proc Natl Acad Sci U S A* **99**, 12877–12882 (2002).
568. Rodemann, H. P. & Müller, G. A. Characterization of human renal fibroblasts in health and disease: II. In vitro growth, differentiation, and collagen synthesis of fibroblasts

from kidneys with interstitial fibrosis. *Am J Kidney Dis* **17**, 684–686 (1991).
569. Tomasek, J. J., Gabbiani, G., Hinz, B., Chaponnier, C. & Brown, R. A. Myofibroblasts and mechano-regulation of connective tissue remodelling. *Nat Rev Mol Cell Biol* **3**, 349–363 (2002).
570. Lukjanenko, L. *et al.* Loss of fibronectin from the aged stem cell niche affects the regenerative capacity of skeletal muscle in mice. *Nat Med* **22**, 897–905 (2016).
571. Bentzinger, C. F. *et al.* Fibronectin regulates Wnt7a signaling and satellite cell expansion. *Cell Stem Cell* **12**, 75–87 (2013).
572. Urciuolo, A. *et al.* Collagen VI regulates satellite cell self-renewal and muscle regeneration. *Nat Commun* **4**, 1964 (2013).
573. Tierney, M. T. *et al.* Autonomous Extracellular Matrix Remodeling Controls a Progressive Adaptation in Muscle Stem Cell Regenerative Capacity during Development. *Cell Rep* **14**, 1940–1952 (2016).
574. Fiore, D. *et al.* Pharmacological blockage of fibro/adipogenic progenitor expansion and suppression of regenerative fibrogenesis is associated with impaired skeletal muscle regeneration. *Stem Cell Res* **17**, 161–169 (2016).
575. Malietzis, G. *et al.* Low Muscularity and Myosteatosis Is Related to the Host Systemic Inflammatory Response in Patients Undergoing Surgery for Colorectal Cancer. *Ann Surg* **263**, 320–325 (2016).
576. Sturlan, S. *et al.* In vivo gene transfer of murine interleukin-4 inhibits colon-26-mediated cancer cachexia in mice. *Anticancer Res* **22**, 2547–2554 (2002).
577. Malecova, B. *et al.* Dynamics of cellular states of fibro-adipogenic progenitors during myogenesis and muscular dystrophy. *Nat Commun* **9**, 3670 (2018).
578. Biferali, B., Proietti, D., Mozzetta, C. & Madaro, L. Fibro-Adipogenic Progenitors Cross-Talk in Skeletal Muscle: The Social Network. *Front Physiol* **10**, 1074 (2019).
579. Kuswanto, W. *et al.* Poor Repair of Skeletal Muscle in Aging Mice Reflects a Defect in Local, Interleukin-33-Dependent Accumulation of Regulatory T Cells. *Immunity* **44**, 355–367 (2016).
580. Mendias, C. L. *et al.* Transforming growth factor-beta induces skeletal muscle atrophy and fibrosis through the induction of atrogin-1 and scleraxis. *Muscle Nerve* **45**, 55–59 (2012).
581. Ismaeel, A. *et al.* Role of Transforming Growth Factor-β in Skeletal Muscle Fibrosis: A Review. *Int J Mol Sci* **20**, E2446 (2019).
582. Krüger-Genge, A., Blocki, A., Franke, R.-P. & Jung, F. Vascular Endothelial Cell Biology: An Update. *Int J Mol Sci* **20**, E4411 (2019).
583. Lee, S. *et al.* Autocrine VEGF signaling is required for vascular homeostasis. *Cell* **130**, 691–703 (2007).
584. Christov, C. *et al.* Muscle satellite cells and endothelial cells: close neighbors and privileged partners. *Mol Biol Cell* **18**, 1397–1409 (2007).
585. Schmalbruch, H. & Hellhammer, U. The number of nuclei in adult rat muscles with special reference to satellite cells. *Anat Rec* **189**, 169–175 (1977).
586. Verma, M. *et al.* Muscle Satellite Cell Cross-Talk with a Vascular Niche Maintains Quiescence via VEGF and Notch Signaling. *Cell Stem Cell* **23**, 530-543.e9 (2018).
587. Wagner, P. D. The critical role of VEGF in skeletal muscle angiogenesis and blood flow. *Biochem Soc Trans* **39**, 1556–1559 (2011).
588. Audet, G. N., Meek, T. H., Garland, T. & Olfert, I. M. Expression of angiogenic regulators and skeletal muscle capillarity in selectively bred high aerobic capacity mice. *Exp Physiol* **96**, 1138–1150 (2011).
589. Hardy, D. *et al.* Comparative Study of Injury Models for Studying Muscle Regeneration in Mice. *PLoS One* **11**, e0147198 (2016).
590. Hansen-Smith, F. M., Hudlicka, O. & Egginton, S. In vivo angiogenesis in adult rat

skeletal muscle: early changes in capillary network architecture and ultrastructure. *Cell Tissue Res* **286**, 123–136 (1996).
591. Roberts, P. & McGeachie, J. K. Endothelial cell activation during angiogenesis in freely transplanted skeletal muscles in mice and its relationship to the onset of myogenesis. *J Anat* **169**, 197–207 (1990).
592. Bryan, B. A. *et al.* Coordinated vascular endothelial growth factor expression and signaling during skeletal myogenic differentiation. *Mol Biol Cell* **19**, 994–1006 (2008).
593. Germani, A. *et al.* Vascular endothelial growth factor modulates skeletal myoblast function. *Am J Pathol* **163**, 1417–1428 (2003).
594. Rhoads, R. P. *et al.* Satellite cell-mediated angiogenesis in vitro coincides with a functional hypoxia-inducible factor pathway. *Am J Physiol Cell Physiol* **296**, C1321-1328 (2009).
595. Borselli, C. *et al.* Functional muscle regeneration with combined delivery of angiogenesis and myogenesis factors. *Proc Natl Acad Sci U S A* **107**, 3287–3292 (2010).
596. Arsic, N. *et al.* Vascular endothelial growth factor stimulates skeletal muscle regeneration in vivo. *Mol Ther* **10**, 844–854 (2004).
597. Ochoa, O. *et al.* Delayed angiogenesis and VEGF production in CCR2-/- mice during impaired skeletal muscle regeneration. *Am J Physiol Regul Integr Comp Physiol* **293**, R651-661 (2007).
598. Zordan, P. *et al.* Macrophages commit postnatal endothelium-derived progenitors to angiogenesis and restrict endothelial to mesenchymal transition during muscle regeneration. *Cell Death Dis* **5**, e1031 (2014).
599. Hiroux, C., Dalle, S., Koppo, K. & Hespel, P. Voluntary exercise does not improve muscular properties or functional capacity during C26-induced cancer cachexia in mice. *J Muscle Res Cell Motil* **42**, 169–181 (2021).
600. Tanaka, M. *et al.* Preventive effects of low-intensity exercise on cancer cachexia-induced muscle atrophy. *FASEB J* **33**, 7852–7862 (2019).
601. Tanaka, M. *et al.* Differential effects of pre-exercise on cancer cachexia-induced muscle atrophy in fast- and slow-twitch muscles. *FASEB J* **34**, 14389–14406 (2020).
602. Ouchi, N. *et al.* Follistatin-like 1, a secreted muscle protein, promotes endothelial cell function and revascularization in ischemic tissue through a nitric-oxide synthase-dependent mechanism. *J Biol Chem* **283**, 32802–32811 (2008).
603. Kadlec, A. O., Chabowski, D. S., Ait-Aissa, K. & Gutterman, D. D. Role of PGC-1α in Vascular Regulation: Implications for Atherosclerosis. *Arterioscler Thromb Vasc Biol* **36**, 1467–1474 (2016).
604. Kim, Y.-M., Mancinelli, G., Grippo, P. & Rehman, J. Abstract 2595: Cancer cachexia is mediated by the suppression of PGC1-alpha expression in the skeletal muscle vasculature. *Cancer Research* **81**, 2595–2595 (2021).
605. Vestweber, D. Relevance of endothelial junctions in leukocyte extravasation and vascular permeability. *Ann N Y Acad Sci* **1257**, 184–192 (2012).
606. Nourshargh, S., Hordijk, P. L. & Sixt, M. Breaching multiple barriers: leukocyte motility through venular walls and the interstitium. *Nat Rev Mol Cell Biol* **11**, 366–378 (2010).
607. Loprinzi, C. L. *et al.* Controlled trial of megestrol acetate for the treatment of cancer anorexia and cachexia. *J Natl Cancer Inst* **82**, 1127–1132 (1990).
608. Temel, J. S. *et al.* Anamorelin in patients with non-small-cell lung cancer and cachexia (ROMANA 1 and ROMANA 2): results from two randomised, double-blind, phase 3 trials. *Lancet Oncol* **17**, 519–531 (2016).
609. Arends, J. *et al.* ESPEN guidelines on nutrition in cancer patients. *Clin Nutr* **36**, 11–48 (2017).

610. Dev, R., Del Fabbro, E. & Bruera, E. Association between megestrol acetate treatment and symptomatic adrenal insufficiency with hypogonadism in male patients with cancer. *Cancer* **110**, 1173–1177 (2007).
611. Loprinzi, C. L., Schaid, D. J., Dose, A. M., Burnham, N. L. & Jensen, M. D. Body-composition changes in patients who gain weight while receiving megestrol acetate. *J Clin Oncol* **11**, 152–154 (1993).
612. Schmid, I. *et al.* Megestrol acetate to correct the nutritional status in an adolescent with growth hormone deficiency: Increase of appetite and body weight but only by increase of body water and fat mass followed by profound cortisol and testosterone depletion. *Klin Padiatr* **214**, 54–57 (2002).
613. Leśniak, W., Bała, M., Jaeschke, R. & Krzakowski, M. Effects of megestrol acetate in patients with cancer anorexia-cachexia syndrome--a systematic review and meta-analysis. *Pol Arch Med Wewn* **118**, 636–644 (2008).
614. Crawford, J. *et al.* Study Design and Rationale for the Phase 3 Clinical Development Program of Enobosarm, a Selective Androgen Receptor Modulator, for the Prevention and Treatment of Muscle Wasting in Cancer Patients (POWER Trials). *Curr Oncol Rep* **18**, 37 (2016).
615. Dobs, A. S. *et al.* Effects of enobosarm on muscle wasting and physical function in patients with cancer: a double-blind, randomised controlled phase 2 trial. *Lancet Oncol* **14**, 335–345 (2013).
616. Basaria, S., Wahlstrom, J. T. & Dobs, A. S. Clinical review 138: Anabolic-androgenic steroid therapy in the treatment of chronic diseases. *J Clin Endocrinol Metab* **86**, 5108–5117 (2001).
617. Mohler, M. L. *et al.* Nonsteroidal selective androgen receptor modulators (SARMs): dissociating the anabolic and androgenic activities of the androgen receptor for therapeutic benefit. *J Med Chem* **52**, 3597–3617 (2009).
618. Wright, T. J. *et al.* A randomized trial of adjunct testosterone for cancer-related muscle loss in men and women. *J Cachexia Sarcopenia Muscle* **9**, 482–496 (2018).
619. Bayliss, T. J., Smith, J. T., Schuster, M., Dragnev, K. H. & Rigas, J. R. A humanized anti-IL-6 antibody (ALD518) in non-small cell lung cancer. *Expert Opin Biol Ther* **11**, 1663–1668 (2011).
620. Jatoi, A. *et al.* A placebo-controlled, double-blind trial of infliximab for cancer-associated weight loss in elderly and/or poor performance non-small cell lung cancer patients (N01C9). *Lung Cancer* **68**, 234–239 (2010).
621. Wiedenmann, B. *et al.* A multicenter, phase II study of infliximab plus gemcitabine in pancreatic cancer cachexia. *J Support Oncol* **6**, 18–25 (2008).
622. Smith, R. C. & Lin, B. K. Myostatin inhibitors as therapies for muscle wasting associated with cancer and other disorders. *Curr Opin Support Palliat Care* **7**, 352–360 (2013).
623. Mantovani, G. *et al.* A phase II study with antioxidants, both in the diet and supplemented, pharmaconutritional support, progestagen, and anti-cyclooxygenase-2 showing efficacy and safety in patients with cancer-related anorexia/cachexia and oxidative stress. *Cancer Epidemiol Biomarkers Prev* **15**, 1030–1034 (2006).
624. Pedersen, B. K. Muscles and their myokines. *J Exp Biol* **214**, 337–346 (2011).
625. Chow, L. S. *et al.* Exerkines in health, resilience and disease. *Nat Rev Endocrinol* **18**, 273–289 (2022).
626. Leuchtmann, A. B., Adak, V., Dilbaz, S. & Handschin, C. The Role of the Skeletal Muscle Secretome in Mediating Endurance and Resistance Training Adaptations. *Front Physiol* **12**, 709807 (2021).
627. Jensen, L., Bangsbo, J. & Hellsten, Y. Effect of high intensity training on

capillarization and presence of angiogenic factors in human skeletal muscle. *J Physiol* **557**, 571–582 (2004).
628. Nalbandian, M. & Takeda, M. Lactate as a Signaling Molecule That Regulates Exercise-Induced Adaptations. *Biology (Basel)* **5**, E38 (2016).
629. Kim, J. & Lee, J. Role of transforming growth factor-β in muscle damage and regeneration: focused on eccentric muscle contraction. *J Exerc Rehabil* **13**, 621–626 (2017).
630. Imai, T. *et al.* Identification and molecular characterization of fractalkine receptor CX3CR1, which mediates both leukocyte migration and adhesion. *Cell* **91**, 521–530 (1997).
631. Takahashi, H. *et al.* TGF-β2 is an exercise-induced adipokine that regulates glucose and fatty acid metabolism. *Nat Metab* **1**, 291–303 (2019).
632. Petersen, A. M. W. & Pedersen, B. K. The anti-inflammatory effect of exercise. *J Appl Physiol (1985)* **98**, 1154–1162 (2005).
633. Colbert, L. H. *et al.* Physical activity, exercise, and inflammatory markers in older adults: findings from the Health, Aging and Body Composition Study. *J Am Geriatr Soc* **52**, 1098–1104 (2004).
634. Mathur, N. & Pedersen, B. K. Exercise as a mean to control low-grade systemic inflammation. *Mediators Inflamm* **2008**, 109502 (2008).
635. Beavers, K. M., Brinkley, T. E. & Nicklas, B. J. Effect of exercise training on chronic inflammation. *Clin Chim Acta* **411**, 785–793 (2010).
636. Tipton, K. D. & Wolfe, R. R. Exercise, protein metabolism, and muscle growth. *Int J Sport Nutr Exerc Metab* **11**, 109–132 (2001).
637. Wong, T. S. & Booth, F. W. Protein metabolism in rat tibialis anterior muscle after stimulated chronic eccentric exercise. *J Appl Physiol (1985)* **69**, 1718–1724 (1990).
638. Pedersen, B. K. & Fischer, C. P. Physiological roles of muscle-derived interleukin-6 in response to exercise. *Curr Opin Clin Nutr Metab Care* **10**, 265–271 (2007).
639. Pedersen, B. K. & Febbraio, M. A. Muscle as an endocrine organ: focus on muscle-derived interleukin-6. *Physiol Rev* **88**, 1379–1406 (2008).
640. Daou, H. N. Exercise as an anti-inflammatory therapy for cancer cachexia: a focus on interleukin-6 regulation. *Am J Physiol Regul Integr Comp Physiol* **318**, R296–R310 (2020).
641. Zinna, E. M. & Yarasheski, K. E. Exercise treatment to counteract protein wasting of chronic diseases. *Curr Opin Clin Nutr Metab Care* **6**, 87–93 (2003).
642. Hurley, B. F., Hanson, E. D. & Sheaff, A. K. Strength training as a countermeasure to aging muscle and chronic disease. *Sports Med* **41**, 289–306 (2011).
643. Röckl, K. S. C., Witczak, C. A. & Goodyear, L. J. Signaling mechanisms in skeletal muscle: acute responses and chronic adaptations to exercise. *IUBMB Life* **60**, 145–153 (2008).
644. Fujimaki, S. *et al.* Functional Overload Enhances Satellite Cell Properties in Skeletal Muscle. *Stem Cells Int* **2016**, 7619418 (2016).
645. Kritikaki, E. *et al.* Exercise Training-Induced Extracellular Matrix Protein Adaptation in Locomotor Muscles: A Systematic Review. *Cells* **10**, 1022 (2021).
646. Peck, B. D. *et al.* A muscle cell-macrophage axis involving matrix metalloproteinase 14 facilitates extracellular matrix remodeling with mechanical loading. *FASEB J* **36**, e22155 (2022).
647. Saito, Y., Chikenji, T. S., Matsumura, T., Nakano, M. & Fujimiya, M. Exercise enhances skeletal muscle regeneration by promoting senescence in fibro-adipogenic progenitors. *Nat Commun* **11**, 889 (2020).
648. Gould, D. W., Lahart, I., Carmichael, A. R., Koutedakis, Y. & Metsios, G. S. Cancer cachexia prevention via physical exercise: molecular mechanisms. *J Cachexia Sarcopenia Muscle* **4**, 111–124 (2013).
649. Lenk, K., Schuler, G. & Adams, V. Skeletal muscle wasting in cachexia and sarcopenia: molecular pathophysiology and impact of exercise training. *J Cachexia*

Sarcopenia Muscle **1**, 9–21 (2010).
650. Sasso, J. P. *et al.* A framework for prescription in exercise-oncology research. *J Cachexia Sarcopenia Muscle* **6**, 115–124 (2015).
651. Thompson, H. J., Jiang, W. & Zhu, Z. Candidate mechanisms accounting for effects of physical activity on breast carcinogenesis. *IUBMB Life* **61**, 895–901 (2009).
652. Filaire, E. *et al.* Lung cancer: what are the links with oxidative stress, physical activity and nutrition. *Lung Cancer* **82**, 383–389 (2013).
653. Betof, A. S., Dewhirst, M. W. & Jones, L. W. Effects and potential mechanisms of exercise training on cancer progression: a translational perspective. *Brain Behav Immun* **30 Suppl**, S75-87 (2013).
654. Loh, S. Y. & Musa, A. N. Methods to improve rehabilitation of patients following breast cancer surgery: a review of systematic reviews. *Breast Cancer (Dove Med Press)* **7**, 81–98 (2015).
655. Kimmel, G. T., Haas, B. K. & Hermanns, M. The role of exercise in cancer treatment: bridging the gap. *Curr Sports Med Rep* **13**, 246–252 (2014).
656. Ka, B., Fg, B., Mm, P., Jm, D. & Ja, C. Effect of exercise on biological pathways in ApcMin/+ mouse intestinal polyps. *Journal of applied physiology (Bethesda, Md. : 1985)* **104**, (2008).
657. Fouladiun, M. *et al.* Daily physical-rest activities in relation to nutritional state, metabolism, and quality of life in cancer patients with progressive cachexia. *Clin Cancer Res* **13**, 6379–6385 (2007).
658. Terada, S. *et al.* Effects of low-intensity prolonged exercise on PGC-1 mRNA expression in rat epitrochlearis muscle. *Biochem Biophys Res Commun* **296**, 350–354 (2002).
659. Pilegaard, H., Saltin, B. & Neufer, P. D. Exercise induces transient transcriptional activation of the PGC-1alpha gene in human skeletal muscle. *J Physiol* **546**, 851–858 (2003).
660. Fernandez-Marcos, P. J. & Auwerx, J. Regulation of PGC-1α, a nodal regulator of mitochondrial biogenesis. *Am J Clin Nutr* **93**, 884S–90 (2011).
661. Handschin, C. *et al.* Skeletal muscle fiber-type switching, exercise intolerance, and myopathy in PGC-1alpha muscle-specific knock-out animals. *J Biol Chem* **282**, 30014–30021 (2007).
662. Bodine, S. C. mTOR signaling and the molecular adaptation to resistance exercise. *Med Sci Sports Exerc* **38**, 1950–1957 (2006).
663. Lai, K.-M. V. *et al.* Conditional activation of akt in adult skeletal muscle induces rapid hypertrophy. *Mol Cell Biol* **24**, 9295–9304 (2004).
664. Ogborn, D. & Schoenfeld, B. J. The Role of Fiber Types in Muscle Hypertrophy: Implications for Loading Strategies. *Strength & Conditioning Journal* **36**, 20–25 (2014).
665. Otis, J. S., Lees, S. J. & Williams, J. H. Functional overload attenuates plantaris atrophy in tumor-bearing rats. *BMC Cancer* **7**, 146 (2007).
666. Anaerobic exercise reduces tumor growth, cancer cachexia and increases macrophage and lymphocyte response in Walker 256 tumor-bearing rats - PubMed. https://pubmed.ncbi.nlm.nih.gov/18688637/.
667. Deuster, P. A., Morrison, S. D. & Ahrens, R. A. Endurance exercise modifies cachexia of tumor growth in rats. *Med Sci Sports Exerc* **17**, 385–392 (1985).
668. Puppa, M. J. *et al.* The effect of exercise on IL-6-induced cachexia in the Apc (Min/+) mouse. *J Cachexia Sarcopenia Muscle* **3**, 117–137 (2012).
669. Ranjbar, K. *et al.* Combined Exercise Training Positively Affects Muscle Wasting in Tumor-Bearing Mice. *Med Sci Sports Exerc* **51**, 1387–1395 (2019).
670. Padilha, C. S. *et al.* Resistance Training's Ability to Prevent Cancer-induced Muscle Atrophy Extends Anabolic Stimulus. *Med Sci Sports Exerc* **53**, 1572–1582 (2021).
671. Patel, D. I. *et al.* Exercise preserves muscle mass and force in a prostate cancer mouse

model. *Eur J Transl Myol* **29**, 8520 (2019).
672. Morinaga, M. *et al.* Aerobic Exercise Ameliorates Cancer Cachexia-Induced Muscle Wasting through Adiponectin Signaling. *Int J Mol Sci* **22**, 3110 (2021).
673. Ruan, H. & Dong, L. Q. Adiponectin signaling and function in insulin target tissues. *J Mol Cell Biol* **8**, 101–109 (2016).
674. Yanai, H. & Yoshida, H. Beneficial Effects of Adiponectin on Glucose and Lipid Metabolism and Atherosclerotic Progression: Mechanisms and Perspectives. *Int J Mol Sci* **20**, E1190 (2019).
675. Egan, B. & Zierath, J. R. Exercise metabolism and the molecular regulation of skeletal muscle adaptation. *Cell Metab* **17**, 162–184 (2013).
676. Mayhew, D. L., Kim, J.-S., Cross, J. M., Ferrando, A. A. & Bamman, M. M. Translational signaling responses preceding resistance training-mediated myofiber hypertrophy in young and old humans. *J Appl Physiol (1985)* **107**, 1655–1662 (2009).
677. Khamoui, A. V. & Kim, J. S. Candidate mechanisms underlying effects of contractile activity on muscle morphology and energetics in cancer cachexia. *Eur J Cancer Care (Engl)* **21**, 143–157 (2012).
678. Sun, D. F., Chen, Y. & Rabkin, R. Work-induced changes in skeletal muscle IGF-1 and myostatin gene expression in uremia. *Kidney Int* **70**, 453–459 (2006).
679. al-Majid, S. & McCarthy, D. O. Resistance exercise training attenuates wasting of the extensor digitorum longus muscle in mice bearing the colon-26 adenocarcinoma. *Biol Res Nurs* **2**, 155–166 (2001).
680. Norton, J. A., Lowry, S. F. & Brennan, M. F. Effect of work-induced hypertrophy on skeletal muscle of tumor- and nontumor-bearing rats. *J Appl Physiol Respir Environ Exerc Physiol* **46**, 654–657 (1979).
681. Padilha, C. S. *et al.* Moderate vs high-load resistance training on muscular adaptations in rats. *Life Sci* **238**, 116964 (2019).
682. Testa, M. T. de J. *et al.* Resistance Training Attenuates Activation of STAT3 and Muscle Atrophy in Tumor-Bearing Mice. *Front Oncol* **12**, 880787 (2022).
683. Solheim, T. S. *et al.* A randomized phase II feasibility trial of a multimodal intervention for the management of cachexia in lung and pancreatic cancer. *J Cachexia Sarcopenia Muscle* **8**, 778–788 (2017).
684. Schink, K. *et al.* Effects of whole-body electromyostimulation combined with individualized nutritional support on body composition in patients with advanced cancer: a controlled pilot trial. *BMC Cancer* **18**, 886 (2018).
685. Uster, A. *et al.* Effects of nutrition and physical exercise intervention in palliative cancer patients: A randomized controlled trial. *Clin Nutr* **37**, 1202–1209 (2018).
686. Galvão, D. A. *et al.* Resistance training and reduction of treatment side effects in prostate cancer patients. *Med Sci Sports Exerc* **38**, 2045–2052 (2006).
687. Wiskemann, J. *et al.* Progressive Resistance Training to Impact Physical Fitness and Body Weight in Pancreatic Cancer Patients: A Randomized Controlled Trial. *Pancreas* **48**, 257–266 (2019).
688. Temel, J. S. *et al.* A structured exercise program for patients with advanced non-small cell lung cancer. *J Thorac Oncol* **4**, 595–601 (2009).
689. Wong, J. N., McAuley, E. & Trinh, L. Physical activity programming and counseling preferences among cancer survivors: a systematic review. *Int J Behav Nutr Phys Act* **15**, 48 (2018).
690. McGowan, E. L. *et al.* Physical activity preferences among a population-based sample of colorectal cancer survivors. *Oncol Nurs Forum* **40**, 44–52 (2013).
691. Philip, E. J. *et al.* Physical activity preferences of early-stage lung cancer survivors. *Support Care Cancer* **22**, 495–502 (2014).

692. Argilés, J. M., Busquets, S., López-Soriano, F. J., Costelli, P. & Penna, F. Are there any benefits of exercise training in cancer cachexia? *J Cachexia Sarcopenia Muscle* **3**, 73–76 (2012).
693. Stene, G. B. *et al.* Effect of physical exercise on muscle mass and strength in cancer patients during treatment--a systematic review. *Crit Rev Oncol Hematol* **88**, 573–593 (2013).
694. Bøhn, S.-K. H., Fosså, S. D., Wisløff, T. & Thorsen, L. Physical activity and associations with treatment-induced adverse effects among prostate cancer patients. *Support Care Cancer* **27**, 1001–1011 (2019).
695. Romero, S. A. D. *et al.* Barriers to physical activity: a study of academic and community cancer survivors with pain. *J Cancer Surviv* **12**, 744–752 (2018).
696. Chan, A. *et al.* Barriers and facilitators to exercise among adult cancer survivors in Singapore. *Support Care Cancer* **30**, 4867–4878 (2022).
697. Hurria, A., Jones, L. & Muss, H. B. Cancer Treatment as an Accelerated Aging Process: Assessment, Biomarkers, and Interventions. *Am Soc Clin Oncol Educ Book* **35**, e516-522 (2016).
698. Belloum, Y., Rannou-Bekono, F. & Favier, F. B. Cancer-induced cardiac cachexia: Pathogenesis and impact of physical activity (Review). *Oncol Rep* **37**, 2543–2552 (2017).
699. Cachexia and asthenia in cancer patients - PubMed. https://pubmed.ncbi.nlm.nih.gov/11905651/.
700. Maddocks, M., Armstrong, S. & Wilcock, A. Exercise as a supportive therapy in incurable cancer: exploring patient preferences. *Psychooncology* **20**, 173–178 (2011).
701. Lowe, S. S., Watanabe, S. M., Baracos, V. E. & Courneya, K. S. Physical activity interests and preferences in palliative cancer patients. *Support Care Cancer* **18**, 1469–1475 (2010).
702. Guo, Y., E Phillips, B., Atherton, P. J. & Piasecki, M. Molecular and neural adaptations to neuromuscular electrical stimulation; Implications for ageing muscle. *Mech Ageing Dev* **193**, 111402 (2021).
703. Gondin, J., Guette, M., Ballay, Y. & Martin, A. Electromyostimulation training effects on neural drive and muscle architecture. *Med Sci Sports Exerc* **37**, 1291–1299 (2005).
704. Hultman, E., Sjöholm, H., Jäderholm-Ek, I. & Krynicki, J. Evaluation of methods for electrical stimulation of human skeletal muscle in situ. *Pflugers Arch* **398**, 139–141 (1983).
705. Maffiuletti, N. A. Physiological and methodological considerations for the use of neuromuscular electrical stimulation. *Eur J Appl Physiol* **110**, 223–234 (2010).
706. Enoka, R. M., Amiridis, I. G. & Duchateau, J. Electrical Stimulation of Muscle: Electrophysiology and Rehabilitation. *Physiology (Bethesda)* **35**, 40–56 (2020).
707. Currier, D. P. & Mann, R. Muscular strength development by electrical stimulation in healthy individuals. *Phys Ther* **63**, 915–921 (1983).
708. Porcari, J. P. *et al.* The effects of neuromuscular electrical stimulation training on abdominal strength, endurance, and selected anthropometric measures. *J Sports Sci Med* **4**, 66–75 (2005).
709. Martin, L., Cometti, G., Pousson, M. & Morlon, B. Effect of electrical stimulation training on the contractile characteristics of the triceps surae muscle. *Eur J Appl Physiol Occup Physiol* **67**, 457–461 (1993).
710. Doucet, B. M., Lam, A. & Griffin, L. Neuromuscular electrical stimulation for skeletal muscle function. *Yale J Biol Med* **85**, 201–215 (2012).
711. Sluka, K. A. & Walsh, D. Transcutaneous electrical nerve stimulation: basic science mechanisms and clinical effectiveness. *J Pain* **4**, 109–121 (2003).
712. Valenti, F. [NEUROMUSCULAR ELECTROSTIMULATION IN CLINICAL PRACTICE]. *Acta Anaesthesiol* **15**, 227–245 (1964).
713. Adams, D., Logerstedt, D. S., Hunter-Giordano, A., Axe, M. J. & Snyder-Mackler, L.

Current concepts for anterior cruciate ligament reconstruction: a criterion-based rehabilitation progression. *J Orthop Sports Phys Ther* **42**, 601–614 (2012).
714. Bickel, C. S., Gregory, C. M. & Dean, J. C. Motor unit recruitment during neuromuscular electrical stimulation: a critical appraisal. *Eur J Appl Physiol* **111**, 2399–2407 (2011).
715. Vanderthommen, M. & Duchateau, J. Electrical stimulation as a modality to improve performance of the neuromuscular system. *Exerc Sport Sci Rev* **35**, 180–185 (2007).
716. Stotz, P. J. & Bawa, P. Motor unit recruitment during lengthening contractions of human wrist flexors. *Muscle Nerve* **24**, 1535–1541 (2001).
717. Henneman, E., Somjen, G. & Carpenter, D. O. Excitability and inhibitability of motoneurons of different sizes. *J Neurophysiol* **28**, 599–620 (1965).
718. Feiereisen, P., Duchateau, J. & Hainaut, K. Motor unit recruitment order during voluntary and electrically induced contractions in the tibialis anterior. *Exp Brain Res* **114**, 117–123 (1997).
719. Gondin, J. *et al.* Neuromuscular electrical stimulation training induces atypical adaptations of the human skeletal muscle phenotype: a functional and proteomic analysis. *J Appl Physiol (1985)* **110**, 433–450 (2011).
720. Jones, S. *et al.* Neuromuscular electrical stimulation for muscle weakness in adults with advanced disease. *Cochrane Database Syst Rev* **10**, CD009419 (2016).
721. Duchateau, J. & Hainaut, K. Training effects of sub-maximal electrostimulation in a human muscle. *Med Sci Sports Exerc* **20**, 99–104 (1988).
722. Miller, C. & Thépaut-Mathieu, C. Strength training by electrostimulation conditions for efficacy. *Int J Sports Med* **14**, 20–28 (1993).
723. Pantović, M., Popović, B., Madić, D. & Obradović, J. Effects of Neuromuscular Electrical Stimulation and Resistance Training on Knee Extensor/Flexor Muscles. *Coll Antropol* **39 Suppl 1**, 153–157 (2015).
724. Lai, H. S., Domenico, G. D. & Strauss, G. R. The effect of different electro-motor stimulation training intensities on strength improvement. *Aust J Physiother* **34**, 151–164 (1988).
725. Pichon, F., Chatard, J. C., Martin, A. & Cometti, G. Electrical stimulation and swimming performance. *Med Sci Sports Exerc* **27**, 1671–1676 (1995).
726. Babault, N., Cometti, G., Bernardin, M., Pousson, M. & Chatard, J.-C. Effects of electromyostimulation training on muscle strength and power of elite rugby players. *J Strength Cond Res* **21**, 431–437 (2007).
727. Brocherie, F., Babault, N., Cometti, G., Maffiuletti, N. & Chatard, J.-C. Electrostimulation training effects on the physical performance of ice hockey players. *Med Sci Sports Exerc* **37**, 455–460 (2005).
728. Maddocks, M. *et al.* Neuromuscular electrical stimulation to improve exercise capacity in patients with severe COPD: a randomised double-blind, placebo-controlled trial. *Lancet Respir Med* **4**, 27–36 (2016).
729. Mohan, S., Stanbrook, M. & Anand, A. Neuromuscular electrical stimulation to improve exercise capacity in patients with severe COPD. *Lancet Respir Med* **4**, e14-16 (2016).
730. Sillen, M. J. H. *et al.* Effects of neuromuscular electrical stimulation of muscles of ambulation in patients with chronic heart failure or COPD: a systematic review of the English-language literature. *Chest* **136**, 44–61 (2009).
731. Chen, R.-C. *et al.* Effectiveness of neuromuscular electrical stimulation for the rehabilitation of moderate-to-severe COPD: a meta-analysis. *Int J Chron Obstruct Pulmon Dis* **11**, 2965–2975 (2016).
732. Ploesteanu, R. L. *et al.* Effects of neuromuscular electrical stimulation in patients with

heart failure - review. *J Med Life* **11**, 107–118 (2018).
733. Wageck, B., Nunes, G. S., Silva, F. L., Damasceno, M. C. P. & de Noronha, M. Application and effects of neuromuscular electrical stimulation in critically ill patients: systematic review. *Med Intensiva* **38**, 444–454 (2014).
734. Righetti, R. F. *et al.* Neuromuscular Electrical Stimulation in Patients With Severe COVID-19 Associated With Sepsis and Septic Shock. *Front Med (Lausanne)* **9**, 751636 (2022).
735. Dal Corso, S. *et al.* Skeletal muscle structure and function in response to electrical stimulation in moderately impaired COPD patients. *Respir Med* **101**, 1236–1243 (2007).
736. Sillen, M. J. H., Janssen, P. P., Akkermans, M. A., Wouters, E. F. M. & Spruit, M. A. The metabolic response during resistance training and neuromuscular electrical stimulation (NMES) in patients with COPD, a pilot study. *Respir Med* **102**, 786–789 (2008).
737. Nuhr, M. J. *et al.* Beneficial effects of chronic low-frequency stimulation of thigh muscles in patients with advanced chronic heart failure. *Eur Heart J* **25**, 136–143 (2004).
738. de Oliveira Melo, M., Aragão, F. A. & Vaz, M. A. Neuromuscular electrical stimulation for muscle strengthening in elderly with knee osteoarthritis - a systematic review. *Complement Ther Clin Pract* **19**, 27–31 (2013).
739. O'Connor, D., Brennan, L. & Caulfield, B. The use of neuromuscular electrical stimulation (NMES) for managing the complications of ageing related to reduced exercise participation. *Maturitas* **113**, 13–20 (2018).
740. Langeard, A., Bigot, L., Chastan, N. & Gauthier, A. Does neuromuscular electrical stimulation training of the lower limb have functional effects on the elderly?: A systematic review. *Exp Gerontol* **91**, 88–98 (2017).
741. Gibson, J. N., Smith, K. & Rennie, M. J. Prevention of disuse muscle atrophy by means of electrical stimulation: maintenance of protein synthesis. *Lancet* **2**, 767–770 (1988).
742. Gould, N., Donnermeyer, D., Pope, M. & Ashikaga, T. Transcutaneous muscle stimulation as a method to retard disuse atrophy. *Clin Orthop Relat Res* 215–220 (1982).
743. Wall, B. T. *et al.* Neuromuscular electrical stimulation increases muscle protein synthesis in elderly type 2 diabetic men. *Am J Physiol Endocrinol Metab* **303**, E614-623 (2012).
744. Benavent-Caballer, V., Rosado-Calatayud, P., Segura-Ortí, E., Amer-Cuenca, J. J. & Lisón, J. F. Effects of three different low-intensity exercise interventions on physical performance, muscle CSA and activities of daily living: a randomized controlled trial. *Exp Gerontol* **58**, 159–165 (2014).
745. Jandova, T. *et al.* Muscle Hypertrophy and Architectural Changes in Response to Eight-Week Neuromuscular Electrical Stimulation Training in Healthy Older People. *Life (Basel)* **10**, E184 (2020).
746. Di Filippo, E. S. *et al.* Neuromuscular electrical stimulation improves skeletal muscle regeneration through satellite cell fusion with myofibers in healthy elderly subjects. *J Appl Physiol (1985)* **123**, 501–512 (2017).
747. Fujiya, H. *et al.* Microcurrent electrical neuromuscular stimulation facilitates regeneration of injured skeletal muscle in mice. *J Sports Sci Med* **14**, 297–303 (2015).
748. Guo, B.-S., Cheung, K.-K., Yeung, S. S., Zhang, B.-T. & Yeung, E. W. Electrical stimulation influences satellite cell proliferation and apoptosis in unloading-induced muscle atrophy in mice. *PLoS One* **7**, e30348 (2012).
749. Sciancalepore, M., Coslovich, T., Lorenzon, P., Ziraldo, G. & Taccola, G. Extracellular stimulation with human 'noisy' electromyographic patterns facilitates myotube activity. *J Muscle Res Cell Motil* **36**, 349–357 (2015).
750. Crevenna, R., Marosi, C., Schmidinger, M. & Fialka-Moser, V. Neuromuscular electrical stimulation for a patient with metastatic lung cancer--a case report. *Support Care*

Cancer **14**, 970–973 (2006).
751. Windholz, T., Swanson, T., Vanderbyl, B. L. & Jagoe, R. T. The feasibility and acceptability of neuromuscular electrical stimulation to improve exercise performance in patients with advanced cancer: a pilot study. *BMC Palliat Care* **13**, 23 (2014).
752. Maddocks, M. *et al.* Randomized controlled pilot study of neuromuscular electrical stimulation of the quadriceps in patients with non-small cell lung cancer. *J Pain Symptom Manage* **38**, 950–956 (2009).
753. Maddocks, M. *et al.* Neuromuscular electrical stimulation of the quadriceps in patients with non-small cell lung cancer receiving palliative chemotherapy: a randomized phase II study. *PLoS One* **8**, e86059 (2013).
754. O'Connor, D., Caulfield, B. & Lennon, O. The efficacy and prescription of neuromuscular electrical stimulation (NMES) in adult cancer survivors: a systematic review and meta-analysis. *Support Care Cancer* **26**, 3985–4000 (2018).
755. Long, D. E. *et al.* Skeletal muscle properties show collagen organization and immune cell content are associated with resistance exercise response heterogeneity in older persons. *J Appl Physiol (1985)* **132**, 1432–1447 (2022).
756. Gundersen, K. Muscle memory and a new cellular model for muscle atrophy and hypertrophy. *J Exp Biol* **219**, 235–242 (2016).
757. Lee, H. *et al.* A cellular mechanism of muscle memory facilitates mitochondrial remodelling following resistance training. *J Physiol* **596**, 4413–4426 (2018).
758. Psilander, N. *et al.* Effects of training, detraining, and retraining on strength, hypertrophy, and myonuclear number in human skeletal muscle. *J Appl Physiol (1985)* **126**, 1636–1645 (2019).
759. Marchildon, F., Fu, D., Lala-Tabbert, N. & Wiper-Bergeron, N. CCAAT/enhancer binding protein beta protects muscle satellite cells from apoptosis after injury and in cancer cachexia. *Cell Death Dis* **7**, e2109 (2016).
760. Fry, C. S. *et al.* Satellite cell activation and apoptosis in skeletal muscle from severely burned children. *J Physiol* **594**, 5223–5236 (2016).
761. Ni, J. & Zhang, L. Cancer Cachexia: Definition, Staging, and Emerging Treatments. *Cancer Manag Res* **12**, 5597–5605 (2020).
762. Winje, I. M. *et al.* Cachexia does not induce loss of myonuclei or muscle fibres during xenografted prostate cancer in mice. *Acta Physiol (Oxf)* **225**, e13204 (2019).
763. MacDonald, K. P., Pettit, A. R., Quinn, C., Thomas, G. J. & Thomas, R. Resistance of rheumatoid synovial dendritic cells to the immunosuppressive effects of IL-10. *J Immunol* **163**, 5599–5607 (1999).
764. Hellenbrand, D. J. *et al.* Sustained interleukin-10 delivery reduces inflammation and improves motor function after spinal cord injury. *J Neuroinflammation* **16**, 93 (2019).
765. Joseph, J., Cho, D. S. & Doles, J. D. Metabolomic Analyses Reveal Extensive Progenitor Cell Deficiencies in a Mouse Model of Duchenne Muscular Dystrophy. *Metabolites* **8**, E61 (2018).
766. Reddy, A. *et al.* pH-Gated Succinate Secretion Regulates Muscle Remodeling in Response to Exercise. *Cell* **183**, 62-75.e17 (2020).
767. De Lerma Barbaro, A. The complex liaison between cachexia and tumor burden (Review). *Oncol Rep* **34**, 1635–1649 (2015).
768. Aoyagi, T., Terracina, K. P., Raza, A., Matsubara, H. & Takabe, K. Cancer cachexia, mechanism and treatment. *World J Gastrointest Oncol* **7**, 17–29 (2015).
769. Kurz, E. *et al.* Exercise-induced engagement of the IL-15/IL-15Rα axis promotes anti-tumor immunity in pancreatic cancer. *Cancer Cell* **40**, 720-737.e5 (2022).
770. Huang, Q., Wu, M., Wu, X., Zhang, Y. & Xia, Y. Muscle-to-tumor crosstalk: The effect of exercise-induced myokine on cancer progression. *Biochim Biophys Acta Rev Cancer*

1877, 188761 (2022).
771. Re Cecconi, A. D. *et al.* Musclin, A Myokine Induced by Aerobic Exercise, Retards Muscle Atrophy During Cancer Cachexia in Mice. *Cancers (Basel)* **11**, E1541 (2019).

ANNEXE

During my thesis, colleagues and I, had the opportunity to participate in the writing of a review that, in the first place, describes the potential different roles that macrophages can play in muscle regeneration *versus* hypertrophy in both humans and animal models. In a second time, we presented the current findings on the potential impact of different immunomodulatory strategies during muscle regeneration and hypertrophy.
We were interested in dealing with this subject because the role of macrophages in physiological adaptations to exercise, like in muscle hypertrophy, is up to now, mostly ignored. In this review, the distinct studies that we have mentioned highlighted considerably the key roles of macrophages during exercise, such as in regulation of satellite cell fusion/myonuclear accretion and modulation of the satellite cell niche to support muscle growth.

Received: 2 September 2022 | Accepted: 12 September 2022

DOI: 10.14814/phy2.15480

INVITED REVIEW

Physiological Reports

Role of macrophages during skeletal muscle regeneration and hypertrophy—Implications for immunomodulatory strategies

Clara Bernard[1] | **Aliki Zavoriti**[1] | **Quentin Pucelle**[2] | **Bénédicte Chazaud**[1] | **Julien Gondin**[1]

[1]Institut NeuroMyoGène, Unité Physiopathologie et Génétique du Neurone et du Muscle, Université Claude Bernard Lyon 1, CNRS UMR 5261, INSERM U1315, Université Lyon, Lyon, France

[2]Université de Versailles Saint-Quentin-En-Yvelines, Versailles, France

Correspondence
Julien Gondin, Institut NeuroMyoGène (INMG), Physiopathologie et Génétique du Neurone et du Muscle (PGNM), CNRS 5261—INSERM U1315—UCBL1, Faculté de Médecine et de Pharmacie, 8 Avenue Rockefeller, 69008 Lyon, France.
Email: julien.gondin@univ-lyon1.fr

Abstract

Skeletal muscle is a plastic tissue that regenerates *ad integrum* after injury and adapts to raise mechanical loading/contractile activity by increasing its mass and/or myofiber size, a phenomenon commonly refers to as skeletal muscle hypertrophy. Both muscle regeneration and hypertrophy rely on the interactions between muscle stem cells and their neighborhood, which include inflammatory cells, and particularly macrophages. This review first summarizes the role of macrophages in muscle regeneration in various animal models of injury and in response to exercise-induced muscle damage in humans. Then, the potential contribution of macrophages to skeletal muscle hypertrophy is discussed on the basis of both animal and human experiments. We also present a brief comparative analysis of the role of macrophages during muscle regeneration versus hypertrophy. Finally, we summarize the current knowledge on the impact of different immunomodulatory strategies, such as heat therapy, cooling, massage, nonsteroidal anti-inflammatory drugs and resolvins, on skeletal muscle regeneration and their potential impact on muscle hypertrophy.

1 | INTRODUCTION

Adult skeletal muscle is a highly plastic organ. Muscle remodels, i.e. adapts to the physical demand, such as during hypertrophy, and regenerates after a damage. The two processes involve different mechanisms (Fukada et al., 2022). Muscle remodeling mainly relies on adaptation of the myofibers while regeneration relies on muscle stem cells (aka satellite cells, MuSCs) that implement adult myogenesis. MuSCs are absolutely required for muscle regeneration (Lepper et al., 2011; Murphy et al., 2011; Sambasivan et al., 2011), but their involvement in remodeling induced by (or consecutive to) skeletal muscle hypertrophy remains a matter of debate (Egner et al., 2016; McCarthy et al., 2011). However, in both situations, MuSCs develop interactions with their neighborhood, which includes inflammatory cells, and particularly macrophages.

Macrophages are known for a long time to be involved in post-injury skeletal muscle regeneration, where they play very important trophic roles for MuSCs and other cells

Bénédicte Chazaud and Julien Gondin equally contributed.

Clara Bernard and Aliki Zavoriti equally contributed.

in the muscle tissue. By extension, macrophages have been investigated in other conditions where muscle remodeling takes place, such as hypertrophy, but the knowledge on their biological functions is far less advanced in that context, both in animal models and human. Here we provide a brief overview on how macrophages regulate muscle regeneration through their interactions with various cell types (references to reviews for more details are given in the text), a prerequisite to understand their role in the regulation of muscle mass. Next, we address for the first time whether and to what extent macrophages are involved in muscle hypertrophy and summarize the recent advances on this topic. Then, we present a brief comparative analysis of the role of macrophages during muscle regeneration versus hypertrophy. Finally, the identification of the biological functions of macrophages in muscle regeneration and remodeling has made possible the rewiring of monitoring inflammation after an injury. Thus, the last section of this review focuses on the management of the inflammatory response through the application of widespread methods used by athletes to improve muscle recovery after an injury or to promote muscle hypertrophy in response to exercise.

2 | MACROPHAGES AND SKELETAL MUSCLE REGENERATION

Adult skeletal muscle regenerates *ad integrum* after an injury induced by myotoxic agents (cardiotoxin, BaCl2) (Arnold et al., 2007; Hardy et al., 2016), physical muscle injury (e.g., crush or freeze injury) (Hardy et al., 2016; Takagi et al., 2011) or unaccustomed exercise (also referred to as exercise-induced muscle damage [EIMD]) (Saclier et al., 2013). The role of macrophages in muscle regeneration is first presented in various animal models of injury and then in response to EIMD in humans.

2.1 | Animal studies

Skeletal muscle regeneration relies on MuSC properties, that exit quiescence, expand, differentiate and fuse to form new functional myofibers. The adult myogenic program is tightly controlled by myogenic transcription factors which expression follows an intrinsic pattern (Yin et al., 2013). However, the last decade evidenced that the MuSC environment impacts on that program: well-orchestrated environmental cues support each step of myogenesis for a harmonious and efficient regeneration. On the contrary, alteration of some properties of that environment delays or impairs the myogenic program, thus the regeneration process as a whole (Dumont et al., 2015).

After an injury, neutrophils are the first immune cells to invade the injury site where they attract monocytes and start the inflammatory response. $Ly6C^{pos}CCR2^{pos}CX3CR1^{lo}$ circulating monocytes enter the damaged muscle area through the CCL2-CCR2 axis (Contreras-Shannon et al., 2007; Martinez et al., 2010; Warren et al., 2005) as well as via the complement protein C3a-C3aR axis (Zhang et al., 2017). After their arrival in the damaged muscle, they become $Ly6C^{pos}$ pro-inflammatory macrophages. They promote the expansion of MuSCs by stimulating their proliferation through the delivery of soluble factors and metabolites (among which IL-6, TNFα, VEGF, IGF1, IL1β; IL13, NAMPT, glutamine) (Baht et al., 2020; Lu et al., 2011; Ratnayake et al., 2021; Shang et al., 2020; Tonkin et al., 2015), they also control the number of fibro-adipo-progenitors (FAPs) by triggering their apoptosis through TNFα production (Lemos et al., 2015). The pro-inflammatory phase is usually short (2–3 days) and ends with the shift towards the acquisition of an anti-inflammatory/restorative phenotype by macrophages. A major role of macrophages is efferocytosis, which consists in the phagocytosis of dead cells and cell debris. This process induces the resolution of inflammation by the modification of the macrophage inflammatory status. Engulfment of dead myoblasts stops the secretion of TNFα and induces that of anti-inflammatory effectors like TGF-β (Arnold et al., 2007). The macrophage shift is characterized by metabolic changes, from a glycolytic to oxidative and glutamine metabolism (for reviews see Juban & Chazaud, 2017, 2021). $Ly6C^{neg}$ restorative macrophages exert a series of functions while dampening the inflammatory response. They stimulate terminal myogenic differentiation and fusion of MuSCs via the secretion of factors (IGF-1, TGF-β, GDF3...) (Arnold et al., 2007; Lu et al., 2011; Saclier et al., 2013; Varga, Mounier, Patsalos, et al., 2016). Restorative macrophages also promote angiogenesis, they stimulate fibroblastic cells for extracellular matrix (ECM) remodeling and secrete themselves ECM components (e.g., proteoglycans, matricellular proteins and assembly proteins) (Varga, Mounier, Horvath, et al., 2016, for reviews see Panci & Chazaud, 2021; Singh & Chazaud, 2021). The kinetics of the inflammatory response is fundamental for the good orchestration of myogenesis and the surrounding supportive biological processes. Indeed, inhibition of the molecular pathways involved in the macrophage shift (including to date IGF-1, MKP1-p38, SRB1-ERK, AMPK, C/EBPβ, STAT3, NFIX, BACH1) leads to a loss of acquisition of the restorative phenotype and therefore to an impairment in muscle regeneration (Baht et al., 2020; Mounier et al., 2013; Patsalos et al., 2022; Perdiguero et al., 2011; Saclier et al., 2020; Tonkin et al., 2015; Zhang et al., 2019, for review see Juban, 2021). Moreover, too early acquisition of the

restorative phenotype also leads to an altered muscle regeneration (Bencze et al., 2012; Caratti et al., 2020; Cheng et al., 2008; Giannakis et al., 2019; Perdiguero et al., 2011; Rigamonti et al., 2013). In vitro analyses using human cells showed that pro-inflammatory macrophages inhibit differentiation and fusion of MuSCs (Saclier et al., 2013), suggesting that in vivo too early appearance of restorative macrophages triggers too early myogenic differentiation/fusion, thus preventing an efficient muscle regeneration.

The various models of skeletal muscle injury, notably in the mouse, have allowed the development of an important field of investigations to understand the cellular and molecular mechanisms regulating adult skeletal muscle regeneration (Figure 1a). A limitation of these models is the extent of the damage, that covers the whole muscle (or most part of it). Thus, although very reproducible and robust, these models poorly represent injuries occurring in humans and are non-physiological.

2.2 | Human studies

Our knowledge on the role of macrophages in skeletal muscle regeneration mainly relies on animal models of muscle injury. In human, the accumulation of macrophages after EIMD is still a matter of debate. This is due to the unclear definition of EIMD and the related use of indirect markers, such as delayed onset muscle soreness and/or blood sampling parameters (e.g., creatine kinase), that mainly reflect symptoms of muscle damage and not necessarily its occurrence and/or magnitude. The evaluation of maximal force loss and recovery after exercise allows to overcome these limitations and is now considered as the best indirect marker of muscle damage severity (Paulsen et al., 2012; Warren et al., 1999). Indeed, a mild muscle damage, which is defined as a force decline of no more than 20% (during the first 24 h) and/or full recovery within 48 h, does not lead to macrophage infiltration in all (Bourgeois et al., 1999; Féasson et al., 2002; Malm et al., 2004) but one (Crameri et al., 2007) studies. Interestingly, a myofiber self-repair/remodeling mechanism, independent of MuSCs, has been recently demonstrated in response to a mild injury (Roman et al., 2021), even though the lack of force measurements does not allow to determine the magnitude of muscle damage in this context. On the contrary, severe muscle damage, which corresponds to a force loss over 50% and/or recovery lasting longer than 1 week, is consistently associated with leukocyte/macrophage infiltration (Beaton et al., 2002; Child et al., 1999; Hikida et al., 1983; Jones et al., 1986; Lauritzen et al., 2009; Mackey et al., 2016; Paulsen et al., 2010; Round et al., 1987; Saclier et al., 2013), thereby illustrating a link between macrophage accumulation and the magnitude of muscle damage. In agreement with animal investigations, severe EIMD in human leads to an accumulation of pro-inflammatory macrophages (i.e., $CD68^{pos}iNOS^{pos}$ and $C68^{pos}COX2^{pos}$ cells) in regenerating areas containing proliferating MuSCs while restorative macrophages (i.e., $CD68^{pos}Arg1^{pos}$, $CD206^{pos}$ and $CD163^{pos}$ cells) were mainly located in areas containing differentiating MuSCs (Saclier et al., 2013). Finally, an elegant analysis of human single myofibers after EIMD shows macrophage infiltration in both necrotic and regenerating muscle regions to remove damaged tissue and promote myogenesis, respectively (Mackey & Kjaer, 2017). These findings illustrate the key role of macrophages in the regulation of MuSC fate to ensure effective human muscle regeneration after a severe injury.

3 | MACROPHAGES AND SKELETAL MUSCLE HYPERTROPHY

Adult skeletal muscle has a remarkable capacity to adapt to increased mechanical loading/contractile activity by increasing its mass and/or myofiber size, a phenomenon commonly refers to as skeletal muscle hypertrophy. Hypertrophy occurs when the rate of protein synthesis exceeds the rate of protein degradation and efforts have been made to decipher the cellular and molecular events occurring within the myofiber and resulting in such increased proteostasis. However, evidence is emerging that efficient muscle hypertrophy is also due to an increased number of myonuclei (i.e., myonuclear accretion) triggered by the fusion of MuSCs with the overloaded myofibers (Egner et al., 2016; McCarthy et al., 2011; Goh & Millay, 2017; Fukuda et al., 2019). So far, the role of macrophages in regulating skeletal muscle mass, possibly through interactions with the myofiber and/or other cell types such as MuSCs, is still poorly understood. Indeed, most of the existing studies have focused their interest on the kinetics of inflammatory cell accumulation in the muscle after a single session of EIMD leading to muscle damage, thus triggering muscle regeneration as described above. On the contrary, the impact of resistance training programs (i.e., multiple bouts of exercise) on the inflammatory process has been scarcely investigated as compared with the plethora of studies focusing on muscle regeneration. Considering that muscle hypertrophy could occur in the absence of substantial muscle injury (Fukada et al., 2022; Fukuda et al., 2019), there is a need for improving our understanding of how and to what extent macrophages are involved in the regulation of skeletal muscle mass.

In the following section, the role of macrophages on skeletal muscle hypertrophy will be first addressed on the

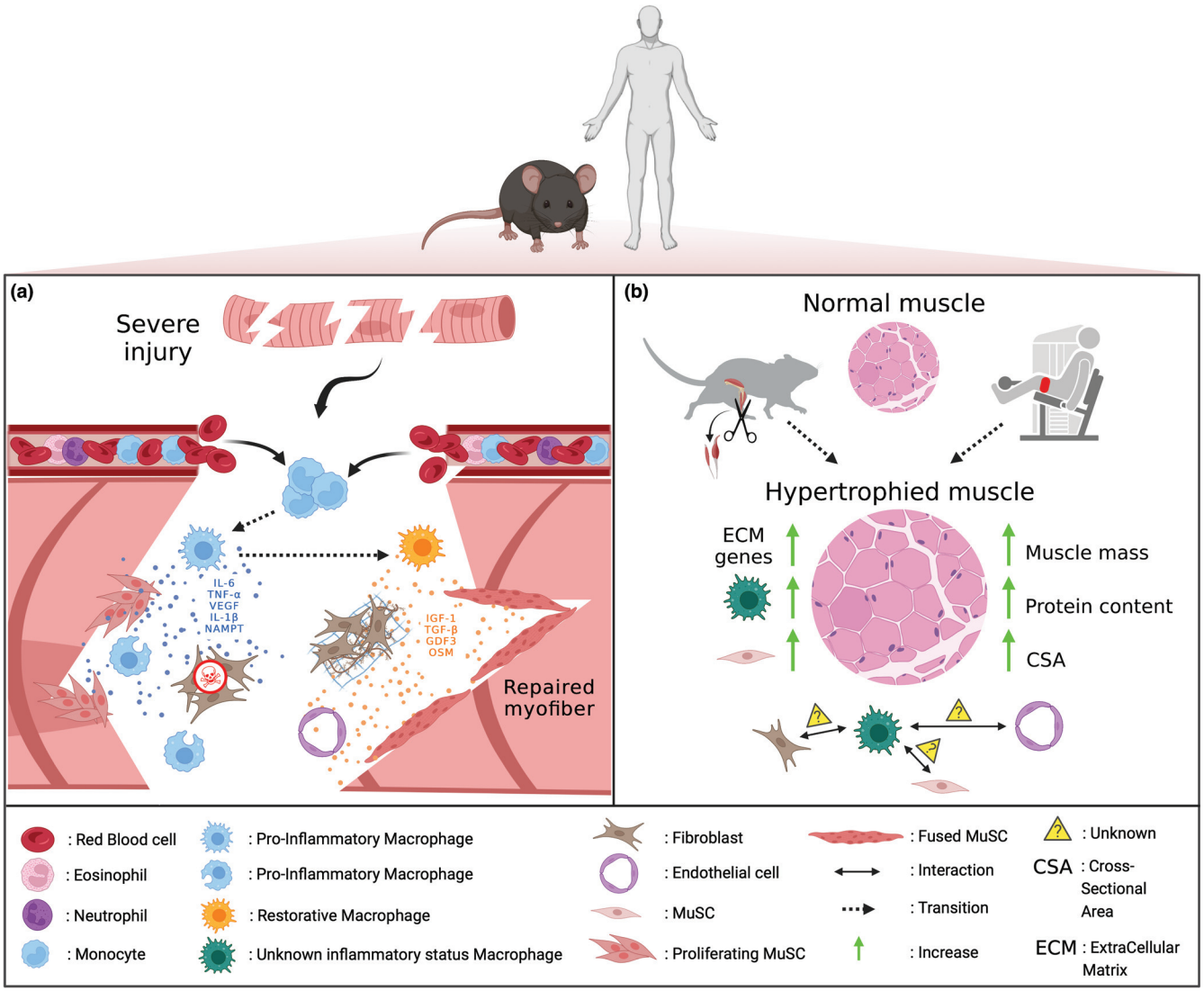

FIGURE 1 Role of macrophages during muscle regeneration and hypertrophy in animals and human. (a) after a severe injury usually induced by injection of a snake venom (e.g., cardiotoxin or notexin) into the mouse muscle, blood circulating monocytes enter the injured muscle and become pro-inflammatory macrophages. They secrete cytokines such as IL-6, TNF-α, VEGF, IL-1β and NAMPT to promote the proliferation of MuSCs and apoptosis of fibroblasts. Thanks to the phagocytosis of cell debris, pro-inflammatory macrophages switch to become restorative macrophages and deliver other effectors such as IGF-1, TGF-β, GDF3 and OSM. They stimulate differentiation and fusion of MuSCs to repair the injured myofibers and promote angiogenesis and extracellular matrix remodeling. Human investigations also reported an accumulation of pro-inflammatory macrophages in regenerating areas containing proliferating MuSCs while restorative macrophages were mainly located in areas containing differentiating MuSCs after a severe exercise-induced muscle damage. (b) Hypertrophy can be induced experimentally by synergistic ablation of hindlimb muscles in animals or by resistance training in human, which is sometimes performed under blood flow restriction (the pneumatic cuff placed around the thigh is represented in red). These models are associated with an increase in muscle mass, myofiber cross-sectional area, protein content, number of MuSCs, expression of genes involved in the regulation of extracellular matrix and macrophage infiltration. However, the inflammatory status of macrophages is not known in this context and how they interact with MuSCs, fibroblasts and endothelial cells to regulate changes in muscle mass has to be determined.

basis of animal experiments. Then, human studies describing the effects of resistance training on muscle mass and macrophages will be presented. We chose to present only the results obtained from healthy muscle so experiments involving atrophic (e.g., unloading/reloading) or diseased muscle will not be considered.

3.1 | Animal studies

The most common animal model to study hypertrophy in rodents consists in the surgical ablation of synergistic hindlimb muscles, usually *gastrocnemius* and *soleus* muscles, leaving only the remaining *plantaris* muscle to perform

the daily functional activities (Armstrong et al., 1979). Such compensatory hypertrophic model (i.e., synergist ablation-induced muscle hypertrophy) increases the mechanical loading (i.e., overload) on the *plantaris* muscle and can lead to a two-fold increase in muscle mass and protein content according to two phases (Armstrong et al., 1979; DiPasquale et al., 2007; Marino et al., 2008). The early changes in muscle mass occurring with the first 3 days post-overload are mainly related to an increase in muscle water content due to edema (Armstrong et al., 1979). Then, an increase in myofiber cross-sectional area (CSA), illustrating skeletal muscle hypertrophy, usually takes places within 14 days of overload (Kandarian & White, 1989; Marino et al., 2008). Interestingly, these two phases are associated with leukocyte invasion in the muscle interstitium (Armstrong et al., 1979). The number of macrophages progressively increases, reaching a peak at day 5–7 (DiPasquale et al., 2007; Marino et al., 2008; Novak et al., 2009) and is either going back to control values (DiPasquale et al., 2007; Novak et al., 2009) or being still present (Marino et al., 2008) at day 14. These discrepancies could be related to an inter-laboratory variability in the management of the mouse model of synergist ablation. In addition, immunohistochemical analysis of macrophage-specific antigens indicates that both pro-inflammatory ($ED1^{pos}$) and anti-inflammatory ($ED2^{pos}$) subpopulations of macrophages increase during muscle hypertrophy, at least in aged rats (Thompson et al., 2006). Overall, synergist ablation-induced muscle hypertrophy is characterized by a sequential infiltration then disappearance of macrophages.

Growing evidence illustrates the potential role of macrophages in hypertrophy. The first evidence was provided by DiPasquale and colleagues (DiPasquale et al., 2007) who showed that the magnitude of skeletal muscle hypertrophy is reduced after depletion of macrophages induced by intraperitoneal injection of clodronate liposomes. It was also demonstrated that hypertrophy is blunted and accumulation of macrophages is reduced in mice deficient in urokinase-type plasminogen activator (uPA), which is in agreement with the role of uPA in macrophage chemotaxis (Bryer et al., 2008), ECM remodeling (Chapman et al., 1988) and the production of growth factors (Bryer et al., 2008). It has been recently showed that RhoA, a small GTPase protein produced by overloaded myofibers, leads to muscle hypertrophy mainly through MuSC fusion (Noviello et al., 2022). Overload-induced myonuclear accretion was ascribed to macrophage recruitment favored by the expression of the chemokines CCL3/CX3CL1 and to ECM remodeling promoted by the upregulation of *Mmp9/Mmp13/Adam8* mRNA expression. Of note, clodronate liposomes-induced depletion of macrophages blunts myofiber growth and diminishes both the number and fusion of MuSCs, illustrating the role of macrophages in the fate of MuSCs in response to muscle overload (Noviello et al., 2022). However, it is noteworthy that the above-mentioned administration of clodronate liposomes results only in a partial reduction in macrophage content, so it remains to determine whether hypertrophy is totally prevented when all macrophages are lacking. Interestingly, mice deficient for β2-integrin (CD18) that is required for leukocyte extravasation, display lower muscle mass and myofiber CSA as compared with WT mice after synergist ablation (Marino et al., 2008). In addition, gene expression of both *MyoD* and *Myogenin* is lower in $CD18^{-/-}$ mice as compared with WT, as well as the proportion of proliferating MuSCs (i.e., $BrdU^{pos}Desmin^{pos}$ cells). However, these effects are not related to a reduction in the number of macrophages because $CD18^{-/-}$ mice actually show a higher macrophage content at day 7 after muscle overload as compared with WT. It remains to determine whether the macrophage status (i.e., pro- vs. anti-inflammatory) and/or the reduced number of neutrophils observed in the absence of CD18 play a role in the defective response to mechanical overload. Finally, Murach and colleagues (Murach et al., 2021) recently demonstrated that MuSCs modulate the expression of several chemokine genes (i.e., *Ccl2*, *Ccl5*, *Ccl7* and *Cxcl1*) in immune cells, FAPs and endothelial cells through extracellular vesicle-mediated miR-206/Wisp1 axis. This indicates a thin and dynamic regulation between myogenic and non-myogenic cells to promote muscle hypertrophy (Figure 1b).

However, and importantly to be pointed out, the large number (i.e., around 25%–30%) of centrally nucleated myofibers (a marker of newly formed myofibers) observed 7 days post-surgery (Marino et al., 2008) suggests that the accumulation of macrophages may be related at least in part to synergist ablation-induced muscle injury, that would trigger regeneration. In addition, even though the use of tenotomy-induced muscle overload could limit the extent of muscle injury (Fukuda et al., 2019; Kaneshige et al., 2022), the magnitude and the rate of muscle hypertrophy (i.e., +30% of muscle mass in 1–3 weeks post-surgery) (Fukuda et al., 2019; Kaneshige et al., 2022; Noviello et al., 2022) largely exceeds what can be achieved in conventional resistance training programs (i.e., +5%–10% of muscle mass after 20–24 weeks of training) (Reggiani & Schiaffino, 2020). Although an increased number of macrophages was reported in the absence of histological alterations after electrically-evoked concentric contractions (McLoughlin et al., 2003), the impact of the corresponding experimental protocols on muscle mass (that would have defined hypertrophy) was not documented. On that basis, the use of newly developed mouse models of exercise-induced muscle hypertrophy

relying on weight pulling mimicking resistance exercise in human (Zhu et al., 2021) or neuromuscular electrical stimulation-induced myonuclear accretion (Zavoriti et al., 2021) could be particularly relevant to decipher the role of macrophages in this context.

3.2 | Human studies

Only a few studies focused on the influence of macrophages on human skeletal muscle hypertrophy following resistance training protocols. It was demonstrated that the increased number of $CD11b^{pos}/CD206^{pos}$ macrophages *per* myofiber is correlated with changes in myofiber CSA, in MuSC number, in transcription of two growth factor genes (*HGF* and *IGF-1*) and in the expression of ECM related genes (i.e., *MMP14*, *SERPIN1*, *SPARC*, *ELN*, *COL5A1*, *COL6A1*, *TGFβ1*, *LOX*) in human skeletal muscle after cycling exercise training (Walton et al., 2019). In agreement with animal studies, this suggests an active role of macrophages in the regulation of MuSCs and ECM to promote muscle growth. More recently, macrophage (i.e., $CD11^{pos}CD206^{pos}$) abundance increases in older adults submitted to 14 weeks of progressive resistance training (PRT) and is positively correlated to changes in muscle fiber size, capillary density, MuSC abundance and number of myonuclei (Peck et al., 2022), the latter suggesting MuSC fusion. Strikingly, matrix metalloproteinase 14 (*Mmp14*) gene is one of the most upregulated genes following PRT and is strongly associated with macrophage number (Peck et al., 2022), indicating that macrophages might be the main contributor of MMP14 secretion. The authors also showed in vitro that mouse macrophages treated with conditioned medium of electrically stimulated myotubes increase the expression of leukemia inhibitory factor (*Lif*) and *Mmp14* and increase collagen degradation (Peck et al., 2022). These data strongly implicate a potential role of macrophages in ECM remodeling and collagen homeostasis that could facilitate skeletal muscle adaptations to PRT through a muscle-cell macrophage axis involving LIF and MMP14. Multiple linear regression analyses also revealed that, before PRT, collagen content/organization and macrophage abundance ($CD11^{pos}CD206^{neg}$) were trending to be associated with poor muscle growth potential (Long et al., 2022). These findings suggest that both collagen organization and macrophage content influence overall muscle growth.

In the same way, healthy individuals undergoing a 4-week-heavy resistance exercise training show an increased content of macrophages in the muscle endomysium near the myotendinous junction (Jakobsen et al., 2017). This elevation is accompanied by increased levels of tenascin-C and collagen content, indicating matrix remodeling, yet it was not shown whether the exercise training protocol induces changes in myofiber CSA (Jakobsen et al., 2017). Two recent studies demonstrated that low-load resistance training performed under blood flow restriction leads to robust muscle hypertrophy (i.e., 20%–40% increase in myofiber CSA) associated with an increase in the number of MuSCs and in the number of myonuclei *per* myofiber (Bjørnsen et al., 2019; Nielsen et al., 2012). Although the number of macrophages slightly increases during the first week of training, when the protocol leads to muscle injury (indirectly assessed by increased creatine kinase [CK] levels) (Bjørnsen et al., 2021), macrophage accumulation mainly occurs 3 weeks after the beginning of the training protocol (Bjørnsen et al., 2021; Nielsen et al., 2017). In agreement with their role in supporting muscle regeneration, macrophages could be required for the last step of myogenesis (e.g., fusion) or for interaction with other cell types such as endothelial cells or fibroblasts to promote angiogenesis and/or ECM remodeling after resistance training programs. Finally, considering that *CCL2* gene expression is increased after repeated bouts of exercise or during skeletal muscle regeneration following injury (Contreras-Shannon et al., 2007; Hubal et al., 2008; Shireman et al., 2007), genetic variations occurring in *CCL2* and its receptor CCR2 were investigated in relation to resistance training-induced changes in skeletal muscle size and strength (Harmon et al., 2010). In individuals undergoing a 12-week resistance-training program, one variant (i.e., rs1024610) in *CCL2* is associated with an increase in maximal voluntary strength, while no variant is associated with changes in skeletal muscle size in response to this training program (Harmon et al., 2010).

Overall, macrophages are mobilized into the skeletal muscle in response to resistance training programs in humans, even though the molecular regulators involved in muscle hypertrophy are still to be determined.

4 | COMPARATIVE ANALYSIS OF THE ROLE OF MACROPHAGES IN MUSCLE REGENERATION VERSUS HYPERTROPHY

Muscle injury leads to myofiber necrosis (at least in animal models) that triggers a massive infiltration of both neutrophils and macrophages at the damaged site. On the contrary, necrosis/death of myofibers may be minimized/prevented in response to muscle overload (Fukuda et al., 2019; Kaneshige et al., 2022), resulting in a lower infiltration of macrophages and absence of efferocytosis. The inflammatory status of macrophages in response to muscle overload remains to be determined. Indeed, a clear delineation between pro-inflammatory and

restorative macrophages has been recently questioned in response to resistance exercise in humans (Jensen et al., 2020). However, the use of CD68, CD11b and CD206 markers does not allow to classify macrophage phenotype into pro-inflammatory and restorative macrophages. Finally, while after a damage, myofibers release their internal content, triggering the inflammatory response, overloaded myofibers secrete various factors such as IL-6 (Guerci et al., 2012; Serrano et al., 2008), IL-4 (Guerci et al., 2012), RhoA (Noviello et al., 2022), that can dynamically regulate the interactions between macrophages, MuSCs and mesenchymal progenitors (Noviello et al., 2022) to promote muscle hypertrophy. Overall, the use of non-damaging models of muscle hypertrophy would allow to improve our understanding of the role of macrophages and their interactions with neighboring cells in the regulation of muscle mass.

5 | MANAGEMENT OF THE INFLAMMATORY RESPONSE

Several strategies have been assessed to modulate/reduce the inflammatory response after either acute or chronic exercise training. Among them, cooling, heating, massage and nonsteroidal anti-inflammatory drugs (NSAIDs) are widespread methods used by athletes. More recently, a class of molecules named resolvins (or specialized pro-resolving mediators) was shown to play a key role in the resolution of inflammation in animal models of regeneration. In this section, we will primarily summarize the current knowledge on the impact of heat therapy, cooling, massage, NSAIDs and resolvins on skeletal muscle regeneration and the known underlying cellular mechanisms (Figure 2). We will also briefly discuss how these immunomodulatory strategies could affect muscle growth in response to overload. Readers can refer to excellent reviews to get a broader picture on how these therapeutic strategies impact other processes involved in skeletal muscle homeostasis (e.g., protein synthesis and degradation, adaptations to endurance/resistance training...) (Costello et al., 2015; Fennel et al., 2022; Howatson & van Someren, 2008; Hyldahl & Peake, 2020; McGorm et al., 2018; Urso, 2013; Van Pelt et al., 2021).

5.1 | Cooling

Cooling induced by topical icing, cold-water immersion or cryotherapy is largely used by athletes to prevent and/or treat subjective (e.g., muscle soreness) and/or objective symptoms (e.g., decrement in performance) of EIMD. However, such strategy may actually alter skeletal muscle regeneration (Shibaguchi et al., 2016; Takagi et al., 2011). Cooling decreases the number of macrophages in various models of muscle damage (Miyakawa et al., 2020; Takagi et al., 2011; Vieira Ramos et al., 2016) as well as it delays the shift towards restorative macrophages, as illustrated by a reduced number of $F4/80^{pos}CD206^{pos}$ cells, a lower IL-10 expression and a higher TNFα expression at day 5 and day 7 post-EIMD, respectively (Kawashima et al., 2021). Indeed, IL-10 participates to the shift in macrophage phenotype (Deng et al., 2012) while pro-inflammatory macrophages robustly express TNFα. In addition, cooling slows the disappearance of necrotic myofibers, suggesting an impairment of efferocytosis (Kawashima et al., 2021). The disturbed phenotypic transition of macrophages could therefore be involved in the delayed activation of MuSCs (Kawashima et al., 2021) and the increase in collagen deposition (Shibaguchi et al., 2016; Takagi et al., 2011), eventually resulting in a reduced myofiber CSA (Kawashima et al., 2021; Takagi et al., 2011).

Human studies further illustrate the lack of functional effects of cooling on muscle repair. Indeed, such strategy do neither accelerate muscle strength recovery nor reduce muscle soreness and CK activity after EIMD (Guilhem et al., 2013; Howatson et al., 2005; Tseng et al., 2013), the latter being even higher after icing as compared with a sham procedure (Tseng et al., 2013). Finally, infiltration of macrophages, changes in *Mac1* (*CD11B*, *ITGAM*), *CD163* and cytokine/chemokine mRNA expression (i.e., *IL1B*, *TNF*, *IL6*, *CCL2*, *CCL4*, *CXCL2*, *IL8* and *LIF*) are similar between cold water immersion and active recovery after a single resistance exercise. However, the moderate increase in CK activity (Peake et al., 2017) and the absence of functional measurements do not allow to ascertain the occurrence of muscle damage in this study. Finally, cold water immersion blunts myonuclear accretion, attenuates the increase in MuSC number and limits myofiber growth in response to strength training (Fyfe et al., 2019; Roberts et al., 2015). It remains however to be determined whether and to what extent these deleterious effects of cooling on muscle hypertrophy are directly due to changes in the number and/or status of macrophages. Overall, contrary to the popular belief and the usual practice, there is so far no evidence regarding the positive effects of cooling application on skeletal muscle regeneration and hypertrophy.

5.2 | Heat therapy

Contrarily to the negative effects of cooling, the use of heat therapy following muscle injury appears as a

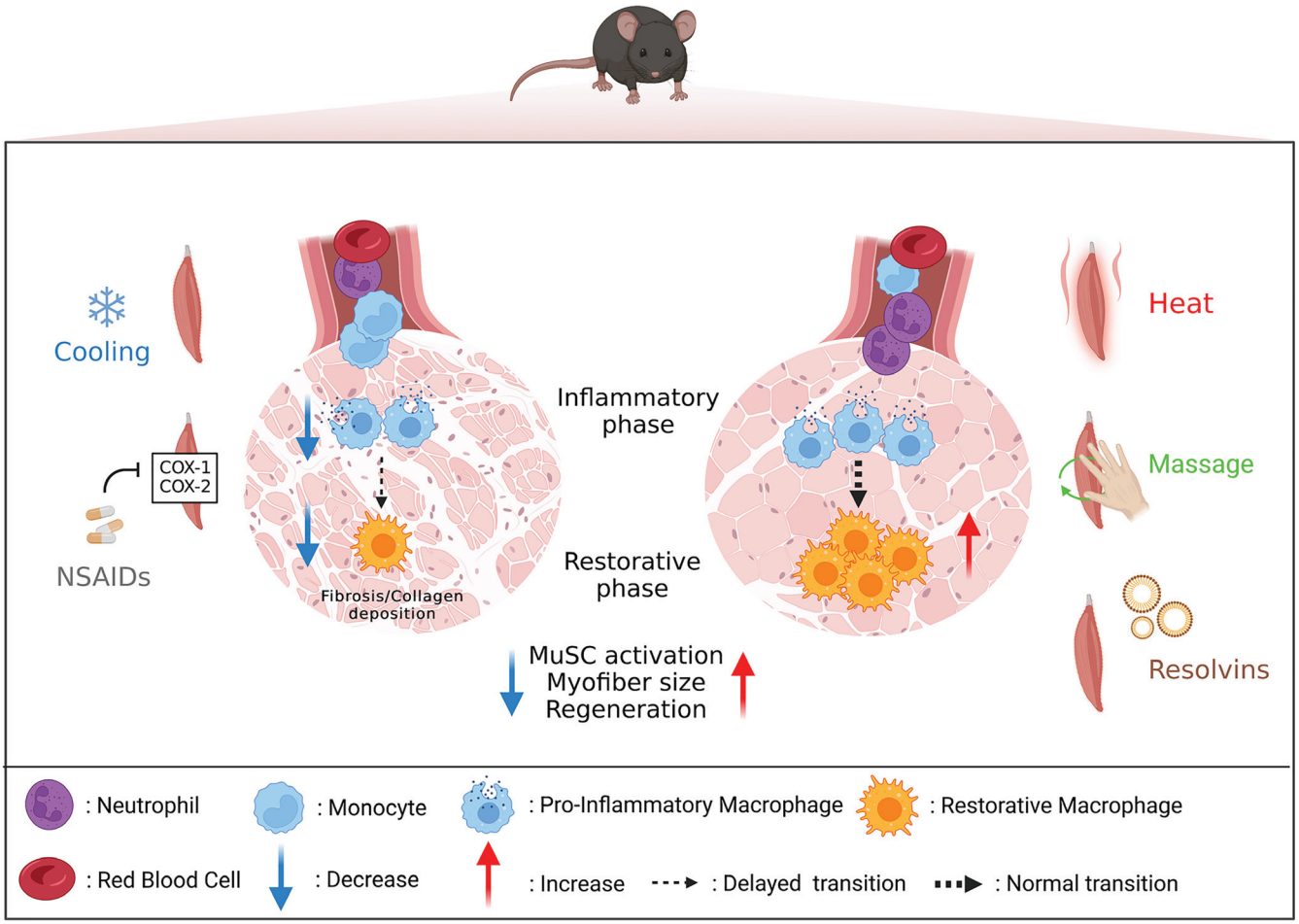

FIGURE 2 Impact of different therapeutic strategies on the muscle regeneration process in animals. Following muscle injury, cooling or administration of nonsteroidal anti-inflammatory drugs administration (NSAIDs) can contribute to muscle regeneration defect and myofiber size decrease. Cooling decreases macrophage number and delays the shift towards anti-inflammatory/restorative macrophages. Similarly, NSAIDs act upstream to reduce or delay macrophage infiltration through the inhibition of cyclooxygenase (COX-1 and COX-2) enzyme activity. As a result of perturbed inflammation, MuSCs are unable to activate properly and to repair damaged muscle fibers leading to the accumulation of necrotic muscle fibers in conjunction with collagen/fibrosis deposition. On the contrary, heating, massage or treatment with resolvins, show beneficial effects on muscle regeneration. Heating results in rapid increase of macrophages capable of resolving faster inflammation. Likewise, massage by applying cyclic movements on the injured muscle contributes to reduce the inflammatory infiltrate and favors early clearance of neutrophils. In addition, resolvins enhance the resolution of inflammation by limiting neutrophil infiltration and increasing macrophage efferocytosis. These mechanisms are associated with a better activation and differentiation of MuSCs.

promising therapeutic approach for promoting skeletal muscle regeneration. Various heat therapies have been used in animal studies such as hot water immersion, exposure to an environmental stress in a dedicated heat chamber or application of packs filled with hot water (Kim, Reid, et al., 2019; Kojima et al., 2007; Oishi et al., 2009; Shibaguchi et al., 2016; Takeuchi et al., 2014). Post-injury heating treatment results in an rapid increase in the number of $ED1^{pos}$ macrophages (Takeuchi et al., 2014), a greater number of MuSCs within the damaged muscle (Kojima et al., 2007; Oishi et al., 2009; Shibaguchi et al., 2016; Takeuchi et al., 2014) and a higher myonuclear accretion (Oishi et al., 2009) together with a faster MyoD and Myogenin protein expression (Hatade et al., 2014; Oishi et al., 2009) in response to crush or toxic injury. This results in a faster muscle regeneration illustrated by a larger myofiber CSA (Oishi et al., 2009; Shibaguchi et al., 2016; Takeuchi et al., 2014), a decrease in intramuscular collagen deposition (Shibaguchi et al., 2016; Takeuchi et al., 2014), and an improved force production after a 3-week treatment in a mouse model of ischemia-induced muscle injury (Kim, Reid, et al., 2019). So far, the cellular mechanisms involved in the beneficial effects of heat therapy on muscle regeneration remain unclear. Heat therapy triggers the expression of several members of the heat shock protein family (HSPs) such as *HSP25*, *HSP27*, *HSP60*, *HSP70*, *HSP72*, *HSP90* (McGorm et al., 2018) with some of them being differentially expressed in the various

stages of myogenesis, suggesting specific roles for individual HSPs in this process (Thakur et al., 2019). For instance, in vitro studies showed that inhibition of HSP70 impairs myoblast differentiation (Fan et al., 2018). Interestingly, *Cd11b* and *Cd68* mRNA expression is reduced in the first 4 days post-injury in the absence of *Hsp70* while sustained inflammation and necrosis, collagen deposition and impaired myofiber regeneration persist several weeks post-injury in Hsp70-deficient mice (Senf et al., 2013). In addition, heat induces the release of IL-6 protein from myoblasts in a temperature-dependent manner. IL-6, which is released by myofibers in response to exercise (Pedersen & Febbraio, 2008), is known as a pleiotropic cytokine associated with the regulation of immune responses.

The substantial differences in the study design (i.e., type of exercise, heating method...) led to conflicting findings in human with studies showing either improved (Vaile et al., 2008) or unchanged (Jayaraman et al., 2004; Kuligowski et al., 1998; Pournot et al., 2011) functional performance after heating post-EIMD. In addition, while heat therapy leads to a greater resistance to fatigue after EIMD resulting in severe functional alterations (i.e., 40%–50% reduction in voluntary strength 1 day after EIMD), it does not influence maximal voluntary strength recovery, nor macrophage content, capillarization and HSP expression (Kim, Kuang, et al., 2019). Overall, the discrepancies between animal and human studies may be related to the heating methods (whole-body vs. localized), timing (pre, during, post-intervention) and duration (single or repeated bouts) of interventions, underlying the need for deciphering the optimal parameters for improving or accelerating muscle regeneration. The potential benefit of heat therapy on the regulation of muscle growth has been recently highlighted (Kim et al., 2020) but the role of macrophages is still unknown.

5.3 | Massage

Massage or mechanical/manual therapy through cyclic muscle tissue compression is a widespread method used by athletes aiming at dampening muscle soreness and/or improving recovery after a strenuous exercise (Davis et al., 2020; Howatson & van Someren, 2008). Indeed, skeletal muscle is composed of various cell types than can sense and respond to mechanical loads, a physiological process refers to as mechanotransduction (Khan & Scott, 2009). Evidence is emerging illustrating the immunomodulatory effects of massage on skeletal muscle homeostasis. In vitro experiments showed that mechanical deformation applied on a scaffold promotes the acquisition of anti-inflammatory/restorative phenotype by macrophages (Ballotta et al., 2014). Interestingly, the application of controlled cyclic compressive loading in uninjured muscle leads to the expression of genes associated with the immune response together with the infiltration of $CD68^{pos}$ and $CD163^{pos}$ cells in a load-dependent manner (Waters-Banker et al., 2014). Several animal studies further demonstrated that four consecutive days of cyclic compression decreases the infiltration of leukocytes/macrophages and facilitates force recovery after EIMD (Butterfield et al., 2008; Haas, Butterfield, Abshire, et al., 2013; Haas, Butterfield, Zhao, et al., 2013). The effectiveness of cyclic compression on muscle regeneration is dependent on the massage timing (i.e., in favor of an immediate application as compared with a delayed intervention; Haas, Butterfield, Abshire, et al., 2013), as well as on the magnitude and frequency of mechanical loading (Haas, Butterfield, Zhao, et al., 2013). In addition, the application of a controlled massage-like treatment after severe muscle injury resulting from notexin injection and hindlimb ischemia attenuates interstitial fibrosis, reduces inflammatory infiltrate, diminishes the proportion of pro-inflammatory $CCR7^{pos}$ macrophages, increases myofiber CSA and improves muscle force 14 days after injury (Cezar et al., 2016). It was suggested that in vivo tissue compression could modulate the inflammatory status of macrophages, reduce the adhesion of pro-fibrotic macrophages and accelerate immune cell and/or metabolic waste product removal through an increased fluid transportation (Cezar et al., 2016). However, a recent study showed that cyclic muscle tissue compression-induced functional improvement is not related to changes in macrophage content and/or inflammatory status but ascribed to an early clearance of neutrophils resulting in a reduction of the expression of several cytokines such as MMP9 and CCL3 that reduce the proliferation and/or promote the differentiation of MuSCs in vitro (Seo et al., 2021). These discrepancies are not easy to explain but could be related to different modalities of tissue compression (electromagnetic linear actuator vs. magnetic actuation of biphasic ferrogel scaffolds) and/or differences in the applied mechanical loads (Cezar et al., 2016; Seo et al., 2021). The use of precise and well-controlled massage-like treatment to animals (rabbits, rats and mice) (Haas, Butterfield, Abshire, et al., 2013; Hunt et al., 2019; Seo et al., 2021) should allow to improve our understanding on the impact of cyclic muscle tissue compression on the complex interaction between immune cells and neighboring cells. Human investigation also revealed that massage attenuates the production of the inflammatory cytokines TNFα and IL-6 and mitigates the nuclear accumulation of the p65 subunit of nuclear factor kB after a cycling exercise until exhaustion (Crane et al., 2012). However, IL-6 can be produced by other cells (e.g., myofibers; Chow et al., 2022; Guerci et al., 2012; Serrano et al., 2008) than macrophages.

It is therefore unclear how and to what extent massage really improves muscle regeneration in humans through the modulation of the inflammatory response inasmuch as the investigations were also limited to the first 3 h post-exercise. Finally, massage-induced mechanotransduction could be beneficial for increasing muscle mass. For instance, RhoA, which controls the expression of MMPs and of macrophage chemoattractants (Noviello et al., 2022), also plays a key role in mechanotransduction by translating physical forces into biochemical signaling pathways and activating specific transcription factors. In addition, it was demonstrated that the expression of the mechanotransduction pathway Yap/Taz in mesenchymal progenitor cells of loaded muscles promotes MuSC proliferation, through a thrombospondin-1/CD47 axis (Kaneshige et al., 2022). Massage could therefore impact macrophages and their microenvironment to promote muscle growth, even though additional studies are warranted in this context.

5.4 | NSAIDs

NSAIDs, a class of medication reducing inflammatory processes through the inhibition of cyclooxygenase (COX-1 and COX-2) enzyme activity which decreases prostaglandin production from arachidonic acid, are excessively used by athletes for both prophylactic and therapeutic purposes (Gorski et al., 2011; Tscholl et al., 2015). Although a NSAID treatment administrated immediately or within 6 h (1–2 times a day for 2–7 days) after muscle injury in mice provides a short-term functional improvement (Lapointe et al., 2002; Mishra et al., 1995; Obremsky et al., 1994), a subsequent decrement in muscle function is observed in the late phase of muscle regeneration (i.e., 28 days post-injury) (Mishra et al., 1995). Indeed, most of the animal studies revealed that NSAIDs negatively affect muscle regeneration by reducing/delaying macrophage infiltration (Almekinders & Gilbert, 1986; Lapointe et al., 2002) and promoting fibrosis/collagen deposition via the upregulation of TGF-β1 expression (Shen et al., 2005). The negative effects of NSAIDs are dependent of COX-2 activity as illustrated by the altered muscle regeneration in mice deficient for COX2 (Bondesen et al., 2004; Shen et al., 2006) or treated with selective COX-2 inhibitors (Bondesen et al., 2004; Shen et al., 2005) and the preserved muscle regeneration in mice treated with a selective COX-1 inhibitor (Bondesen et al., 2004). This could be ascribed to the role of COX-2 in macrophage chemotaxis (Reding et al., 2006) and in uPA activity. It was further demonstrated that prostaglandin E2 plays a key role in the proliferation of MuSCs (Ho et al., 2017) and that NSAIDs may exert a negative effect on MuSC fate in vitro (Liao et al., 2019) and in vivo (Ho et al., 2017). Overall, a consensus is emerging on the deleterious effects of NSAIDs in animal models of skeletal muscle regeneration even though it remains to be determined how they disturb cellular interactions in this context.

Contrarily to animal experiments, findings are still controversial regarding the role of NSAIDs after EIMD in humans. These discrepancies could be related, at least in part, to the magnitude of histological alterations (e.g., number of desmin-negative myofibers) and the extent of macrophage infiltration which can be less severe in human as compared with animals (see Section 1). It has been consistently demonstrated that NSAID treatment has no effect on the number of macrophages (Mikkelsen et al., 2009; Paulsen et al., 2010; Vella et al., 2016) or on the mRNA levels of *Cd68* (Mackey et al., 2016), suggesting that the effects of NSAIDs on human muscle function are not necessarily mediated by the regulation of immune cells. Interestingly, NSAIDs could affect the fate of MuSCs after exercise, even though this is not a universal finding (Paulsen et al., 2010). Two studies reported that NSAIDs attenuate the increase of MuSC number after voluntary endurance or eccentric exercise that are not associated with overt signs of muscle injury/regeneration (e.g., absence of desmin-negative myofibers or embryonic myosin heavy chain positive myofibers) (Mackey et al., 2007; Mikkelsen et al., 2009), illustrating a role for the COX pathway in the regulation of MuSC activity in humans. This is consistent with in vitro studies showing that prostaglandins are involved in the fusion of primary chick myoblasts (Zalin, 1977). On the contrary, a greater increase in the proportion of MuSCs was observed after administration of NSAIDs as compared with placebo 7 days after a severe muscle injury induced by electrical stimulation applied during lengthening contractions (Mackey et al., 2016). In addition, NSAIDs induce a faster muscle repair as illustrated by the return of both MuSC content and ECM gene expression to baseline values, suggesting dynamic interactions between MuSCs and fibroblastic cells while the role of macrophages is not described in this context. Overall, one could assume that NSAIDs differentially impact macrophages and their interactions with neighboring cells in damaging versus non-damaging conditions. However, independently of the extent of injury, NSAIDs seem to fasten muscle function recovery when assessed 24–48 h post exercise (Bourgeois et al., 1999; Hasson et al., 1993) but do not result in long-term functional improvement (Mackey et al., 2016; Paulsen et al., 2010). The contradictory findings in humans could be due to the large differences in the exercise protocols and the related severity of injury, the timing (prophylactic vs. therapeutic) and/or the duration of treatment (e.g., single dose (Hasson et al., 1993) vs. a 6-week treatment (Mackey et al., 2016)), the number

of included subjects, as well as the type of drugs (i.e., selective vs. non-selective COX inhibitors). Finally, blunted skeletal muscle hypertrophy has also been reported after chronic administration of NSAIDs (Lilja et al., 2018; Novak et al., 2009; Soltow et al., 2006) at least in young healthy muscles. This was associated with a reduced macrophage infiltration (Novak et al., 2009) which is in agreement with the role of COX-2 in macrophage chemotaxis (Reding et al., 2006). On the contrary, positive effects of NSAIDs on skeletal muscle mass and/or force have been described in healthy elderly adults (Trappe et al., 2011), suggesting that the efficacy of this strategy may rely on the basal inflammatory status. Further studies are needed to illustrate how macrophages are impacted by NSAIDs in response to overload in both young and older muscles.

5.5 | Resolvins

The inflammatory response is sustained by different classes of lipid mediators: the pro-inflammatory phase is associated with prostaglandins (which synthesis relies on COX1 and COX2) and leukotrienes. The repair/healing phase is supported by a series of more than 40 lipids with anti-inflammatory properties including lipoxins, resolvins, maresins and protectins, called Specialized Pro-resolving Mediators (or SPM) (Serhan, 2014). Resolvins are a family of more than 20 members formed from omega-3 essential polyunsaturated fatty acids, docosahexaenoic acid (DHA), eicosapentaenoic acid (EPA) and docosapentaenoic acid (n-3 DPA) giving rise to the D-, E- and T-series resolvins, respectively (Serhan, 2014). So far, five resolvin receptors have been identified (A lipoxin and formyl peptide receptor 2 [ALX/FPR2], DRV1/GPR32, DRV2/GPR18, ERV1/ChemR23, GPR101) belonging to the seven transmembrane G-protein coupled receptor family (Cash et al., 2014; Flak et al., 2020). Resolvins actively participate in the resolution of inflammation, notably by limiting neutrophil infiltration and increasing macrophage efferocytosis.

In skeletal muscle, promising results have been recently obtained with the use of resolvins. In a hindlimb ischemia injury model, where skeletal myofibers are injured and therefore where muscle operates regeneration, a daily treatment with Resolvin D2 from 24 h after injury improves angiogenesis and increases the number of regenerating myofibers 14 days after injury, associated with a decrease in neutrophil infiltration in the muscle at early time points (Zhang et al., 2016). Treatment with Resolvin D1 leads to a similar improvement and requires signaling through its ALX/FPR2 receptor on macrophages. Indeed, in $LysM^{Cre}$;$ALX/FPR2^{flox}$ mice, where the gene is deleted in myeloid cells, the expression of a provascularization phenotype of macrophages in blunted (Sansbury et al., 2020). In both toxin-induced muscle injury and EIMD, the lipid mediator class shift usually observed during the inflammatory response occurs at the time of resolution of inflammation, notably in macrophages (Giannakis et al., 2019; Markworth et al., 2020). A single intramuscular injection of Resolvin D2 in early regenerating muscle (day 2–3 after toxic injury) improves both muscle mass and force recovery, and increases the number of $Ly6C^{neg}$ restorative macrophages (Giannakis et al., 2019). A single intraperitoneal injection of Resolvin D2 at the time of injury strongly decreases neutrophil infiltration at early time points (from day 1 post-toxic injury) and induces the expression of the restorative phenotype of macrophages at a later stage (increased expression of *Alox12*, *Arg1*, *IL1b*) (day 5), associated with an improvement of the myogenic process (Markworth et al., 2020). In both studies, resolvin administration leads to increased myofiber CSA and muscle strength (Juban, 2021; Trappe et al., 2011). It is noteworthy that Resolvins also impact on myogenesis, at least in vitro. Resolvin D1 at 100 nM has no impact on myogenesis in the murine myoblast cell line C2C12 but counteracts the deleterious effect of high concentrations of TNFα (20 ng/ml) on myogenesis (Markworth et al., 2020). Resolvin D2 at 200 nM directly stimulates primary mouse MuSC differentiation and myogenesis, through the GPR18 receptor that is expressed in differentiating muscle stem cells (Dort et al., 2021).

Most interestingly, these studies have directly compared the impact of resolvins and other anti-inflammatory treatments. Resolvins have a superior benefit for muscle regeneration than NSAIDs (ibuprofen), that acutely inhibits the pro-inflammatory prostanoids, but their expression rebounds later on, driving strong unbalance of the kinetics of macrophage subtypes (the transition to the acquisition of the restorative phenotype is impaired) (Giannakis et al., 2019) and that glucocorticoids (prednisolone is less efficient and with only short-term benefit) (Dort et al., 2021).

6 | CONCLUSION

Macrophages are at the heart of the regeneration process by interacting with MuSCs and other cell types to restore skeletal muscle structure and function. Growing evidence is also emerging on their role on skeletal muscle hypertrophy. The use of non-damaging mouse models of exercise should allow to determine how they participate in the regulation of myofiber size. This should clearly highlight the specific role of macrophages and their interactions with neighboring cells in muscle regeneration versus hypertrophy. Animal studies highlight the key role of several

immunomodulatory strategies to favor muscle regeneration and evidence is emerging illustrating that the modulation of the inflammatory response could be relevant to favor muscle hypertrophy. Rather than blunting the pro-inflammatory phase, promoting the active resolution of inflammation to establish the regenerative inflammation appears a good strategy to improve/accelerate muscle regeneration as well as to promote muscle growth.

AUTHOR CONTRIBUTIONS

Clara Bernard, Aliki Zavoriti, Quentin Pucelle, Bénédicte Chazaud and Julien Gondin contributed to the conception and design of this review. Clara Bernard, Aliki Zavoriti, Quentin Pucelle, Bénédicte Chazaud and Julien Gondin interpreted and synthesized the data. Clara Bernard, Aliki Zavoriti, Quentin Pucelle, Bénédicte Chazaud and Julien Gondin wrote the draft manuscript. All authors contributed to and revised the final manuscript. All authors read and approved the final manuscript.

ORCID

Julien Gondin https://orcid.org/0000-0002-3108-605X

REFERENCES

Almekinders, L. C., & Gilbert, J. A. (1986). Healing of experimental muscle strains and the effects of nonsteroidal antiinflammatory medication. *The American Journal of Sports Medicine*, *14*, 303–308. https://doi.org/10.1177/036354658601400411

Armstrong, R. B., Marum, P., Tullson, P., & Saubert, C. W. (1979). Acute hypertrophic response of skeletal muscle to removal of synergists. *Journal of Applied Physiology: Respiratory, Environmental and Exercise Physiology*, *46*, 835–842. https://doi.org/10.1152/jappl.1979.46.4.835

Arnold, L., Henry, A., Poron, F., Baba-Amer, Y., van Rooijen, N., Plonquet, A., Gherardi, R. K., & Chazaud, B. (2007). Inflammatory monocytes recruited after skeletal muscle injury switch into antiinflammatory macrophages to support myogenesis. *The Journal of Experimental Medicine*, *204*, 1057–1069. https://doi.org/10.1084/jem.20070075

Baht, G. S., Bareja, A., Lee, D. E., Rao, R. R., Huang, R., Huebner, J. L., Bartlett, D. B., Hart, C. R., Gibson, J. R., Lanza, I. R., Kraus, V. B., Gregory, S. G., Spiegelman, B. M., & White, J. P. (2020). Meteorin-like facilitates skeletal muscle repair through a Stat3/IGF-1 mechanism. *Nature Metabolism*, *2*, 278–289. https://doi.org/10.1038/s42255-020-0184-y

Ballotta, V., Driessen-Mol, A., Bouten, C. V. C., & Baaijens, F. P. T. (2014). Strain-dependent modulation of macrophage polarization within scaffolds. *Biomaterials*, *35*, 4919–4928. https://doi.org/10.1016/j.biomaterials.2014.03.002

Beaton, L. J., Tarnopolsky, M. A., & Phillips, S. M. (2002). Contraction-induced muscle damage in humans following calcium channel blocker administration. *Journal of Physiology (London)*, *544*, 849–859.

Bencze, M., Negroni, E., Vallese, D., Yacoub-Youssef, H., Chaouch, S., Wolff, A., Aamiri, A., Di Santo, J. P., Chazaud, B., Butler-Browne, G., Savino, W., Mouly, V., & Riederer, I. (2012). Proinflammatory macrophages enhance the regenerative capacity of human myoblasts by modifying their kinetics of proliferation and differentiation. *Molecular Therapy*, *20*, 2168–2179. https://doi.org/10.1038/mt.2012.189

Bjørnsen, T., Wernbom, M., Løvstad, A., Paulsen, G., D'Souza, R. F., Cameron-Smith, D., Flesche, A., Hisdal, J., Berntsen, S., & Raastad, T. (2019). Delayed myonuclear addition, myofiber hypertrophy, and increases in strength with high-frequency low-load blood flow restricted training to volitional failure. *Journal of Applied Physiology (Bethesda, MD: 1985)*, *126*, 578–592. https://doi.org/10.1152/japplphysiol.00397.2018

Bjørnsen, T., Wernbom, M., Paulsen, G., Markworth, J. F., Berntsen, S., D'Souza, R. F., Cameron-Smith, D., & Raastad, T. (2021). High-frequency blood flow-restricted resistance exercise results in acute and prolonged cellular stress more pronounced in type I than in type II fibers. *Journal of Applied Physiology (Bethesda, MD: 1985)*, *131*, 643–660. https://doi.org/10.1152/japplphysiol.00115.2020

Bondesen, B. A., Mills, S. T., Kegley, K. M., & Pavlath, G. K. (2004). The COX-2 pathway is essential during early stages of skeletal muscle regeneration. *American Journal of Physiology. Cell Physiology*, *287*, C475–C483. https://doi.org/10.1152/ajpcell.00088.2004

Bourgeois, J., MacDougall, D., MacDonald, J., & Tarnopolsky, M. (1999). Naproxen does not alter indices of muscle damage in resistance-exercise trained men. *Medicine and Science in Sports and Exercise*, *31*, 4–9. https://doi.org/10.1097/00005768-199901000-00002

Bryer, S. C., Fantuzzi, G., Van Rooijen, N., & Koh, T. J. (2008). Urokinase-type plasminogen activator plays essential roles in macrophage chemotaxis and skeletal muscle regeneration. *Journal of Immunology*, *180*, 1179–1188. https://doi.org/10.4049/jimmunol.180.2.1179

Butterfield, T. A., Zhao, Y., Agarwal, S., Haq, F., & Best, T. M. (2008). Cyclic compressive loading facilitates recovery after eccentric exercise. *Medicine and Science in Sports and Exercise*, *40*, 1289–1296. https://doi.org/10.1249/MSS.0b013e31816c4e12

Caratti, G., Desgeorges, T., Juban, G., Koenen, M., Kozak, B., Théret, M., Chazaud, B., Tuckermann, J. P., & Mounier, R. (2020). AMPKα1 is essential for Glucocorticoid Receptor triggered anti-inflammatory macrophage activation. *bioRxiv*. https://doi.org/10.1101/2020.01.02.892836

Cash, J. L., Norling, L. V., & Perretti, M. (2014). Resolution of inflammation: Targeting GPCRs that interact with lipids and peptides. *Drug Discovery Today*, *19*, 1186–1192. https://doi.org/10.1016/j.drudis.2014.06.023

Cezar, C. A., Roche, E. T., Vandenburgh, H. H., Duda, G. N., Walsh, C. J., & Mooney, D. J. (2016). Biologic-free mechanically induced muscle regeneration. *Proceedings of the National Academy of Sciences of the United States of America*, *113*, 1534–1539. https://doi.org/10.1073/pnas.1517517113

Chapman, H. A., Reilly, J. J., & Kobzik, L. (1988). Role of plasminogen activator in degradation of extracellular matrix protein by live human alveolar macrophages. *The American Review of Respiratory Disease*, *137*, 412–419. https://doi.org/10.1164/ajrccm/137.2.412

Cheng, M., Nguyen, M.-H., Fantuzzi, G., & Koh, T. J. (2008). Endogenous interferon-gamma is required for efficient skeletal muscle regeneration. *American Journal of Physiology. Cell Physiology*, *294*, C1183–C1191. https://doi.org/10.1152/ajpcell.00568.2007

Child, R., Brown, S., Day, S., Donnelly, A., Roper, H., & Saxton, J. (1999). Changes in indices of antioxidant status, lipid peroxidation and inflammation in human skeletal muscle after eccentric muscle actions. *Clinical Science (London, England)*, *96*, 105–115.

Chow, L. S., Gerszten, R. E., Taylor, J. M., Pedersen, B. K., van Praag, H., Trappe, S., Febbraio, M. A., Galis, Z. S., Gao, Y., Haus, J. M., Lanza, I. R., Lavie, C. J., Lee, C.-H., Lucia, A., Moro, C., Pandey, A., Robbins, J. M., Stanford, K. I., Thackray, A. E., … Snyder, M. P. (2022). Exerkines in health, resilience and disease. *Nature Reviews. Endocrinology*, *18*, 273–289. https://doi.org/10.1038/s41574-022-00641-2

Contreras-Shannon, V., Ochoa, O., Reyes-Reyna, S., Sun, D., Michalek, J., Kuziel, W., McManus, L., & Shireman, P. (2007). Fat accumulation with altered inflammation and regeneration in skeletal muscle of CCR2−/− mice following ischemic injury. *American Journal of Physiology. Cell Physiology*, *292*, C953–C967. https://doi.org/10.1152/ajpcell.00154.2006

Costello, J. T., Baker, P. R. A., Minett, G. M., Bieuzen, F., Stewart, I. B., & Bleakley, C. (2015). Whole-body cryotherapy (extreme cold air exposure) for preventing and treating muscle soreness after exercise in adults. *Cochrane Database of Systematic Reviews*, CD010789. https://doi.org/10.1002/14651858.CD010789.pub2

Crameri, R. M., Aagaard, P., Qvortrup, K., Langberg, H., Olesen, J., & Kjaer, M. (2007). Myofibre damage in human skeletal muscle: Effects of electrical stimulation versus voluntary contraction. *Journal of Physiology (London)*, *583*, 365–380. https://doi.org/10.1113/jphysiol.2007.128827

Crane, J. D., Ogborn, D. I., Cupido, C., Melov, S., Hubbard, A., Bourgeois, J. M., & Tarnopolsky, M. A. (2012). Massage therapy attenuates inflammatory signaling after exercise-induced muscle damage. *Science Translational Medicine*, *4*, 119ra13. https://doi.org/10.1126/scitranslmed.3002882

Davis, H. L., Alabed, S., & Chico, T. J. A. (2020). Effect of sports massage on performance and recovery: A systematic review and meta-analysis. *BMJ Open Sport & Exercise Medicine*, *6*, e000614. https://doi.org/10.1136/bmjsem-2019-000614

Deng, B., Wehling-Henricks, M., Villalta, S. A., Wang, Y., & Tidball, J. G. (2012). IL-10 triggers changes in macrophage phenotype that promote muscle growth and regeneration. *Journal of Immunology*, *189*, 3669–3680. https://doi.org/10.4049/jimmunol.1103180

DiPasquale, D. M., Cheng, M., Billich, W., Huang, S. A., van Rooijen, N., Hornberger, T. A., & Koh, T. J. (2007). Urokinase-type plasminogen activator and macrophages are required for skeletal muscle hypertrophy in mice. *American Journal of Physiology-Cell Physiology*, *293*, C1278–C1285. https://doi.org/10.1152/ajpcell.00201.2007

Dort, J., Orfi, Z., Fabre, P., Molina, T., Conte, T. C., Greffard, K., Pellerito, O., Bilodeau, J.-F., & Dumont, N. A. (2021). Resolvin-D2 targets myogenic cells and improves muscle regeneration in Duchenne muscular dystrophy. *Nature Communications*, *12*, 6264. https://doi.org/10.1038/s41467-021-26516-0

Dumont, N. A., Wang, Y. X., & Rudnicki, M. A. (2015). Intrinsic and extrinsic mechanisms regulating satellite cell function. *Development*, *142*, 1572–1581. https://doi.org/10.1242/dev.114223

Egner, I. M., Bruusgaard, J. C., & Gundersen, K. (2016). Satellite cell depletion prevents fiber hypertrophy in skeletal muscle. *Development*, *143*, 2898–2906. https://doi.org/10.1242/dev.134411

Fan, W., Gao, X. K., Rao, X. S., Shi, Y. P., Liu, X. C., Wang, F. Y., Liu, Y. F., Cong, X. X., He, M. Y., Xu, S. B., Shen, W. L., Shen, Y., Yan, S. G., Luo, Y., Low, B. C., Ouyang, H., Bao, Z., Zheng, L. L., & Zhou, Y. T. (2018). Hsp70 interacts with mitogen-activated protein kinase (MAPK)-activated protein kinase 2 to regulate p38MAPK stability and myoblast differentiation during skeletal muscle regeneration. *Molecular and Cellular Biology*, *38*, e00211-18. https://doi.org/10.1128/MCB.00211-18

Féasson, L., Stockholm, D., Freyssenet, D., Richard, I., Duguez, S., Beckmann, J. S., & Denis, C. (2002). Molecular adaptations of neuromuscular disease-associated proteins in response to eccentric exercise in human skeletal muscle. *The Journal of Physiology*, *543*, 297–306. https://doi.org/10.1113/jphysiol.2002.018689

Fennel, Z. J., Amorim, F. T., Deyhle, M. R., Hafen, P. S., & Mermier, C. M. (2022). The heat shock connection: Skeletal muscle hypertrophy and atrophy. *American Journal of Physiology. Regulatory, Integrative and Comparative Physiology*, *323*, R133–R148. https://doi.org/10.1152/ajpregu.00048.2022

Flak, M. B., Koenis, D. S., Sobrino, A., Smith, J., Pistorius, K., Palmas, F., & Dalli, J. (2020). GPR101 mediates the pro-resolving actions of RvD5n-3 DPA in arthritis and infections. *The Journal of Clinical Investigation*, *130*, 359–373. https://doi.org/10.1172/JCI131609

Fukada, S. I., Higashimoto, T., & Kaneshige, A. (2022). Differences in muscle satellite cell dynamics during muscle hypertrophy and regeneration. *Skeletal Muscle*, *12*, 17. https://doi.org/10.1186/s13395-022-00300-0

Fukuda, S., Kaneshige, A., Kaji, T., Noguchi, Y.-T., Takemoto, Y., Zhang, L., Tsujikawa, K., Kokubo, H., Uezumi, A., Maehara, K., Harada, A., Ohkawa, Y., & Fukada, S.-I. (2019). Sustained expression of HeyL is critical for the proliferation of muscle stem cells in overloaded muscle. *eLife*, *8*, e48284. https://doi.org/10.7554/eLife.48284

Fyfe, J. J., Broatch, J. R., Trewin, A. J., Hanson, E. D., Argus, C. K., Garnham, A. P., Halson, S. L., Polman, R. C., Bishop, D. J., & Petersen, A. C. (2019). Cold water immersion attenuates anabolic signaling and skeletal muscle fiber hypertrophy, but not strength gain, following whole-body resistance training. *Journal of Applied Physiology (Bethesda, MD: 1985)*, *127*, 1403–1418. https://doi.org/10.1152/japplphysiol.00127.2019

Giannakis, N., Sansbury, B. E., Patsalos, A., Hays, T. T., Riley, C. O., Han, X., Spite, M., & Nagy, L. (2019). Dynamic changes to lipid mediators support transitions among macrophage subtypes during muscle regeneration. *Nature Immunology*, *20*, 626–636. https://doi.org/10.1038/s41590-019-0356-7

Goh, Q., & Millay, D. P. (2017). Requirement of myomaker-mediated stem cell fusion for skeletal muscle hypertrophy. *eLife*, *6*, e20007. https://doi.org/10.7554/eLife.20007

Gorski, T., Cadore, E. L., Pinto, S. S., da Silva, E. M., Correa, C. S., Beltrami, F. G., & Kruel, L. F. M. (2011). Use of NSAIDs in triathletes: Prevalence, level of awareness and reasons for use. *British Journal of Sports Medicine*, *45*, 85–90. https://doi.org/10.1136/bjsm.2009.062166

Guerci, A., Lahoute, C., Hébrard, S., Collard, L., Graindorge, D., Favier, M., Cagnard, N., Batonnet-Pichon, S., Précigout, G., Garcia, L., Tuil, D., Daegelen, D., & Sotiropoulos, A. (2012). Srf-dependent paracrine signals produced by myofibers control satellite

cell-mediated skeletal muscle hypertrophy. *Cell Metabolism*, *15*, 25–37. https://doi.org/10.1016/j.cmet.2011.12.001

Guilhem, G., Hug, F., Couturier, A., Regnault, S., Bournat, L., Filliard, J.-R., & Dorel, S. (2013). Effects of air-pulsed cryotherapy on neuromuscular recovery subsequent to exercise-induced muscle damage. *The American Journal of Sports Medicine*, *41*, 1942–1951. https://doi.org/10.1177/0363546513490648

Haas, C., Butterfield, T. A., Abshire, S., Zhao, Y., Zhang, X., Jarjoura, D., & Best, T. M. (2013). Massage timing affects postexercise muscle recovery and inflammation in a rabbit model. *Medicine and Science in Sports and Exercise*, *45*, 1105–1112. https://doi.org/10.1249/MSS.0b013e31827fdf18

Haas, C., Butterfield, T. A., Zhao, Y., Zhang, X., Jarjoura, D., & Best, T. M. (2013). Dose-dependency of massage-like compressive loading on recovery of active muscle properties following eccentric exercise: Rabbit study with clinical relevance. *British Journal of Sports Medicine*, *47*, 83–88. https://doi.org/10.1136/bjsports-2012-091211

Hardy, D., Besnard, A., Latil, M., Jouvion, G., Briand, D., Thépenier, C., Pascal, Q., Guguin, A., Gayraud-Morel, B., Cavaillon, J.-M., Tajbakhsh, S., Rocheteau, P., & Chrétien, F. (2016). Comparative study of injury models for studying muscle regeneration in mice. *PLoS ONE*, *11*, e0147198. https://doi.org/10.1371/journal.pone.0147198

Harmon, B. T., Orkunoglu-Suer, E. F., Adham, K., Larkin, J. S., Gordish-Dressman, H., Clarkson, P. M., Thompson, P. D., Angelopoulos, T. J., Gordon, P. M., Moyna, N. M., Pescatello, L. S., Visich, P. S., Zoeller, R. F., Hubal, M. J., Tosi, L. L., Hoffman, E. P., & Devaney, J. M. (2010). CCL2 and CCR2 variants are associated with skeletal muscle strength and change in strength with resistance training. *Journal of Applied Physiology (Bethesda, MD: 1985)*, *109*, 1779–1785. https://doi.org/10.1152/japplphysiol.00633.2010

Hasson, S. M., Daniels, J. C., Divine, J. G., Niebuhr, B. R., Richmond, S., Stein, P. G., & Williams, J. H. (1993). Effect of ibuprofen use on muscle soreness, damage, and performance: A preliminary investigation. *Medicine and Science in Sports and Exercise*, *25*, 9–17. https://doi.org/10.1249/00005768-199301000-00003

Hatade, T., Takeuchi, K., Fujita, N., Arakawa, T., & Miki, A. (2014). Effect of heat stress soon after muscle injury on the expression of MyoD and myogenin during regeneration process. *Journal of Musculoskeletal & Neuronal Interactions*, *14*, 325–333.

Hikida, R. S., Staron, R. S., Hagerman, F. C., Sherman, W. M., & Costill, D. L. (1983). Muscle fiber necrosis associated with human marathon runners. *Journal of the Neurological Sciences*, *59*, 185–203. https://doi.org/10.1016/0022-510x(83)90037-0

Ho, A. T. V., Palla, A. R., Blake, M. R., Yucel, N. D., Wang, Y. X., Magnusson, K. E. G., Holbrook, C. A., Kraft, P. E., Delp, S. L., & Blau, H. M. (2017). Prostaglandin E2 is essential for efficacious skeletal muscle stem-cell function, augmenting regeneration and strength. *Proceedings of the National Academy of Sciences of the United States of America*, *114*, 6675–6684. https://doi.org/10.1073/pnas.1705420114

Howatson, G., Gaze, D., & van Someren, K. A. (2005). The efficacy of ice massage in the treatment of exercise-induced muscle damage. *Scandinavian Journal of Medicine & Science in Sports*, *15*, 416–422.

Howatson, G., & van Someren, K. A. (2008). The prevention and treatment of exercise-induced muscle damage. *Sports Medicine*, *38*, 483–503. https://doi.org/10.2165/00007256-200838060-00004

Hubal, M. J., Chen, T. C., Thompson, P. D., & Clarkson, P. M. (2008). Inflammatory gene changes associated with the repeated-bout effect. *American Journal of Physiology. Regulatory, Integrative and Comparative Physiology*, *294*, R1628-37. https://doi.org/10.1152/ajpregu.00853.2007

Hunt, E. R., Confides, A. L., Abshire, S. M., Dupont-Versteegden, E. E., & Butterfield, T. A. (2019). Massage increases satellite cell number independent of the age-associated alterations in sarcolemma permeability. *Physiological Reports*, *7*, e14200. https://doi.org/10.14814/phy2.14200

Hyldahl, R. D., & Peake, J. M. (2020). Combining cooling or heating applications with exercise training to enhance performance and muscle adaptations. *Journal of Applied Physiology (Bethesda, MD: 1985)*, *129*, 353–365. https://doi.org/10.1152/japplphysiol.00322.2020

Jakobsen, J. R., Mackey, A. L., Knudsen, A. B., Koch, M., Kjaer, M., & Krogsgaard, M. R. (2017). Composition and adaptation of human myotendinous junction and neighboring muscle fibers to heavy resistance training. *Scandinavian Journal of Medicine & Science in Sports*, *27*, 1547–1559. https://doi.org/10.1111/sms.12794

Jayaraman, R. C., Reid, R. W., Foley, J. M., Prior, B. M., Dudley, G. A., Weingand, K. W., & Meyer, R. A. (2004). MRI evaluation of topical heat and static stretching as therapeutic modalities for the treatment of eccentric exercise-induced muscle damage. *European Journal of Applied Physiology*, *93*, 30–38. https://doi.org/10.1007/s00421-004-1153-y

Jensen, S. M., Bechshøft, C. J. L., Heisterberg, M. F., Schjerling, P., Andersen, J. L., Kjaer, M., & Mackey, A. L. (2020). Macrophage subpopulations and the acute inflammatory response of elderly human skeletal muscle to physiological resistance exercise. *Frontiers in Physiology*, *11*, 811. https://doi.org/10.3389/fphys.2020.00811

Jones, D. A., Newham, D. J., Round, J. M., & Tolfree, S. E. (1986). Experimental human muscle damage: Morphological changes in relation to other indices of damage. *The Journal of Physiology*, *375*, 435–448.

Juban, G. (2021). Transcriptional control of macrophage inflammatory shift during skeletal muscle regeneration. *Seminars in Cell & Developmental Biology*, *119*, 82–88. https://doi.org/10.1016/j.semcdb.2021.06.011

Juban, G., & Chazaud, B. (2017). Metabolic regulation of macrophages during tissue repair: Insights from skeletal muscle regeneration. *FEBS Letters*, *591*, 3007–3021. https://doi.org/10.1002/1873-3468.12703

Juban, G., & Chazaud, B. (2021). Efferocytosis during skeletal muscle regeneration. *Cell*, *10*, 3267. https://doi.org/10.3390/cells10123267

Kandarian, S., & White, T. (1989). Force deficit during the onset of muscle hypertrophy. *Journal of Applied Physiology (Bethesda, MD: 1985)*, *67*, 2600–2607. https://doi.org/10.1152/jappl.1989.67.6.2600

Kaneshige, A., Kaji, T., Zhang, L., Saito, H., Nakamura, A., Kurosawa, T., Ikemoto-Uezumi, M., Tsujikawa, K., Seno, S., Hori, M., Saito, Y., Matozaki, T., Maehara, K., Ohkawa, Y., Potente, M., Watanabe, S., Braun, T., Uezumi, A., & Fukada, S.-I. (2022). Relayed signaling between mesenchymal progenitors and muscle stem cells ensures adaptive stem cell response to increased mechanical load. *Cell Stem Cell*, *29*, 265, e6–280. https://doi.org/10.1016/j.stem.2021.11.003

Kawashima, M., Kawanishi, N., Tominaga, T., Suzuki, K., Miyazaki, A., Nagata, I., Miyoshi, M., Miyakawa, M., Sakuraya, T., Sonomura, T., & Arakawa, T. (2021). Icing after eccentric contraction-induced muscle damage perturbs the disappearance of necrotic muscle fibers and phenotypic dynamics of macrophages in mice. *Journal of Applied Physiology (Bethesda, MD: 1985)*, *130*, 1410–1420. https://doi.org/10.1152/japplphysiol.01069.2020

Khan, K. M., & Scott, A. (2009). Mechanotherapy: How physical therapists' prescription of exercise promotes tissue repair. *British Journal of Sports Medicine*, *43*, 247–252. https://doi.org/10.1136/bjsm.2008.054239

Kim, K., Kuang, S., Song, Q., Gavin, T. P., & Roseguini, B. T. (2019). Impact of heat therapy on recovery after eccentric exercise in humans. *Journal of Applied Physiology (Bethesda, MD: 1985)*, *126*, 965–976. https://doi.org/10.1152/japplphysiol.00910.2018

Kim, K., Monroe, J. C., Gavin, T. P., & Roseguini, B. T. (2020). Skeletal muscle adaptations to heat therapy. *Journal of Applied Physiology (Bethesda, MD: 1985)*, *128*, 1635–1642. https://doi.org/10.1152/japplphysiol.00061.2020

Kim, K., Reid, B. A., Ro, B., Casey, C. A., Song, Q., Kuang, S., & Roseguini, B. T. (2019). Heat therapy improves soleus muscle force in a model of ischemia-induced muscle damage. *Journal of Applied Physiology (Bethesda, MD: 1985)*, *127*, 215–228. https://doi.org/10.1152/japplphysiol.00115.2019

Kojima, A., Goto, K., Morioka, S., Naito, T., Akema, T., Fujiya, H., Sugiura, T., Ohira, Y., Beppu, M., Aoki, H., & Yoshioka, T. (2007). Heat stress facilitates the regeneration of injured skeletal muscle in rats. *Journal of Orthopaedic Science*, *12*, 74–82. https://doi.org/10.1007/s00776-006-1083-0

Kuligowski, L. A., Lephart, S. M., Giannantonio, F. P., & Blanc, R. O. (1998). Effect of whirlpool therapy on the signs and symptoms of delayed-onset muscle soreness. *Journal of Athletic Training*, *33*, 222–228.

Lapointe, B. M., Frémont, P., & Côté, C. H. (2002). Adaptation to lengthening contractions is independent of voluntary muscle recruitment but relies on inflammation. *American Journal of Physiology. Regulatory, Integrative and Comparative Physiology*, *282*, R323-9. https://doi.org/10.1152/ajpregu.00339.2001

Lapointe, B. M., Frenette, J., & Cote, C. H. (2002). Lengthening contraction-induced inflammation is linked to secondary damage but devoid of neutrophil invasion. *Journal of Applied Physiology*, *92*, 1995–2004.

Lauritzen, F., Paulsen, G., Raastad, T., Bergersen, L. H., & Owe, S. G. (2009). Gross ultrastructural changes and necrotic fiber segments in elbow flexor muscles after maximal voluntary eccentric action in humans. *Journal of Applied Physiology (Bethesda, MD: 1985)*, *107*, 1923–1934. https://doi.org/10.1152/japplphysiol.00148.2009

Lemos, D. R., Babaeijandaghi, F., Low, M., Chang, C.-K., Lee, S. T., Fiore, D., Zhang, R.-H., Natarajan, A., Nedospasov, S. A., & Rossi, F. M. V. (2015). Nilotinib reduces muscle fibrosis in chronic muscle injury by promoting TNF-mediated apoptosis of fibro/adipogenic progenitors. *Nature Medicine*, *21*, 786–794. https://doi.org/10.1038/nm.3869

Lepper, C., Partridge, T. A., & Fan, C.-M. (2011). An absolute requirement for Pax7-positive satellite cells in acute injury-induced skeletal muscle regeneration. *Development*, *138*, 3639–3646. https://doi.org/10.1242/dev.067595

Liao, C.-H., Lin, L.-P., Yu, T.-Y., Hsu, C.-C., Pang, J.-H. S., & Tsai, W.-C. (2019). Ibuprofen inhibited migration of skeletal muscle cells in association with downregulation of p130cas and CrkII expressions. *Skeletal Muscle*, *9*, 23. https://doi.org/10.1186/s13395-019-0208-z

Lilja, M., Mandić, M., Apró, W., Melin, M., Olsson, K., Rosenborg, S., Gustafsson, T., & Lundberg, T. R. (2018). High doses of anti-inflammatory drugs compromise muscle strength and hypertrophic adaptations to resistance training in young adults. *Acta Physiologica (Oxford, England)*, *222*, e12948. https://doi.org/10.1111/apha.12948

Long, D. E., Peck, B. D., Lavin, K. M., Dungan, C. M., Kosmac, K., Tuggle, S. C., Bamman, M. M., Kern, P. A., & Peterson, C. A. (2022). Skeletal muscle properties show collagen organization and immune cell content are associated with resistance exercise response heterogeneity in older persons. *Journal of Applied Physiology (Bethesda, MD: 1985)*, *132*, 1432–1447. https://doi.org/10.1152/japplphysiol.00025.2022

Lu, H., Huang, D., Saederup, N., Charo, I. F., Ransohoff, R. M., & Zhou, L. (2011). Macrophages recruited via CCR2 produce insulin-like growth factor-1 to repair acute skeletal muscle injury. *The FASEB Journal*, *25*, 358–369. https://doi.org/10.1096/fj.10-171579

Mackey, A. L., & Kjaer, M. (2017). The breaking and making of healthy adult human skeletal muscle in vivo. *Skeletal Muscle*, *7*, 24. https://doi.org/10.1186/s13395-017-0142-x

Mackey, A. L., Kjaer, M., Dandanell, S., Mikkelsen, K. H., Holm, L., Døssing, S., Kadi, F., Koskinen, S. O., Jensen, C. H., Schrøder, H. D., & Langberg, H. (2007). The influence of anti-inflammatory medication on exercise-induced myogenic precursor cell responses in humans. *Journal of Applied Physiology (Bethesda, MD: 1985)*, *103*, 425–431. https://doi.org/10.1152/japplphysiol.00157.2007

Mackey, A. L., Rasmussen, L. K., Kadi, F., Schjerling, P., Helmark, I. C., Ponsot, E., Aagaard, P., Durigan, J. L. Q., & Kjaer, M. (2016). Activation of satellite cells and the regeneration of human skeletal muscle are expedited by ingestion of nonsteroidal anti-inflammatory medication. *The FASEB Journal*, *30*, 2266–2281. https://doi.org/10.1096/fj.201500198R

Malm, C., Sjödin, T. L. B., Sjöberg, B., Lenkei, R., Renström, P., Lundberg, I. E., & Ekblom, B. (2004). Leukocytes, cytokines, growth factors and hormones in human skeletal muscle and blood after uphill or downhill running. *Journal of Physiology (London)*, *556*, 983–1000. https://doi.org/10.1113/jphysiol.2003.056598

Marino, J. S., Tausch, B. J., Dearth, C. L., Manacci, M. V., McLoughlin, T. J., Rakyta, S. J., Linsenmayer, M. P., & Pizza, F. X. (2008). β_2-integrins contribute to skeletal muscle hypertrophy in mice. *American Journal of Physiology-Cell Physiology*, *295*, C1026–C1036. https://doi.org/10.1152/ajpcell.212.2008

Markworth, J. F., Brown, L. A., Lim, E., Floyd, C., Larouche, J., Castor-Macias, J. A., Sugg, K. B., Sarver, D. C., Macpherson, P. C., Davis, C., Aguilar, C. A., Maddipati, K. R., & Brooks, S. V. (2020). Resolvin D1 supports skeletal myofiber regeneration via actions on myeloid and muscle stem cells. *JCI Insight*, *5*, 137713. https://doi.org/10.1172/jci.insight.137713

Martinez, C. O., McHale, M. J., Wells, J. T., Ochoa, O., Michalek, J. E., McManus, L. M., & Shireman, P. K. (2010). Regulation of skeletal muscle regeneration by CCR2-activating chemokines is directly related to macrophage recruitment. *American Journal of*

Physiology. Regulatory, Integrative and Comparative Physiology, *299*, R832-42. https://doi.org/10.1152/ajpregu.00797.2009

McCarthy, J. J., Mula, J., Miyazaki, M., Erfani, R., Garrison, K., Farooqui, A. B., Srikuea, R., Lawson, B. A., Grimes, B., Keller, C., Van Zant, G., Campbell, K. S., Esser, K. A., Dupont-Versteegden, E. E., & Peterson, C. A. (2011). Effective fiber hypertrophy in satellite cell-depleted skeletal muscle. *Development*, *138*, 3657–3666. https://doi.org/10.1242/dev.068858

McGorm, H., Roberts, L. A., Coombes, J. S., & Peake, J. M. (2018). Turning up the heat: An evaluation of the evidence for heating to promote exercise recovery, muscle rehabilitation and adaptation. *Sports Medicine*, *48*, 1311–1328. https://doi.org/10.1007/s40279-018-0876-6

McLoughlin, T. J., Mylona, E., Hornberger, T. A., Esser, K. A., & Pizza, F. X. (2003). Inflammatory cells in rat skeletal muscle are elevated after electrically stimulated contractions. *Journal of Applied Physiology (Bethesda, MD: 1985)*, *94*, 876–882. https://doi.org/10.1152/japplphysiol.00766.2002

Mikkelsen, U. R., Langberg, H., Helmark, I. C., Skovgaard, D., Andersen, L. L., Kjaer, M., & Mackey, A. L. (2009). Local NSAID infusion inhibits satellite cell proliferation in human skeletal muscle after eccentric exercise. *Journal of Applied Physiology*, *107*, 1600–1611. https://doi.org/10.1152/japplphysiol.00707.2009

Mishra, D. K., Fridén, J., Schmitz, M. C., & Lieber, R. L. (1995). Anti-inflammatory medication after muscle injury. A treatment resulting in short-term improvement but subsequent loss of muscle function. *Journal of Bone and Joint Surgery*, *77*, 1510–1519. https://doi.org/10.2106/00004623-199510000-00005

Miyakawa, M., Kawashima, M., Haba, D., Sugiyama, M., Taniguchi, K., & Arakawa, T. (2020). Inhibition of the migration of MCP-1 positive cells by icing applied soon after crush injury to rat skeletal muscle. *Acta Histochemica*, *122*, 151511. https://doi.org/10.1016/j.acthis.2020.151511

Mounier, R., Théret, M., Arnold, L., Cuvellier, S., Bultot, L., Göransson, O., Sanz, N., Ferry, A., Sakamoto, K., Foretz, M., Viollet, B., & Chazaud, B. (2013). AMPKα1 regulates macrophage skewing at the time of resolution of inflammation during skeletal muscle regeneration. *Cell Metabolism*, *18*, 251–264. https://doi.org/10.1016/j.cmet.2013.06.017

Murach, K. A., Peck, B. D., Policastro, R. A., Vechetti, I. J., Van Pelt, D. W., Dungan, C. M., Denes, L. T., Fu, X., Brightwell, C. R., Zentner, G. E., Dupont-Versteegden, E. E., Richards, C. I., Smith, J. J., Fry, C. S., McCarthy, J. J., & Peterson, C. A. (2021). Early satellite cell communication creates a permissive environment for long-term muscle growth. *iScience*, *24*, 102372. https://doi.org/10.1016/j.isci.2021.102372

Murphy, M. M., Lawson, J. A., Mathew, S. J., Hutcheson, D. A., & Kardon, G. (2011). Satellite cells, connective tissue fibroblasts and their interactions are crucial for muscle regeneration. *Development*, *138*, 3625–3637. https://doi.org/10.1242/dev.064162

Nielsen, J. L., Aagaard, P., Bech, R. D., Nygaard, T., Hvid, L. G., Wernbom, M., Suetta, C., & Frandsen, U. (2012). Proliferation of myogenic stem cells in human skeletal muscle in response to low-load resistance training with blood flow restriction. *The Journal of Physiology*, *590*, 4351–4361. https://doi.org/10.1113/jphysiol.2012.237008

Nielsen, J. L., Aagaard, P., Prokhorova, T. A., Nygaard, T., Bech, R. D., Suetta, C., & Frandsen, U. (2017). Blood flow restricted training leads to myocellular macrophage infiltration and upregulation of heat shock proteins, but no apparent muscle damage. *The Journal of Physiology*, *595*, 4857–4873. https://doi.org/10.1113/jp273907

Novak, M. L., Billich, W., Smith, S. M., Sukhija, K. B., McLoughlin, T. J., Hornberger, T. A., & Koh, T. J. (2009). COX-2 inhibitor reduces skeletal muscle hypertrophy in mice. *American Journal of Physiology-Regulatory, Integrative and Comparative Physiology*, *296*, R1132-9. https://doi.org/10.1152/ajpregu.90874.2008

Noviello, C., Kobon, K., Delivry, L., Guilbert, T., Britto, F., Julienne, F., Maire, P., Randrianarison-Huetz, V., & Sotiropoulos, A. (2022). RhoA within myofibers controls satellite cell microenvironment to allow hypertrophic growth. *iScience*, *25*, 103616. https://doi.org/10.1016/j.isci.2021.103616

Obremsky, W. T., Seaber, A. V., Ribbeck, B. M., & Garrett, W. E. (1994). Biomechanical and histologic assessment of a controlled muscle strain injury treated with piroxicam. *The American Journal of Sports Medicine*, *22*, 558–561. https://doi.org/10.1177/036354659402200420

Oishi, Y., Hayashida, M., Tsukiashi, S., Taniguchi, K., Kami, K., Roy, R. R., & Ohira, Y. (2009). Heat stress increases myonuclear number and fiber size via satellite cell activation in rat regenerating soleus fibers. *Journal of Applied Physiology (Bethesda, MD: 1985)*, *107*, 1612–1621. https://doi.org/10.1152/japplphysiol.91651.2008

Panci, G., & Chazaud, B. (2021). Inflammation during post-injury skeletal muscle regeneration. *Seminars in Cell & Developmental Biology*, *119*, 32–38. https://doi.org/10.1016/j.semcdb.2021.05.031

Patsalos, A., Halasz, L., Medina-Serpas, M. A., Berger, W. K., Daniel, B., Tzerpos, P., Kiss, M., Nagy, G., Fischer, C., Simandi, Z., Varga, T., & Nagy, L. (2022). A growth factor-expressing macrophage subpopulation orchestrates regenerative inflammation via GDF-15. *The Journal of Experimental Medicine*, *219*, e20210420. https://doi.org/10.1084/jem.20210420

Paulsen, G., Egner, I. M., Drange, M., Langberg, H., Benestad, H. B., Fjeld, J. G., Hallén, J., & Raastad, T. (2010). A COX-2 inhibitor reduces muscle soreness, but does not influence recovery and adaptation after eccentric exercise. *Scandinavian Journal of Medicine & Science in Sports*, *20*, e195–e207. https://doi.org/10.1111/j.1600-0838.2009.00947.x

Paulsen, G., Mikkelsen, U. R., Raastad, T., & Peake, J. M. (2012). Leucocytes, cytokines and satellite cells: What role do they play in muscle damage and regeneration following eccentric exercise? *Exercise Immunology Review*, *18*, 42–97.

Peake, J. M., Roberts, L. A., Figueiredo, V. C., Egner, I., Krog, S., Aas, S. N., Suzuki, K., Markworth, J. F., Coombes, J. S., Cameron-Smith, D., & Raastad, T. (2017). The effects of cold water immersion and active recovery on inflammation and cell stress responses in human skeletal muscle after resistance exercise. *The Journal of Physiology*, *595*, 695–711. https://doi.org/10.1113/jp272881

Peck, B. D., Murach, K. A., Walton, R. G., Simmons, A. J., Long, D. E., Kosmac, K., Dungan, C. M., Kern, P. A., Bamman, M. M., & Peterson, C. A. (2022). A muscle cell-macrophage axis involving matrix metalloproteinase 14 facilitates extracellular matrix remodeling with mechanical loading. *The FASEB Journal*, *36*, e22155. https://doi.org/10.1096/fj.202100182RR

Pedersen, B. K., & Febbraio, M. A. (2008). Muscle as an endocrine organ: Focus on muscle-derived interleukin-6. *Physiological*

Reviews, *88*, 1379–1406. https://doi.org/10.1152/physrev.90100.2007

Perdiguero, E., Sousa-Victor, P., Ruiz-Bonilla, V., Jardí, M., Caelles, C., Serrano, A. L., & Muñoz-Cánoves, P. (2011). p38/MKP-1-regulated AKT coordinates macrophage transitions and resolution of inflammation during tissue repair. *The Journal of Cell Biology*, *195*, 307–322. https://doi.org/10.1083/jcb.201104053

Pournot, H., Bieuzen, F., Duffield, R., Lepretre, P.-M., Cozzolino, C., & Hausswirth, C. (2011). Short term effects of various water immersions on recovery from exhaustive intermittent exercise. *European Journal of Applied Physiology*, *111*, 1287–1295. https://doi.org/10.1007/s00421-010-1754-6

Ratnayake, D., Nguyen, P. D., Rossello, F. J., Wimmer, V. C., Tan, J. L., Galvis, L. A., Julier, Z., Wood, A. J., Boudier, T., Isiaku, A. I., Berger, S., Oorschot, V., Sonntag, C., Rogers, K. L., Marcelle, C., Lieschke, G. J., Martino, M. M., Bakkers, J., & Currie, P. D. (2021). Macrophages provide a transient muscle stem cell niche via NAMPT secretion. *Nature*, *591*, 281–287. https://doi.org/10.1038/s41586-021-03199-7

Reding, T., Bimmler, D., Perren, A., Sun, L.-K., Fortunato, F., Storni, F., & Graf, R. (2006). A selective COX-2 inhibitor suppresses chronic pancreatitis in an animal model (WBN/Kob rats): Significant reduction of macrophage infiltration and fibrosis. *Gut*, *55*, 1165–1173. https://doi.org/10.1136/gut.2005.077925

Reggiani, C., & Schiaffino, S. (2020). Muscle hypertrophy and muscle strength: Dependent or independent variables? A provocative review. *European Journal of Translational Myology*, *30*, 9311. https://doi.org/10.4081/ejtm.2020.9311

Rigamonti, E., Touvier, T., Clementi, E., Manfredi, A. A., Brunelli, S., & Rovere-Querini, P. (2013). Requirement of inducible nitric oxide synthase for skeletal muscle regeneration after acute damage. *Journal of Immunology*, *190*, 1767–1777. https://doi.org/10.4049/jimmunol.1202903

Roberts, L. A., Raastad, T., Markworth, J. F., Figueiredo, V. C., Egner, I. M., Shield, A., Cameron-Smith, D., Coombes, J. S., & Peake, J. M. (2015). Post-exercise cold water immersion attenuates acute anabolic signalling and long-term adaptations in muscle to strength training. *The Journal of Physiology*, *593*, 4285–4301. https://doi.org/10.1113/JP270570

Roman, W., Pinheiro, H., Pimentel, M. R., Segalés, J., Oliveira, L. M., García-Domínguez, E., Gómez-Cabrera, M. C., Serrano, A. L., Gomes, E. R., & Muñoz-Cánoves, P. (2021). Muscle repair after physiological damage relies on nuclear migration for cellular reconstruction. *Science*, *374*, 355–359. https://doi.org/10.1126/science.abe5620

Round, J. M., Jones, D. A., & Cambridge, G. (1987). Cellular infiltrates in human skeletal muscle: Exercise induced damage as a model for inflammatory muscle disease? *Journal of the Neurological Sciences*, *82*, 1–11. https://doi.org/10.1016/0022-510x(87)90002-5

Saclier, M., Lapi, M., Bonfanti, C., Rossi, G., Antonini, S., & Messina, G. (2020). The transcription factor Nfix requires RhoA-ROCK1 dependent phagocytosis to mediate macrophage skewing during skeletal muscle regeneration. *Cell*, *9*, E708. https://doi.org/10.3390/cells9030708

Saclier, M., Yacoub-Youssef, H., Mackey, A. L., Arnold, L., Ardjoune, H., Magnan, M., Sailhan, F., Chelly, J., Pavlath, G. K., Mounier, R., Kjaer, M., & Chazaud, B. (2013). Differentially activated macrophages orchestrate myogenic precursor cell fate during human skeletal muscle regeneration. *Stem Cells*, *31*, 384–396. https://doi.org/10.1002/stem.1288

Sambasivan, R., Yao, R., Kissenpfennig, A., Van Wittenberghe, L., Paldi, A., Gayraud-Morel, B., Guenou, H., Malissen, B., Tajbakhsh, S., & Galy, A. (2011). Pax7-expressing satellite cells are indispensable for adult skeletal muscle regeneration. *Development*, *138*, 3647–3656. https://doi.org/10.1242/dev.067587

Sansbury, B. E., Li, X., Wong, B., Patsalos, A., Giannakis, N., Zhang, M. J., Nagy, L., & Spite, M. (2020). Myeloid ALX/FPR2 regulates vascularization following tissue injury. *Proceedings of the National Academy of Sciences of the United States of America*, *117*, 14354–14364. https://doi.org/10.1073/pnas.1918163117

Senf, S. M., Howard, T. M., Ahn, B., Ferreira, L. F., & Judge, A. R. (2013). Loss of the inducible Hsp70 delays the inflammatory response to skeletal muscle injury and severely impairs muscle regeneration. *PLoS ONE*, *8*, e62687. https://doi.org/10.1371/journal.pone.0062687

Seo, B. R., Payne, C. J., McNamara, S. L., Freedman, B. R., Kwee, B. J., Nam, S., de Lázaro, I., Darnell, M., Alvarez, J. T., Dellacherie, M. O., Vandenburgh, H. H., Walsh, C. J., & Mooney, D. J. (2021). Skeletal muscle regeneration with robotic actuation-mediated clearance of neutrophils. *Science Translational Medicine*, *13*, eabe8868. https://doi.org/10.1126/scitranslmed.abe8868

Serhan, C. N. (2014). Pro-resolving lipid mediators are leads for resolution physiology. *Nature*, *510*, 92–101. https://doi.org/10.1038/nature13479

Serrano, A. L., Baeza-Raja, B., Perdiguero, E., Jardí, M., & Muñoz-Cánoves, P. (2008). Interleukin-6 is an essential regulator of satellite cell-mediated skeletal muscle hypertrophy. *Cell Metabolism*, *7*, 33–44. https://doi.org/10.1016/j.cmet.2007.11.011

Shang, M., Cappellesso, F., Amorim, R., Serneels, J., Virga, F., Eelen, G., Carobbio, S., Rincon, M. Y., Maechler, P., De Bock, K., Ho, P.-C., Sandri, M., Ghesquière, B., Carmeliet, P., Di Matteo, M., Berardi, E., & Mazzone, M. (2020). Macrophage-derived glutamine boosts satellite cells and muscle regeneration. *Nature*, *587*, 626–631. https://doi.org/10.1038/s41586-020-2857-9

Shen, W., Li, Y., Tang, Y., Cummins, J., & Huard, J. (2005). NS-398, a cyclooxygenase-2-specific inhibitor, delays skeletal muscle healing by decreasing regeneration and promoting fibrosis. *The American Journal of Pathology*, *167*, 1105–1117. https://doi.org/10.1016/S0002-9440(10)61199-6

Shen, W., Prisk, V., Li, Y., Foster, W., & Huard, J. (2006). Inhibited skeletal muscle healing in cyclooxygenase-2 gene-deficient mice: The role of PGE2 and PGF2alpha. *Journal of Applied Physiology (Bethesda, MD: 1985)*, *101*, 1215–1221. https://doi.org/10.1152/japplphysiol.01331.2005

Shibaguchi, T., Sugiura, T., Fujitsu, T., Nomura, T., Yoshihara, T., Naito, H., Yoshioka, T., Ogura, A., & Ohira, Y. (2016). Effects of icing or heat stress on the induction of fibrosis and/or regeneration of injured rat soleus muscle. *The Journal of Physiological Sciences*, *66*, 345–357. https://doi.org/10.1007/s12576-015-0433-0

Shireman, P. K., Contreras-Shannon, V., Ochoa, O., Karia, B. P., Michalek, J. E., & McManus, L. M. (2007). MCP-1 deficiency causes altered inflammation with impaired skeletal muscle regeneration. *Journal of Leukocyte Biology*, *81*, 775–785. https://doi.org/10.1189/jlb.0506356

Singh, P., & Chazaud, B. (2021). Benefits and pathologies associated with the inflammatory response. *Experimental Cell Research*, *409*, 112905. https://doi.org/10.1016/j.yexcr.2021.112905

Soltow, Q. A., Betters, J. L., Sellman, J. E., Lira, V. A., Long, J. H. D., & Criswell, D. S. (2006). Ibuprofen inhibits skeletal muscle hypertrophy in rats. *Medicine and Science in Sports and Exercise*, *38*, 840–846. https://doi.org/10.1249/01.mss.0000218142.98704.66

Takagi, R., Fujita, N., Arakawa, T., Kawada, S., Ishii, N., & Miki, A. (2011). Influence of icing on muscle regeneration after crush injury to skeletal muscles in rats. *Journal of Applied Physiology (Bethesda, MD: 1985)*, *110*, 382–388. https://doi.org/10.1152/japplphysiol.01187.2010

Takeuchi, K., Hatade, T., Wakamiya, S., Fujita, N., Arakawa, T., & Miki, A. (2014). Heat stress promotes skeletal muscle regeneration after crush injury in rats. *Acta Histochemica*, *116*, 327–334. https://doi.org/10.1016/j.acthis.2013.08.010

Thakur, S. S., James, J. L., Cranna, N. J., Chhen, V. L., Swiderski, K., Ryall, J. G., & Lynch, G. S. (2019). Expression and localization of heat-shock proteins during skeletal muscle cell proliferation and differentiation and the impact of heat stress. *Cell Stress & Chaperones*, *24*, 749–761. https://doi.org/10.1007/s12192-019-01001-2

Thompson, R. W., McClung, J. M., Baltgalvis, K. A., Davis, J. M., & Carson, J. A. (2006). Modulation of overload-induced inflammation by aging and anabolic steroid administration. *Experimental Gerontology*, *41*, 1136–1148. https://doi.org/10.1016/j.exger.2006.08.013

Tonkin, J., Temmerman, L., Sampson, R. D., Gallego-Colon, E., Barberi, L., Bilbao, D., Schneider, M. D., Musarò, A., & Rosenthal, N. (2015). Monocyte/macrophage-derived IGF-1 orchestrates murine skeletal muscle regeneration and modulates autocrine polarization. *Molecular Therapy*, *23*, 1189–1200. https://doi.org/10.1038/mt.2015.66

Trappe, T. A., Carroll, C. C., Dickinson, J. M., LeMoine, J. K., Haus, J. M., Sullivan, B. E., Lee, J. D., Jemiolo, B., Weinheimer, E. M., & Hollon, C. J. (2011). Influence of acetaminophen and ibuprofen on skeletal muscle adaptations to resistance exercise in older adults. *American Journal of Physiology. Regulatory, Integrative and Comparative Physiology*, *300*, R655–R662. https://doi.org/10.1152/ajpregu.00611.2010

Tscholl, P. M., Vaso, M., Weber, A., & Dvorak, J. (2015). High prevalence of medication use in professional football tournaments including the world cups between 2002 and 2014: A narrative review with a focus on NSAIDs. *British Journal of Sports Medicine*, *49*, 580–582. https://doi.org/10.1136/bjsports-2015-094784

Tseng, C.-Y., Lee, J.-P., Tsai, Y.-S., Lee, S.-D., Kao, C.-L., Liu, T.-C., Lai, C.-H., Harris, M. B., & Kuo, C.-H. (2013). Topical cooling (icing) delays recovery from eccentric exercise-induced muscle damage. *Journal of Strength and Conditioning Research*, *27*, 1354–1361. https://doi.org/10.1519/JSC.0b013e318267a22c

Urso, M. L. (2013). Anti-inflammatory interventions and skeletal muscle injury: Benefit or detriment? *Journal of Applied Physiology (Bethesda, MD: 1985)*, *115*, 920–928. https://doi.org/10.1152/japplphysiol.00036.2013

Vaile, J., Halson, S., Gill, N., & Dawson, B. (2008). Effect of hydrotherapy on the signs and symptoms of delayed onset muscle soreness. *European Journal of Applied Physiology*, *102*, 447–455. https://doi.org/10.1007/s00421-007-0605-6

Van Pelt, D. W., Lawrence, M. M., Miller, B. F., Butterfield, T. A., & Dupont-Versteegden, E. E. (2021). Massage as a mechanotherapy for skeletal muscle. *Exercise and Sport Sciences Reviews*, *49*, 107–114. https://doi.org/10.1249/JES.0000000000000244

Varga, T., Mounier, R., Horvath, A., Cuvellier, S., Dumont, F., Poliska, S., Ardjoune, H., Juban, G., Nagy, L., & Chazaud, B. (2016). Highly dynamic transcriptional signature of distinct macrophage subsets during sterile inflammation, resolution, and tissue repair. *Journal of Immunology*, *196*, 4771–4782. https://doi.org/10.4049/jimmunol.1502490

Varga, T., Mounier, R., Patsalos, A., Gogolák, P., Peloquin, M., Horvath, A., Pap, A., Daniel, B., Nagy, G., Pintye, E., Póliska, S., Cuvellier, S., Larbi, S. B., Sansbury, B. E., Spite, M., Brown, C. W., Chazaud, B., & Nagy, L. (2016). Macrophage PPARγ, a lipid activated transcription factor controls the growth factor GDF3 and skeletal muscle regeneration. *Immunity*, *45*, 1038–1051. https://doi.org/10.1016/j.immuni.2016.10.016

Vella, L., Markworth, J. F., Paulsen, G., Raastad, T., Peake, J. M., Snow, R. J., Cameron-Smith, D., & Russell, A. P. (2016). Ibuprofen ingestion does not affect markers of post-exercise muscle inflammation. *Frontiers in Physiology*, *7*, 86. https://doi.org/10.3389/fphys.2016.00086

Vieira Ramos, G., Pinheiro, C. M., Messa, S. P., Delfino, G. B., Marqueti, R.d. C., Salvini, T.d. F., & JLQ, D. (2016). Cryotherapy reduces inflammatory response without altering muscle regeneration process and extracellular matrix remodeling of rat muscle. *Scientific Reports*, *6*, 18525. https://doi.org/10.1038/srep18525

Walton, R. G., Kosmac, K., Mula, J., Fry, C. S., Peck, B. D., Groshong, J. S., Finlin, B. S., Zhu, B., Kern, P. A., & Peterson, C. A. (2019). Human skeletal muscle macrophages increase following cycle training and are associated with adaptations that may facilitate growth. *Scientific Reports*, *9*, 969. https://doi.org/10.1038/s41598-018-37187-1

Warren, G. L., Hulderman, T., Mishra, D., Gao, X., Millecchia, L., O'Farrell, L., Kuziel, W. A., & Simeonova, P. P. (2005). Chemokine receptor CCR2 involvement in skeletal muscle regeneration. *The FASEB Journal*, *19*, 413–415. https://doi.org/10.1096/fj.04-2421fje

Warren, G. L., Lowe, D. A., & Armstrong, R. B. (1999). Measurement tools used in the study of eccentric contraction-induced injury. *Sports Medicine*, *27*, 43–59.

Waters-Banker, C., Butterfield, T. A., & Dupont-Versteegden, E. E. (2014). Immunomodulatory effects of massage on nonperturbed skeletal muscle in rats. *Journal of Applied Physiology (Bethesda, MD: 1985)*, *116*, 164–175. https://doi.org/10.1152/japplphysiol.00573.2013

Yin, H., Price, F., & Rudnicki, M. A. (2013). Satellite cells and the muscle stem cell niche. *Physiological Reviews*, *93*, 23–67. https://doi.org/10.1152/physrev.00043.2011

Zalin, R. J. (1977). Prostaglandins and myoblast fusion. *Developmental Biology*, *59*, 241–248. https://doi.org/10.1016/0012-1606(77)90258-5

Zavoriti, A, Fessard, A., Rahmati, M., Carmine, P. D., Chazaud, B., & Gondin, J. (2021). *Individualized isometric neuromuscular electrical stimulation training promotes myonuclear accretion in mouse skeletal muscle.*

Zhang, C., Wang, C., Li, Y., Miwa, T., Liu, C., Cui, W., Song, W.-C., & Du, J. (2017). Complement C3a signaling facilitates skeletal muscle regeneration by regulating monocyte function

and trafficking. *Nature Communications*, *8*, 2078. https://doi.org/10.1038/s41467-017-01526-z

Zhang, J., Qu, C., Li, T., Cui, W., Wang, X., & Du, J. (2019). Phagocytosis mediated by scavenger receptor class BI promotes macrophage transition during skeletal muscle regeneration. *The Journal of Biological Chemistry*, *294*, 15672–15685. https://doi.org/10.1074/jbc.RA119.008795

Zhang, M. J., Sansbury, B. E., Hellmann, J., Baker, J. F., Guo, L., Parmer, C. M., Prenner, J. C., Conklin, D. J., Bhatnagar, A., Creager, M. A., & Spite, M. (2016). Resolvin D2 enhances Postischemic revascularization while resolving inflammation. *Circulation*, *134*, 666–680. https://doi.org/10.1161/CIRCULATIONAHA.116.021894

Zhu, W. G., Hibbert, J. E., Lin, K. H., Steinert, N. D., Lemens, J. L., Jorgenson, K. W., Newman, S. M., Lamming, D. W., & Hornberger, T. A. (2021). Weight pulling: A novel mouse model of human progressive resistance exercise. *Cell*, *10*, 2459. https://doi.org/10.3390/cells10092459

SUPPORTING INFORMATION

Additional supporting information can be found online in the Supporting Information section at the end of this article.

How to cite this article: Bernard, C., Zavoriti, A., Pucelle, Q., Chazaud, B., & Gondin, J. (2022). Role of macrophages during skeletal muscle regeneration and hypertrophy—Implications for immunomodulatory strategies. *Physiological Reports*, *10*, e15480. https://doi.org/10.14814/phy2.15480

Study of the muscle stem cell microenvironment in cancer cachexia and the benefits of a neuromuscular electrical stimulation therapy

Cancer cachexia (CC) is a multifactorial syndrome in patients with cancer that leads to unintentional body weight loss mainly caused by loss of skeletal muscle tissue (*i.e.,* muscle atrophy). CC negatively affects muscle strength and quality of life of cancer patients, consequently leading to increased mortality. To date no curative treatment, exist to overcome CC. Recently, CC was proposed to result from dysfunction of the muscle stem cells, the satellite cells (SCs), required for muscle homeostasis. In the presence of tumor, notably SCs are unable to differentiate and fuse. Also, the fate of SCs is regulated by different cell types (immune cells, fibro-adipogenic progenitors (FAPs), and endothelial cells) that compose the SC niche and might also be altered in CC. SC fate impairment could result from altered cellular interactions within the cachectic niche leading to muscle weakness and wasting. However, characterization of these dysfunctions remains largely unknown in this context. Exercise promotes SC fusion (*i.e.*, myonuclear accretion) and regulates the SC niche to sustain muscle growth in response to increased contractile activity. Implementing exercise as a therapeutic strategy is challenging in cancer patients who usually have low tolerance to exercise. Neuromuscular electrical stimulation (NMES) represents an alternative approach to exercise to increase muscle contractile activity. The aim of this work was first to develop a NMES training protocol that relies on the main function of skeletal muscle, *i.e.*, force production in response to electrical stimuli. Our individualized and carefully-monitored NMES positively regulated SC fate by inducing myonuclear accretion and led to muscle hypertrophy in the absence of muscle damage in healthy mice. Our second aim was to determine whether CC alters SC niche and whether NMES could serve as a therapy to counteract muscle weakness and wasting and the alterations in SC and its niche from two complementary mouse models of CC (*i.e.,* C26 et *Apc*$^{Min/+}$ mouse models). We first demonstrated that the number and function of SCs were altered in the cachectic animals together with increases in macrophages and FAPs accumulation. Our findings from the *in vitro* experiments emphasized that the interactions between these cell types could be impaired. NMES improved muscle force and mass in the C26 cachectic mice as well as SC fate, while it changed macrophage inflammatory status. NMES preserved myofiber size in the *Apc*$^{Min/+}$ mice independently of regulation in SCs. Increased muscle contractions by NMES can limit the deleterious consequences of CC on muscle function, mass or myofiber size and positively modulate SC niche. This work sheds new light on a potential non-pharmacological therapy.

Étude du microenvironnement des cellules souches musculaires dans la cachexie cancéreuse et bénéfices d'une thérapie par électrostimulation neuromusculaire

La cachexie cancéreuse (CC) est un syndrome multifactoriel qui touchent les patients atteints de cancer et qui entraîne une perte de poids corporel involontaire provoquée principalement par la fonte de muscles squelettiques. La CC affecte négativement la force musculaire et la qualité de vie des patients atteints de cancer, réduisant leur taux de survie. À ce jour, la CC reste incurable. Il a été récemment proposé que la CC résulte d'un dysfonctionnement des cellules souches musculaires (CSM) nécessaires à l'homéostasie du muscle. En présence d'une tumeur, les CSM sont incapables de se différencier et de fusionner. Aussi, le destin des CSM est régulé par différents types cellulaires (*i.e.*, cellules immunes, progéniteurs fibro-adipogéniques (FAP) et cellules endothéliales) qui composent la niche des CSM et qui pourraient être également altérés lors de la CC. L'altération du destin des CSM pourrait donc résulter d'une altération dans les interactions cellulaires au sein de la niche cachectique, entraînant une faiblesse et une fonte musculaires. Cependant, les interactions cellulaires dans la CC sont peu connues. Il est admis que l'exercice favorise la fusion des CSM (*i.e.,* accrétion myonucléaire) et régule la niche pour soutenir la croissance musculaire en réponse à une activité contractile accrue. La pratique de l'exercice physique pour limiter la cachexie reste difficile chez les patients cachectiques qui souvent sont affaiblis. L'électrostimulation neuromusculaire (ESNM) constitue une approche alternative à l'exercice pour augmenter l'activité contractile des muscles. Notre premier objectif était de développer un protocole d'entraînement par ESNM qui s'appuie sur la principale fonction du muscle squelettique, à savoir la production de force en réponse à une neurostimulation. Nous démontrons qu'un protocole d'ESNM individualisé et soigneusement contrôlé régule positivement le devenir des CSM en induisant une accrétion myonucléaire et une hypertrophie musculaire en l'absence de lésions musculaires chez des souris saines. Notre second objectif était d'évaluer comment la cachexie altère la niche des CSM et si une augmentation de l'activité musculaire par ESNM permet de limiter les altérations du muscle, les dysfonctions de CSM et de leur niche dans deux modèles murins de CC (Les modèles murins C26 et *Apc*$^{Min/+}$). Nous démontrons que la CC induit des altérations dans le nombre de CSM, de macrophages et des FAPs tout comme elle altère la fonction de CSM. Aussi, nous mettons en évidence *in vitro* que la CC affecte les interactions entre ces différents types cellulaires. Enfin, nous démontrons que le protocole d'ESNM améliore la force et la masse musculaires chez les souris cachectiques C26, ainsi que le devenir des cellules souches tout en modifiant le statut inflammatoire des macrophages. Le NMES a préservé la taille des myofibres chez les souris *Apc*$^{Min/+}$ indépendamment d'une régulation de la CSM. L'augmentation des contractions musculaires par le ESNM peut limiter les conséquences délétères de la CC sur la fonction et la masse musculaires ou la taille de myofibres et moduler positivement la niche des CSM. Ce travail apporte un nouvel éclairage sur une thérapie non pharmacologique potentielle.